



University of Kentucky  
**UKnowledge**

---

Theses and Dissertations--Pharmacy

College of Pharmacy

---

2018

## CHARACTERIZATION AND ENGINEERING OF HUMAN PROTEINS AS THERAPEUTIC CANDIDATES

Kyungbo Kim

University of Kentucky, [kyungbo.kim85@uky.edu](mailto:kyungbo.kim85@uky.edu)

Digital Object Identifier: <https://doi.org/10.13023/etd.2018.354>

[Right click to open a feedback form in a new tab to let us know how this document benefits you.](#)

---

### Recommended Citation

Kim, Kyungbo, "CHARACTERIZATION AND ENGINEERING OF HUMAN PROTEINS AS THERAPEUTIC CANDIDATES" (2018). *Theses and Dissertations--Pharmacy*. 91.

[https://uknowledge.uky.edu/pharmacy\\_etds/91](https://uknowledge.uky.edu/pharmacy_etds/91)

This Doctoral Dissertation is brought to you for free and open access by the College of Pharmacy at UKnowledge. It has been accepted for inclusion in Theses and Dissertations--Pharmacy by an authorized administrator of UKnowledge. For more information, please contact [UKnowledge@lsv.uky.edu](mailto:UKnowledge@lsv.uky.edu).

## **STUDENT AGREEMENT:**

I represent that my thesis or dissertation and abstract are my original work. Proper attribution has been given to all outside sources. I understand that I am solely responsible for obtaining any needed copyright permissions. I have obtained needed written permission statement(s) from the owner(s) of each third-party copyrighted matter to be included in my work, allowing electronic distribution (if such use is not permitted by the fair use doctrine) which will be submitted to UKnowledge as Additional File.

I hereby grant to The University of Kentucky and its agents the irrevocable, non-exclusive, and royalty-free license to archive and make accessible my work in whole or in part in all forms of media, now or hereafter known. I agree that the document mentioned above may be made available immediately for worldwide access unless an embargo applies.

I retain all other ownership rights to the copyright of my work. I also retain the right to use in future works (such as articles or books) all or part of my work. I understand that I am free to register the copyright to my work.

## **REVIEW, APPROVAL AND ACCEPTANCE**

The document mentioned above has been reviewed and accepted by the student's advisor, on behalf of the advisory committee, and by the Director of Graduate Studies (DGS), on behalf of the program; we verify that this is the final, approved version of the student's thesis including all changes required by the advisory committee. The undersigned agree to abide by the statements above.

Kyungbo Kim, Student

Dr. Chang-Guo Zhan, Major Professor

Dr. David J. Feola, Director of Graduate Studies

CHARACTERIZATION AND ENGINEERING OF HUMAN PROTEINS  
AS THERAPEUTIC CANDIDATES

---

DISSERTATION

---

A dissertation submitted in partial fulfillment of  
the requirements for the degree of Doctor of Philosophy in the  
College of Pharmacy  
at the University of Kentucky

By  
Kyungbo Kim  
Lexington, Kentucky  
Director: Dr. Chang-Guo Zhan, Professor of Pharmacy  
Lexington, Kentucky  
2018

Copyright © Kyungbo Kim 2018

## ABSTRACT OF DISSERTATION

### CHARACTERIZATION AND ENGINEERING OF HUMAN PROTEINS AS THERAPEUTIC CANDIDATES

Protein engineering has been a useful tool in the fight against human diseases. Human insulin was the first recombinant DNA-derived therapeutic protein (Humulin®) approved by the US FDA in 1982. However, many of the early protein drugs were only recombinant versions of natural proteins with no modification of their primary amino acid sequence and most of them did not make optimal drug products mainly due to their short half-life or suboptimal affinity, leading to poor therapeutic efficacy. The difficulty in the large-scale production of some therapeutic proteins was another important issue. In the past three decades, different protein engineering platforms have been developed to overcome the obstacles seen in the first generations of these treatments. With the help of these new techniques, proteins have been purposefully modified to improve their clinical potential. The focus of my dissertation is the engineering of potential protein drugs to make them therapeutically useful and more valuable. Previously, our research group has developed cocaine hydrolases (CocHs) from human butyrylcholinesterase (BChE) for treatment of cocaine addiction and prevention of acute cocaine intoxication. In the first project, CocHs were further engineered to improve their performance, e.g., Fc-fused CocHs with an extended serum half-life. Then, I investigated the potential application of a long-lasting CocH for protection against the acute toxic and stimulant effects of cocaine. In the second project, I investigated the potential inhibition of CocH-mediated cocaine hydrolysis by heroin (3,6-diacetylmorphine) or its initial host metabolite, 6-monoacetylmorphine (6-MAM). The investigation of this possible inhibition was important to determine the *in vivo* efficacy of CocHs, as heroin is one of the most commonly co-abused drugs by cocaine-dependent individuals, as well as a possible metabolite of CocHs. In the third project, I expressed and characterized the recombinant human UDP-glucuronosyltransferase 1A10 (UGT1A10) enzyme, which can inactivate many therapeutically valuable substances. In the fourth and final project, prostate apoptosis response-4 (Par-4), a tumor suppressor protein, was engineered to have a prolonged duration of action so that it may be more therapeutically valuable for cancer treatment.

KEYWORDS: CocH, UGT, Cocaine, Heroin, Morphine, Par-4

Kyungbo Kim  
Student's Signature

7/18/2018  
Date

CHARACTERIZATION AND ENGINEERING OF HUMAN PROTEINS AS  
THERAPEUTIC CANDIDATES

By

Kyungbo Kim

Chang-Guo Zhan  
Director of Dissertation

David J. Feola  
Director of Graduate Studies

07/18/2018  
Date

*I would like to dedicate this dissertation to dear wife (Soonmi Shim) and beloved family members (Myeonghee Lee, Jae Hong Kim, and Kyung Min Kim). Your love, support, and encouragement have sustained me throughout my life.*

## ACKNOWLEDGEMENTS

I would like to begin by thanking my advisor, Dr. Chang-Guo Zhan, for trusting and supporting me to complete my PhD program. I have learned a lot in his lab and really respect him as a brilliant scientist and principal investigator. I have enjoyed time on my working place and will miss those moments. I also would like to appreciate Dr. Markos Leggas, Dr. Shuxia Wang, Dr. Sylvie Garneau-Tsodikova, and Dr. Jurgen Rohr for serving as my Dissertation Committee members providing invaluable guidance and assistance over the years. I also thank Dr. Yinan Wei for serving as the outside examiner. In addition, I would like to send my more thanks to Dr. Mark Leggas again who always gave me sincere advices when I needed help. I am also very grateful to Dr. Fang Zheng for her good advices.

I want to thank the current and previous lab members of Dr. Chang-Guo Zhan's lab for their help, especially those (Dr. Zhenyu Jin, Ting Zhang, Ding Kai, Xirong Zheng, Dr. Chunhui Zhang, Dr. Jinling Zhang, and Dr. Ziyuan Zhou) who have worked together with me in some projects. I send my special thanks to Dr. Ting Zhang for her great kindness and encouraging me a lot. Shuo Zhou is a smart colleague for intellectual discussions. I also thank Dr. Ding Kai for his precious works and love for everyone in the lab. Dr. Zhenyu Jin, I am very grateful to you for treating me like a family member. I also appreciate Dr. Vivek M. Rangnekar, Dr. Nikhil Hebbar, and Nathalia Vitoria Pereira Araujo who have worked with me on my Par-4 project. I also should thank Alexander Williams for helping me to revise my dissertation.

I also would like to express my gratitude to my friends outside the department. Na-Ra Lee provides the wise suggestions to improve my scientific challenges. I learned a lot from Chanung Wang while I was working with him in Korean Bioscientists Association at



University of Kentucky. June-Sun Yoon (Sunny) is a wonderful friend and scientist who inspired me a lot with his brilliant ideas and great enthusiasm. It is my luck to have him in my life.

Finally, I would like to express sincere appreciation to my former advisers who taught and trusted me. I could dream of becoming a scientist in the lab of Dr. Sang-Bong Choi during my university years. I have learned a lot from Dr. Woon Lee about how to organize my projects. Dr. Kyungbo-Bo Kim always gives me professional or personal advice with a bright smile. Dr. Dong-Eun Kim is a scientist and teacher who I respect the most. He has been a very important reason why I want to do science for a living.

## TABLE OF CONTENTS

ACKNOWLEDGEMENTS .....	iii
LIST OF TABLES .....	xi
LIST OF FIGURES .....	xii
Chapter I. Introduction.....	1
1.1 Protein therapeutics.....	1
1.2 Improvement of activity.....	2
1.3 Fusion proteins for half-life extension of protein therapeutics.....	3
Chapter II. Development of a Long-acting Cocaine Hydrolase for Cocaine Abuse Treatment .....	6
2.1 Treatment for cocaine abuse .....	8
2.1.1 Cocaine overdose and addiction .....	8
2.1.2 Physical and psychological dependence on cocaine.....	9
2.1.3 Effect of cocaine on dopaminergic neurotransmission .....	11
2.1.4 Relapse.....	13
2.1.5 Specific goals to be achieved for treatment of substance abuse disorder .....	14
2.1.6 Pharmacokinetic approach for cocaine abuse treatment.....	16
2.1.7 Enzyme-based therapy for cocaine abuse .....	17
2.2 The focuses of this research.....	19
2.3 Results & Discussion .....	20

2.3.1 Insights from molecular modeling .....	20
2.3.2 Characterization of CocH3-fused with human IgG1 Fc variants.....	21
2.3.3 Determination of biological half-life in rats .....	27
2.3.4 Effectiveness of CocH3-Fc(3m) in blocking the striatal dopamine transporter trafficking induced by cocaine.....	30
2.4 Experimental details.....	35
2.4.1 Materials & Animals .....	35
2.4.2 Construction of gene expression plasmids.....	35
2.4.3 A recombinant lentiviral packaging system for stable cell generation .....	35
2.4.4 Transient expression and purification of soluble single-chain FcRn (sFcRn) .	36
2.4.5 Large-scale protein expression and purification of Fc-fused CocHs .....	38
2.4.6 Enzyme-linked immunosorbent assay (ELISA) .....	40
2.4.7 Pharmacokinetic studies in rats.....	41
2.4.8 DAT cellular distribution assay.....	42
Chapter III. Kinetic Characterization of Cholinesterases and a Therapeutically Valuable Cocaine Hydrolase for Their Catalytic Activities against Heroin and Its Metabolite 6- monoacetylmorphine.....	44
3.1 Heroin hydrolysis to morphine by human cholinesterase.....	45
3.2 The focuses of this research.....	47
3.3 Results & Discussion .....	47

3.3.1 Identification of Fc variants with altered binding.....	47
3.3.2 Hydrolysis of free 6-MAM to morphine by human recombinant BChE and AChE.....	49
3.3.3 Kinetics of heroin hydrolysis by BChE, AChE, and Coch1 .....	50
3.3.4 Kinetics of 6-MAM hydrolysis by BChE, AChE, and Coch1 .....	55
3.3.5 Insights from molecular modeling .....	60
3.3.6 Main outcomes of this research .....	64
3.4 Experimental details.....	65
3.4.1 Materials .....	65
3.4.2 Construction of mammalian expression plasmids .....	65
3.4.3 Protein Expression and Purification.....	66
3.4.4 Enzyme Activity Assays .....	67
3.4.5 Molecular modelling.....	68
Chapter IV. Oligomerization and Catalytic Parameters of Human UDP-glucuronosyltransferase 1A10 .....	69
4.1 UDP-glucuronosyltransferase (UGT) .....	70
4.2 The focuses of this research.....	72
4.3 Results.....	72
4.3.1 Overexpression of human UGT1A10 in CHO and HEK293 cells .....	72
4.3.2 Quantification of the levels of recombinant UGT1A10 in microsomes prepared	

from stable cells .....	75
4.3.3 Kinetics of morphine glucuronidation by recombinant human UGT1A10 .....	78
4.3.4 Kinetics of entacapone glucuronidation by recombinant human UGT1A10...	81
4.4 Discussion and Conclusion .....	85
4.5 Experimental details.....	90
4.5.1 Chemicals and Materials.....	90
4.5.2 Generation of the stable cell line by lentivirus infection .....	90
4.5.3 Microsomal preparation .....	91
4.5.4 Purification of UGT1A10 .....	91
4.5.5 Enzyme Activity Assays .....	92
4.5.6 Hydrolysis by $\beta$ -glucuronidase .....	93
4.5.7 Western blot assay.....	93
Chapter V. Development of a New Par-4 Entity with a Prolonged Duration of Action...	95
5.1 The role of Par-4 as a tumor suppressor .....	95
5.2 The focuses of this research.....	97
5.3 Results.....	98
5.3.1 The short serum persistence <i>in vivo</i> of recombinant Par-4 (Par-4).....	98
5.3.2 Development of a method for large-scale production of Fc-fused Par-4.....	99
5.3.3 <i>E. coli</i> -derived Par-4 proteins induce apoptosis in cancer cells.....	111
5.3.4 Characterization of the <i>in vivo</i> profiles of recombinant Par-4 .....	113

5.3.5 <i>In vivo</i> characterization of recombinant Par-4 proteins for their potency in inhibiting metastatic tumor growth.....	115
5.4 Discussion .....	117
5.5 Experimental details.....	121
5.4.1 Cloning, expression and purification of 6xHis-Par-4 and Fc(M1)-Par-4 .....	121
5.4.2 Western blot .....	123
5.4.3 Immunocytochemistry and apoptosis analysis.....	123
5.4.4 Pharmacokinetics studies in mice .....	124
5.4.5 Lung metastasis of E0771 cells.....	125
5.4.6 Statistical analysis.....	126
Chapter VI. Conclusions and Future Directions .....	127
6.1 Cocaine abuse treatment .....	127
6.2 Oligomerization and catalytic parameters of human UGT1A10 .....	128
6.3 Cancer treatment .....	129
Chapter VII. Other Unpublished Works.....	131
7.1 Development of potential antibody therapeutics for opioid use disorders .....	131
7.1.1 The main purpose of this study .....	131
7.1.2 Introduction.....	131
7.1.3 Results and discussion .....	134
7.1.4 Materials and methods .....	137

7.2 Development of mPGES-1 specific inhibitor as an anticancer agent for multiple therapeutic areas.....	139
7.2.1 The main purpose of this study .....	139
7.2.2 Results and discussion .....	139
7.2.3 Materials and methods .....	148
References.....	149
Vitae .....	174

## LIST OF TABLES

Table 2.1 Treatment options for cocaine detox withdrawal symptoms.....	10
Table 2.2 The reported neurochemical differences between cocaine addicts and healthy individuals.....	11
Table 2.3 Drugs in phase II clinical trials for cocaine addiction.....	15
Table 2.4 The new generations of CocH with an improved catalytic efficiency against cocaine.....	19
Table 2.5 Summary of determined equilibrium dissociation constants ( $K_D$ ) of interaction of Fc-fused CocHs with FcRn molecules (at pH 6.0, (nM)).....	27
Table 2.6 The determined biological half-lives of Fc-fused CocH3 proteins in rats.....	30
Table 2.7 The referred DNA sequences for FcRn expression.....	37
Table 3.1 The reported kinetic parameters of human BChE for heroin hydrolysis.....	47
Table 3.2 Kinetic parameters of BChE, AChE, and CocH1 against heroin.....	54
Table 3.3 Kinetic parameters of BChE, AChE, and CocH1 against heroin.....	58
Table 4.1 Kinetic constants for morphine 3- and 6-glucuronide formation by human recombinant UDP-glucuronosyltransferases stably expressed in HEK293 cells .....	71
Table 4.2 Kinetic parameters of human UGT1A10-6xHis against morphine .....	80
Table 4.3 Kinetic parameters of human UGT1A10-6xHis against entacapone.....	85
Table 5.1 The determined biological half-lives of recombinant Par-4 proteins in mice..	115
Table 7.1 $IC_{50}$ values ( $\mu M$ ) of BAR002, Cisplatin, Erlotinib, or PTX after 48 h of exposure (n = 3, mean $\pm$ SD).....	141
Table 7.2 $IC_{50}$ values ( $\mu M$ ) of BAR002, Cisplatin, Erlotinib, or PTX after 48 h of exposure (n = 3, mean $\pm$ SD).....	145



## LIST OF FIGURES

Figure 2.1 Cocaine metabolic pathways in physiological condition.....	18
Figure 2.2 Schematic presentation of the soluble single-chain FcRn proteins of different species.....	24
Figure 2.3 Schematic presentation of the newly designed Fc-fused CocH3 proteins.....	25
Figure 2.4 Serum concentration (%) versus time profiles of Fc-fused CocH3 proteins in rats.....	29
Figure 2.5 The schematic presentation of DAT cellular distribution assay.....	32
Figure 2.6 The cell surface distribution of dopamine transporter (DAT) in the striatum of adult rats.....	33
Figure 3.1 Schematic presentation of heroin hydrolysis to morphine.....	46
Figure 3.2 Enzymatic activity of BChE and AChE on the hydrolysis of heroin. ....	48
Figure 3.3 Enzymatic activity of BChE and AChE on the hydrolysis of 6-MAM. ....	50
Figure 3.4 Kinetic analysis of heroin hydrolysis by BChE, AChE, and CocH1. ....	52
Figure 3.5 Kinetic analysis of 6-MAM hydrolysis by BChE, AChE, and CocH1. ....	56
Figure 3.6 (–)-Cocaine hydrolysis by CocH1. Both the enzyme (100 ng/ml) and (–)-cocaine (100 $\mu$ M) were incubated together with 100 $\mu$ M opioid (heroin or 6-MAM).....	60
Figure 3.7 Modeled structures of the AChE, BChE, and CocH1 (E14-3) binding with heroin and 6-MAM. ....	63
Figure 4.1 Western blot analysis of UGT1A10 protein in microsomes prepared from UGT1A10-6xHis-overexpressing stable CHO and HEK293 cell lines. ....	73
Figure 4.2 Analysis of recombinant UGT1A10 expression. SDS-polyacrylamide gel electrophoresis of microsomes under different denaturing conditions, followed by	

immunoblot analysis.....	75
Figure 4.3 Quantification of the levels of UGT1A10 in microsomes. ....	77
Figure 4.4 Kinetic analysis of the formation of morphine-3-glucuronide (M3G) by UGT1A10.....	79
Figure 4.5 HPLC analysis of the formation of entacapone 3- <i>O</i> -glucuronide using microsomes prepared from UGT1A10-6xHis-overexpressing stable cell lines. ....	82
Figure 4.6 Kinetic analysis of entacapone 3- <i>O</i> -glucuronide formation by UGT1A10....	83
Figure 4.7 The modeled van der Waals surface of the UGT1A10 protein structure, showing three solvent-accessible cysteine residues (C72, C183, and C277 in green color).....	88
Figure 5.1 SDS-PAGE of the TRX-fused or hexa-histidine tagged Par-4 (TRX-Par-4 and 6xHis-Par-4, respectively) purified by immobilized cobalt ion affinity chromatography.....	99
Figure 5.2 The limited serum persistence of recombinant Par-4 proteins in mice.....	100
Figure 5.3 The schematic presentation of the fusion protein of Par-4 to Fc(M1). ‘ss’ represents the leader peptide sequence of mouse IgG kappa-chain.....	102
Figure 5.4 SDS-PAGE of the purified Fc(M1)-Par-4.....	104
Figure 5.5 Recombinant Par-4 protein is expressed at a scale of 100 ml using each of TransIT-PRO™ and PEI. ....	105
Figure 5.6 Preparation of Fc(M1)-Par-4. (A) The schematic presentation of Fc(M1)-Par- 4. (B) Western blot analysis of Par-4 protein in bacterial extract transformed with pET- 22b(+)/6xhis-Par-4 and induced with IPTG.....	106

Figure 5.7 Rare codons found in the coding region of Fc(M1)-Par4 gene.....	108
Figure 5.8 SDS-PAGE analysis of Fc(M1)-Par-4 in the <i>E. coli</i> BL21 (DE3) and Rosetta (DE3) transformed with pET-22b(+)/Fc(M1)-Par-4.....	108
Figure 5.9 Effects of computational codon optimization of Fc(M1)-Par-4 gene on its bacterial expression.....	109
Figure 5.10 Growth curves of the <i>E. coli</i> BL21 (DE3) transformed with pET-22b(+)/Fc(M1)-Par-4 .....	111
Figure 5.11 Comparison between IPTG-induced and uninduced growth of the transformed <i>E. coli</i> BL21 (DE3) at 18°C in TB at 350 rpm.....	111
Figure 5.12 Effects of the induction variables (OD600) on the expression of Fc(M1)-Par-4 in the <i>E. coli</i> BL21 (DE3) transformed with the gene.....	112
Figure 5.13 Recombinant Par-4 elicits apoptosis in E0771 (murine breast cancer cell line) cells.....	113
Figure 5.14 Serum concentration (%) versus time profiles of recombinant Par-4 proteins in mice.....	115
Figure 5.15 Recombinant Par-4 protein suppresses the metastatic growth of tumor (E0771). .....	117
Figure 7.1 SDS-PAGE of the purified mAb MMBCmAb-H6M.....	136
Figure 7.2 The modeled structure and in vitro activities of mAb MMBCmAb-H6M....	137
Figure 7.3 Dose-response curves of Cisplatin, Erlotinib, or PTX in DU-145 cells. (48 h of exposure, n = 3, mean $\pm$ SD).....	141
Figure 7.4 Combination assays of BAR002 and anticancer agents Cisplatin, Erlotinib, and PTX. DU-145 cells were exposed to a different concentration of an anticancer agent with	

0.78 $\mu$ M BAR002.....	143
Figure 7.5 Dose-response curves of Cisplatin, Erlotinib, or PTX in A549 cells. (48 h of exposure, n = 3, mean $\pm$ SD).....	145
Figure 7.6 Combination assays of BAR002 and anticancer agents Cisplatin, Erlotinib, and PTX. A549 cells were exposed to a different concentration of an anticancer agent with 0.78 $\mu$ M BAR002.....	146
Figure 7.7 Viability was measured over 5 days by MTT reduction after DU-145 cells were exposed to different concentrations of BAR002 (closed squares) and or controls (closed circles).....	148

## Chapter I. Introduction

### 1.1 Protein therapeutics

Multiple human proteins have been developed as therapeutic protein drugs since the introduction of recombinant human insulin in 1982.<sup>1</sup> Therapeutic protein drugs have a critical advantage over small-molecule drugs that are currently more dominant in the pharmaceutical market.<sup>2-4</sup> They perform highly specific and complex functions that are not easily mimicked by small molecules.<sup>5-6</sup> For example, some human diseases that were previously not treatable or are characterized by congenital deficiency or acquired loss of a functional endogenous protein (*e.g.* diabetes,<sup>7</sup> dwarfism,<sup>8-9</sup> infertility,<sup>10</sup> chronic renal failure,<sup>11</sup> Gaucher disease,<sup>12-13</sup> and certain cancer types<sup>14-17</sup>) can now be successfully managed by using protein therapeutics.<sup>18</sup> Indeed, protein replacement therapy has been considered a suitable alternative to gene (replacement) therapy for the disease conditions where gene therapy is currently inapplicable to treatment.<sup>19-20</sup> The development of new protein drugs has accelerated the changes in the treatment paradigm of many different diseases.

Natural human proteins were not originally evolved for therapeutic purposes. Therefore, most of them do not have the intrinsic activity, affinity, and/or stability sufficient to treat diseases within patients.<sup>5, 21-23</sup> They usually have a short circulating half-life, low thermal stability at physiological temperature, or suboptimal affinity, which in turn results in limited therapeutic efficacy and frequent dosage.<sup>24</sup> In addition to this, many of them are difficult to produce in large-scale,<sup>25-27</sup> which usually leads to a greatly increased cost of pharmaceutical commercialization.<sup>27</sup> In general, the use of these drugs is limited in routine

clinical practice due to the high cost.<sup>26</sup> Because of these reasons, substantial improvements have been made in the stability, pharmacokinetics, pharmacodynamics, and production yield of multiple human proteins to make them become therapeutically and commercially viable.<sup>14, 28</sup>

## **1.2 Improvement of activity**

Improved versions of human protein therapies can be developed by improving both functionality and efficiency.<sup>34-39</sup> Our increasing understanding of the structural and functional relationship of multiple human proteins to their mechanisms of action enables us to more rationally re-design and engineer them to induce an improved activity or even novel functionality.<sup>29-30</sup> A number of protein engineering strategies are currently in use for not only the optimization of existing therapeutic proteins, but for the introduction of novel protein drugs for specific clinical applications as well.<sup>29-32</sup> Here, I will describe an example of rational modifications to a current protein drug, accomplished by protein engineering, that has resulted in both the development of the next generation of therapeutic proteins and the approval of novel therapeutic proteins for the treatment of other diseases. Human Interleukin 2 (IL-2) is an example of a protein has been genetically modified for clinical use. Proleukin® (Chiron Corporation) was the first recombinant human IL-2 variant produced in *E. coli*.<sup>33-35</sup> This aglycosylated therapeutic protein differs from natural human IL-2 by a substitution of cysteine for serine at position 125 for increased stability and the removal of an N-terminal alanine residue for increased production yield in *E. coli*. The biological activity of Proleukin® was proven similar to that of the wild-type human IL-2,<sup>36</sup> and the drug has been approved by the FDA for treatment of metastatic melanoma and

metastatic renal cell carcinoma.<sup>33, 37</sup> However, it has been reported that high doses of IL-2 utilized for treatment of these types of cancer causes significant toxicity to humans due to its capability to activate natural killer (NK) cells.<sup>38-39</sup> Therefore, in order to reduce toxicity and improve tumor suppressor activity, IL-2 has been further engineered to have an increased binding affinity for its receptor (known as CD25 ) observed on the cell surface of human T cells, but with no increased interaction with IL-2 receptors on NK cells. The discovered high-affinity IL-2 variant has proven considerably more potent in activating human T cells compared to that of the native human IL2.<sup>40-41</sup> This may imply that enhanced T cell activation by the IL-2 analog would permit lower dosage in the clinic and therefore a reduced chance for adverse effects. In addition, fusion of IL-2 to a toxin (*e.g.* Aerolysin,<sup>42</sup> diphtheria toxin,<sup>43-44</sup> Denileukin diftitox (Ontak®)<sup>45-46</sup>) has been developed for other clinical applications such as the treatment of cutaneous T-cell lymphoma expressing high levels of the CD25 component of the IL-2 receptor.<sup>47-48</sup> In this case, IL-2 is used as a homing molecule to deliver a conjugated toxin to the target lymphoma.

### **1.3 Fusion proteins for half-life extension of protein therapeutics**

The therapeutic efficacy of a therapeutic protein drug in the human body also can be greatly increased by improving its pharmacokinetic profile.<sup>28, 49-54</sup> Market pressures for better patient compliance and treatment cost-effectiveness have created a great demand for a therapeutic protein drug whose therapeutic efficacy can be sustained even at long dosing intervals. Because of these reasons, multiple protein engineering platforms have been developed to extend the circulating half-life of a therapeutic protein. Examples of such platform technologies include protein PEGylation<sup>55</sup> and protein fusion with the Fc region

of human IgG1 (IgG Fc)<sup>56-57</sup> or human serum albumin (HSA).<sup>58</sup> These strategies have been the most widely employed to prolong the duration of action of protein therapeutics.

The endothelial cellular neonatal Fc receptor (FcRn) has a critical role in maintaining the high circulating levels of IgG and HSA.<sup>59-60</sup> Indeed, immunoglobulin G has a prolonged circulating half-life of 21 days mainly due to FcRn-mediated recycling that protects against intracellular endocytic-lysosomal degradation.<sup>61-62</sup> Intriguingly, this property is also shared with HSA. IgG Fc or HSA strongly interacts with FcRn in the acidic endosomal compartment (pH 6.0) after being internalized into endocytic vesicles.<sup>63</sup> These receptor-bound proteins are then returned to the cell membrane for extracellular release, whereas other serum proteins in the vascular endothelium are eventually degraded by the endocytic-lysosomal system.<sup>64-65</sup> Fusion to IgG Fc or HSA prolongs the circulating half-life of a therapeutic protein by exploiting the FcRn-mediated recycling mechanism.<sup>66-68</sup>

Interestingly, genetic conjugation to IgG Fc or HSA also provides additional benefits such as increasing both protein production and secretion,<sup>69-70</sup> and enabling simple purification by affinity chromatography.<sup>57, 71-72</sup> A number of Fc- and albumin-fused bio-therapeutics have been approved by the FDA or are currently under development.<sup>73</sup> A significant research effort on engineering the Fc region and HSA for improved pharmacokinetics has demonstrated that enhanced binding affinity at pH 6 for FcRn further extends the biological half-lives of the fusion proteins.<sup>74-77</sup> For example, when a Fc variant with improved FcRn binding affinity was constructed in the context of bevacizumab (Avastin®, Genentech/Roche),<sup>78</sup> a humanized anti-VEGF IgG1 antibody, the Fc engineered antibody showed an approximately three and five-fold extension of the naïve bevacizumab's half-life in human FcRn transgenic mice and a non-primate model,



respectively.<sup>76, 79-81</sup> Inspired by these promising pharmacokinetic bioengineering technologies, we have developed several novel therapeutic proteins with a prolonged duration of action for treatment of cocaine addiction or cancer. These novel therapeutic entities are expected to not only be more protective against elimination by cellular endolysosomal degradation, but also eventually provide greater dosing convenience for treatment.

This thesis research consists of four different projects. The first project is described in Chapter II. In the first project, cocaine hydrolases (CocHs) were engineered to have a prolonged duration of action *in vivo*. Then, I investigated the potential application of a long-lasting CocH for protection against the acute toxicity and stimulant effects of cocaine.

In the second project included in Chapter III, I investigated the potential inhibition of CocH-catalyzed cocaine hydrolysis by heroin (3,6-diacetylmorphine) or its initial host metabolite, 6-monoacetylmorphine (6-MAM). Because heroin is one of the most commonly co-abused drugs by cocaine-dependent individuals, as well as a possible metabolite of CocHs, the investigation of this possible inhibition was important to determine the *in vivo* efficacy of CocHs.

In the third project described in Chapter IV, I expressed and characterized extrahepatic human UDP-glucuronosyltransferase 1A10 (UGT1A10) enzyme, which can inactivate many therapeutically valuable substances including morphine.

In the last project included in Chapter V of this dissertation, prostate apoptosis response-4 (Par-4), a tumor suppressor protein, was genetically engineered to have a prolonged duration of action so that the protein may become more valuable for treatment of metastatic tumor.

## Chapter II. Development of a Long-acting Cocaine Hydrolase for Cocaine Abuse Treatment

Cocaine, a highly pleasurable drug, is well-known for its high propensity to produce dependent behavior as well as physical harm to the users.<sup>82-83</sup> Cocaine use causes two different, but closely related problems; addiction and overdose. Overall purpose of this study is to develop a long-lasting enzyme therapy for treatment of cocaine addiction as well as prevention of cocaine overdose. For this purpose, through a combination of computational and experimental approaches, we have previously developed highly active cocaine hydrolases (CocHs) by engineering butyrylcholinesterase (BChE). Especially, CocH3 is proven to hydrolyze cocaine into biologically and physiologically inactive forms with an approximately 2000-fold higher catalytic efficiency, compared to wild-type BChE. However, according to our pharmacokinetic study of recombinant BChE and CocHs prepared from mammalian expression systems, compared to natural BChE (11 days in human), these recombinant enzymes are estimated to have limited *in vivo* half-lives (2-3 days in human),<sup>84</sup> requiring twice weekly *i.v.* administration to retain its protective anti-cocaine activity in the circulatory system of human.<sup>85</sup>

To date, a number of commercially and clinically successful therapeutic proteins have been generated as a fusion of both protein and the Fc region of immunoglobulin or human serum albumin (HSA). Such fusions provide therapeutic proteins with the IgG or HSA-like property of a long biological half-life as well as several other benefits such as the increasing expression and secretion of the fusion protein and allowing simple purification by affinity chromatography (protein A and ALBUPURE<sup>®</sup> chromatography). In this study,<sup>86</sup> we made the effort to improve the pharmacokinetic (PK) properties and

potency of CocH3 by generating fusion proteins of CocH3 and the Fc region of human IgG1 or HSA. It has been demonstrated that the fusion of CocH3 to our newly designed human Fc variants (Fc(3m), Fc(4m), and Fc(6m)) have a substantially higher binding affinity at pH 6 for human FcRn. These fusion CocHs had an increased half-life of more than 28-fold in rats, compared to unfused CocH3. In addition, it was observed that FcRn-mediated improvement of the enzyme further extended the duration of anti-cocaine activity of CocH3 in the circulatory systems of rats and mice.<sup>87</sup> These results might bridge the gap for enhanced patient dosing convenience with the clinical need of maintaining therapeutic efficacy of CocHs for cocaine addiction treatment. Moreover, the results of our protection experiment demonstrated that pretreatment of rats with 3 mg/kg CocH3-Fc(3m) (*i.v.*) before *i.p.* administration of a lethal dose (60 mg/kg) of cocaine completely blocked physiological effects of cocaine on the brain. The pretreatment of CocH3-Fc(3m) not only fully protected the animals from the hyperlocomotor activity induced by cocaine, but also completely prevented changes in the subcellular localization of dopamine transporter (DAT) from cytosol to the plasma membrane.

A manuscript for the results described in this chapter will be submitted for consideration of publication. Both animal behavior and pharmacokinetic studies described in this chapter were mainly performed by Ting Zhang and Xirong Zheng. Jing Deng prepared the rat brain samples for the DAT distribution assay. The molecular modeling study was performed by Drs. Yanyan Zhu and Yaxia Yuan. Dr. Zhenyu Jin helped me to prepare cocaine hydrolases. Dr. Jinling Zhang contributed to FcRn binding assay. I designed and performed all the rest experimental procedures described in this chapter.

## **2.1 Treatment for cocaine abuse**

### **2.1.1 Cocaine overdose and addiction**

Cocaine is one of the most harmful drugs in the world.<sup>82</sup> According to the 2007 National Survey on Drug Use and Health reports, about 36 million Americans aged above 12 years have abused cocaine at least once in their lifetime. At present, cocaine is the most abused illicit drugs in America and was involved in 40.3% of illicit drug-related visits to hospital emergency departments (EDs) in 2011 within the US.

Cocaine is well known for its euphoric high, physical harm, and high propensity to produce dependence to the users.<sup>83</sup> The physical harm caused by cocaine abuse is primarily attributed to the strong cardiovascular effects of cocaine.<sup>88-93</sup> Cocaine produces the feeling of euphoria by majorly inhibiting the reuptake of dopamine, but it can also act as a norepinephrine (noradrenaline) reuptake inhibitor (NRI).<sup>94-97</sup> In the presence of cocaine, more norepinephrine molecules remain active in the synaptic cleft for a longer than normal duration. This leads to an exaggerated sympathetic nervous system response, imposing a severe strain on the cardiovascular system. Indeed, when the activities of the heart are intensified, a great cardiac need for oxygen and nutrients is created. However, the constriction of capillaries induced by cocaine restricts the flow of blood to the heart muscle. Consequently, the cardiovascular system becomes overburdened and, in the process, cocaine users may encounter life-threatening heart issues such as myocardial infarction (heart attack), and myocarditis (inflammatory cardiomyopathy). In fact, the continual use of cocaine drastically increases the risk for these mentioned conditions as well as several other cardiovascular issues within cocaine-addicted patients.<sup>98-99</sup>

Cocaine is often abused for recreational purposes and can cause serious substance

addiction (AKA, substance use disorder).<sup>100-101</sup> In general, substance addiction is defined as a relapsing and chronic brain disorder that is characterized by uncontrollable and compulsive seeking of a drug, despite the negative health and social consequences associated with their use. Powerful psychoactive molecules such as cocaine and heroin produce a two-part reaction in a user, the rush and high. The “rush” is an immensely intense feeling resulting from the initial and acute psychological effects of a drug, and the euphoric feeling following the rush is named as the “high” which often lasts over a period of several hours after the drug intake.<sup>83</sup> In fact, the psychostimulant effect of a drug is largely dependent on not only its pharmacodynamic efficacy, but also how much of the drug enters into the brain over a short time span. This is why street drugs are usually formulated in ways allowing the users to smoke, snort, or intravenously inject them, and with these introduction methods, effects on the brain can take place within half a minute. The short-term and intensive pleasurable effects of stimulants are closely connected with the high risk for abuse and dependence. Due to this connection, cocaine can induce powerful dependent behaviors within the users.<sup>102-103</sup>

### **2.1.2 Physical and psychological dependence on cocaine**

In general, addiction encompasses both physical and psychological dependence on a substance. Physical reliance is characterized by the adaptive changes occurring within the body in response to the chronic use of a drug. These changes mainly involve increasing tolerance (*i.e.* a progressively increasing dose being required for the same effect).<sup>104-108</sup> For instance, if a long-term or heavy user of cocaine either cuts down or quits taking the drug, physical reliance typically manifests through intense withdrawal reactions (e.g., depression,

diarrhea, tremors, sleeplessness, and sweating) and drug craving. These symptoms are often intolerable, and in the case of untreated or uncontrolled depression, are considered a danger associated with an increased risk of suicide for cocaine addicts admitted to treatment.<sup>109-111</sup> Although there are currently no FDA-approved medications specific for the treatment of cocaine withdrawal, some medications listed in the Table 2.1 have been used to alleviate the withdrawal symptoms, but only during the period of cocaine detoxication.<sup>112-114</sup> In addition, some research also has shown that propranolol,<sup>115-118</sup> buprenorphine,<sup>119-120</sup> and naltrexone<sup>121</sup> might be beneficial for those suffering from cocaine withdrawal.

**Table 2.1** Treatment options for cocaine detox withdrawal symptoms

Medicine	Notes
Gabapentin	A medication prescribed for prevention of seizures. This drug helps to recover feelings of wellbeing by encouraging the release of the GABA.
Modafinil	A medication prescribed to alleviate the fatigue associated with cocaine withdrawal by helping healthy nighttime sleep and increasing dopamine production.
Topiramate	A medication prescribed to ease agitation by decreasing activity in the central nervous system.
Vigabatrin	This drug may alleviate cocaine cravings by encouraging production of GABA.
Baclofen	A medicine prescribed as a muscle relaxant. Baclofen may be utilized to induce the release of GABA in cocaine recovery.

Treatment for psychological dependence on cocaine begins when physical reliance on the drug is addressed by the medically supervised process of cocaine detoxification, allowing the patient's body to re-adjust to the absence of cocaine. Psychological reliance

on a drug is generally defined as a compulsive or perceived need for drug use and is characterized by continual use of a substance without increasing tolerance or the withdrawal symptoms resulting from physical dependence on a drug. In fact, in case of cocaine addition, the developed habitual is driven more by the psychological addiction on the drug than the physical withdrawal symptoms. Research from animal studies and human trials have shown that an intense psychological craving for cocaine is caused by the adaptive changes occurring within the brain due to the continuous presence of the drug.<sup>122</sup> It has been observed that cocaine affects multiple major neurotransmitter receptor systems in the central nervous system (CNS) including the dopaminergic neurotransmission system.

**Table 2.2** The reported neurochemical differences between cocaine addicts and healthy individuals

Neurotransmitter system	Component	Difference compared to healthy individuals	Ref.
Dopaminergic neurotransmission	Dopamine transporter	Increased cell surface availability	123-126
	D <sub>2</sub> receptor	Decreased availability on cell surface	127-129
	VMAT2*	Decreased availability	130-132
Serotonergic neurotransmission	5-HT transporter	Increased expression	133
	Extracellular 5-HT	Increased levels	134
	5-HT <sub>18</sub> receptor	Decreased availability	135
Glutamatergic neurotransmission	Glutamate/creatine ratio	Decreased glutamate levels	136
GABA neurotransmission	GABA	Decreased baseline GABA levels	137

\* VMAT2: Vesicular monoamine transporter type 2

### 2.1.3 Effect of cocaine on dopaminergic neurotransmission

Dopamine is a major neurotransmitter responsible for regulating pleasurable

feelings and the reward system in the brain.<sup>82, 138-141</sup> Once cocaine molecules accumulate in the brain, they proceed to preserve high dopamine levels in the synapse and consequently induce more intense signaling.<sup>142</sup> It is generally believed by scientists that this intensified dopaminergic neurotransmission is directly involved in the pleasurable feelings produced by cocaine.

Importantly, it was demonstrated that there is a frightening trade-off associated with the artificially elevated levels of dopamine in the reward circuits of the brain. Artificially raising dopamine leads to significant changes in the expression of the genes related to dopaminergic neurotransmission, leading to a reduced sensitivity of the dopaminergic reward system to dopamine. Examples of such altered gene expression include the increased cell surface expression of dopamine transporter (DAT) which increases the flux of dopamine through the cell,<sup>143</sup> and the downregulation of dopamine receptors.<sup>122</sup> It was also observed that bringing the changed dopaminergic function back to pre-abuse levels is a very slow process, usually requiring at least a month.<sup>143</sup> As cocaine wears off, fewer dopamine molecules than usual are available in the synapse for signaling due to the accelerated rate of dopamine re-uptake by the previously mentioned increase of cell surface DATs. This substantial reduction in dopamine levels quickly ends the euphoric state and results in craving and intense emotional stress. For example, when the euphoric state ends in drug users, they typically begin to feel empty and may suffer from anxiousness, restlessness, and agitation. This prompts them seek out cocaine to relax or re-achieve the euphoric state. However, this seeking of cocaine may prove fruitless, largely due to the decreased sensitivity of the dopaminergic system.



#### **2.1.4 Relapse**

Relapse is considered the most refractory aspect of substance addiction.<sup>144</sup> Relapse means that a drug-addicted individual makes a conscious decision to abandon his/her recovery plan and return to drug use. The National Institute on Drug Abuse (NIDA) has estimated that approximately 50% of recovering drug addicts undergo relapse. Relapse can occur unexpectedly, but it is typically brought on by triggers. Drug craving is regarded as the main trigger for relapse, which can be triggered by positive reinforcement (i.e., an increased desire to use drug due to its euphoric effects), negative reinforcement (i.e., an increased desire to use drug to alleviate withdrawal symptoms), or environment factors, such as being exposed to stress and drug-related stimuli.<sup>145</sup> Therefore, the main goals of relapse prevention for the drug addicts are to understand the issue of relapse and to learn how to prevent or manage its occurrence during drug rehabilitation.<sup>146</sup>

Technically, drug craving by cocaine-addicts is more attributed to their psychological addiction to the drug.<sup>83</sup> Unfortunately, there are no currently FDA-approved drugs that can specifically treat or manage mental reliance on cocaine. Along with this scarcity of treatment options, the priming effect of cocaine makes it even more difficult to treat cocaine addiction. Exposure to a single dose of cocaine can greatly intensify drug craving behavior and eventually lead to full-blown relapse, no matter how many years of abstinence the patients have achieved.<sup>147-148</sup> It was also observed that the re-use of cocaine after abstinence sharply increases the risk of cocaine overdose in the cocaine-addicted patients due to their reduced tolerance to the drug with duration of abstinence.<sup>149</sup> Considering that cocaine addicts admitted to treatment are still very vulnerable to the temptation to relapse, they should be safeguarded against any exposure to cocaine; not only

to prevent cocaine-primed relapse, but also to protect them against acute cocaine intoxication which potentially happens on their journey from addiction to recovery.

#### **2.1.5 Specific goals to be achieved for treatment of substance abuse disorder**

Technically speaking, there are specific goals to be achieved for treatment of substance abuse disorder.<sup>148</sup> First, withdrawal symptoms should be properly addressed during detoxication process. Second, drug craving needs to be prevented and properly managed. Third, any physiological functions that are affected by drug use (*e.g.* the function of the brain's communication system) must be nurtured back to a more normal state. Finally, and most importantly, the stimulant effects of a drug of abuse must be antagonized during addiction recovery process.

However, in reality, it may be impractical to expect that all of these requirements for addiction treatment can be accomplished separately. Since cocaine addicts admitted to treatment are susceptible to the temptation to relapse, the lack of treatment options for drug craving may make it difficult to successfully complete a painful and time-consuming process of physiological re-adaptation to the absence of cocaine. As mentioned above, the repeated use of cocaine leads to the adaptive changes related to a state of abnormal physiological functioning in the user's body and brain, which makes a major contribution to drug craving behavior. Therefore, to achieve a better outcome in the treatment of cocaine addiction, it seems necessary to first completely block the physiological effects of cocaine in the body so that the reinforcing action of the drug can be decreased for a sufficiently long period of time required to achieve long-term extinction of the drug-craving behavior.

For the treatment of cocaine abuse, considerable research effort has been focused

on development of pharmacological agents which target the major neurotransmitter transporter/receptor systems affected by cocaine (*e.g.* dopaminergic, GABAergic, serotonergic, and glutamatergic systems).<sup>148, 150-151</sup>

**Table 2.3** Drugs in phase II clinical trials for cocaine addiction

Neurotransmitter system	Name	Ref.
Dopaminergic drugs	Amphetamine	152-154
	Modafinil	121, 155-160
	Ropinirole	161-163
	Levodopa	155, 163
	Aripiprazole	164-167
Glutamate/GABA drugs	Topiramate	167-174
	Baclofen	175-176
Noradrenergic drugs	Doxazosin	177-179
	Propranolol	180-183

Although phase II clinical trials using the therapeutic compounds above have produced promising results, over the last three decades, the traditional pharmacological approaches for cocaine addiction treatment have not yet yielded a single treatment which is both safe in human use and effective for treatment. This difficulty is mainly due to several reasons as follows.<sup>149, 151, 184</sup> First, the target-based, therapeutic small molecules are designed to act at the sites of action of cocaine to antagonize the effects of the drug. However, given that cocaine affects multiple neuromodulatory systems in the CNS, targeting just one or several neurotransmitter systems for treatment might not be enough for actual recovery from cocaine addiction. In addition, the current limited understanding of the neuropharmacological mechanisms influenced by the stimulant action of cocaine

makes it more difficult to antagonize the effects of the drug. Second, many therapeutic lead compounds for possible treatments of cocaine addiction have safety issues mainly due to their high abuse potential. Due to the mechanism of these drugs targeting neuro-communication system, they generally risk the possibility of being abused. Third, many drug candidates in clinical trials have displayed inappropriate pharmacokinetic properties for human use although they have proven very effective in preclinical studies.

#### **2.1.6 Pharmacokinetic approach for cocaine abuse treatment**

In view of these difficulties, a new treatment strategy that directly targets and inactivates cocaine has received increasing clinical attention.<sup>82</sup> This pharmacokinetic (PK) strategy aims to keep cocaine below its threshold concentration required to induce any physiological effect at its sites of action. Indeed, this anti-cocaine effect is expected to be beneficial in three clinical contexts. First, the chance of acute cocaine intoxication may be substantially decreased or completely prevented due to the altered distribution of cocaine and the acceleration of its clearance. Second, the cocaine-addicted patients on an effective anti-cocaine treatment may also be protected from experiencing the reinforcing effects of cocaine, which are required to reduce the chances of relapse primed by cocaine. Considering the long-term anti-cocaine effect, the patients would also have a better opportunity to naturally recover their damaged neuromodulatory systems. Third, long-term cocaine abstinence achieved by the PK strategy might also facilitate the physiological re-adaptation to the absence of the drug by preventing cocaine actions in peripheral tissues.

Pharmacokinetic approaches for cocaine addiction treatment can be achieved by either using a cocaine-specific antibody or through an efficient cocaine-hydrolyzing

enzyme. In general, these protein-based PK agents are not expected to result in the same side effects seen with therapeutic small molecules targeting the neurotransmitter transporter/receptor systems in the CNS. This is because they barely cross the BBB to reach the CNS. Both types of PK agents have proven effective for preventing the rapid distribution of cocaine molecules into the CNS after drug intake in both pre-clinical and clinical studies.<sup>185-189</sup> However, using an efficient cocaine-hydrolyzing enzyme has a theoretical, but critical, advantage over antibody-based approaches (active and passive immunization) in that it would be very difficult for the cocaine-addicted patients to increase drug intake sufficient to overwhelm the therapeutic effect of efficient cocaine-hydrolyzing enzyme. This is in contrast to the therapeutic antibodies which could be possibly saturated by cocaine molecules allowing most of the drug to remain free and available for action.

### **2.1.7 Enzyme-based therapy for cocaine abuse**

In our previous studies, we (our lab at the University of Kentucky) have designed and discovered high-activity butyrylcholinesterase (BChE) mutants, also known as cocaine hydrolases (CocHs), that can rapidly convert naturally occurring, biologically active (–)-cocaine to physiologically inactive metabolites ecgonine methyl ester (EME) and benzoic acid. In particular, the first one of our designed CocHs (denoted as CocH1), *i.e.* the A199S/S287G/A328W/Y332G mutant, demonstrated a ~1000-fold improved catalytic efficiency against (–)-cocaine compared with the wild-type BChE ( $k_{\text{cat}} = 4.1 \text{ min}^{-1}$  and  $K_M = 4.5 \text{ }\mu\text{M}$ )<sup>190-191</sup> and an effectiveness as an enzyme or gene therapy for cocaine abuse treatment without significant adverse effects in animal experiments.<sup>192-195</sup>

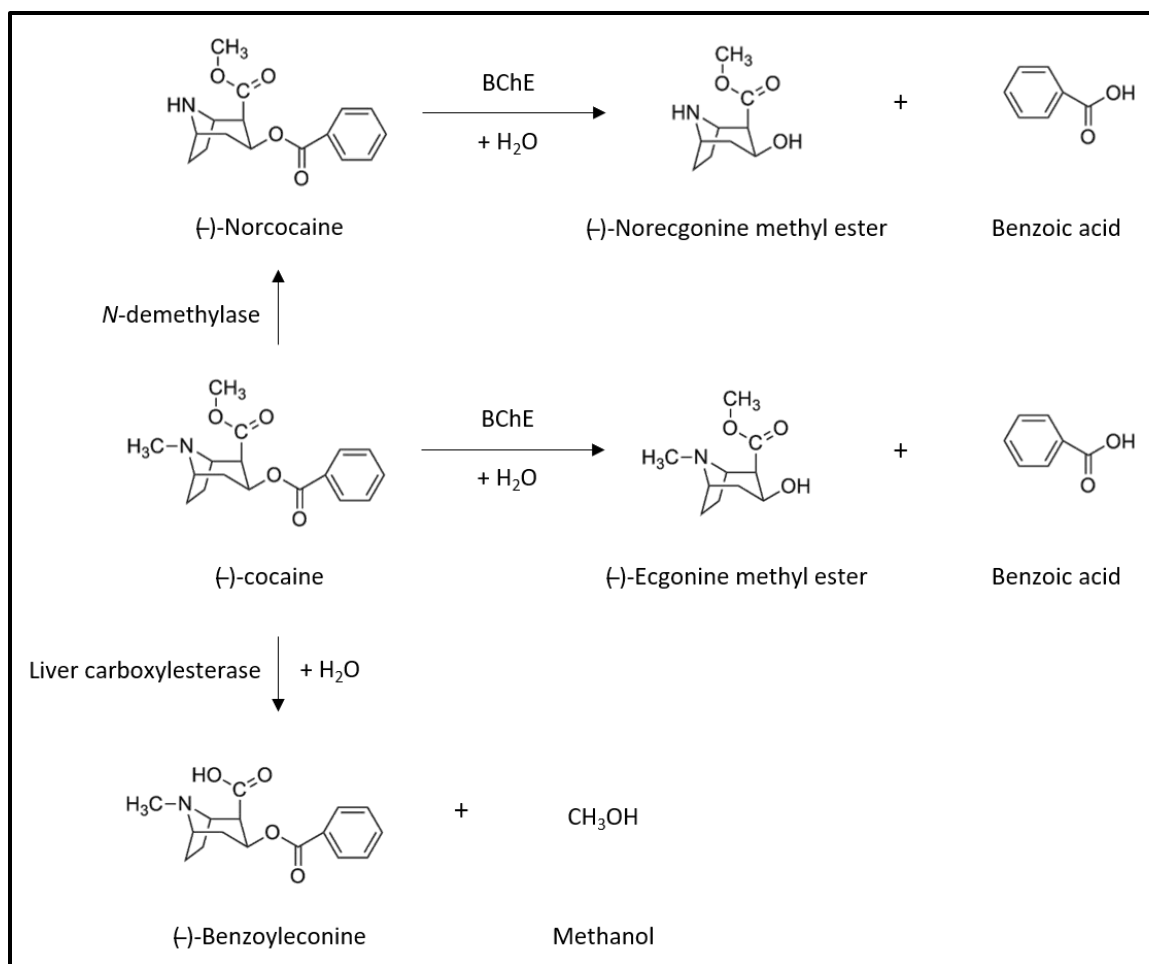


**Figure 2.1** Cocaine metabolic pathways in physiological condition.<sup>196-197</sup>

Further, CocH1 truncated after amino acid 529 was fused with human serum albumin (HSA) to prolong the biological half-life without changing the catalytic activity of CocH1 against cocaine.<sup>198</sup> The HSA-fused CocH1 (known as Albu-CocH, Albu-CocH1, AlbuBChE or TV-1380 in the literature) has been proven safe and promising for use in animals and humans in preclinical and clinical studies.<sup>84, 199</sup> However, its actual therapeutic value for cocaine addiction treatment is limited by an insufficiently long biological half-life (~8 h in rats<sup>198</sup> or 43-77 h in humans<sup>84</sup>). Recently, a Phase II clinical trial of TV-1380 for cocaine addiction treatment did not show statistically significant efficacy with the once-

weekly dosing schedule due to its relatively short biological half-life.<sup>85</sup> Nevertheless, it has been concluded that “*Although the continued development of TV-1380 appears unlikely, its promising clinical profile should embolden efforts to develop new enzyme products that are capable of delivering greater catabolic activity*”<sup>85</sup> in order to be effective with the desirable once-weekly dosing schedule for cocaine addiction treatment. Our most recently reported studies in various animal models of cocaine overdose treatment show that Albu-CocH1 (or TV-1380) itself would be more appropriate for cocaine overdose treatment.<sup>200-201</sup>

## **2.2 The focuses of this research**

In order to meet the requirements to be an effective enzyme therapeutic for cocaine addiction, CocH1 has further engineered so that the next generation of CocHs have even higher catalytic activity compared to that of CocH1 and, more importantly, have a sufficiently long biological half-life for human cocaine addiction treatment. Indeed, a growing body of preclinical data including our animal study results have shown that the catalytic efficiency of a cocaine-metabolizing enzyme is a major factor determining the efficacy in protecting animals against acute cocaine intoxication and reinstatement (equivalent to relapse within humans) provoked by the cocaine priming effect. Therefore, to deliver greater catabolic activity to human body, our research group has made effort on development of the next generation of CocHs whose cocaine-hydrolyzing activities are substantially higher than that of CocH1 (Table 2.4). At the same time, for the same reason, CocHs whose biological half-lives are sufficiently long for human cocaine addiction treatment are currently under development. In this chapter, I described our efforts to develop novel CocH entities with a prolonged duration of action.

**Table 2.4** The new generation of CocHs with an improved catalytic efficiency against cocaine

<sup>a</sup> Relative catalytic efficiency ( $k_{\text{cat}}/K_M$ ).

Enzyme	$k_{\text{cat}}$ ( $\text{min}^{-1}$ )	$K_M$ ( $\mu\text{M}$ )	RCE <sup>a</sup>	Ref.
BChE wt	4.1	4.5	1	
CocH1 (A199S/S287G/A328W/Y332G)	3060	3.1	1080	190
CocH2 (A199S/F227A/S287G/A328W/E441D)	1730	1.1	1800	202
CocH3 (A199S/F227A/S287G/A328W/Y332G)	5700	3.1	2020	203
CocH5 (A199S/F227A/P285A/S287G/A328W/Y332G)	14600	3.7	4400	204
CocH6 (A199S/F227S/P285Q/S287G/A328W/Y332G)	15500	3.1	5500	US Patent # 9365841

## 2.3 Results & Discussion

### 2.3.1 Insights from molecular modeling

Molecular modeling studies were performed in our lab to study how neonatal Fc receptor (FcRn) binding with human IgG1 Fc variants<sup>205</sup> and the corresponding fusion proteins. Through the modeling studies, the relative binding affinities of various fusion proteins with the FcRn at pH 6 were estimated. Based on the computationally estimated binding affinities, several Fc variants, including Fc(3m), Fc(4m), and Fc(6m) (as indicated below), were predicted to have significantly improved binding affinities with the FcRn. Hence, the experimental studies described below were focused on these Fc variants.



### **2.3.2 Characterization of CochH3-fused with human IgG1 Fc variants**

Altered binding to FcRn can lead to significant changes in the biological half-lives of therapeutic protein drugs (*e.g.* therapeutic antibodies, and HSA- or Fc-fused biotherapeutics) in both humans and animals. Therefore, it is interesting to characterize their binding affinities with FcRn from clinically relevant species (human, monkey, rat, and mouse). This *in vitro* analysis helps predict whether positive results obtained from the pharmacokinetic studies in animal models can be translated and applied when utilized in human clinical trials.

In this study, we generated a comprehensive data set on the binding of Fc-fused CochH3 proteins with FcRn proteins from four different species (human, monkey, rat, and mouse) and these results can be utilized to predict whether the increased FcRn binding affinity of CochH3 translates to pharmacokinetic benefit in nonhuman primates or humans.

#### ***2.3.2.1 Design and expression of FcRn as a single-chain like fusion protein***

The neonatal Fc receptor (FcRn) was first discovered as the receptor which is responsible for the transfer of maternal Immunoglobulin Gs (IgGs) from breast milk to babies across their intestinal epithelial cells. FcRn also enables maternal IgGs to cross the materno-fetal barrier during pregnancy.<sup>206</sup> This cell surface protein consists of two protein subunits, a transmembrane alpha chain (denoted as heavy chain for convenience) and a beta 2 microglobulin (B2M), these subunits non-covalently interact with each other at a 1:1 molar ratio. Currently, FcRn has received increased clinical attention because of its pivotal role in regulating the homeostasis of IgG and albumin in mammals through its distinctive pH-dependent physical interaction with specific serum proteins. Indeed, the Fc

region of IgG or albumin strongly interacts with FcRn at a slightly acidic condition, but the formed complex is easily dissociated at the physiological pH.<sup>207</sup> With the help of this unique binding feature of FcRn, the IgG and albumin captured in endosomes can escape from cellular endolysosomal degradation and eventually be returned to the circulatory system for reuse.<sup>208-210</sup> In functional FcRn-deficient ( $\beta 2m^{-/-}$ ) mice, it was observed that both the serum half-life and endogenous level of IgG substantially decrease by a factor of about 6 and 10, respectively,<sup>211</sup> and the lifespan of albumin also shortened significantly.<sup>212-213</sup> This clearly indicates the importance of FcRn for the long serum persistence of both IgG and albumin. Added to this, many studies have shown that this specific function of FcRn is well conserved across different species including human,<sup>214</sup> monkey,<sup>215-217</sup> rat,<sup>218</sup> mice,<sup>211, 219-220</sup> and even chickens.<sup>221</sup>

Currently, there is a large market pressure for a treatment that both improves patient convenience and compliance *via* a less frequent dosing schedule of a therapeutic protein drug.<sup>77</sup> Because enhanced binding affinity to FcRn at a certain range can greatly improve the pharmacokinetic profile and therapeutic efficacy of a protein drug,<sup>56-57</sup> much of the research effort has been spent on the engineering of these protein drugs (*e.g.* therapeutic antibodies and HSA- or Fc-fused bio-therapeutics) to increase their FcRn binding affinities. However, these attempts were limited due to the difficulty of obtaining the required amount of functional FcRn proteins for use in the binding affinity assays.

Many different methods have been employed for the large-scale production of soluble functional FcRn. In previous studies, two genes encoding each of the different subunits of FcRn, a C-terminal transmembrane domain truncated heavy chain variant and the wild-type B2M, were frequently co-expressed in mammalian or insect cells and the

resultant heterodimer complexes secreted into the culture medium were then purified.<sup>77, 214,</sup>  
<sup>220</sup> This type of soluble FcRn protein was proven fully functional in binding to antibody or albumin, and have been widely used to improve our understanding of FcRn itself and its interaction with IgG or albumin. However, there is an unresolved issue in this approach. The heavy chain variant is not as strongly expressed in both insect and mammalian systems, whereas B2M is highly produced, which restricts the overall production yield of functional FcRn. As an alternative approach to the large-scale production of soluble FcRn, the receptor was also expressed in *Pichia pastoris* (a species of yeast),<sup>222</sup> and *E. coli*.<sup>223</sup> However, against all expectations, the FcRn protein expressed in *Pichia pastoris* was not glycosylated and *E. coli*-derived FcRn proteins formed inclusion bodies in the cytoplasm.<sup>209, 224</sup>

Recently, it was reported by Yang Feng *et. al.* that soluble, fully-functional human FcRn can be expressed in mammalian cells as a single fusion protein.<sup>206</sup> The B2M was genetically conjugated to the N-terminus of the transmembrane domain truncated heavy chain variant through a short amino acid linker. The generated soluble single-chain FcRn (sFcRn) was not only highly expressed in mammalian cells, but also could be easily purified through simple affinity chromatography *via* its C-terminal hexa-histidine tag. In addition, the purified sFcRn proteins were also fully functional.

Inspired by the design of the soluble human FcRn reported by Yang Feng *et. al.*,<sup>206</sup> multi-species FcRn proteins (human, monkey, rat, and mouse) were designed to be expressed as a soluble single-chain protein in the present study. The designed sFcRn genes were expressed and purified as described below. As shown in Fig. 2.2, the N-terminal sequence for the leader peptide of B2M was first replaced with the leader peptide sequence

of mouse Ig kappa-chain to facilitate the secretion of the fusion proteins from the cytosol to the extracellular space. Both the signal peptide and transmembrane domain of the corresponding heavy chain were excluded from the design of the new fusion genes. Then, a mature B2M sequence was genetically conjugated to the N-terminus of the mature sequence of its corresponding heavy chain *via* a flexible amino acid linker ((GGGGS)<sub>3</sub>). A hexa-histidine tag (Hisx6) was introduced at the C-terminal end of all the fusion gene when they were synthesized by GenScript to simplify the protein purification process.

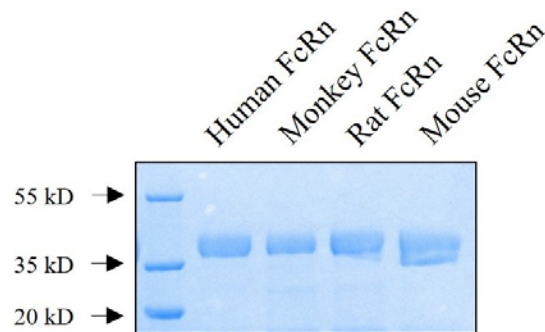
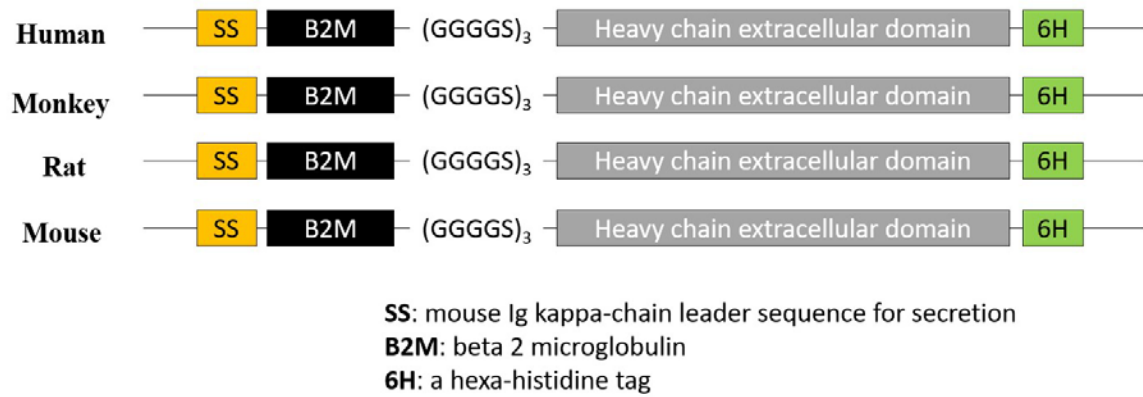


**Figure 2.2** Schematic presentation of the soluble single-chain FcRn proteins of different species.

Each fusion gene was cloned into a mammalian expression vector, pCMV-MCS. The fusion proteins were expressed in 293 FreeStyle cells (293FS), an engineered HEK293 cell-line, and then purified by immobilized metal ion affinity chromatography.

### 2.3.2.2 Preparation of Fc-fused CocH3 proteins

For the extension of biological half-life, CocH3 truncated after amino acid 529 was fused with either the wild-type Fc region of human IgG1 (*i.e.* CocH3-Fc) or the IgG1-Fc variants (*i.e.* CocH3-Fc<sub>(v)</sub>) that we designed. (Fig. 2.2) These proteins were expressed and purified as described below.

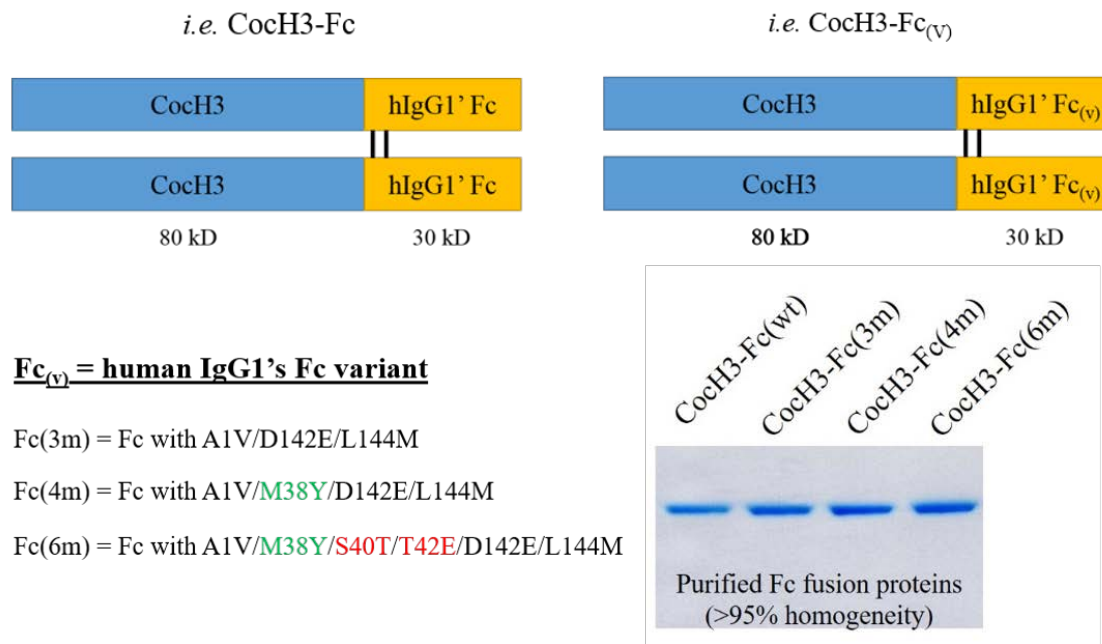


**Figure 2.3** Schematic presentation of the newly designed Fc-fused CocH3 proteins.

### 2.3.2.3 Binding affinity of Fc-fused CocH3 toward different FcRn

To identify the Fc-fused CocH3's increased binding affinity toward human FcRn, and to examine whether the selected enzyme also shows increased binding affinity for FcRn

of other preclinical species (monkey, rat, and mouse), we investigated the interaction of different Fc-fused Coch3 proteins with these FcRn proteins. The FcRn binding was analyzed by ELISA. Results are summarized in Table 2.5. The determined  $K_D$  value of Coch3-Fc toward human FcRn is in good agreement with the values determined by others for the binding of the wild-type human IgG1.<sup>75, 225</sup>

As expected, the six amino acid substitutions (A1V/M38Y/S40T/T42E/D142E/L144M) introduced into the Fc portion of Coch3-Fc greatly increased the affinity of the fusion protein toward human and monkey FcRn at pH 6.0, approximately 48- and 45-fold, respectively. However, the same increase in affinity was not seen toward mouse FcRn with only a 9-fold increase. It is likely that this difference is mainly attributed to the innate high affinity of human Fc to mouse FcRn. Interestingly, it was also observed that the affinities for the binding of Fc-fused Coch3 proteins to monkey FcRn are almost the same as with human FcRn, which strongly suggests that all the newly designed six residues interact with human and monkey FcRn at pH 6.0 in a very similar manner.

In addition, we observed that none of the Coch3-Fc<sub>(v)</sub> proteins have higher binding affinity for rat FcRn than Coch3-Fc. However, Coch3-Fc(4m) and Coch3-Fc(6m) show significantly increased affinity for rat FcRn, compared with Coch3-Fc with A1V/D142E/L144M (*i.e.* Coch3-Fc(3m)). These results suggest that the introduction of A1V/D142E/L144M into the Fc portion negatively affects the binding of Coch3-Fc to rat FcRn at pH 6.0. Indeed, previous reports already show that rat FcRn has strong binding affinity at pH 6.0 for different subclasses of human IgG including IgG1 and IgG2 ( $K_D$  = 35 and 20 nM, respectively)<sup>216, 226</sup> and rat FcRn retains significant binding with human IgG1 even at neutral pH ( $K_D$  = 1389 nM).<sup>226</sup>

**Table 2.5** Summary of determined equilibrium dissociation constants ( $K_D$ ) of interaction of Fc-fused CochHs with FcRn (at pH 6.0, (nM))

Fc-fused CochH3	Neonatal Fc receptor (FcRn)			
	Human	Monkey	Rat	Mouse
CochH3-Fc(wt)	~ 2500	~ 2500	$37.46 \pm 7.07$	$95.65 \pm 13.22$
CochH3-Fc(3m)	$991.6 \pm 24.7$	$1004 \pm 165$	$159.40 \pm 6.40$	$50.73 \pm 10.25$
CochH3-Fc(4m)	$326.9 \pm 14.6$	$325.2 \pm 18.6$	$61.29 \pm 6.90$	$11.96 \pm 2.62$
CochH3-Fc(6m)	$52.14 \pm 3.54$	$56.65 \pm 5.09$	$50.74 \pm 4.89$	$10.06 \pm 1.55$

Results are representative of three independent experiments and each experiment was performed as triplicate. The values are expressed as mean  $\pm$  S.D.

### 2.3.3 Determination of biological half-life in rats

To examine whether enhanced binding affinity at pH 6 for FcRn improves the biological half-life of Fc-fused CochH3, a pharmacokinetic (PK) study was carried out in rats (*Rattus norvegicus*). The *in vivo* data were based on intravenous (*i.v.*) injection of the enzymes in the tested animal model. The generated PK data are depicted in Fig. 2.4 and the biological half-lives obtained are summarized in Table 2.6. The results clearly show that the fusion proteins of the truncated CochH3 (without the tetramerization domain) to the N-terminus of the Fc portion of IgG1 have substantially longer biological half-lives (up to ~200 h) than that (~7 h) of the full-length CochH3, denoted as CochH3 in Fig. 2.4. Among the Fc-fused CochH3 proteins tested here, CochH3-Fc with A1V/M38Y/D142E/L144M (*i.e.* CochH3-Fc(4m)) displays the longest biological half-life (~200 h) in rats and the introduction of these

four mutations increases the biological half-life of Coch3-Fc more than 2-fold. Coch3-Fc(6m) also has a long biological half-life comparable to that of Coch3-Fc(4m), but the A1V/D142E/L144M mutations of Fc(4m) extend the biological half-life of Coch3-Fc only by ~23 h, suggesting that the M38Y on the Fc region plays a critical role in interaction with rat FcRn at pH 6.0.

Intriguingly, it was also observed that Coch3-Fc does not show the longest biological half-life despite of its strongest rat FcRn binding affinity, which suggests that some other factors such as the delayed release of Coch3-Fc at neutral pH or its relatively low thermal stability might have negative effects on the serum persistence of Coch3-Fc in rats. Indeed, it was previously reported that extended serum persistence of human IgG due to the benefits of increased FcRn binding at pH 6.0 can be offset by increasing neutral pH FcRn affinity in rats.<sup>75</sup>

Considering that Coch3-Fc(6m) rather than Coch3-Fc(4m) shows substantially higher binding affinity toward both human and monkey FcRn, there may be a good possibility that Coch3-Fc(6m) has a much longer biological half-life in a following animal study using monkeys and human clinical trials, compared to Coch3-Fc(4m).



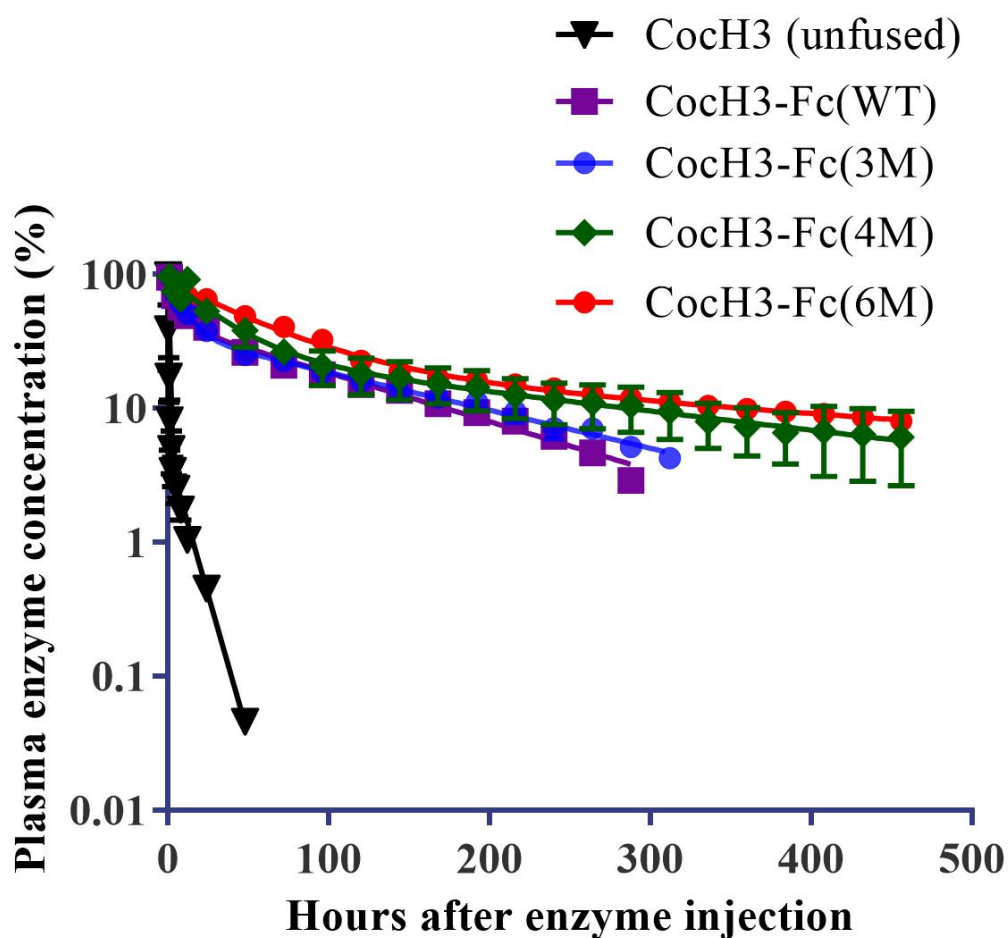


**Figure 2.4** Serum concentration (%) *versus* time profiles of Fc-fused CocH3 proteins in rats. All enzymes were administered *via i.v.* infusion at 0.06 mg/kg body weight and the serum concentrations of Fc-fused CocH3 were determined by a sensitive radiometric assay using [ $^3\text{H}$ ](–)-cocaine. Results are shown as mean  $\pm$  standard error. Other lab members (Ting Zhang and Xirong Zheng *et al.*) kindly provided the data for this figure.

**Table 2.6** The determined distribution and biological half-lives of Fc-fused Coch3 proteins in rats in comparison with the unfused Coch3 in rats. The parameters were obtained from fitting to the well-known double-exponential equation<sup>227</sup> by GraphPad Prism 7.04:  $([E]_t = Ae^{-k_1t} + Be^{-k_2t})$  which accounts for both the enzyme distribution process (the fast phase, associated with  $k_1$ ) and elimination process (the slow phase, associated with  $k_2$ ). The half-life ( $t_{1/2}$ ) associated with the enzyme elimination rate constant  $k_2$  is known as the elimination half-life or biological half-life.

Protein	Distribution $t_{1/2}$ (hr)	Biological $t_{1/2}$ (hr)
Coch3	0.2	7
Coch3-Fc(wt)	4.9	85
Coch3-Fc(3m)	6.4	107
Coch3-Fc(4m)	23	218
Coch3-Fc(6m)	35	222

#### **2.3.4 Effectiveness of Coch3-Fc(3m) in blocking the striatal dopamine transporter trafficking induced by cocaine**

Dopamine is a monoaminergic neurotransmitter which mediates a number of brain activities including reward, emotion, learning, and motivation.<sup>228</sup> The dopamine transporter (DAT) is a key determinant of the level of synaptic dopamine. DAT pumps excess dopamine molecules from the synaptic cleft back into presynaptic neurons when it is expressed on their cell surface, and in turn terminates the signal of the neurotransmitter.<sup>229</sup> It has been demonstrated that different DAT substrates or inhibitors such as cocaine facilitate the translocation of DAT from cytosol to cell surface for an increased function.

The altered surface expression or malfunction of human DAT (hDAT) is well-known to be a major cause of psychiatric and neurological disorders such as clinical depression, bipolar disorder, and substance use disorder, also known as drug addiction,<sup>230-231</sup> thus hDAT has been a clinically valuable target for the treatment of these serious brain diseases.<sup>232-234</sup>

Cocaine is believed to produce the feeling of euphoria by primarily inhibiting DAT in the central nervous system. Many pre-clinical and clinical studies have shown how altered DAT function contributes to substance use disorder. For example, exposure of brain to a psychoactive stimulant like cocaine leads to a rapid increase in the extracellular fluid (ECF) levels of dopamine<sup>235-237</sup> and in turn increases in the reuptake of dopamine.<sup>238-239</sup> These immediate effects of cocaine on the brain consequently cause the reduction of sensitivity of the brain to dopaminergic neurotransmission, which contributes to the drug craving. Indeed, the facilitated dopamine reuptake after exposure to cocaine is mainly attributed to the increasing cell surface expression of DAT and cocaine is proven to rapidly and strongly induce the trafficking of dopamine to cell surface in both DAT expressing cells and brain.<sup>128, 240-242</sup> In addition, it has been observed that the changed dopaminergic neurotransmission especially in the specific brain regions related to the reward circuits (*e.g.* striatum and nucleus accumbens) is more closely associated with drug abuse potential.<sup>141,</sup>

243-244

To exam whether the pretreatment of rats with 3 mg/kg CocH3-Fc(3m) (*i.v.*) before the *i.p.* administration of cocaine efficiently protects rats from the physiological effects of the drug on the brain, we performed a DAT cell redistribution assay.

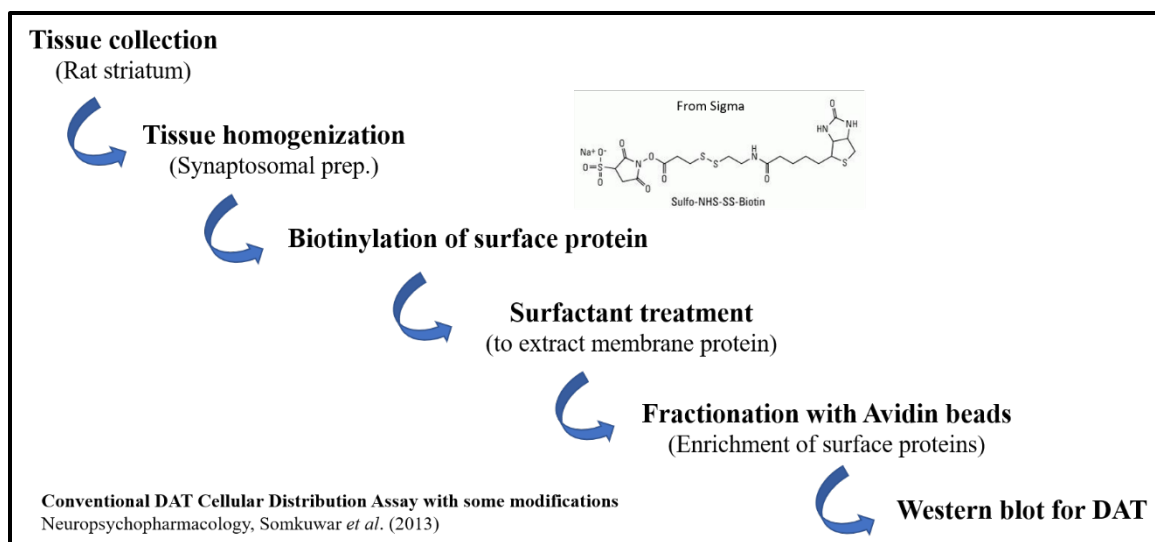


**Figure 2.5** The schematic presentation of DAT cellular distribution assay.

As shown in Fig. 2.6, most DAT proteins were observed in the non-biotinylated fraction of the striatal synaptosomes prepared from both the saline controls and the enzyme control without the cocaine injection. Considering that synaptosomes are an isolated synaptic terminal from a neuron, these findings implicate that the majority of DAT is originally located within the intracellular space of synaptic neurons and the *i.v.* administration of 3 mg/kg CocH3-Fc(3m) lead to no significant change in the subcellular localization of the transporter. Importantly, it was also observed that the pretreatment of CocH3-Fc(3m) (3 mg/kg *i.v.*) 3 min prior to a lethal dose of cocaine (60 mg/kg *i.p.*) not only saves all the rats tested from acute cocaine intoxication, but also completely blocks the DAT trafficking-induced by the lethal cocaine dose. This may indicate that the accelerated cocaine clearance achieved by the enzyme is able to suppress cocaine below its threshold concentration in the body ( $0.22 \pm 0.07 \mu\text{M}$ ) required to elicit physiological effects.<sup>245</sup>

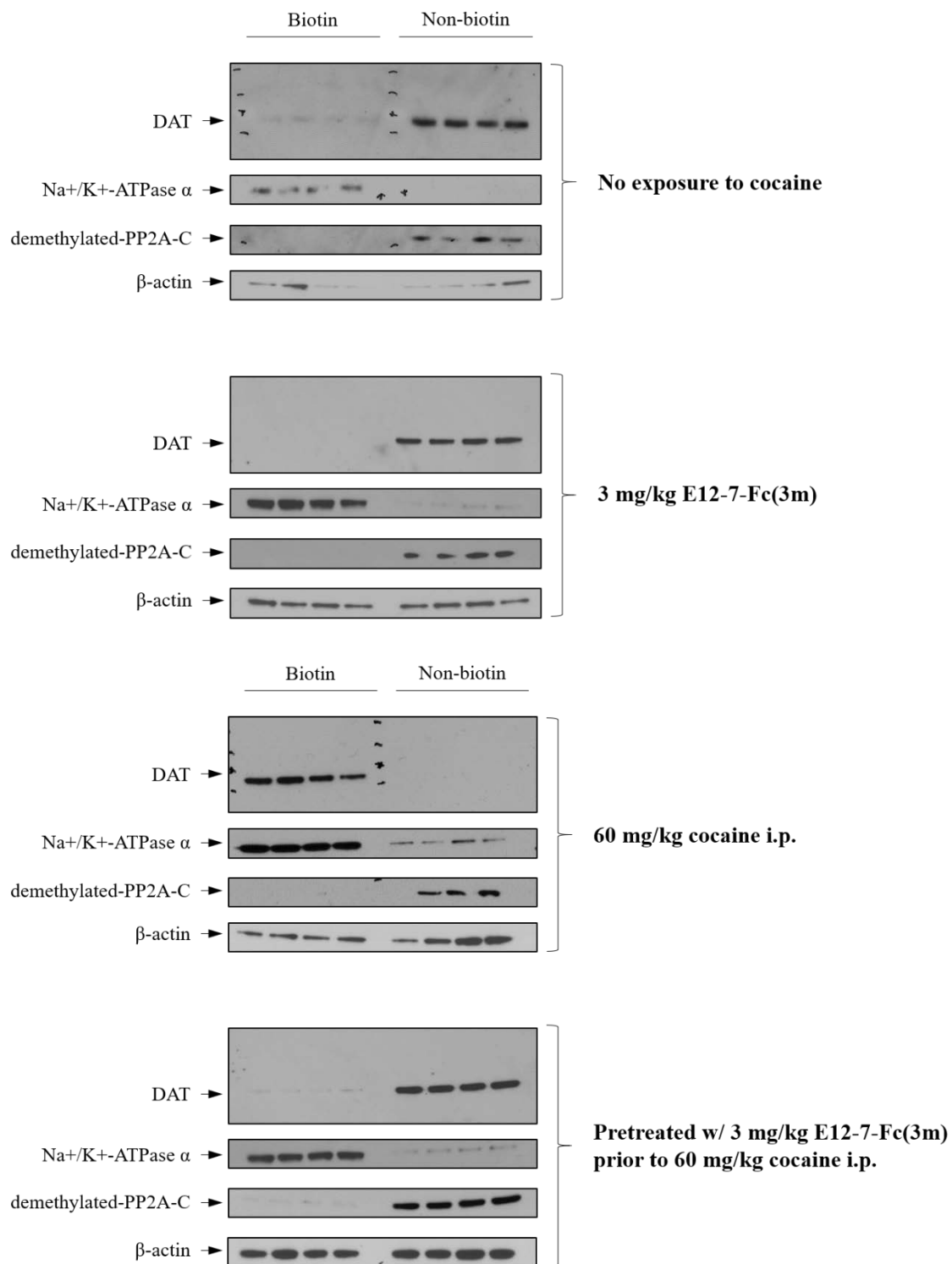


**Figure 2.6** The cell surface distribution of dopamine transporter (DAT) in the striatum of adult rats. Saline or 3 mg/kg CocH3-Fc(3m) was injected *i.v.* in rats (n = 4), 3 min before *i.p.* administration of a dose of cocaine (60 mg/kg). Representative blots for DAT distribution between biotinylated (Biotin; cell surface) and non-biotinylated (Non-biotin; intracellular) fractions in striatal synaptosomes from the rats. Na<sup>+</sup>/K<sup>+</sup> ATPase and demethylated-phosphatase A (demethylated-PP2A-C) were used as a marker for membrane protein and cytosolic fraction, respectively. These markers were served to ascertain the biotinylation efficiency of surface proteins whereas  $\beta$ -actin was used as a loading control.

## **2.4 Experimental details**

### **2.4.1 Materials & Animals**

(-)-Cocaine was kindly provided by the National Institute on Drug Abuse (NIDA) Drug Supply Program (Bethesda, MD) and radioactive [ $^3\text{H}$ ]( $-$ )-Cocaine was obtained from PerkinElmer (Waltham, Massachusetts). All other chemicals were ordered from Sigma-Aldrich (St. Louis, MO) and Thermo Fisher Scientific (Waltham, MA). Male Sprague-Dawley rats (220–250 g) were purchased from Harlan (Harlan, Indianapolis, IN). All the animal experiments were performed in a same colony room in accordance with the Guide for the Care and Use of Laboratory Animals as adopted and promulgated by the National Institutes of Health. The animal protocol was approved by the IACUC (Institutional Animal Care and Use Committee) at the University of Kentucky.

### **2.4.2 Construction of gene expression plasmids**

For recombinant lentiviral packaging to generate stable cell lines expressing the gene of interest, the C-terminal of truncated CocHs were first genetically fused to the N-terminal of the Fc portion of wild-type human IgG, a Fc variant, or the wild-type HSA by overlapping extension PCR with Phusion DNA polymerase. Then, the PCR products were digested with restriction endonucleases Hind III and XbaI. The gel purified PCR products were then ligated to the pCSC lentiviral vector using T4 DNA ligase. The resulting DNA constructs were used for the following recombinant lentiviral packing experiment (2.4.3).

### **2.4.3 A recombinant lentiviral packaging system for stable cell generation**

To package the recombinant lentivirus particles carrying the gene of Fc- or HSA-

fused Coch3, 293FS cells were cultured and prepared in DMEM medium containing 10% Fetal Bovine Serum (FBS) (Life Technologies). When the cell reached 70% confluence, a lentivirus plasmid encoding the gene of interest was transfected into the cell with the two packaging vectors (pMDLg/pRRE and pRSV-Rev) and one envelope plasmid (pCMV-VSV-G) by lipofection at a mass ratio of 10:6.5:2.5:3.5. For transfection of 293FS cells in a 10 cm dish, those DNA plasmids (approximately 22.5 µg in total) were first mixed with 1 ml of Opti-MEM® (Life Technologies) without serum. 25 µl of the TransIT-PRO Transfection Kit (Mirus Bio LLC, Madison, WI) was then gently mixed with the medium followed by incubation at RT for 10 min. The transfection complex was carefully added to the cell in a dropwise manner and the cells were incubated at 3% CO<sub>2</sub> at 37°C. 16 h after transfection, the culture medium was exchanged with a fresh complete medium. From this point, the culture medium was replaced with a fresh complete medium and collected every following 24 h for three days. The collected media were then filtered through a 0.45-µm cellulose acetate filter followed by ultra-centrifugation in Beckman SW28 rotor at 800,000 × g for 1.5 h at 4°C to obtain the pellet of the recombinant lentiviral particles. The resulting pellet were then suspended in Hank's balanced salt solution and freshly utilized for generation of stable CHO-S cells. The lentivirus titration was performed using QuickTiter™ lentivirus rapid quantitation kit (Cell Biolabs, San Diego, CA).

#### **2.4.4 Transient expression and purification of soluble single-chain FcRn (sFcRn)**

The DNA sequences of the beta 2 microglobulin chain (B2M) and heavy chain (AKA, Fc fragment of IgG receptor and transporter) of FcRn are based on the reported sequences in the GenBank database (National Center for Biotechnology Information)



(Table 2.4) and codons were optimized for expression in HEK293 cells.

**Table 2.7** The referred DNA sequences for FcRn expression

<b>Species (Binomial name)</b>	<b>B2M</b>	<b>heavy chain</b>
Human ( <i>homo sapiens</i> )	NM_004048	NM_004107
Monkey ( <i>Macaca fascicularis</i> )	NM_001284689	NM_001284551
Rat ( <i>Rattus norvegicus</i> )	NM_012512	NM_033351
Mouse ( <i>Mus musculus</i> )	NM_009735	NM_010189

FcRn proteins from clinically relevant species (human, monkey, rat, mouse) were expressed as a single chain-like fusion protein. Briefly, the highly hydrophilic B2M was genetically inked to a transmembrane domain truncated variant of the heavy chain *via* a flexible amino acid linker as described in the Results and Discussion section (2.3.2.1). All the newly designed fusion genes were synthesized by GenScript to facilitate the purification of the proteins. Each fusion gene was cloned into a mammalian expression vector, pCMV-MCS. 293 FreeStyle cells (293FS) (Life Technologies), an engineered HEK293 cell-line, were incubated in (serum-free) FreeStyle 293 Expression Medium (Life Technologies) at 37°C in a humidified atmosphere with 8% CO<sub>2</sub> and transfected with gene expression DNA constructs encoding the protein of interest using the TransIT-PRO Transfection Kit (Mirus Bio LLC, Madison, WI) when the number of the cells reached  $1.5 \times 10^6$  cells/mL. The culture medium was harvested 6 days after transfection. The FcRn protein secreted into the culture medium was purified by Immobilized Cobalt Affinity Chromatography (ICAC). After removing cells by centrifugation, the cell-free culture

medium was mixed with rmp HisPur Cobalt Resin (Thermo Fisher Scientific) pre-equilibrated with 20 mM Tris·HCl, pH 7.4, containing 200 mM NaCl and incubated for overnight at 6°C with occasional stirring. Then, the suspension was packed in a column and washed with 10 column volume (CV) of Washing buffer (20 mM Tris·HCl, pH 7.4, containing 20 mM imidazole and 200 mM NaCl) until an  $OD_{280} < 0.02$  was achieved; then the resin-bound proteins were eluted by Elution buffer (20 mM Tris·HCl, pH 7.4, containing 200 mM imidazole and 200 mM NaCl). The eluate was then dialyzed in storage buffer (50 mM Hepes, 20% sorbitol, 1 M glycine, pH 7.4) by Millipore Centrifugal Filter Units. The entire purification process was conducted on ice and the purified FcRn proteins were stored at  $-20^{\circ}\text{C}$  until use. Their purity was analyzed by SDS-PAGE on a 4–12% NuPAGE Novex Bis-Tris gel (Life Technologies).

#### **2.4.5 Large-scale protein expression and purification of Fc-fused CochHs**

For the scaled-up preparation of Fc-fused and HSA-fused CochHs, FreeStyle™ CHO-S cells (CHO-S) (Life Technologies) were first infected with recombinant lentivirus containing the gene of interest and then the transduced cells were resuspended and incubated in FreeStyle CHO Expression Medium (Life Technologies) with 8 mM L-glutamine (Life Technologies) at  $37^{\circ}\text{C}$  in a humidified atmosphere with 8%  $\text{CO}_2$ . The day before infection, the cells were seeded at a concentration of  $0.5 \times 10^5$  viable cells/well in 12-well plate and stabilized in freestyle CHO expression medium containing 1% FBS and 8 mM L-glutamine and. In the presence of 1% FBS, CHO-S cells quickly attach to the tissue culture plate. For successful lentiviral transduction, the recombinant lentiviral particles harboring the gene of interest were incubated with the cells. Simultaneously,

positive charged Polybrene (Santa Cruz Biotechnology) (1  $\mu$ l/ml) was added into the cell culture medium to improve the infection efficiency *via* neutralization of the electrical charge repulsion between the cell surface and lentiviral particles. 24 h after transduction, the medium was exchanged with a fresh medium and then incubated usually for 3 days for complete recovery of the cells from the infection. The transduced cells were then suspended by trypsinization and separated into two halves. One half was utilized for the next round of transduction with the expectation of improved target protein expression *via* increasing gene copy number of the protein of interest inside of the cells. The other half was used for protein yield determination. After each infection, efficiencies of the achieved stable cell pools were examined and the pool with the highest expression yield was chosen for scaled-up production. For large-scale production, the selected cell pool was incubated in an agitated bioreactor BioFlo/CelliGen 115 (Eppendorf). The cells were amplified at 37 °C in shake flasks to the designated volume and density before they are transferred to a bioreactor. The cells were seeded in a bioreaction at a concentration of  $0.8 \times 10^6$  viable cells/ml. The bioreactor was operated in a batch model and the temperature and pH of the cell culture medium were kept at 7.4 and at 32 °C. 10 days after cell seeding, the culture medium was harvested, and the enzymes were purified.

The Fc-fused Coch3 proteins secreted into the culture medium was purified by protein A affinity chromatography. After removing cells by centrifugation, the cell-free culture medium was mixed with rmp Protein A Sepharose Fast Flow (GE Healthcare Life Sciences) pre-equilibrated with 20 mM Tris·HCl, pH 7.4, and incubated for overnight at 6°C with continual shaking. Then, the mixture was packed in a column and washed with 5 column volume (CV) of 20 mM Tris·HCl, pH 7.4, containing 200 mM NaCl until an OD<sub>280</sub>

< 0.02 was achieved; then the protein was eluted by 50 mM sodium acetate, pH 4.0, containing 200 mM NaCl. HSA-fused CocH1 was also expressed in the method described above. Using the AlbuPure matrix (Prometic Life Sciences Inc., Laval, Canada), CocH1-HSA was purified where the cell-free culture medium was loaded onto packed bed pre-equilibrated with 50 mM sodium acetate (pH 5.3), extensively washed with 8 CV of equilibration buffer. Then, the resin bound protein was eluted with 5 CV of 50 mM ammonium acetate, pH 7.4. For buffer exchange, the eluate was dialyzed in storage buffer (50 mM Hepes, 20% sorbitol, 1 M glycine, pH 7.4) by Millipore Centrifugal Filter Units. The entire purification process was performed in a cold room at 8°C and the purified proteins were stored at -80°C until use.

#### **2.4.6 Enzyme-linked immunosorbent assay (ELISA)**

##### ***Binding of Fc-fused CocH3 to different FcRn proteins***

400 ng of 6xHis-tagged schFcRn in 100 µl 0.05M PBS, pH 7.4, was immobilized in a 96 well flat-bottomed EIA plate (Corning) at 4 °C overnight (or 37 °C for 2 h). At the same time, corresponding empty wells without FcRn coating were left as a negative control. The liquid was dumped from the plates and the rest was drained on paper towel. Coated wells were blocked with blocking buffer (0.05M PBS, pH 6.0, containing 1 mg/ml casein) (250 µL/well) at RT for 1 h. After washing twice with washing buffer (0.05M PBS, pH 6.0) (250 µL/well), 100 µl of Fc fusion protein diluted in blocking buffer, pH 6.0 was added to each well at a range of concentrations. The plate was then covered with an adhesive plastic and incubated, with continual shaking, at RT for 1 h. After washing three times with washing buffer, the HRP-conjugated antibody (anti-human IgG-Fc Ab-HRP) (70 µl/well),

diluted with blocking buffer at a ratio of 1:20,000, was added into each well and incubated at RT for 30 min on a shaker. The wells were then washed three times with washing buffer (250 µl/well) before 250 µl TMB substrate was added to the wells. The ELISA plate was kept in the dark until the desired color develops. The reaction was stopped with 100µL of 0.5M HCl. The absorbance (= the developed blue color) was measured at 450 nm using a microplate reader. All measurements were performed in triplicate or quadruplicate.

#### **2.4.7 Pharmacokinetic studies in rats**

Rats were injected with Fc-fused Coch3 proteins through the tail vein at a dose of 0.06 mg/kg body weight for Albu-Coch1; and 0.06 mg/kg. Blood samples were then obtained by needle puncture of the saphenous vein. Approximately 100 µL of blood was collected into a heparin-treated capillary tube at differing time points after protein injection. The plasma was separated from the collected blood samples by centrifugation (15 min, at  $5,000 \times g$ ). The concentration of Fc-fused Coch3 in plasma was determined by a highly sensitive radiometric assay as described in our previous report.<sup>246</sup> The obtained PK data (time dependent enzyme concentrations) ( $[E]_t$ ) were fitted to a double-exponential equation<sup>247</sup> by GraphPad Prism 5.01 software:  $[E]_t = Ae^{-k_1t} + Be^{-k_2t}$ , which explains both the distribution process (the fast phase, associated with  $k_1$ ) and the elimination process (the slow phase, associated with  $k_2$ ) of the Fc-fused Coch3 protein in animals. The  $t_{1/2}$  associated with the elimination rate constant  $k_2$  of the fusion protein is known as the biological  $t_{1/2}$  or elimination  $t_{1/2}$ .

#### **2.4.8 DAT cellular distribution assay**

All steps were performed on ice or at 4 °C.

##### ***Preparation of synaptosomal pellets***

Striatum of one cocaine-treated and one vehicle-treated rat were homogenized in individual tissue homogenizers, containing 3 ml of sucrose solution (0.32 M sucrose and 5 mM NaHCO<sub>3</sub>, pH 7.4). Synaptosomal suspensions were exposed to two centrifugation steps (2,000g, 10 min, 4 °C followed by 20,000g, 17 min, 4 °C). The resulting pellets were then resuspended in the sucrose solution.

##### ***Biotinylation of cell surface protein***

Synaptosomal suspensions included about 250 µg protein for striatum. Suspensions were then incubated (at 4 °C for 1 hr on a shaking) in 500 µl of 1.5 mg/ml bifunctional cross-linker (sulfo-NHS biotin) in PBS/Ca/Mg buffer (2.7 mM KCl, 138 mM NaCl, 0.1 mM CaCl<sub>2</sub>, 1.5 mM KH<sub>2</sub>PO<sub>4</sub>, 9.6 mM Na<sub>2</sub>HPO<sub>4</sub>, 1 mM MgCl<sub>2</sub>, pH 7.4), which labels all the membrane proteins with biotin. Free sulfo-NHS biotin molecules were then removed by centrifugation (8000g, 4 min, 4 °C), followed by washing with 1 ml of 100 mM glycine in PBS/Ca/Mg buffer. This washing step was repeated twice. Samples were then centrifuged (8000g, 5 min, 4 °C) and washed twice with 1 ml of PBS/Ca/Mg buffer with no glycine. The surface-biotinylated synaptosomes were then broken by sonication for 5 seconds followed by incubation (at 4 °C for 20 min on a shaker) in Triton X-100 buffer (150 µl for striatal synaptosomes; 10 mM Tris, 150 mM NaCl, 1 mM EDTA, 1.0% Triton X-100, 250 µM phenylmethanesulfonyl fluoride, 1 µg/ml leupeptin, 1 µg/ml aprotinin, 1 µM pepstatin, pH 7.4). Lysates were then exposed to centrifugation (13,000g, 1 hr, 4 °C). The resulting supernatants represent the total protein fraction.

### ***Isolation of biotinylated proteins***

To separate the biotinylated cell surface proteins from the non-biotinylated intracellular proteins, the supernatant was incubated with Avidin-coated beads at RT for 1 hr on a shaker, and then centrifuged (13,000g, 2 min, 4 °C). The resulting supernatant represent the intracellular fraction. The Avidin-bound biotinylated proteins constituted the cell surface fraction. The precipitated Avidin beads were washed five times with 1% Triton-X-100 buffer. Then, the beads were boiled for 10 min in SDS-loading buffer to separate the biotinylated cell surface proteins from the biotin- Avidin complex. Finally, the resulting cell surface and intracellular fractions were stored at -20 °C until use for western blot analysis.

### ***Western blotting***

Biotinylated and non-biotinylated fractions were subjected to gel electrophoresis. Blots were then incubated, with continuous shaking, for 1 hr at RT with primary antibody for DAT, followed by incubation with HRP-conjugated secondary antibody (30 min, RT). DAT protein (72 kDa) was detected using chemiluminescence. Na<sup>+</sup>/K<sup>+</sup> ATPase (a plasma-membrane enriched protein; 100 kDa) or demethylated PP2A-C (an intracellular protein; 34 kDa) were also detected on blots and these molecular markers served to ascertain the efficiency of biotinylation of surface proteins.  $\beta$ -actin (a cytoskeletal protein; 42 kDa) was used as an internal loading control.

### **Chapter III. Kinetic Characterization of Cholinesterases and a Therapeutically Valuable Cocaine Hydrolase for Their Catalytic Activities against Heroin and Its Metabolite 6-monoacetylmorphine**

As the most popularly abused one of opioids, heroin is actually a prodrug. In the body, heroin is hydrolyzed/activated to 6-monoacetylmorphine (6-MAM) first and then to morphine to produce its toxic and physiological effects. It has been known that heroin hydrolysis to 6-MAM and morphine is accelerated by cholinesterases, including acetylcholinesterase (AChE) and/or butyrylcholinesterase (BChE). However, there has been controversy over the specific catalytic activities and functional significance of the cholinesterases, which requires for the more careful kinetic characterization under the same experimental conditions. In this study,<sup>248</sup> the kinetic characterization of AChE, BChE, and a therapeutically promising cocaine hydrolase (CocH1) for heroin and 6-MAM hydrolyses under the same experimental conditions. The research described in this chapter has been published in *Chemico-Biological Interactions*.<sup>249</sup> It has been demonstrated that AChE and BChE have similar  $k_{\text{cat}}$  values (2100 and 1840  $\text{min}^{-1}$ , respectively) against heroin, but with a large difference in  $K_{\text{M}}$  (2170 and 120  $\mu\text{M}$ , respectively). Both AChE and BChE can catalyze 6-MAM hydrolysis to morphine, with relatively lower catalytic efficiency compared to the heroin hydrolysis. CocH1 can also catalyze hydrolysis of heroin ( $k_{\text{cat}}=2150 \text{ min}^{-1}$  and  $K_{\text{M}}=245 \mu\text{M}$ ) and 6-MAM ( $k_{\text{cat}}=0.223 \text{ min}^{-1}$  and  $K_{\text{M}}=292 \mu\text{M}$ ), with relatively larger  $K_{\text{M}}$  values and lower catalytic efficiency compared to BChE. Notably, the  $K_{\text{M}}$  values of CocH1 against both heroin and 6-MAM are all much larger than previously reported maximum serum heroin and 6-MAM concentrations observed in heroin users. We also found that (–)-cocaine degradation by CocH1 was not significantly changed in the presence of even an abnormally high concentration (100  $\mu\text{M}$ ) of heroin or 6-MAM. These findings



imply that the heroin use along with cocaine will not drastically affect the catalytic activity of CocH1 against cocaine in the CocH1-based enzyme therapy for cocaine abuse.

Dr. Jianzhuang Yao performed molecular modeling study. Dr. Zhenyu Jin helped me to prepare cocaine hydrolases. I performed all the rest experiments described in this chapter.

### **3.1 Heroin hydrolysis to morphine by human cholinesterase**

Heroin (3,6-diacetylmorphine) is one of the drugs most commonly co-abused by cocaine-dependent individuals.<sup>250-255</sup> The concurrent use of cocaine and heroin has received increasing clinical attentions because it not only causes more serious morbid psychopathology<sup>256-257</sup> and poor addiction treatment outcomes,<sup>258-259</sup> but also considerably increases the risk of severe drug overdose which ends in death.<sup>260</sup>

Considering the frequent use of cocaine in combination with heroin by addicts, a question is whether or not cocaine degradation by CocH1, the first one of our discovered high-activity mutants of human BChE, is significantly inhibited by heroin or its metabolites 6-monoacetylmorphine (6-MAM) and morphine. In fact, heroin is quickly converted to 6-MAM and then more slowly to morphine in the circulating system<sup>261-263</sup> and two human cholinesterases, plasma BChE and erythrocyte acetylcholinesterase (AChE), are generally regarded as the principal enzymes involved in both the majority of 6-MAM formation and significant morphine production from heroin.

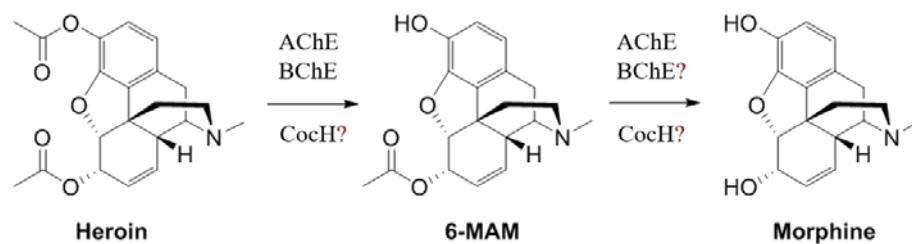


**Figure 3.1** Schematic presentation of heroin hydrolysis to morphine.

It has been demonstrated that 6-MAM is the primary metabolite responsible for heroin's acute psychoactive effects (the rush) and intoxication, but the euphoria following the rush is more due to the stimulant effects of morphine produced from 6-MAM hydrolysis,<sup>264-267</sup> indicating the importance of the rates of 6-MAM formation and degradation in the onset of heroin effects on the central nervous system. At heroin blood concentrations attainable *in vivo*  $\leq 270$  nM,<sup>261, 264, 268-269</sup> ~80% of the total heroin hydrolysis in blood is accounted for plasma and erythrocyte cytosol where BChE and AChE are located, respectively.<sup>270-272</sup> *In vitro* enzyme kinetic studies using purified native human cholinesterases further demonstrated that BChE, rather than AChE, is mainly responsible for degradation of heroin to 6-MAM with a higher catalytic efficiency under first-order kinetics.<sup>273</sup> However, there has been controversy over the catalytic activity and functional significance of the cholinesterases (AChE and BChE) on the hydrolysis of 6-MAM to morphine,<sup>250, 273-274</sup> which makes it difficult to interpret their actual roles in 6-MAM degradation. In addition, the reported values of the kinetic parameters ( $k_{cat}$  and  $K_M$ ) for BChE against heroin ranged from 12.9 to 540 min<sup>-1</sup> and from 0.11 to 3.5 mM, respectively,<sup>250, 273-274</sup> requiring for the more careful kinetic characterization under the same experimental conditions.

**Table 3.1** The reported kinetic parameters of human BChE for heroin hydrolysis

Protein	Reference	Protein source	$K_M$	$k_{cat}$	Incubation condition			
			( $\mu M$ )	( $\text{min}^{-1}$ )	Temp.	pH	Heroin conc. (mM)	Buffer
Human BChE	Lockridge et al., 1980	Human plasma	110	500	25 °C	7.4	0.16 to 2	67 mM Sodium phosphate
	Salmon et al., 1999	Human serum	110	540	37 °C	7.4	0.032 to 4	100 mM Sodium phosphate
	Kamendulis et al., 1996	Human serum	$3500 \pm 400$	$12.9 \pm 0.5$	37 °C	7.5	0 to 12	50 mM Potassium phosphat

### 3.2 The focuses of this research

Here we kinetically compared CHO cell-expressed human recombinant AChE, BChE, and CocH1 with the aims to examine their catalytic efficiencies against heroin and 6-MAM and to assess the possible interaction between cocaine and heroin or 6-MAM in their hydrolysis reactions catalyzed by CocH1 in comparison with human enzymes AChE and BChE. The complete catalytic parameters obtained for AChE, BChE, and CocH1 against heroin and 6-MAM reveal how the abused drugs (cocaine and heroin) can possibly affect each other in terms of their hydrolysis reactions and detoxification under various conditions. The insights from the kinetic characterization will be valuable in guiding further development of novel enzyme therapies for the drug detoxification. In particular, concurrent use of heroin and cocaine is not expected to significantly affect the efficacy of CocH1 (or its fusion protein form TV-1380) in cocaine detoxification.

### 3.3 Results & Discussion

#### 3.3.1 Identification of Fc variants with altered binding

Two previously reported studies led to contradictory findings over the ability of BChE to catalyze hydrolysis of 6-MAM to morphine,<sup>250, 273-274</sup> which limits the interpretation of the data concerning the actual contributions of the enzymes to the drug

metabolism to morphine in blood. In 1999, Salmon and his colleagues reported that only AChE, but not BChE, further hydrolyzes 6-MAM to morphine from heroin,<sup>273</sup> but these findings are opposite to the previous observations of Kamendulis *et al.* showing the capability of BChE to catalyze 6-MAM into morphine ( $k_{\text{cat}} = 0.25 \text{ min}^{-1}$  and  $K_M = 8.6 \text{ mM}$ ).<sup>250</sup> Therefore, we first tested whether or not heroin is metabolized to 6-MAM and then eventually into morphine by recombinant human BChE or AChE. For each enzyme, 1 mM heroin was incubated with 4  $\mu\text{M}$  enzyme. As shown in Fig. 3.2, in the presence of either BChE or AChE, after 25 minutes of incubation, heroin has completely been converted to 6-MAM, and some 6-MAM has further been converted to morphine. Both BChE and AChE were highly active in metabolizing heroin to 6-MAM, but they were less active in further degrading 6-MAM to morphine. These results clearly show that like AChE, BChE is capable of hydrolyzing heroin to morphine eventually, which are in agreement with the findings of Kamendulis *et al.*,<sup>250</sup> but unlike the observations of Salmon *et al.*.<sup>273</sup> We also observed that AChE produced more morphine than BChE in the given reaction condition, implying the relatively lower catalytic efficiency of BChE against 6-MAM.

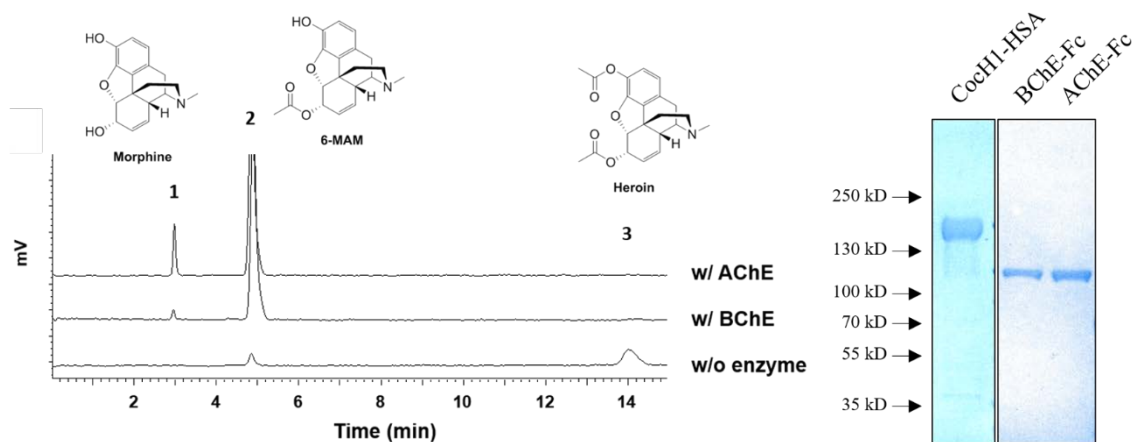


**Figure 3.2** Enzymatic activity of BChE and AChE on the hydrolysis of heroin.

Chromatograms for the deacetylation of heroin in the presence or absence of BChE or AChE. Peak 1 (morphine) with retention time 3.8 min, peak 2 (6-MAM) with retention time 4.9 min and peak 3 (heroin) with retention time 14 min. The enzyme (AChE or BChE) was incubated with 1 mM substrate concentration at 40  $\mu$ M designated enzyme at 37°C for 25 min.

### **3.3.2 Hydrolysis of free 6-MAM to morphine by human recombinant BChE and AChE**

In a previous report by Salmon *et al.*,<sup>273</sup> it was noted that AChE hydrolyzes 6-MAM only when 6-MAM is produced from heroin within its active site and free 6-MAM molecules only serve as an inhibitor for AChE.<sup>273</sup> This led us to examine whether free 6-MAM molecules can serve as a substrate for BChE or not. To address this question, the enzymatic activity of the enzyme (BChE or AChE) was studied using synthetic 6-MAM which we added to the reaction system. 1 mM 6-MAM was mixed and incubated with either 4  $\mu$ M enzyme (BChE or AChE) under the incubation condition mentioned above. The results showed that direct incubation of 6-MAM with BChE produced the amount of morphine which is significantly larger than that in the control (without an enzyme), demonstrating that free 6-MAM molecules can serve as a substrate for BChE (Fig. 3.3). Interestingly, AChE also converted synthetic 6-MAM to morphine in a significant amount comparable to that of morphine produced from heroin by AChE (Fig. 3.2 & 3.3). Overall, these observations clearly indicate that both free heroin and 6-MAM molecules produced after heroin uptake in the circulatory system can be metabolized to morphine by both cholinesterases (AChE and BChE) in blood.

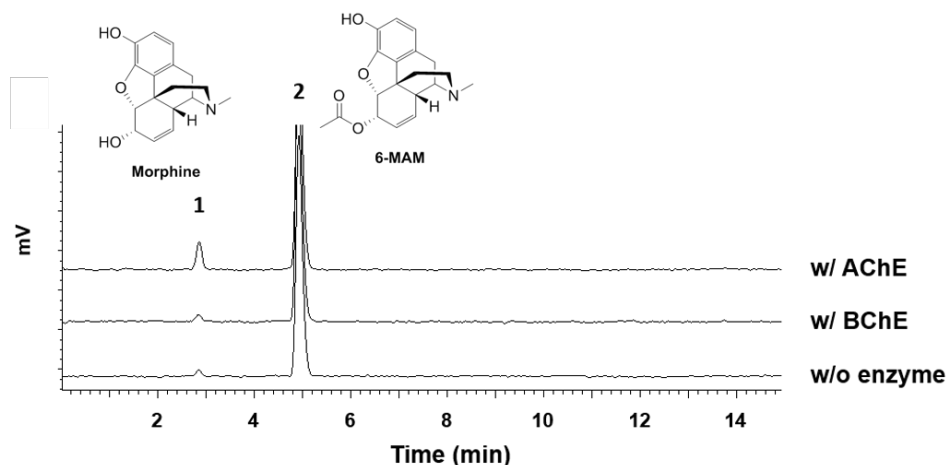


**Figure 3.3** Enzymatic activity of BChE and AChE on the hydrolysis of 6-MAM. Chromatograms for the deacetylation of 6-MAM in the presence or absence of BChE or AChE. Peak 1 (morphine) with retention time 3.8 min and peak 2 (6-MAM) with retention time 4.9 min. The enzyme (AChE or BChE) was incubated with 1 mM substrate concentration at 40  $\mu$ M designated enzyme at 37°C for 25 min.

### 3.3.3 Kinetics of heroin hydrolysis by BChE, AChE, and Coch1

As a potential anti-cocaine medication, Coch1 has a considerably improved catalytic efficiency ( $k_{\text{cat}} = 3060 \text{ min}^{-1}$ ,  $K_{\text{M}} = 3.1 \text{ }\mu\text{M}$ , and  $k_{\text{cat}}/K_{\text{M}} = 9.9 \times 10^8 \text{ min}^{-1} \cdot \text{M}^{-1}$ ) compared to the wild-type BChE ( $k_{\text{cat}} = 4.1 \text{ min}^{-1}$ ,  $K_{\text{M}} = 4.5 \text{ }\mu\text{M}$ , and  $k_{\text{cat}}/K_{\text{M}} = 9.1 \times 10^5 \text{ min}^{-1} \cdot \text{M}^{-1}$ ) against (–)-cocaine. Thus, Coch1 may be used to effectively block the drug reward for a given dose of cocaine. Considering that Coch1 is developed from human BChE capable of metabolizing all of (–)-cocaine, heroin and its initial host metabolite 6-MAM, (–)-cocaine degradation by Coch1 can be affected by the drug-drug interaction with heroin or 6-MAM. Specifically, if heroin or 6-MAM can also be hydrolyzed by Coch1, we would like to know the  $K_{\text{M}}$  or the binding affinity ( $K_{\text{d}}$ ) of the drug (heroin or 6-MAM) with

CocH1 in order to estimate how heroin or 6-MAM could competitively inhibit CocH1 for its catalytic activity against (–)-cocaine. In principle, for a competitive inhibition of an enzyme, the inhibitory constant ( $K_i$ ) value is equal to the corresponding  $K_d$  value ( $K_i = K_d$ ). However, the  $K_d$  value can be different from the corresponding  $K_M$  value. Nevertheless,  $K_d \approx K_M$  value under the well-known rapid equilibrium assumption<sup>275</sup> which is usually true for enzyme-substrate binding. Hence, we may reasonably use an experimentally measured  $K_M$  of CocH1 against heroin or 6-MAM to estimate the potential inhibitory activity of heroin or 6-MAM against CocH1-catalyzed hydrolysis of another substrate like (–)-cocaine when  $K_i \approx K_M$ .

In order to know whether heroin or 6-MAM can significantly inhibit CocH1-catalyzed hydrolysis of (–)-cocaine, we investigated kinetics of heroin degradation to 6-MAM by CocH1, BChE, and AChE. Under the experimental conditions generating the kinetic data depicted in Fig. 3.4, we only observed the metabolite 6-MAM, and there were no detectable levels of morphine, indicating that the enzyme activity for converting 6-MAM to morphine is much lower than that for converting heroin to 6-MAM.

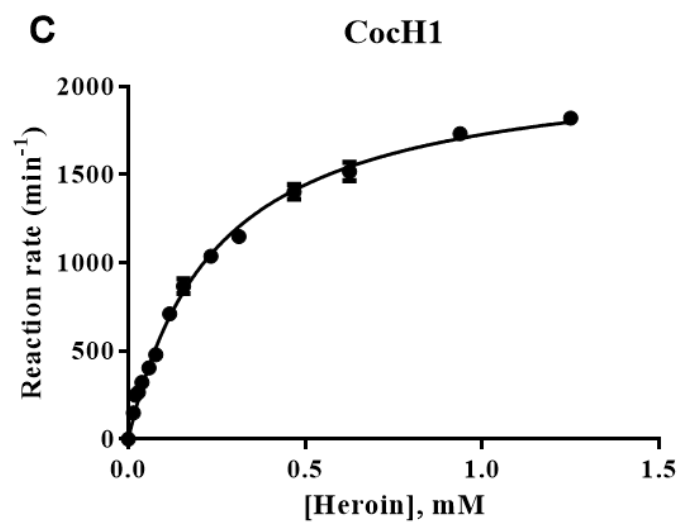
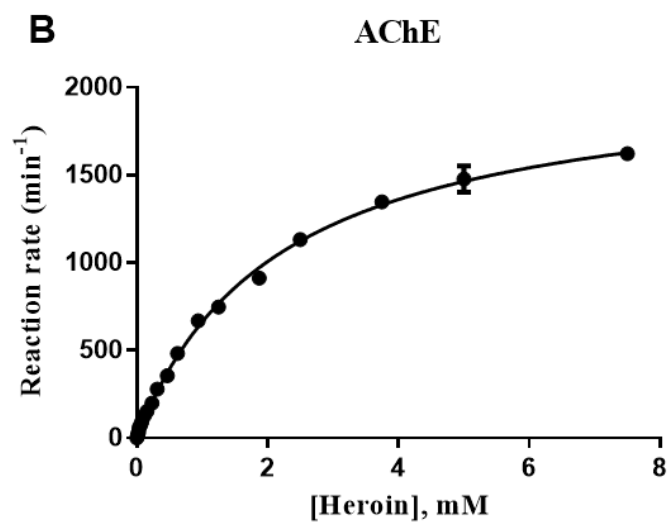
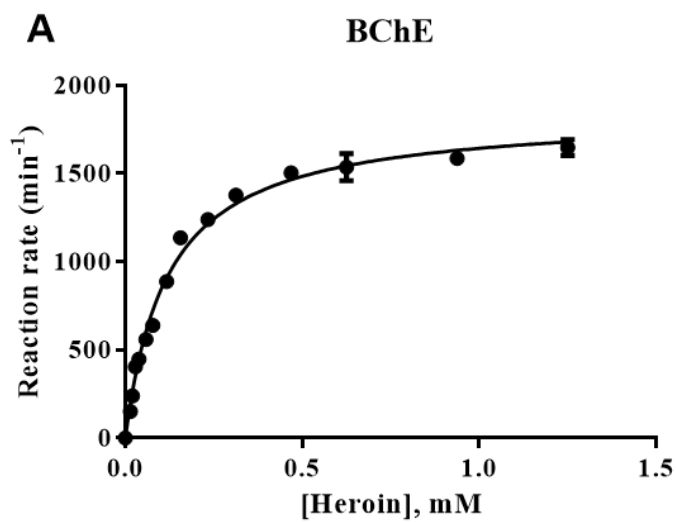




**Figure 3.4** Kinetic analysis of heroin hydrolysis by BChE, AChE, and CocH1. The hydrolysis of heroin to 6-MAM by BChE (A), AChE (B), and CocH1 (C) were determined at substrate concentrations of 0.015-1.25 mM (BChE and CocH1) or 0.015-7.5 mM (AChE). Kinetic parameters ( $k_{cat}$  and  $K_M$ ) were determined by fitting the measured reaction rate data to the Michaelis-Menten kinetic equation using the Prism5.01 software. Each dot is the representative of the average of triplicates and its values are expressed as the mean  $\pm$  standard deviation.

The obtained kinetic data are depicted in Fig. 3.4, and the kinetic parameters obtained are summarized in Table 3.2. As shown in Table 3.2, compared to BChE, CocH1 has a higher  $K_M$  value (245  $\mu$ M compared to 120  $\mu$ M) and a similar  $k_{cat}$  value (2150  $\text{min}^{-1}$  compared to 1840  $\text{min}^{-1}$ ). The determined  $K_M$  of CocH1 against heroin is ~900-fold larger than the previously reported blood heroin concentrations attainable *in vivo* ( $\leq 0.27 \mu\text{M}$ ),<sup>261, 264, 268-269</sup> and ~76-fold larger than its reported  $K_M$  value against (–)-cocaine (3.1  $\mu\text{M}$ ).<sup>190-191</sup> Generally speaking, for a given inhibitor, when the  $K_i$  value is ~900-fold larger than the inhibitor concentration, the inhibitor can only decrease the enzyme activity by less than ~0.1%, suggesting that the blood heroin levels usually achieved by the heroin users are not expected to significantly change the enzymatic hydrolysis of (–)-cocaine by CocH1. Moreover, as one can see from the kinetic data in Table 3.2, AChE has ~18-fold larger  $K_M$  value (2170  $\mu\text{M}$ ) compared to that of BChE, but with a similar  $k_{cat}$  value (2100  $\text{min}^{-1}$  compared to 1840  $\text{min}^{-1}$ ), against heroin. These data indicate that the major difference between wild-type AChE and BChE in the catalytic efficiency against heroin ( $k_{cat}/K_M = 1.53 \times 10^7 \text{ min}^{-1} \cdot \text{M}^{-1}$  for BChE *vs*  $k_{cat}/K_M = 9.68 \times 10^5 \text{ min}^{-1} \cdot \text{M}^{-1}$  for AChE) is mainly

attributed to their difference in the binding affinity with heroin. Our kinetic data strongly support the argument<sup>276</sup> that plasma BChE is the prime enzyme responsible for the rapid enzymatic hydrolysis of the 3'-phenolic ester of heroin in the blood.

**Table 3.2** Kinetic parameters of BChE, AChE, and CocH1 against heroin

<sup>a</sup> Relative catalytic efficiency ( $k_{\text{cat}}/K_{\text{M}}$ )

Enzyme	$k_{\text{cat}}$ ( $\text{min}^{-1}$ )	$K_{\text{M}}$ ( $\mu\text{M}$ )	$k_{\text{cat}}/K_{\text{M}}$ ( $\text{min}^{-1} \cdot \text{M}^{-1}$ )	RCE <sup>a</sup>	R <sup>2</sup>
BChE	1840 ± 24	120 ± 5	$1.53 \times 10^7$	1	0.991
AChE	2100 ± 26	2170 ± 6	$9.68 \times 10^5$	0.06	0.997
CocH1	2150 ± 31	245 ± 9	$8.78 \times 10^6$	0.57	0.994

In this study, our experimental  $K_{\text{M}}$  value of BChE against heroin (120  $\mu\text{M}$ ) is consistent with the earlier  $K_{\text{M}}$  of 110  $\mu\text{M}$  reported by Lockridge *et al.*<sup>250, 273-274</sup> and cited by Salmon *et al.*,<sup>273</sup> but quite different from the number of Kamendulis *et al.* (3.5 mM).<sup>250, 273-274</sup> The catalytic rate constant ( $k_{\text{cat}} = 1840 \text{ min}^{-1}$ ) determined is also substantially higher than the wide range (from 12.9 to 540  $\text{min}^{-1}$ ) reported by those research groups.<sup>250, 273-274</sup> Moreover, the kinetic parameter values of AChE determined for the hydrolysis of heroin to 6-MAM ( $k_{\text{cat}} = 2100 \text{ min}^{-1}$  and  $K_{\text{M}} = 2170 \mu\text{M}$ ) are higher than the values ( $k_{\text{cat}} = 351 \text{ min}^{-1}$  and  $K_{\text{M}} = 620 \mu\text{M}$ ) reported by Salmon *et al.*<sup>273</sup> It is likely that the differences in the catalytic parameters determined for the same enzymatic reactions are largely dependent on how enzymes are prepared if all of the kinetic assays are all in readily controlled experimental conditions. Generally, natural protein sources, especially from human or animal tissues, have the difficulty to meet the requirements for higher retention of functional properties including their enzymatic activities, mainly due to the complicated

collection, treatment, storage, and extraction processes. These processes may affect the protein structure accompanied with a change (usually a decrease) in its binding affinity and activity, and result in inactivation or overall diminished enzymatic activity. Whereas the kinetic studies of Lockridge *et al.*,<sup>250, 273-274</sup> Salmon *et al.*,<sup>273</sup> and Kamendulis *et al.*<sup>250, 273-274</sup> were found on the use of natural BChE or AChE extracted from human blood samples, all the kinetic analysis in the present study were performed using the freshly expressed and purified BChE and AChE for comparison. In addition, another external factor affecting the enzymatic reaction kinetics is the temperature. The kinetic studies of Salmon *et al.*<sup>273</sup>, and Kamendulis *et al.*<sup>250, 273-274</sup> were performed at 37°C, but that of Lockridge *et al.*<sup>250, 273-274</sup> was accomplished at 25°C. In this study, the same enzymatic kinetic analysis was carried out at 37°C and the protein samples used this study are shown to have higher binding affinity and catalytic efficiency (reflected by the lower  $K_M$  and higher  $k_{cat}/K_M$ , respectively). These observations strongly suggest that the kinetic parameters determined in the present study are more likely to reasonably reflect the actual enzymatic activity of human BChE and AChE against heroin.

#### **3.3.4 Kinetics of 6-MAM hydrolysis by BChE, AChE, and Coch1**

As mentioned above, 6-MAM may also potentially inhibit Coch1-catalyzed cocaine hydrolysis because 6-MAM can also serve as a substrate for wild-type BChE (Fig. 3.2 & 3.3). To access this possibility, we examined the kinetics of 6-MAM degradation to morphine by Coch1 as well as wild-type BChE and AChE. The catalytic parameters  $k_{cat}$  and  $K_M$  were determined for BChE against 6-MAM, and then were compared with those of AChE and Coch1 (Fig. 3.5 and Table 3.3).

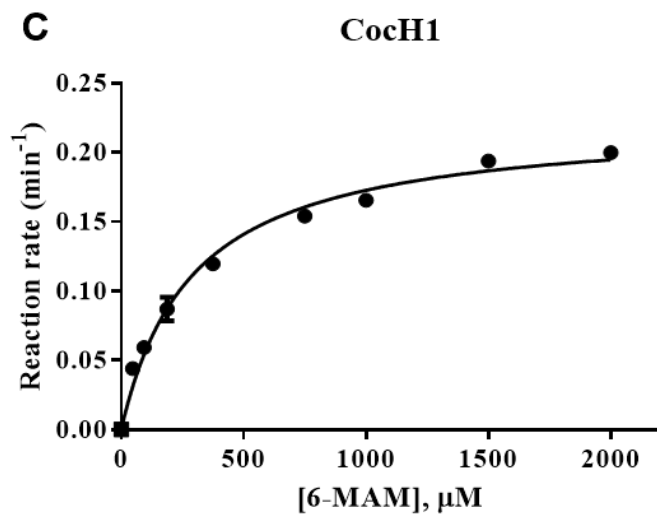
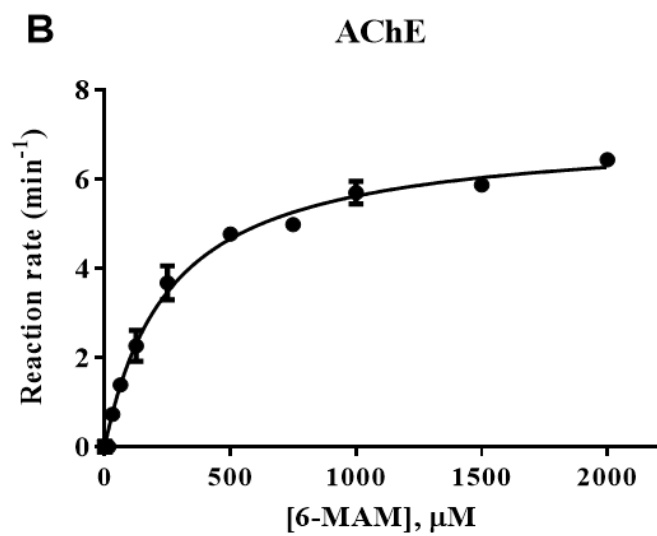
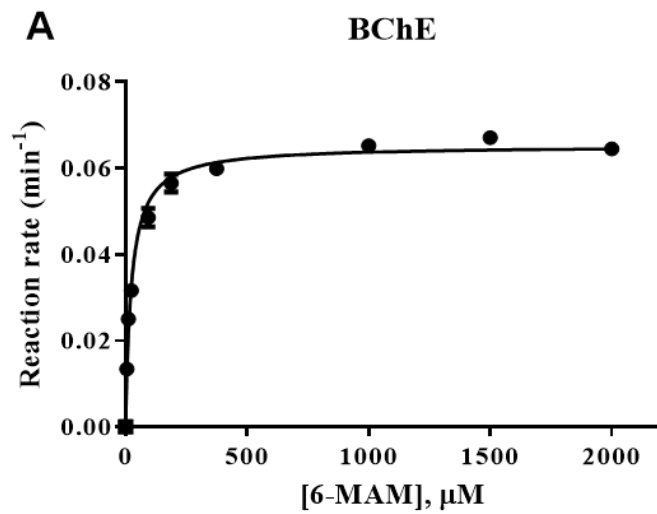


**Figure 3.5** Kinetic analysis of 6-MAM hydrolysis by BChE, AChE, and CocH1. The hydrolysis of heroin to 6-MAM by BChE (A), AChE (B), and CocH1 (C) were determined at substrate concentrations of 5-2000  $\mu\text{M}$ . Kinetic parameters ( $k_{\text{cat}}$  and  $K_{\text{M}}$ ) were determined by fitting the generated reaction rate data to the Michaelis-Menten kinetic equation using the Prism5.01 software. Each dot is the representative of the average of triplicates and its values are expressed as the mean  $\pm$  standard deviation.

As seen in Table 3.3, the  $K_{\text{M}}$  value of CocH1 against 6-MAM was determined to be 292  $\mu\text{M}$  which is ~94-fold-larger than the reported  $K_{\text{M}}$  value (3.1  $\mu\text{M}$ ) of CocH1 against (–)-cocaine. Given that the maximum serum concentration ( $C_{\text{max}}$ ) of 6-MAM in humans has been reported to range from 5.2 to 17.5  $\mu\text{M}$  after intravenous heroin administration,<sup>277-279</sup> the  $K_{\text{M}}$  (292  $\mu\text{M}$ ) of CocH1 against 6-MAM is still ~16-56-fold larger than the  $C_{\text{max}}$  of 6-MAM achieved by heroin users. In comparison, the observed peak blood (–)-cocaine concentrations were ~3-fold higher than the  $K_{\text{M}}$  of CocH1 against (–)-cocaine. Overall, these data suggest that when both 6-MAM and (–)-cocaine reach their corresponding peak concentrations in the blood, CocH1-catalyzed (–)-cocaine hydrolysis can only be inhibited by 6-MAM for ~0.45-1.5%. The lower the 6-MAM concentration, the less the inhibition. The potential inhibition by 6-MAM would not be significant. Hence, CocH1 can still efficiently degrade (–)-cocaine at the 6-MAM concentrations usually achieved by heroin users.

**Table 3.3** Kinetic parameters of BChE, AChE, and CocH1 against 6-MAM<sup>a</sup> Relative catalytic efficiency ( $k_{\text{cat}}/K_{\text{M}}$ )

Enzyme	$k_{\text{cat}}$ ( $\text{min}^{-1}$ )	$K_{\text{M}}$ ( $\mu\text{M}$ )	$k_{\text{cat}}/K_{\text{M}}$ ( $\text{min}^{-1} \cdot \text{M}^{-1}$ )	RCE <sup>a</sup>	R <sup>2</sup>
BChE	0.065 $\pm$ 0.001	24 $\pm$ 1.4	$2.71 \times 10^3$	1	0.990
AChE	7.078 $\pm$ 0.141	259 $\pm$ 18	$2.73 \times 10^4$	10.1	0.990
CocH1	0.223 $\pm$ 0.005	292 $\pm$ 22	$0.764 \times 10^3$	0.282	0.987

According to the kinetic data in Table 3.3, the determined  $k_{\text{cat}}/K_{\text{M}}$  value ( $2.73 \times 10^4 \text{ min}^{-1} \cdot \text{M}^{-1}$ ) of AChE against 6-MAM was approximately 10 times greater than that ( $2.71 \times 10^3 \text{ min}^{-1} \cdot \text{M}^{-1}$ ) of BChE against 6-MAM. Notably, these findings are in agreement with the findings of Kamendulis *et al.*<sup>250, 273-274</sup> in that BChE catalyzes the hydrolysis of 6-MAM into morphine. However, our experimental  $K_{\text{M}}$  and  $k_{\text{cat}}$  values are much different from the corresponding kinetic parameters reported by Kamendulis *et al.*<sup>250, 273-274</sup> Our experimental  $K_{\text{M}}$  of 24  $\mu\text{M}$  is considerably smaller than their  $K_{\text{M}}$  of 8.6 mM and our determined catalytic rate constant ( $k_{\text{cat}} = 0.065 \text{ min}^{-1}$ ) is also much different from the earlier  $k_{\text{cat}}$  of 0.25  $\text{min}^{-1}$ . Accounting for all of the kinetic parameters, the catalytic efficiency ( $k_{\text{cat}}/K_{\text{M}} = 2.71 \times 10^3 \text{ min}^{-1} \text{ M}^{-1}$ ) obtained for the same enzymatic hydrolysis in the present study is ~93-fold larger than that ( $k_{\text{cat}}/K_{\text{M}} = 2.91 \times 10^1 \text{ min}^{-1} \text{ M}^{-1}$ ) reported by Kamendulis *et al.*<sup>250, 273-274</sup> As mentioned above, the differences in the catalytic parameters determined for the same enzymatic reaction seem to largely rely on how BChE is prepared for the kinetic assay. Compared to our kinetic analysis using the freshly expressed and purified BChE, the previous kinetic analysis by Kamendulis *et al.*<sup>250, 273-274</sup> was based on the use of natural BChE extracted from human plasma samples.

Overall, all of our experimental kinetic data strongly suggest that BChE and AChE

play distinct roles in heroin metabolism into morphine. BChE catalyzes hydrolysis of heroin to 6-MAM with a much higher catalytic efficiency than AChE. For the further degradation of 6-MAM to morphine, BChE has a relatively lower catalytic efficiency than AChE.

Further, we tested whether (–)-cocaine degradation by CocH1 will be affected by the drug-drug interaction when heroin or 6-MAM is present in the reaction system. According to the results obtained (Fig. 3.6), (–)-cocaine degradation by CocH1 was not significantly changed in the presence of even an abnormally high concentration (100  $\mu$ M) of heroin or 6-MAM.

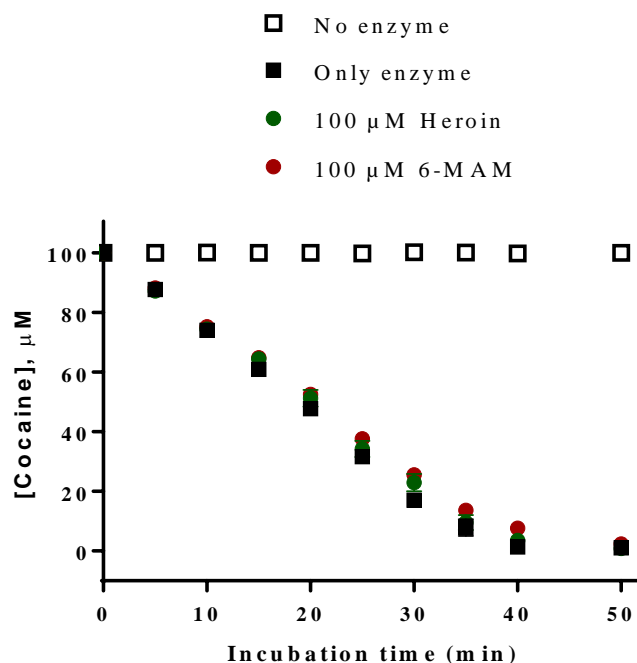


**Figure 3.6** (–)-Cocaine hydrolysis by CocH1. Both the enzyme (100 ng/ml) and (–)-cocaine (100 μM) were incubated together with 100 μM opioid (heroin or 6-MAM). Presented are the residual concentrations of cocaine *versus* time (○, no enzyme control; ■, only enzyme control, without opioid; ●, enzyme plus heroin; ●, enzyme plus 6-MAM). Cocaine concentrations were determined by using sensitive radiometric assays using [<sup>3</sup>H](–)-cocaine. Results represent two independent experiments and the values are expressed as mean ± standard deviations.

### 3.3.5 Insights from molecular modeling

The reaction pathways of cholinesterase-catalyzed hydrolyses of heroin and 6-MAM were studied in our previous computational studies<sup>280-281</sup> through first-principles quantum mechanics and molecular mechanics-free energy (QM/MM-FE) simulations. The optimized reactant complexes (*e.g.* BChE complexed with heroin and 6-MAM, and AChE



complexed with 6-MAM) obtained from our previous QM/MM studies show a couple of important enzyme-substrate interaction features. One is the interaction between the acetyl groups of heroin and 6-MAM and the oxyanion hole consisting of Gly116, Gly117, and Ala199 in BChE (corresponding to Gly121, Gly122, and Ala204 in AChE). The other is the interaction between the positively charged amino-groups of heroin and 6-MAM and the sidechain of Trp82 in BChE (corresponding to Trp86 in AChE). Guided by the aforementioned interactions, the substrate (heroin or 6-MAM) was docked into the active site of the enzyme (AChE, BChE, or Coch1). The molecular docking enabled us to understand how heroin may bind with human AChE, BChE, and Coch11 compared to 6-MAM binding with the corresponding enzymes. According to the enzyme-substrate binding structures obtained from molecular docking (as shown in Fig. 3.7), the binding mode for each enzyme (AChE, BChE, and Coch1) with heroin is similar to that with 6-MAM in terms of the overall hydrogen bonding with the oxyanion hole, particularly for the crucial interactions between the carbonyl oxygen of the substrate and the oxyanion hole of the enzyme. In particular, there are always two hydrogen bonds between the carbonyl oxygen of the substrate and backbone amide groups of the oxyanion hole residues (Gly120 and Gly121 of AChE corresponding to Gly116 and Gly117 of BChE and Coch11) no matter whether the substrate is heroin or 6-MAM. There are also two hydrogen bonds between the carbonyl oxygen of the substrate and the oxyanion hole of Coch1 (sidechain of Ser199 and backbone of Gly117), no matter whether the substrate is heroin or 6-MAM. The modelling results depicted in Fig. 3.7 reveal that, no matter whether the enzyme is AChE, BChE, or Coch1, the acetyl-group of heroin forms stronger hydrogen bonds in the oxyanion hole compared to 6-MAM with the same enzyme. Hence, all of the enzymes

concerned in the present study are expected to have a significantly better catalytic efficiency against heroin compared to 6-MAM. In particular, although a novel hydrogen bond from Ser199 of CocH1 is introduced to stabilize the acetyl-group of the substrate (heroin or 6-MAM), the hydrogen bond with Gly116 is lost compared to wild-type BChE. Therefore, CocH1 concerned in the present study is not expected to have a significantly improved catalytic efficiency against heroin or 6-MAM in comparison with BChE. The computational insight is supported by the measured kinetic parameters discussed above.

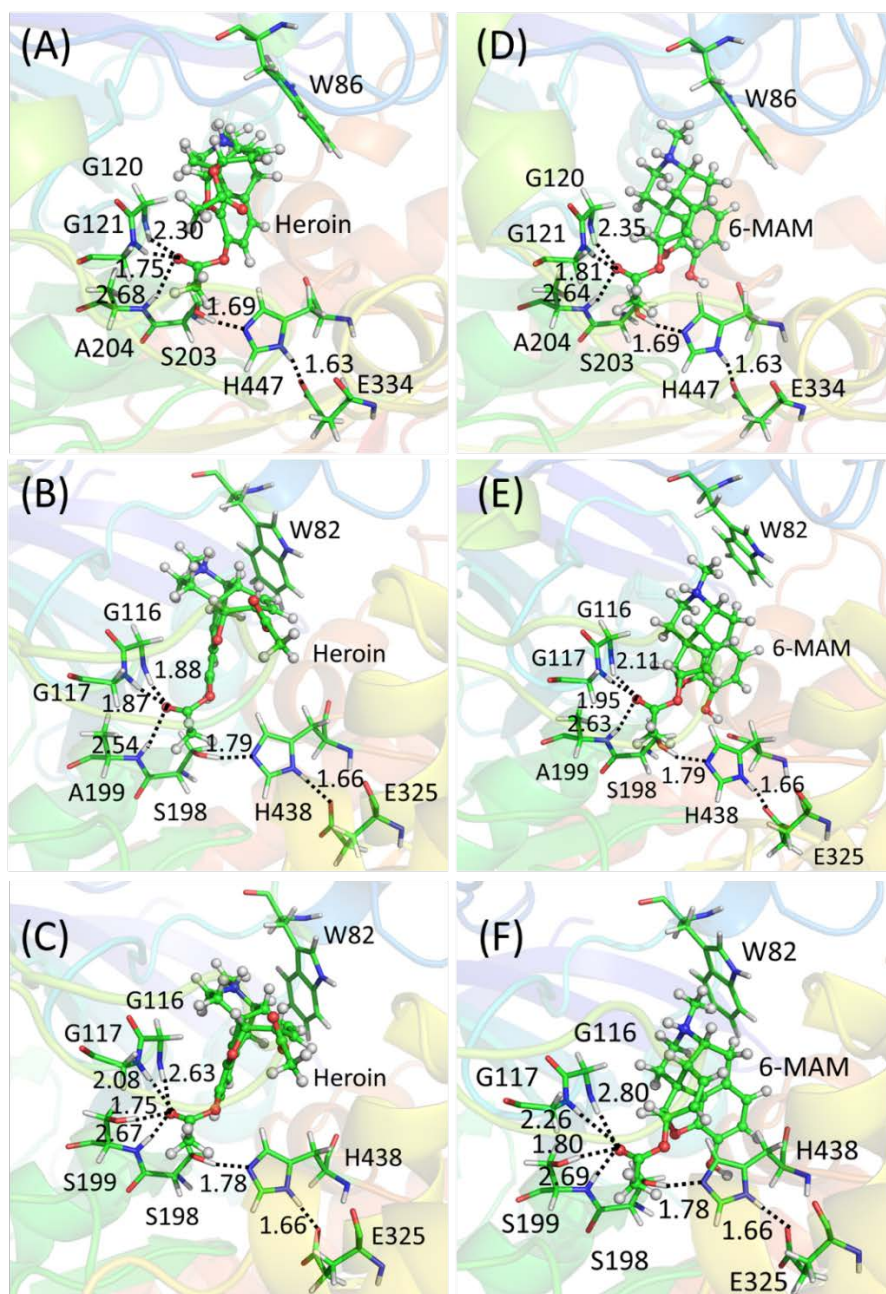


**Figure 3.7** Modeled structures of the AChE, BChE, and CocH1 (E14-3) binding with heroin and 6-MAM. (A) Wild-type AChE binding with heroin; (B) Wild-type BChE binding with heroin; (C) CocH1 binding with heroin; (D) Wild-type AChE binding with 6-MAM; (E) Wild-type BChE binding with 6-MAM; (F) CocH1 binding with 6-MAM. This figure was provided by Dr. Jianzhuang Yao in our lab.

### 3.3.6 Main outcomes of this research

The catalytic activities of wild-type AChE, wild-type BChE, and CocH1 against heroin and 6-MAM have been characterized under the same experimental conditions for comparison. According to the determined kinetic parameters  $k_{\text{cat}}$  and  $K_{\text{M}}$  for all of these enzymatic reactions, wild-type AChE and BChE have similar  $k_{\text{cat}}$  values ( $k_{\text{cat}} = 2100 \text{ min}^{-1}$  for AChE and  $k_{\text{cat}} = 1840 \text{ min}^{-1}$  for BChE) against heroin. However, BChE has a ~16 fold-higher catalytic efficiency than AChE ( $k_{\text{cat}}/K_{\text{M}} = 1.53 \times 10^7 \text{ min}^{-1} \cdot \text{M}^{-1}$  for BChE vs  $k_{\text{cat}}/K_{\text{M}} = 9.67 \times 10^5 \text{ min}^{-1} \cdot \text{M}^{-1}$  for AChE), mainly because BChE has a ~18-fold stronger binding affinity with heroin compared to AChE ( $K_{\text{d}} \approx K_{\text{M}} = 120 \text{ }\mu\text{M}$  for BChE vs  $K_{\text{d}} \approx K_{\text{M}} = 2170 \text{ }\mu\text{M}$  for AChE). Besides, both AChE and BChE can catalyze 6-MAM hydrolysis to morphine, with relatively lower catalytic efficiency compared to the corresponding enzyme catalyzing heroin hydrolysis.

CocH1 can also catalyze hydrolysis of heroin ( $k_{\text{cat}} = 2150 \text{ min}^{-1}$  and  $K_{\text{M}} = 245 \text{ }\mu\text{M}$ ) and 6-MAM ( $k_{\text{cat}} = 0.223 \text{ min}^{-1}$  and  $K_{\text{M}} = 292 \text{ }\mu\text{M}$ ), with relatively larger  $K_{\text{M}}$  values and relatively lower catalytic efficiency compared to wild-type BChE. Notably, the  $K_{\text{M}}$  values of CocH1 against both heroin and 6-MAM are all much larger than previously reported maximum serum heroin and 6-MAM concentrations observed in heroin users, implying that the heroin use along with cocaine use will not significantly affect the catalytic activity of CocH1 against cocaine in the CocH1-based enzyme therapy for cocaine abuse.

### **3.4 Experimental details**

#### **3.4.1 Materials**

Phusion DNA polymerases, restriction enzymes, and T4 DNA ligase were purchased from New England Biolabs. All oligonucleotides were purchased from Eurofins MWG Operon. Vector pCMV-MCS was obtained from Agilent Technologies. Chinese hamster ovary (CHO)-S cells and FreeStyle™ CHO Expression Medium, hypoxanthine/thymidine (HT) supplement, l-glutamine, 4–12% Tris-glycine Mini Protein Gel, and SimpleBlue SafeStain were purchased from Life Technologies (Carlsbad, CA). Reduction-modified protein (rmp) Protein A Sepharose Fast Flow was ordered from GE Healthcare Life Sciences (Pittsburgh, PA). Centrifugal filter units were ordered from Millipore (Burlington, MA). Heroin, 6-MAM, and morphine were provided by the National Institute on Drug Abuse (NIDA) Drug Supply Program. All other chemicals as well as the solvents used in high-performance liquid chromatography (HPLC), were of HPLC grade and purchased from Sigma-Aldrich (St. Louis, MO).

#### **3.4.2 Construction of mammalian expression plasmids**

CocH1 truncated after amino acid 529 was fused with human serum albumin (HSA) for the extension of biological half-life.<sup>282</sup> For protein expression in mammalian cells, the cDNA for the CocH1 (the A199S/F227A/S287G/A328W mutant of human BChE) containing C-terminal HSA was generated and cloned in to pCMV-MCS in our previous studies.<sup>190-191, 283</sup> Two expression plasmids, pCMV-BChE-Fc(WT), and pCMV-AChE-Fc(WT), were constructed as described previously.<sup>87</sup> Briefly, the C-terminal of truncated human enzyme (BChE or AChE) was genetically fused to the N-terminal of the Fc portion

of wild-type human IgG (Fc(WT)) by overlapping extension PCR with Phusion DNA polymerase. Then, the PCR products were digested with restriction endonucleases Hind III and Bgl II. The gel purified PCR products were then ligated to the pCMV-MCS expression vector using T4 DNA ligase.

### **3.4.3 Protein Expression and Purification**

CHO-S cells were incubated in FreeStyle CHO Expression Medium (Life Technologies) with 8 mM l-glutamine (Life Technologies) at 37°C in a humidified atmosphere with 8% CO<sub>2</sub> and transfected with gene expression DNA constructs encoding the protein of interest using the TransIT-PRO Transfection Kit (Mirus Bio LLC, Madison, WI)) when the number of the cells reached  $1.0 \times 10^6$  cells/mL. The culture medium was harvested 6 days after transfection. The Fc-fused protein (BChE or AChE) secreted into the culture medium was purified by protein A affinity chromatography. After removing cells by centrifugation, the cell-free culture medium was mixed with rmp Protein A Sepharose Fast Flow (GE Healthcare Life Sciences) pre-equilibrated with 20 mM Tris·HCl, pH 7.4, and incubated for overnight at 6°C with occasional stirring. Then, the suspension was packed in a column and washed with 5 column volume (CV) of 20 mM Tris·HCl, pH 7.4, containing 200 mM NaCl until an OD<sub>280</sub> < 0.02 was achieved; then the protein was eluted by adjustment of the pH and salt concentration. HSA-fused Coch1 was also expressed as described above. Using the AlbuPure matrix (Prometic Life Sciences Inc., Laval, Canada), Coch1-HSA was purified where the cell-free culture medium was loaded onto packed bed pre-equilibrated with 50 mM sodium acetate, pH 5.3, extensively washed with 8 CV of equilibration buffer. Then, the resin bound protein was eluted with 5 CV of

50 mM ammonium acetate, pH 7.4. For buffer exchange, the eluate was dialyzed in storage buffer (50 mM Hepes, 20% sorbitol, 1 M glycine, pH 7.4) by Millipore Centrifugal Filter Units. The entire purification process was performed in a cold room at 8°C and the purified proteins were stored at -80°C until the activity tests.

#### **3.4.4 Enzyme Activity Assays**

Enzymatic hydrolyses of heroin to 6-MAM and 6-MAM to morphine were tested under the following assay conditions. Incubations (50 µl final volume) contained purified enzyme and heroin or 6-monoacetylmorphine (6-MAM) in 0.1 M phosphate buffer, pH 7.4. All the activity assays were performed at 37°C. For heroin hydrolysis, 0.02 to 2.5 mM heroin was incubated with 35 nM designated enzyme. For 6-MAM hydrolysis, 0.002 to 2 mM 6-MAM was incubated with 2 µM designated enzyme. The reaction time and concentration were adjusted such that no more than 10% of substrate was depleted during reaction. The reaction was terminated, and protein was precipitated by the addition of 100 µl of iced 50% acetonitrile/0.5 M hydrochloric acid, followed by 5 min centrifugation at 15,000 g. The resulting supernatants were subjected to reverse-phase HPLC (RP-HPLC) on a 5 µm C18 110 Å column (250 × 4.6 mm; Gemini) (Life Technologies) and RP-HPLC was performed using the mobile phase consisting of 20% acetonitrile in 0.1% TFA. The remaining substrate and resulting products were monitored by a fluorescence detector with an excitation wavelength of 230 nm and emission wavelength of 315 nm and by monitoring UV absorbance at 230 nm. The quantification was based on a standard curve prepared using an authentic standard compound.

### 3.4.5 Molecular modelling

Heroin and 6-MAM binding with human AChE, BChE, and CocH1 were modelled by using our previously modelled structures of the same enzymes.<sup>280-281, 284-285</sup> Our previous molecular dynamics (MD) simulations on the structures of enzyme-substrate complexes started from the X-Ray crystal structures deposited in the protein databank (PDB) (AChE: code 1B41; BChE: 2XQF and 1P0P). Molecular docking and subsequent optimization were carried out using a similar protocol described previously.<sup>280</sup> Briefly, the acetyl group of the substrate (heroin or 6-MAM) was positioned in the oxyanion hole (consisting of Gly116, Gly117, and Ala199 in BChE, or Gly121, Gly122, and Ala204 in AChE, or Gly116, Gly117, and Ser199 in CocH1), and the positively charged amino-group of the substrate (heroin and 6-MAM) was placed in the choline-binding site near Trp82 in BChE and CocH1 or Trp86 in AChE. Finally, the binding models of heroin and 6-MAM in the corresponding enzyme-substrate complexes were optimized by performing the energy minimization.



## Chapter IV. Oligomerization and Catalytic Parameters of Human UDP-glucuronosyltransferase 1A10

Uridine 5'-diphospho-glucuronosyltransferase (UDP-glucuronosyltransferase, UGT), as an integral membrane protein localized in the endoplasmic reticulum, has the ability to detoxify potentially hazardous xenobiotic substances. Most UGTs are expressed in liver, but UGT1A10 has proven an extra-hepatic enzyme considerably expressed throughout the gastrointestinal track. Earlier studies indicated that different UGT isoforms could exist in higher-order homo-oligomers or at least dimers within the membrane, but the formation of intermolecular disulfide bridges between UGT molecules was not often observed. In this study,<sup>286</sup> we expressed recombinant human UGT1A10 in HEK293 and CHO cells to examine its oligomeric states and characterize its enzymatic activities against two therapeutically interesting substrates, morphine and entacapone, including determination of the catalytic rate constant ( $k_{cat}$ ) values for the first time. The research described in this chapter has been published in to *Drug Metabolism and Distribution*.<sup>287</sup> It was observed that majority of the UGT1A10 protein expressed in HEK293 cells existed in covalently cross-linked higher-order oligomers *via* formation of intermolecular disulfide bonds, whereas formation of the intermolecular disulfide bonds was not observed in the UGT1A10 protein expressed in CHO cells. Due to the formation of the covalently cross-linked higher-order oligomers, the UGT1A10 protein expressed in HEK293 cells had much lower catalytic activities (particularly the catalytic rate constant  $k_{cat}$ ) against both morphine and entacapone, compared to the UGT1A10 protein form expressed in CHO cells against the corresponding substrates.

#### 4.1 UDP-glucuronosyltransferase (UGT)

UGTs are membrane-bound proteins localized in the endoplasmic reticulum (ER). These proteins catalyze the glucuronic acid transfer from UDP-glucuronic acids (UDP-GA) to small molecules (substrates). Human UGTs are divided into two gene families, UGT1 and UGT2, based on evolutionary divergence<sup>288</sup> and play a crucial role in detoxification and excretion of potentially hazardous xenobiotics as well as endogenous substances. However, it has been difficult to study the catalytic activity of an individual UGT in native tissues because many different UGTs are expressed in the same tissues such as liver and their substrate specificities have proven overlapped frequently. Therefore, it has become common in the field to use recombinant enzymes exogenously expressed in different cell lines, when testing whether a specific substrate of interest is converted by a UGT isomer into a glucuronide form and comparing the catalytic efficiencies of UGT isoforms against a specific substrate. Added to this, the absence of a suitable method to purify UGTs as sufficiently active and mono-dispersed proteins has limited the studies toward understanding the structure-function relationships of these proteins.

Morphine remains the most valuable opioid analgesic for the management of moderate to severe pain.<sup>289</sup> Morphine undergoes a considerable first-pass metabolism by UGTs in animals and humans after oral administration. The inactive morphine-3-glucuronide (M3G) and analgesically potent morphine-6-glucuronide (M6G) are the major metabolites of morphine in the body and they are mainly excreted by the urinary system.<sup>290-292</sup> Although human liver still appears to be a prime organ responsible for the formation of morphine glucuronides,<sup>290</sup> the respective contribution of the gastrointestinal tract and liver to the first-pass extraction of orally administered morphine remains unclear.<sup>292</sup> In 2003, a

systemic study of the recombinant human UGT isoforms related to morphine glucuronidation showed that UGT1A10, an extra-hepatic enzyme restrictively expressed in the digestive tract, catalyzes the conversion of morphine to M3G, not M6G, with a relatively higher rate, compared to the other UGT1A isoforms tested (UGT1A1, 1A3, 1A6, 1A8, and 1A9).<sup>293</sup> However, their report only compared the measured  $V_{\max}$  and  $K_M$  values of UGT isomers for the M3G formation, and they were unable to determine their actual catalytic rate constant ( $k_{\text{cat}}$ ) values, which limits the interpretation of the kinetic data concerning the actual catalytic activities of individual UGTs.

**Table 4.1** Kinetic constants for morphine 3- and 6-glucuronide formation by human recombinant UDP-glucuronosyltransferases stably expressed in HEK293 cells.<sup>293</sup>

Human UGTs	$V_{\max}$ (pmol/min/mg)	$K_M$ (mM)
UGT1A10	$628.2 \pm 92.4$	$12.6 \pm 2.6$
UGT2B7	$183.3 \pm 15.4$	$58.3 \pm 3.2$
UGT1A9	$31.7 \pm 3.1$	$37.4 \pm 5.6$
UGT1A6	$20.8 \pm 2.6$	$18.0 \pm 3.7$
UGT1A8	$12.9 \pm 1.0$	$2.6 \pm 0.3$
UGT1A3	$10.3 \pm 0.6$	$3.2 \pm 0.3$
UGT1A1	$4.5 \pm 0.2$	$18.7 \pm 1.4$

## **4.2 The focuses of this research**

In the present study, we first analyzed the expression of recombinant human UGT1A10 protein in HEK293 and CHO cells by western blotting. Then, we kinetically characterized its glucuronidating activities for two different substrates, morphine and entacapone, an inhibitor of catechol-O-methyltransferase (COMT) used in the treatment of Parkinson's disease. The kinetic characterization has allowed us to determine the  $k_{cat}$  values of UGT1A10 against morphine and entacapone for the first time. It has also been demonstrated that recombinant human UGT1A10 protein expressed in HEK293 cells forms oligomerized complexes that are covalently cross-linked by disulfide bonds, but that expressed in CHO cells barely forms cross-linked disulfide bonds. In addition, the complete catalytic parameters obtained for membrane-bound UGT1A10 against morphine and entacapone reveal that the catalytic activities of recombinant UGT1A10 proteins are remarkably different, depending on which type of cell line is used to express the protein.

## **4.3 Results**

### **4.3.1 Overexpression of human UGT1A10 in CHO and HEK293 cells**

When expressed in CHO and HEK293 cells, recombinant human UGT1A10 protein was detected majorly at ~65 kDa (monomeric size) by immunoblotting with an anti-UGT1A antiserum. After longer exposure UGT1A10 protein was also observed as unexpected bands at approximately ~130 kDa, and higher than ~130 kDa in both microsomes prepared from UGT1A10-6xHis-overexpressing stable CHO or HEK293 cells (three independent western blotting tests showed the same bands) (Fig. 4.1). The bands with molecular weight higher than ~65 kDa are neither endogenous UGT1A nor UGT2B

isoforms as they were not detected in the microsomal proteins of native CHO and HEK293 cells by immunoblotting with anti-UGT1A or UGT1B antiserum (data not shown), which indicates that the unexpected high molecular-weight bands were extremely stable homo-oligomers of UGT1A10 or hetero-oligomeric complexes with another protein.

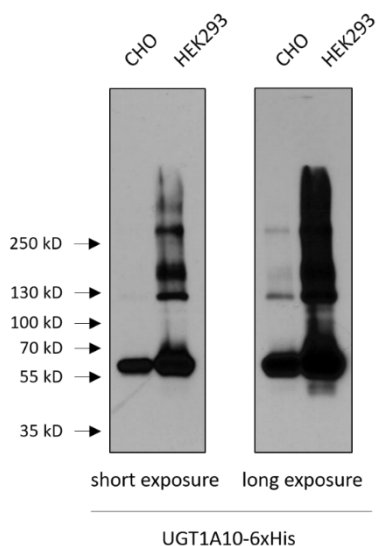


**Figure 4.1** Western blot analysis of UGT1A10 protein in microsomes prepared from UGT1A10-6xHis-overexpressing stable CHO and HEK293 cell lines. Microsomes were boiled at 95°C for 10 min in the presence of 100 mM dithiothreitol (DTT) prior to electrophoresis

Previously, Matern *et al.*<sup>294</sup> showed that a form of active rat UGT extracted from rat liver appears with an apparent molecular mass = 316 kDa and the subunit molecular weight was determined as ~54 kDa, suggesting that the formation of oligomeric UGT complexes occurred naturally or inadvertently after purification. In line with this, recent reports also support<sup>295-297</sup> that the UGT proteins existed in the membrane tissue as higher-order oligomers (at least dimers). These observations led us to test whether the majority of

recombinant human UGT1A10 enzyme in CHO and HEK293 cells are also highly organized within the membrane of ER and exist as homo-oligomeric complexes. For this purpose, UGT1A10 proteins in microsomes prepared from the stable cell lines indicated above were first exposed to different denaturing conditions then separated on SDS-PAGE followed by immunoblot detection with anti-UGT1A antibody as described in the material method section. We found that the majority of HEK293-expressed UGT1A10 (UGT1A10<sup>HEK293</sup>) enzyme molecules formed the higher-order oligomers that were completely resolved to the monomeric size of UGT1A10 upon SDS-PAGE after treatment with dithiothreitol (DTT) and the minority migrate as a dimer after reduction. However, the covalently cross-linked higher-order oligomers were not observed in the CHO-expressed UGT1A10 (UGT1A10<sup>CHO</sup>). Boiling the samples neither formed aggregates of UGT1A10 proteins nor made changes in the results (Fig. 4.2). To examine whether the oligomeric UGT1A10 complexes seen in the stable HEK293 cells are homeric or heteromeric, anti-UGT1A immunoprecipitation was performed. However, whereas UGT1A10<sup>CHO</sup> enzyme was efficiently precipitated, UGT1A10<sup>HEK293</sup> enzyme was not in the same experimental condition.

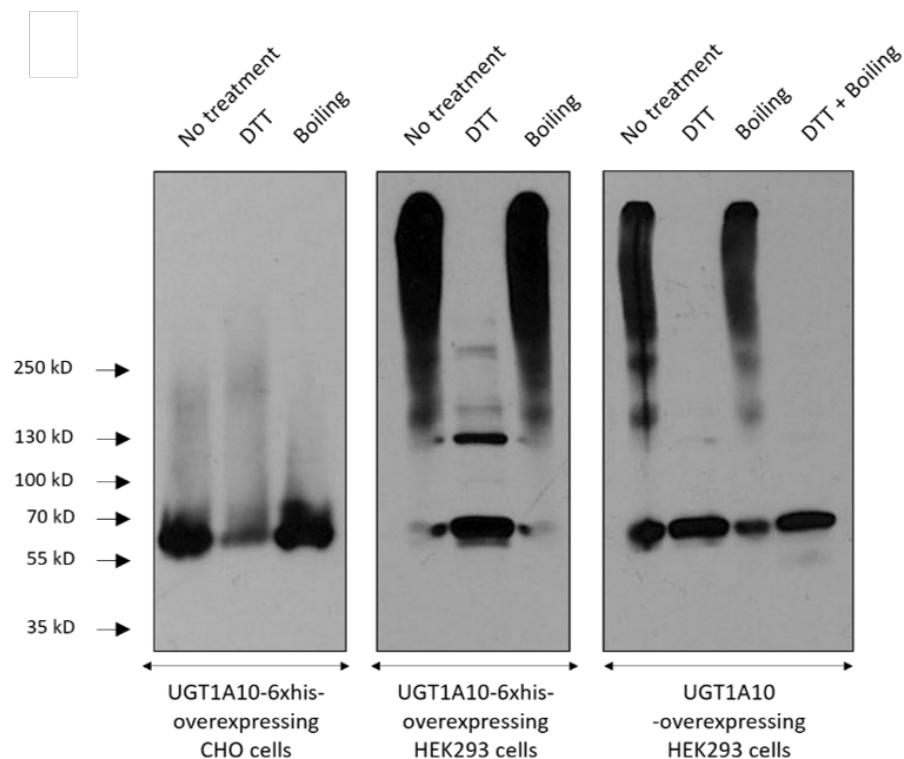


**Figure 4.2** Analysis of recombinant UGT1A10 expression. SDS-polyacrylamide gel electrophoresis of microsomes under different denaturing conditions, followed by immunoblot analysis. DTT, electrophoresis after reduction with 100 mM DTT; Boiling, electrophoresis after boiling; No treatment, No DTT and boiling before electrophoresis.

#### 4.3.2 Quantification of the levels of recombinant UGT1A10 in microsomes prepared from stable cells

Considering that disulfide bridges considerably contribute to the interaction of UGT1A10 expressed in HEK293, but not in CHO cells, a question was whether the UGT1A10 enzyme activity may be altered by the formation of intermolecular crosslinks *via* disulfide bonds between UGT1A10 molecules. To address the question, the concentrations of UGT1A10 expressed using the two stable cell lines were first determined

and then their kinetic parameters ( $k_{\text{cat}}$  and  $K_M$ ) values were evaluated and compared in subsequent kinetic assays. As shown in Fig. 4.3A, we purified UGT1A10 from microsome prepared from the UGT1A10-6xHis-overexpressing stable CHO cells and determined its concentration as noted in the Materials and Method section. Differing amounts of purified UGT1A10 were then loaded as indicated to obtain a single blot with densitometric readings on the linear part of the curve for membrane-bound UGT1A10 in microsomes (Fig 4.3B & C). The concentrations of membrane-bound UGT1A10 in microsomes prepared from the stable HEK293 and CHO cells were determined to be 6.69 and 3.02 ng/ $\mu\text{g}$  of microsomal proteins, respectively.



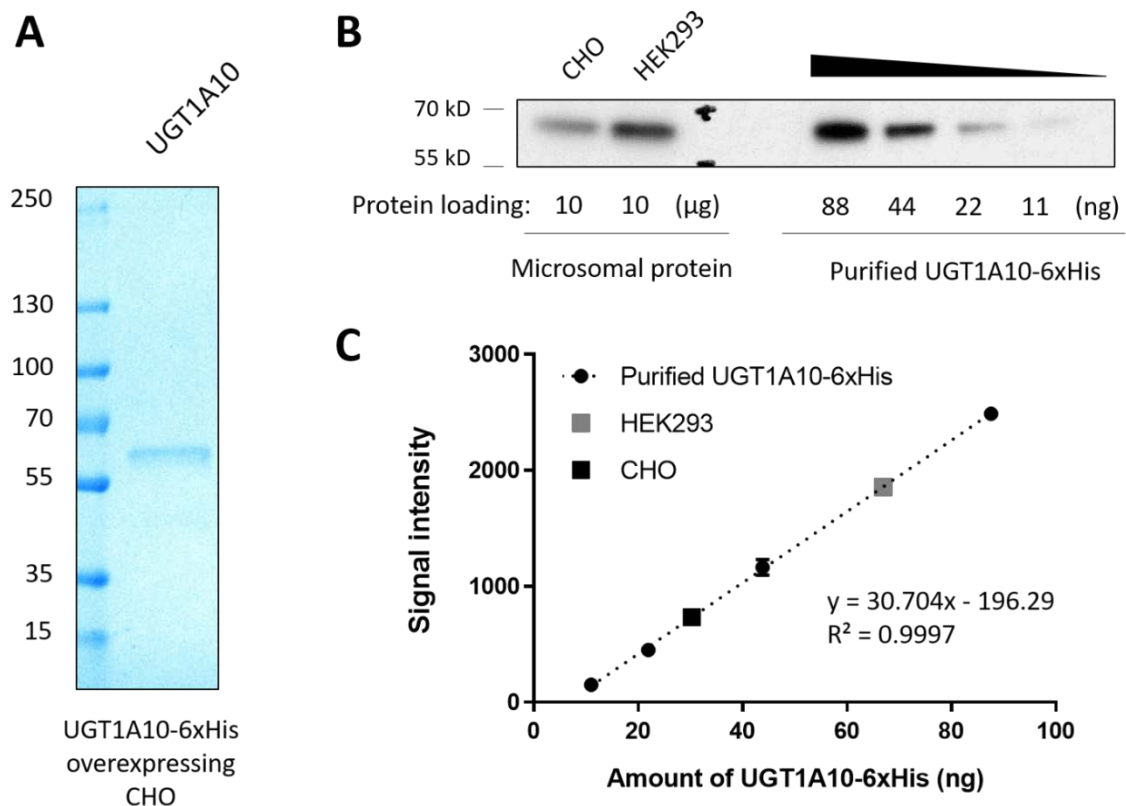


**Figure 4.3** Quantification of the levels of UGT1A10 in microsomes. (A) SDS-PAGE analysis of pure UGT1A10-6xHis extracted from microsome prepared from UGT1A10-6xHis-overexpressing stale CHO cells. The sizes of the molecular mass markers are indicated on the *left* in kDa. (B) Chemiluminescent blot of dilution series of purified UGT1A10-6xHis and two unknown amounts of membrane-bound UGT1A10-6xHis. (C) The linear dynamic range of film-based detection for UGT1A10-6xHis. The graph shows a quantitative level of UGT1A10-6xHis protein for the corresponding chemiluminescence signal intensity. Each dot represents the average of duplicates and its values are expressed as the mean  $\pm$  standard deviation.

### 4.3.3 Kinetics of morphine glucuronidation by recombinant human UGT1A10

To test whether HEK293- and CHO-expressed UGT1A10 proteins forms have a similar catalytic activity against morphine, we investigated the kinetics for the formation of morphine-3-glucuronide (M3G) catalyzed by UGT1A10. As shown in a representative of HPLC chromatograms depicting the peak for M3G (Fig. 4.4A), the glucuronidation activity was observed for both membrane-bound UGT1A10<sup>CHO</sup> or UGT1A10<sup>HEK293</sup> enzymes against morphine (Fig. 4.4, top and middle) and the peak (M3G) with a retention time of 5.4 min disappeared after  $\beta$ -glucuronidase was added to the reaction (Fig. 4.4, bottom).

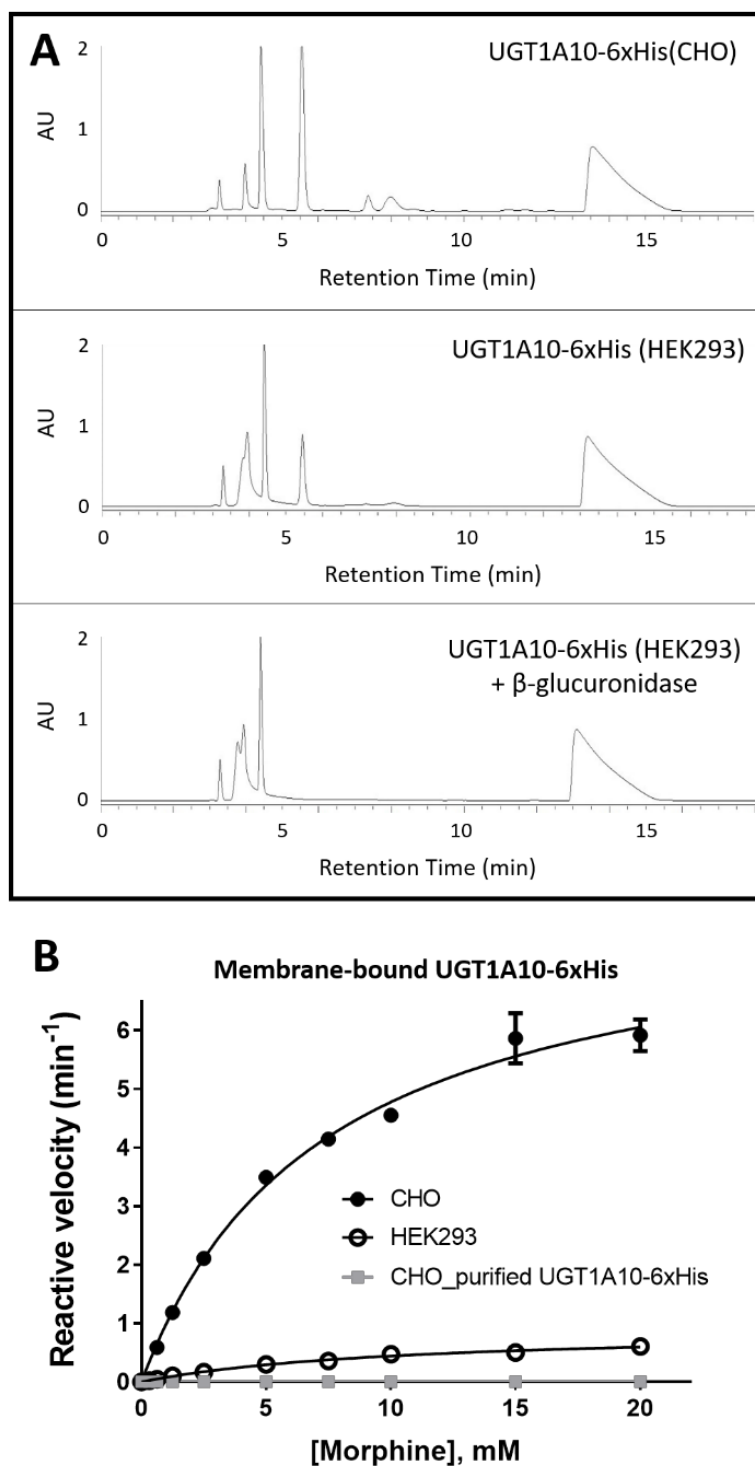


**Figure 4.4** Kinetic analysis of the formation of morphine-3-glucuronide (M3G) by UGT1A10. (A) High-performance liquid chromatography (HPLC) analysis of M3G

formation using microsomes prepared from UGT1A10-6xHis-overexpressing stable cell lines. Top, membrane-bound UGT1A10-6xHis expressed in CHO cells; middle, membrane-bound UGT1A10-6xHis expressed in HEK293 cells; bottom, membrane-bound UGT1A10-6xHis expressed in HEK293 cells with treatment with  $\beta$ -glucuronidase. (B) M3G formation by membrane-bound UGT1A10-6xHis enzymes in CHO cells (●) or in HEK293 cells (○), or by purified UGT1A10-6xHis protein (■) were determined at substrate concentrations of 0.1 to 20 mM. Kinetic parameters ( $k_{cat}$  and  $K_M$ ) were determined by fitting the measured reaction rate data to the Michaelis-Menten kinetic equation using the Prism5.01 software. Each dot is the representative of the average of triplicates and its values are expressed as the mean  $\pm$  standard deviation.

The generated kinetic data are depicted in Fig. 4.4B, and the kinetic parameters obtained are summarized in Table 4.2. As shown in Table 4.2, compared to membrane-bound UGT1A10<sup>HEK293</sup>, membrane-bound UGT1A10<sup>CHO</sup> had a higher  $k_{cat}$  value (8.26 min<sup>-1</sup> compared to 0.90 min<sup>-1</sup>) and a slightly lower  $K_M$  value (7.3 mM compared to 10.4 mM). These data indicate that the major difference between membrane-bound UGT1A10<sup>CHO</sup> and UGT1A10<sup>HEK293</sup> in the catalytic efficiency against morphine ( $k_{cat}/K_M = 1.13 \times 10^3$  min<sup>-1</sup> · M<sup>-1</sup> for UGT1A10<sup>CHO</sup> vs  $k_{cat}/K_M = 86.5$  min<sup>-1</sup> · M<sup>-1</sup> for UGT1A10<sup>HEK293</sup>) is largely attributed to their turnover numbers ( $k_{cat}$ ) for the M3G formation. However, glucuronidation of morphine by the purified UGT1A10 was not observed under the experimental conditions generating the kinetic data depicted in Fig. 4.4B.

**Table 4.2** Kinetic parameters of human UGT1A10-6xHis against morphine<sup>a</sup> Relative catalytic efficiency ( $k_{\text{cat}}/K_{\text{M}}$ )

UGT1A10-6xHis	$K_{\text{M}}$	$k_{\text{cat}}$	$k_{\text{cat}}/K_{\text{M}}$	RCE <sup>a</sup>	R <sup>2</sup>
	<i>mM</i>	<i>min</i> <sup>-1</sup>	<i>min</i> <sup>-1</sup> · <i>M</i> <sup>-1</sup>		
Membrane-bound_HEK293	10.4 ± 0.96	0.90 ± 0.04	86.5	1	0.994
Membrane-bound_CHO	7.30 ± 0.81	8.26 ± 0.38	1.13 × 10 <sup>3</sup>	13.0	0.988

**4.3.4 Kinetics of entacapone glucuronidation by recombinant human UGT1A10**

Entacapone is an inhibitor of catechol-O-methyltransferase (COMT) used in the treatment of Parkinson's disease. Entacapone is known to be metabolized into entacapone 3-*O*-glucuronide by different UGTs. As shown in Fig. 4.5, the peak for entacapone 3-*O*-glucuronide (retention time = 9.9 min) appeared in the presence of membrane-bound UGT1A10<sup>CHO</sup> or UGT1A10<sup>HEK293</sup> (top and middle) enzyme, and the peak was no longer found if the reaction was further incubated with β-glucuronidase (bottom), indicating that entacapone was recognized by both the membrane-bound UGT1A10 enzyme forms as a substrate.

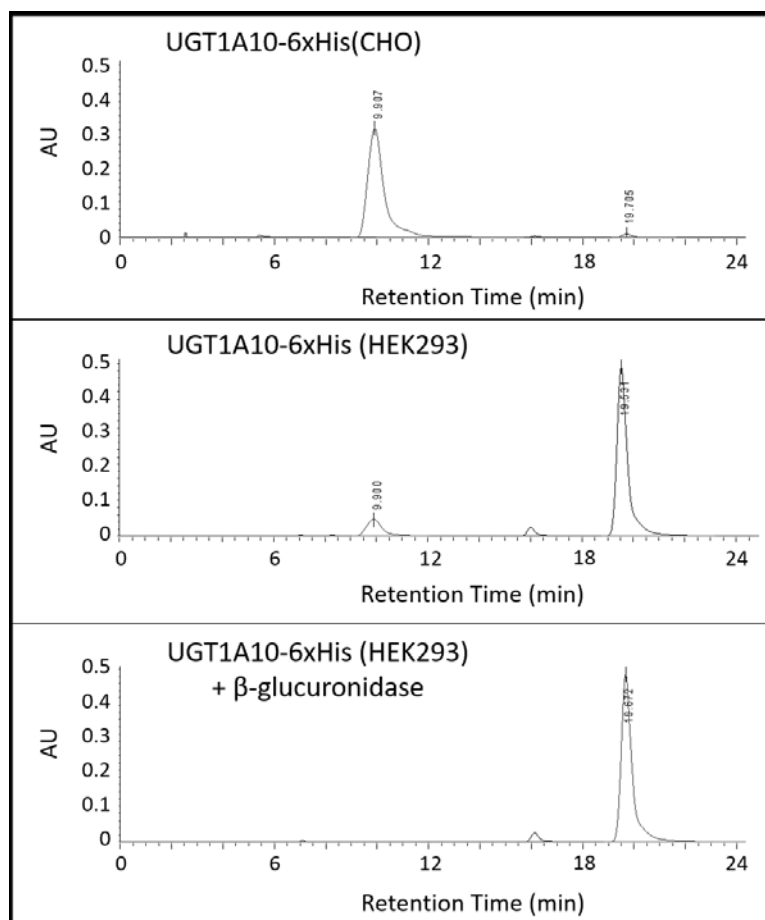


**Figure 4.5** HPLC analysis of the formation of entacapone 3-*O*-glucuronide using microsomes prepared from UGT1A10-6xHis-overexpressing stable cell lines. Top, membrane-bound UGT1A10-6xHis expressed in CHO cells; middle, membrane-bound UGT1A10-6xHis expressed in HEK293 cells; bottom, membrane-bound UGT1A10-6xHis expressed in HEK293 cells with treatment with  $\beta$ -glucuronidase.

To assess whether the observed differences in the catalytic activity against morphine between membrane-bound UGT1A10<sup>CHO</sup> and UGT1A10<sup>HEK293</sup> are also manifested against a different substrate, additional kinetic assay was performed against entacapone. The obtained kinetic data are depicted in Fig. 4.6A, and the kinetic parameters determined are summarized in Table 4.3.

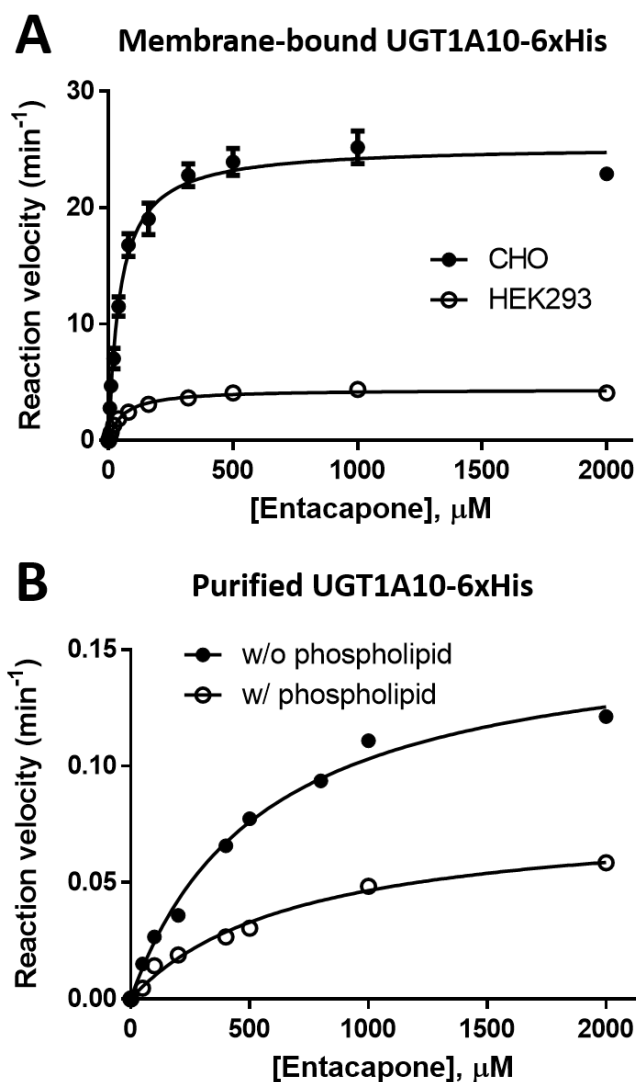


**Figure 4.6** Kinetic analysis of entacapone 3-*O*-glucuronide formation by UGT1A10. (A) Formation of entacapone 3-*O*-glucuronide by membrane-bound UGT1A10-6xHis protein

in CHO cells (●), or in HEK293 cells (○) were determined at substrate concentrations of 3 to 2000  $\mu\text{M}$ . (B) Formation of entacapone 3-*O*-glucuronide by purified UGT1A10-6xHis protein was determined at substrate concentrations of 3 to 2000  $\mu\text{M}$  in the presence (●) or absence (○) of 1 mg/ml of phosphatidylcholine type X-E. Kinetic parameters ( $k_{\text{cat}}$  and  $K_{\text{M}}$ ) were determined by fitting the generated reaction rate data to the Michaelis-Menten kinetic equation using the Prism5.01 software. Each dot refers to the average of duplicate or triplicates and its values are expressed as the mean  $\pm$  standard deviation.

As shown in Table 4.3, the expected similar differences in glucuronidation kinetics for entacapone were also observed between membrane-bound UGT1A10<sup>CHO</sup> and UGT1A10<sup>HEK293</sup>. A substantially higher catalytic efficiency against entacapone was observed for membrane-bound UGT1A10<sup>CHO</sup> compared to UGT1A10<sup>HEK293</sup> ( $5.53 \times 10^5 \text{ min}^{-1} \cdot \text{M}^{-1}$  compared to  $7.71 \times 10^4 \text{ min}^{-1} \cdot \text{M}^{-1}$ ) and this difference is mainly due to a substantially higher  $k_{\text{cat}}$  value ( $25.3 \text{ min}^{-1}$  compared to  $4.39 \text{ min}^{-1}$ ) and a slightly lower  $K_{\text{M}}$  value ( $45.7 \mu\text{M}$  compared to  $56.9 \mu\text{M}$ ) of membrane-bound UGT1A10<sup>CHO</sup> compared to membrane-bound UGT1A10<sup>HEK293</sup>.

Added to this, although the purified UGT1A10 showed a detectable enzymatic activity toward entacapone, the experimental  $K_{\text{M}}$  and  $k_{\text{cat}}$  values of membrane UGT1A10<sup>CHO</sup> were indeed increased by a factor of about 15 ( $45.7 \mu\text{M}$  compared to  $703 \mu\text{M}$ ) and decreased by a factor of about 320 ( $25.3 \text{ min}^{-1}$  compared to  $0.079 \text{ min}^{-1}$ ), respectively, during the purification process (Table 4.3). Moreover, it was observed that the rate constant of entacapone glucuronidation by the purified UGT1A10 was only slightly increased by the addition of phospholipid sonicated (Fig. 4.6B & Table 4.3).



**Table 4.3** Kinetic parameters of human UGT1A10-6xHis against entacapone<sup>a</sup> Relative catalytic efficiency ( $k_{\text{cat}}/K_{\text{M}}$ )

UGT1A10-6xHis	$K_{\text{M}}$	$k_{\text{cat}}$	$k_{\text{cat}}/K_{\text{M}}$	RCE <sup>a</sup>	R <sup>2</sup>
	$\mu\text{M}$	$\text{min}^{-1}$	$\text{min}^{-1} \cdot \text{M}^{-1}$		
Membrane-bound_HEK293	$56.9 \pm 4.1$	$4.39 \pm 0.07$	$7.71 \times 10^4$	1	0.987
Membrane-bound_CHO	$45.7 \pm 4.5$	$25.3 \pm 0.6$	$5.53 \times 10^5$	7.17	0.992
Purified_CHO w/o phospholipid	$703 \pm 116$	$0.079 \pm 0.005$	$1.12 \times 10^2$	$1.45 \times 10^{-3}$	0.991
Purified_CHO w/ phospholipid	$554 \pm 72$	$0.16 \pm 0.01$	$2.88 \times 10^2$	$3.74 \times 10^{-3}$	0.995

#### 4.4 Discussion and Conclusion

An extrahepatic human UGT1A10 was expressed as an active enzyme using lentivirus-infected HEK293 and CHO cells. Our recombinant UGT1A10 has a C-terminal hexa-histidine tag which allows for efficient single-step chromatographic purification using IMAC. Indeed, human recombinant UGTs containing a His tag at the C-terminus have been widely used for the enzymatic characterization, structure determination, and substrate screening studies of the UGTs.<sup>137, 298-301</sup> Zhang *et al.*<sup>302</sup> demonstrated that only mild increase in the  $K_{\text{M}}$  values was observed in UGT1A9 and 2B7 containing the C-terminal His-tag, but no differences in parameters such as the kinetic model. In consistent with the findings, we also found that CHO-expressed recombinant UGT1A10 proteins displayed a similar  $K_{\text{M}}$  values for morphine ( $K_{\text{M}} = 7.30 \pm 0.81$  mM for UGT1A10-6xHis vs  $K_{\text{M}} = 6.60 \pm 0.33$  mM for UGT1A10), regardless of whether or not it had the addition of a His tag to its C-terminal end, which suggests that UGT1A10-6xHis is a good model for the functional studies.

Previously, Kurkela *et al.*<sup>298</sup> reported a good method to purify human UGT1A9 as

an active form using Triton X-100. In this study, we demonstrated that their method also works for purification of active UGT1A10 which shares about 93.2% identical protein sequence with UGT1A9. However, the purification process caused an irreversible and considerable decrease in UGT1A10 enzymatic activity, which cannot be merely compensated by phospholipid addition. Actually, this observation is consistent with the findings of Kurkela *et al.*<sup>298</sup> Compared to membrane-bound UGT1A10<sup>CHO</sup>, the  $K_M$  and  $k_{cat}$  values for entacapone were reduced ~15 and ~320 times, respectively, during the purification process.

The oligomeric states of the UGTs have been studied for more than two decades. One of the main reasons for the attempts was to answer the question concerning whether or not the enzymatic activities of the UGTs are affected by their oligomeric states. The two previous studies studying pure UGT isoforms extracted from the native tissues showed that UGTs could be present as tetramers or even higher-order oligomers.<sup>294, 303</sup> By nearest-neighbor cross-linking and yeast two-hybrid analysis, Ghosh *et al.*<sup>295</sup> also revealed that recombinant human UGT1A1 enzymes within microsomal membrane form homo-oligomers. Added to this, a study using fluorescence resonance energy transfer as a tool to demonstrate oligomerization of UGT1A7 proteins reported<sup>296</sup> that ~90% of UGT1A7 proteins existed as homo-oligomeric complexes in live cells. In this study, we found that most of recombinant human UGT1A10 enzymes expressed in HEK293 cells formed the covalently cross-linked higher-order oligomers *via* intermolecular disulfide bonds (Fig. 4.2). To the best of our knowledge, this is not only the first demonstration of the oligomerized UGT1A10 complexes, but also the first evidence to show the presence of complicated disulfide bridges to form higher-order UGT complexes bigger than a dimer.

Considering that the covalently cross-linked homo-oligomers are not frequently observed in recombinant human UGT1A1, 1A4, and 1A6 enzymes expressed in HEK293 cells, as reported by Fujiwara *et al.*,<sup>304</sup> the observed multiple disulfide bonds formed in the oligomerized UGT1A10 complexes seem to be unique.

Interestingly, we also found that CHO-expressed UGT1A10 was barely cross-linked *via* disulfide bridges, unlike the HEK293-expressed UGT1A10 (Fig. 4.1 & 4.2). This finding led us to ask whether there is any difference in activity between these UGT1A10 enzyme forms. Our kinetic assays on the HEK- and CHO-expressed UGT1A10 enzyme forms for their catalytic activities against morphine and entacapone revealed that HEK293-expressed UGT1A10 had a similar  $K_M$  value, but a substantially decreased  $k_{cat}$  value, compared to the CHO-expressed UGT1A10. These findings suggest that the intermolecular disulfide bonds in the HEK293-expressed UGT1A10 protein would substantially decrease the catalytic activities of the enzyme against both of the substrates (Tables 4.2 & 4.3). However, since the UGT1A10 enzyme forms in the microsomal fractions, not the purified enzyme forms, were utilized for our enzyme activity assays, we still cannot completely rule out alternative possibilities such as the presence of another key determinant of UGT1A10 enzyme activity. Indeed, we also tested whether an enzymatic activity of HEK293-expressed UGT1A10 can increase by disrupting the S-S bonds. It was observed that both membrane-bound UGT1A10<sup>HEK293</sup> and UGT1A10<sup>CHO</sup> became inactive after incubated with 100 mM DTT for 1 hr, which strongly suggests that the intramolecular disulfide bonds of UGT1A10 enzyme are crucial for its activity or stability. Despite of the experimental limitation, our observations clearly indicate that the enzymatic activity and post-translational modification of UGT1A10 can be significantly affected by the cell line

used to express the protein. In addition, according to the modeled van der Waals surface of the UGT1A10 protein structure (Fig. 4.7),<sup>287</sup> UGT1A10 has three cysteine residues (C72, C183, and C277) on the protein surface. C183 of one UGT1A10 molecule could form a disulfide bond with C72 or C277 of another UGT1A10 molecule, *i.e.* forming intermolecular disulfide bonds. Further, there are multiple asparagine residues (that are potential glycosylation sites) nearby C72 and C277 on the protein surface. Different glycan structures formed in different types of cells could have differential effects on formation of the intermolecular disulfide crosslinks, which helps us to understand the observed remarkable oligomerization difference between the two cell lines.

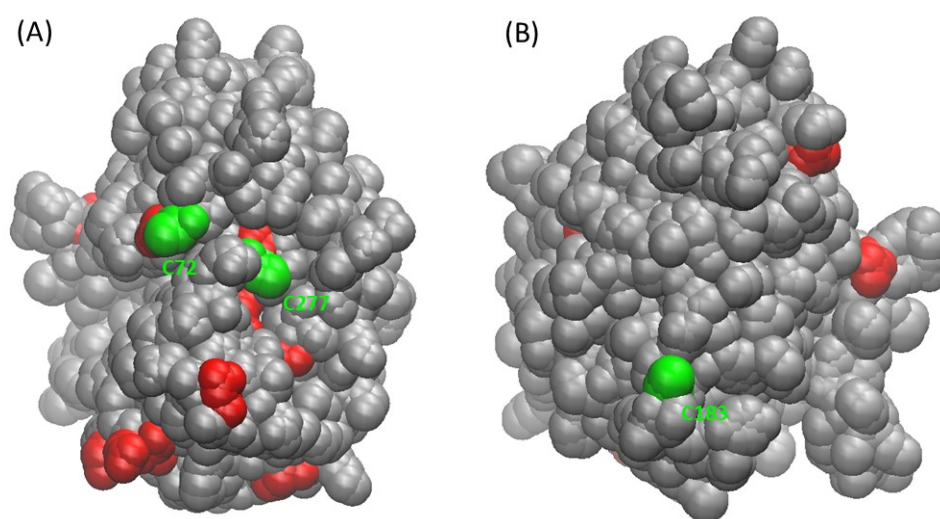


**Figure 4.7** The modeled van der Waals surface of the UGT1A10 protein structure, showing three solvent-accessible cysteine residues (C72, C183, and C277 in green color). Panels A and B show two sides of the protein, with C72 and C277 on one side and C183 on the opposite side. Indicated in red color are solvent-accessible asparagine residues (potential glycosylation sites). C72 and C277 are close to the entrance of the enzyme active-site

pocket. C72 or C277 of a UGT1A10 molecule may form a disulfide bond with C183 or C72 or C277 of another UGT1A10 molecule for crosslinking *via* intermolecular disulfide bonds. The crosslinking disulfide bonds involving C72 or C277 are expected to block the entrance of the enzyme active-site pocket and, thus, decrease the catalytic activity of the enzyme. The figure was provided by Drs. Kuo-Hao Lee and Yaxia Yuan.

Considering that a non-hepatic UGT1A10 enzyme is substantially expressed in human small intestine and colon with UGT1A1, 2B7, 2B15, and 2B17,<sup>305-308</sup> there still remains notable interest in the potential contributions of these enzymes to the first-pass metabolism of morphine in the gastrointestinal track after oral uptake. This is the first report of the complete kinetic parameters ( $k_{\text{cat}}$  and  $K_M$ ) of UGT1A10 against morphine and entacapone. Extending the lines of this study using the UGTs mentioned above will help to enhance our understanding of their significant contributions to the first-pass extraction of orally administered drugs including morphine.

## **4.5 Experimental details**

### **4.5.1 Chemicals and Materials**

Phusion DNA polymerases, restriction enzymes, and T4 DNA ligase were purchased from New England Biolabs (Ipswich, MA). All oligonucleotides were purchased from Eurofins MWG Operon (Louisville, KY). Chinese hamster ovary (CHO)–S cells, 293 human embryonic kidney–F (HEK293) cells, HEK-293FT, FreeStyle™ CHO Expression Medium, FreeStyle™ 293 Expression Medium, hypoxanthine/thymidine (HT) supplement, l-glutamine, 4–12% Tris-glycine Mini Protein Gel, and SimpleBlue SafeStain were purchased from Life Technologies (Carlsbad, CA). Morphine was provided by the National Institute on Drug Abuse (NIDA) Drug Supply Program. Morphine-3-glucuronide, entacapone, entacapone 3-*O*-glucuronide, UDP-GA, Triton X-100, saccharolactone,  $\beta$ -glucuronidase, phospholipids (phosphatidylcholine type X-E) and the solvents used in high-performance liquid chromatography (HPLC) were purchased from Sigma-Aldrich (St. Louis, MO). HisPur™ Cobalt Resin was obtained from Thermo Fisher Scientific (Waltham, MA). Centrifugal filter units were ordered from Millipore (Burlington, MA).

### **4.5.2 Generation of the stable cell line by lentivirus infection**

Cell lines stably overexpressing human UGT1A10 were generated using a lentivirus-based method described in our previous report.<sup>309</sup> The human UGT1A10-6xHis gene was first synthesized by Genscript Corporation (Piscataway, NJ) based on the published sequence in GenBank (NM\_019075.2) and inserted in the pCSC-SP-PW vector, lentivirus plasmid. In order to package the lentivirus particles carrying UGT1A10-6xHis gene, lentivirus was produced by co-transfecting pCSC-human UGT1A10-6xHis plasmid

with the two packaging vectors (pMDLg/pRRE and pRSV-Rev) and one envelope plasmid (pCMV-VSV-G) into HEK-293FT cells by lipofection. CHO-S and HEK293F cells were then transduced with the packaged lentivirus particles. The infected cells were recovered from the infection for 2 days or more and transferred to a shake flask for scaled-up culture. The obtained stable cell pools were kept frozen before use.

#### **4.5.3 Microsomal preparation**

Cells were washed with Tris-buffered saline (25 mM Tris base, pH 7.4, 138 mM NaCl, and 2.7 mM KCl) followed by a centrifugation at  $2,000 \times g$  for 5 min at 4°C. The cell homogenates were prepared through resuspending the cell pellets in 25 mM Tris-Cl, pH 7.4 and subjecting them to sonication. In order to remove cell debris or unbroken cells, the total cell homogenates were exposed to centrifugation at  $10,000 \times g$  for 20 min. Microsomes were prepared by ultracentrifugation of the supernatant at  $100,000 \times g$  for 1.5 hr and resuspending the resulting microsomal fraction in 25 mM Tris-Cl, pH 7.4. Microsomes (10 mg protein/ml) were stored at -70°C before use and their concentrations were determined using the Bradford assay from Thermo Fisher Scientific (Waltham, MA).

#### **4.5.4 Purification of UGT1A10**

The purification of recombinant human UGT1A10-6xHis protein followed a method described by Mika Kurkela,<sup>298</sup> except that a HisPur™ Cobalt Resin from Thermo Fisher Scientific (Waltham, MA) was utilized rather than a nickel-charged His Hi-Trap column from GE Healthcare Life Sciences (Pittsburgh, PA). Briefly, microsomes were suspended in an extraction buffer (25 mM Tris, pH 7.4, 500 mM NaCl, and 1% Triton X-

100) at 2 mg/ml of concentration followed by incubation for 10 min with shaking at 4°C. The suspension was centrifuged at  $100,000 \times g$  for 1 hr. The resultant supernatant was loaded onto a HisPur™ Cobalt Resin (Thermo Fisher Scientific) which has been pre-equilibrated with a washing buffer (25 mM Tris, pH 7.4, 500 mM NaCl, 0.05% Triton X-100, and 50 mM imidazole). After extensive washing with the washing buffer, bound His-tagged proteins were eluted by a stepwise gradient elution with imidazole in the presence of 0.05% Triton X-100 and 150 mM NaCl. The eluents were analyzed by SDS-PAGE and western blot for UGT1A. The concentration of purified UGT1A10-6xHis protein was determined using the Bradford assay (Thermo Fisher Scientific).

#### **4.5.5 Enzyme Activity Assays**

Enzymatic glucuronidation of morphine or entacapone was tested under the following assay conditions. All enzyme assays (100 µl final volume) contained 0.1 M phosphate buffer, pH 7.4, 5 mM MgCl<sub>2</sub>, 5 mM saccharolactone, 5 mM UDPGA, and 100 µg of microsomal protein or 50 ng of purified UGT1A10-6xHis. Phospholipid (1 mg/ml) was added to the assay mixtures containing the purified UGT1A10-6xhis. The concentrations of aglycone substrate ranged from 0.1 to 20 mM (for morphine) or from 3 to 2000 µM (for entacapone). To initiate the reactions, UDPGA (5 mM in incubation) was added to give a 100 µl final volume and then the reactions were incubated at 37°C with shaking. The reaction time was adjusted such that no more than 10% of substrate was depleted during reaction. Blank incubations were performed in the same manner, but without UDPGA. The reaction was terminated with 100 µl glycine-HCl, pH 2, containing 1% (v/v) Triton X-100. The stopped reactions were centrifuged to pellet precipitated



protein. The resulting supernatants were subjected to reverse-phase HPLC (RP-HPLC) on a 5  $\mu$ m C18 110 Å column (250  $\times$  4.6 mm; Gemini) (Life Technologies) and RP-HPLC was performed using the mobile phase consisting of 10% acetonitrile in 0.1% TFA and the remaining substrate and resulting products were monitored by monitoring UV absorbance at 230 nm (morphine and its glucuronide) or 315 nm (entacapone and its glucuronide). The quantification was based on a standard curve prepared using an authentic standard compound. All samples were prepared in duplicate or triplicate. GraphPad Prism 5.01 software (San Diego, CA) was utilized to analyze the kinetic data.

#### **4.5.6 Hydrolysis by $\beta$ -glucuronidase**

The reaction mixture was centrifuged at 13,000  $\times g$  for 10 min and the resultant supernatant was transferred to a new 1.5 ml microcentrifuge tube.  $\beta$ -Glucuronidase was added to the supernatant at final concentration of 4 U/ml. The sample was incubated at 37°C for 2 hr before the reaction was terminated by 100  $\mu$ l glycine-HCl, pH 2 containing 1% (v/v) Triton X-100.

#### **4.5.7 Western blot assay**

The levels of membrane-bound UGT1A10 protein in microsomes prepared from human UGT1A10-6xHis overexpressing cell lines were measured by western blot analysis using mouse anti-human UGT1A IgG obtained from Santa Cruz Biotechnology (Dallas, Texas) (1:3000 dilution as described in the manufacturer's instructions). HRP-conjugated goat anti-mouse IgG (Santa Cruz Biotechnology) was used at 1:4000 as a secondary antibody and UGT1A10 protein was finally detected by chemiluminescence using the

SuperSignal West Dura Extended Duration Substrate from Pierce Biotechnology (Waltham, MA). The levels of UGT1A10 were further quantified against a known amount of purified UGT1A10-6xHis protein by densitometric scanning of the blots using Quantity One software (Bio-Rad, Hercules, CA).

## **Chapter V. Development of a New Par-4 Entity with a Prolonged Duration of Action**

Prostate apoptosis response-4 (Par-4) is one of tumor suppressors which protect against neoplastic transformation. Par-4 is capable of inducing apoptosis selectively in cancer cells through either the intrinsic or extrinsic pathway. Especially, extrinsic apoptosis can be triggered by binding of extracellular Par-4 to cell surface GRP78 detected in various tumor types. In this study, we found that recombinant Par-4 protein shows a limited serum persistence in mice which may diminish its antitumor activity *in vivo*. Therefore, to improve the performance of short-lived Par-4 protein, Par-4 was genetically conjugated to a fragment crystallizable (Fc) of human IgG1 and expressed using the *E. coli* expression system for large-scale production. The results of apoptosis assay demonstrated that *E. coli*-derived novel Par-4 form (denoted as Fc(M1)-Par-4) retains significant proapoptotic activity. In addition, the pharmacokinetic study of Fc(M1)-Par-4 in mice revealed that Fc fusion leads to approximately 7-fold increase in the biological half-life of Par-4. We also demonstrated that a prolonged circulating half-life by Fc fusion improves the ability of Par-4 protein to suppress metastatic tumor growth *in vivo*.

A manuscript for the results described in this chapter will be submitted for consideration of publication. Dr. Ziyuan Zhou and Xirong Zhang helped multiple blood sample collections for the pharmacokinetic studies of Par-4 proteins in mice. Cell-based anti-cancer activity assay and *in vivo* anti-tumor activity assay were performed by Dr. Nikhil Hebbar and Nathalia Vitoria Pereira Araujo in the lab of Dr. Vivek M. Rangnekar.

### **5.1 The role of Par-4 as a tumor suppressor**

Prostate apoptosis response-4 (Par-4) is a tumor suppressor protein expressed

ubiquitously in a number of tissues. In 1994, the Par-4 gene was first discovered as an early apoptotic gene in a rat prostate cancer cell line incubated with ionomycin for apoptotic cell death.<sup>310-311</sup> It was demonstrated that overexpression of Par-4 is sufficient to elicit apoptotic cell death in most cancer cells.<sup>312</sup> In line with this observation, the Par-4 gene has been reported to be often deleted or significantly down-regulated in many different types of cancer including gastric and pancreatic cancer,<sup>313</sup> lymphoma,<sup>314</sup> and neuroblastoma.<sup>306</sup>

The core domain of Par-4 (amino-acid residues 145-204 in human Par-4; and 137-195 in rat Par-4), designated Selective for Apoptosis in Cancer cells (SAC), serves as the effector domain responsible for its pro-apoptotic activity.<sup>315</sup> Notably, this domain is 100% conserved in mouse, rat, and human homologs, which implies that Par-4 plays a critical role in the surveillance against tumors.<sup>315</sup> Indeed, mature Par-4 protein and its SAC domain both are capable to induce apoptotic cell death through both an intrinsic pathway (activated by intrinsic stimuli such as biochemical stress or DNA damage, and mainly modulated by Bcl-2 and Bax)<sup>316</sup> and extrinsic pathway (activated in response to external stimuli such as Fas ligand).<sup>317</sup> At first, it was believed that Par-4 protein localizes and acts only in both the cytoplasm and the nucleus for apoptosis induction,<sup>310, 318</sup> but subsequent studies revealed that Par-4 protein can be secreted to the extracellular space for action.<sup>311</sup> Extracellular Par-4 protein can induce apoptosis *via* caspase-3 and 8 activation when interacting with the stress response protein, *i.e.* glucose regulated protein 78 (GRP78), expressed on the surface of cancer cells.<sup>311</sup> It has been also demonstrated that exposure to purified recombinant Par-4 protein not only induce apoptosis in multiple types of cancer cells, but also inhibit tumor growth *in vivo*.<sup>312, 320-324</sup> Therefore, the current research of Par-4 related drug discovery has focused on development of small-molecule drugs that can facilitate Par-4 secretion from

normal cells for Par-4-dependent inhibition of tumor growth. Arylquin 1<sup>319</sup> and chloroquine (CQ), an anti-malarial drug,<sup>320</sup> have been discovered as a strong inducer of Par-4 secretion from normal or cancer cells.

## **5.2 The focuses of this research**

However, the purpose of our study on Par-4 is different. In the present study, we have engineered Par-4 to improve its *in vivo* stability, and investigated the potential application of the engineered Par-4 protein as a novel protein therapeutic itself for cancer treatment. We found that the tested recombinant Par-4 proteins stay in the circulatory system of mice only for a very short period of time, and especially 6xHis-Par-4 protein whose mass is below the threshold for glomerular filtration ( $\leq \sim 40$  kD) undergoes much rapid clearance from the blood. These results suggest a possibility that the therapeutic efficacy of natural or recombinant Par-4 protein for cancer treatment increases with enhanced *in vivo* performance. To address this possibility, Fc-fused Par-4 protein was generated and produced using the *E. coli* expression system. It is demonstrated that Fc-fusion enhances the performance of Par-4 in mice, which leads to increase in its potency to inhibit metastatic tumor growth *in vivo*. These results also strongly support that the tumor-suppressing activity of secreted Par-4 is potentially diminished due to its limited serum persistence *in vivo*. In this study, we discovered a novel Par-4 entity which is more suitable for potentially promising Par-4-based protein or gene therapy, and developed a new method for large-scale production of this therapeutically more valuable Par-4 entity.

## 5.3 Results

### 5.3.1 The short serum persistence *in vivo* of recombinant Par-4 (Par-4)

In a previous report by Zhao *et al.*,<sup>321</sup> it was demonstrated that the intravenous administration of recombinant TRX-Par-4 or TRX-SAC protein (prepared in *E. coli*) in immunocompetent C57/BL6 mice significantly suppressed lung metastasis of LLC1 (Lewis lung carcinoma line 1) cells in mice,<sup>321</sup> which implies that both extracellular Par-4 and SAC proteins are capable of inhibiting metastatic tumor growth *in vivo*. Thioredoxin (TRX) fusion protein is a frequently used tool to increase the solubility and expression of mammalian proteins when they are expressed heterologously in *E. coli*.<sup>322</sup> However, the pharmacokinetic profiles of both TRX-Par-4 and TRX-SAC proteins have not yet been studied despite of their considerable *in vitro* and *in vivo* anti-tumor activity against different cancer cells.<sup>311, 320-321</sup> Therefore, we first determined how long TRX-Par-4 or unfused Par-4 protein can stay in the circulatory system of mice. To address this question, Par-4 protein fused to the C-terminus of TRX or 6xHis-tag was prepared using the bacterial expression system (TRX-Par-4 and 6xHis-Par-4, respectively; see Fig. 5.1A), and each purified protein was then infused at the dose of 5 mg/kg in mice through tail vein injection. Blood samples were collected at varying time points after protein injection and analyzed by western blotting using anti-Par-4 antibody. The results revealed that both TRX-Par-4 (~50 kD) and 6xHis-Par-4 (~35 kD) proteins are quickly removed from the circulatory system. (Fig. 5.1B & C) TRX-Par-4 concentration decreased *in vivo* at a relatively slower than that of 6xHis-Par-4, with the former able to be observed up to 90 min after *i.v.* injection, while 6xHis-Par-4 could be detected at very low signal up to 30 min. These findings suggest the possibility that the *in vivo* anti-tumor activity of Par-4 protein is limited or underestimated

due to its short circulating half-life. Therefore, we decided to investigate the hypothesis that extended exposure due to improved biological half-life by Fc fusion enhances *in vivo* antitumor activity of Par-4 protein in a mouse model for tumor metastasis.

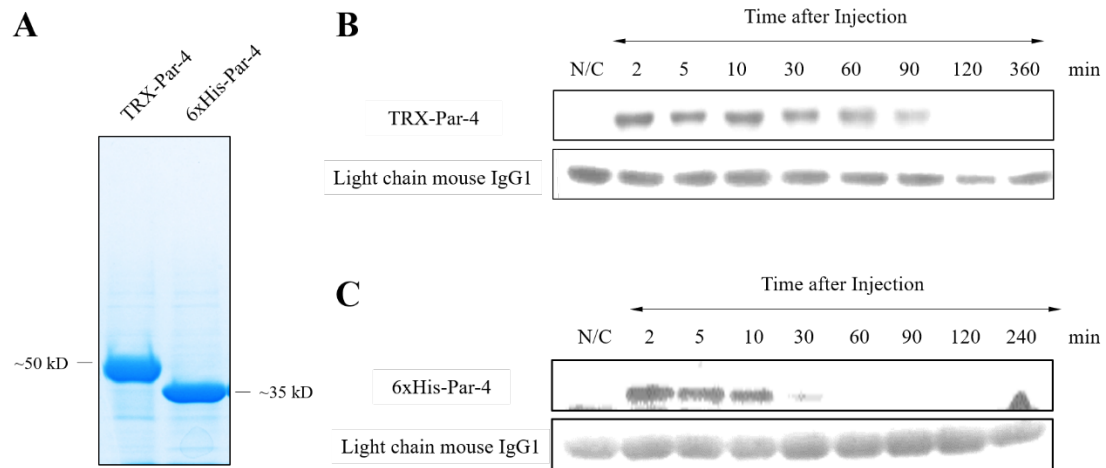


**Figure 5.1** The limited serum persistence of recombinant Par-4 proteins in mice. (A) SDS-PAGE of the purified TRX-fused or hexa-histidine tagged Par-4 (TRX-Par-4 and 6xHis-Par-4, respectively). Mice were injected intravenously with 5 mg/kg TRX-Par-4 or 6xHis-Par-4. Relative serum concentrations of TRX-Par-4 (B) and 6xHis-Par-4 (C) were evaluated at periodic intervals by western blotting. The recombinant Par-4 proteins were detected with antibody against Par-4 and visualized by chemiluminescence. The light chain of mouse IgG1 was used as an internal loading control. The two panels are representative blots of two mice.

### 5.3.2 Development of a method for large-scale production of Fc-fused Par-4

We first designed a novel Par-4 entity with a prolonged duration of action. A great

effort was also made to obtain a sufficient amount of the protein material for *in vivo* characterization. Our protein engineering in this study started from rat Par-4, rather than human Par-4, because the engineered novel Par-4 entity would be tested *in vivo* using rodents (mice and rats).

#### **5.3.2.1 Design of a new Par-4 entity with a prolonged half-life**

The therapeutic efficacy of a therapeutic protein drug can be greatly increased by improving its pharmacokinetic profile.<sup>28, 49-54</sup> Protein fusion with the Fc region of human IgG1 (IgG Fc) is one of the most commonly used strategies to prolong the duration of action of protein therapeutics.<sup>56-57</sup> An A1Q/C6S/C12S/C15S/P24S human Fc variant (denoted as Fc(M1) for convenience) is a monomeric Fc variant and has been successfully utilized to improve the half-life time of abatacept, a therapeutic antibody drug.<sup>323</sup> To extend the biological half-life of Par-4, the gene was first genetically fused to the C-terminus of Fc(M1). The leader peptide sequence of mouse Ig kappa-chain was then added to the N-terminus of the fusion gene to facilitate its secretion from the cytosol to the extracellular space (Fig. 5.2). The resultant gene of Fc(M1)-Par-4 (~70 kD) was first prepared using the CHO expressing system to obtain the amount of protein sufficient for the *in vivo* characterization study of the protein. Purification of the *E. coli*-derived soluble Fc(M1)-Par-4 protein was performed using protein A affinity chromatography (Fig. 5.4).



**Figure 5.2** The schematic presentation of the fusion protein of Par-4 to Fc(M1). ‘ss’ represents the leader peptide sequence of mouse IgG kappa-chain.



### 5.3.2.2 Passage number-related effects on stable CHO-S cells expressing Fc-fused Par-4

As described in the methods section, a lentiviral vector-mediated gene transfer method was employed to generate stable CHO lines for efficient production of recombinant Par-4 protein. However, contrary to our expectations, we found that the generated cell lines at high passage numbers underwent alterations in the efficiency of Fc(M1)-Par-4 production, compared to lower passage cells. The expression levels of the recombinant Par-4 protein rapidly and gradually decreased as the passage number increased (Fig. 5.3). In fact, for more rapid establishment of a stable cell line, our protocol for generation of stable CHO cells does not include any antibiotics selection process which is usually required for screening and selecting a more stable and productive clone from the cell population transduced with recombinant lentiviral particles. Considering that the growth rate of the resulting transduced pooled cell population was slightly decreased when compared to that of naïve CHO cell, the cell viability or proliferation activity of the transduced CHO cells in the pooled cell population might be more specifically and negatively affected by the combinational activity of extracellular and intracellular recombinant Par-4 protein.

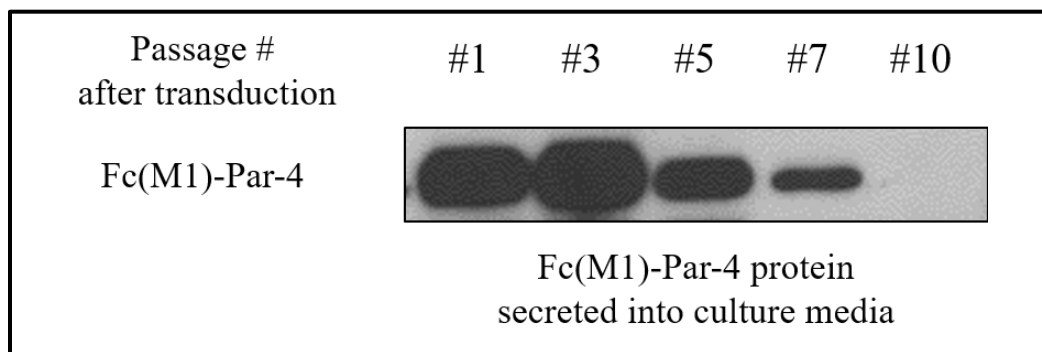


**Figure 5.3** The secretion levels of a recombinant Par-4 protein to the culture media. Each 10  $\mu$ l of culture medium was analyzed by western blot for Par-4.

#### ***5.3.2.3 Expression of Fc(M1)-Par-4 protein by transient transfection***

We were able to obtain a sufficient amount of Fc(M1)-Par-4 protein for its pharmacokinetic study in mice by transient gene expression in CHO-S cells using a commercially available transfection reagent (TransIT-PRO™), but the obtained quantity was still not sufficient for a planned *in vivo* antitumor activity study (Fig 5.4). In reality, transient gene expression using a commercially available transfection agent such as TransIT-PRO, Cellfectin, and Lipofectamine is not generally considered a suitable method for a large-scale protein production mainly due to the high cost of the reagents.

Polyethylenimine (PEI) has been widely used as a transfection reagent largely due to its low cost, despite of its non-negligible cytotoxicity. PEI is a cationic polymer which can introduce nucleic acids such as DNA or RNA into mammalian cells with the polymer.<sup>324</sup> PEI condenses DNA molecules into positively charged particles that interact favorably with the negatively charged phospholipid membrane of cell surface. Consequently, the complexes of DNA and PEI are internalized into cells by endocytosis and the DNA is then released into the cytosol.<sup>325</sup> Indeed, a number of cell lines are proven to be efficiently transfected with PEI. Especially, CHO-S and HEK 293 cells have displayed a relatively higher recombinant protein expression than other cell lines.<sup>326</sup> Therefore, to test the possibility that PEI can be utilized for large-scale production of Fc(M1)-Par-4 protein, the gene was transiently expressed in CHO-S cells using either PEI or TransIT-PRO™ for comparison. As shown in Fig. 5.5, a substantially decreased

production of Fc(M1)-Par-4 protein was observed in the CHO cells transfected with PEI, compared to that of the CHO cell transfected with TransIT-PRO™. Interestingly, it was also observed that the CHO cells transfected with PEI or TransIT-PRO™ show a similar level of 6xHis-Par-4 expression. Given that Fc-fused Par-4 protein might be exposed to a more complicated modification process than 6xHis-Par-4 protein in CHO cells because of its Fc part which requires for proper post-translational modification, the difference in a way of delivering DNA to cells between PEI or TransIT-PRO™ seems to specifically affect Fc-fused-Par-4 expression in CHO cells, but not significantly affect the expression of 6xHis-tagged one. Overall, these data indicate that it is not suitable to use PEI for Fc(M1)-Par-4 expression, but it seems okay to use the reagent for 6xHis-Par-4 expression.

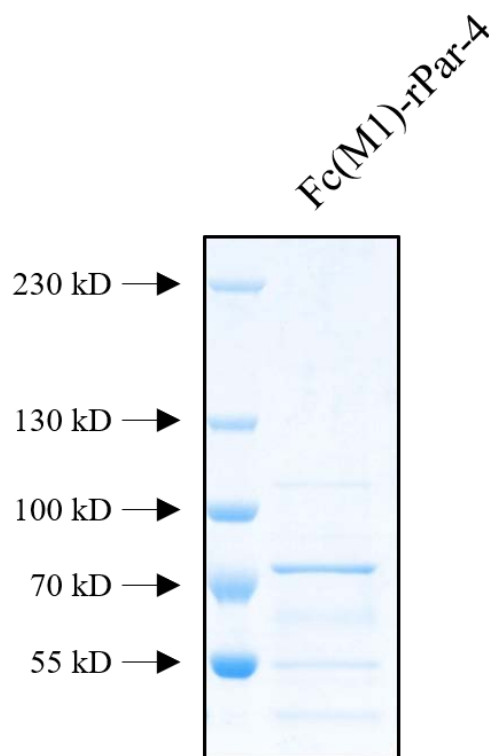


**Figure 5.4** SDS-PAGE of the purified Fc(M1)-Par-4.

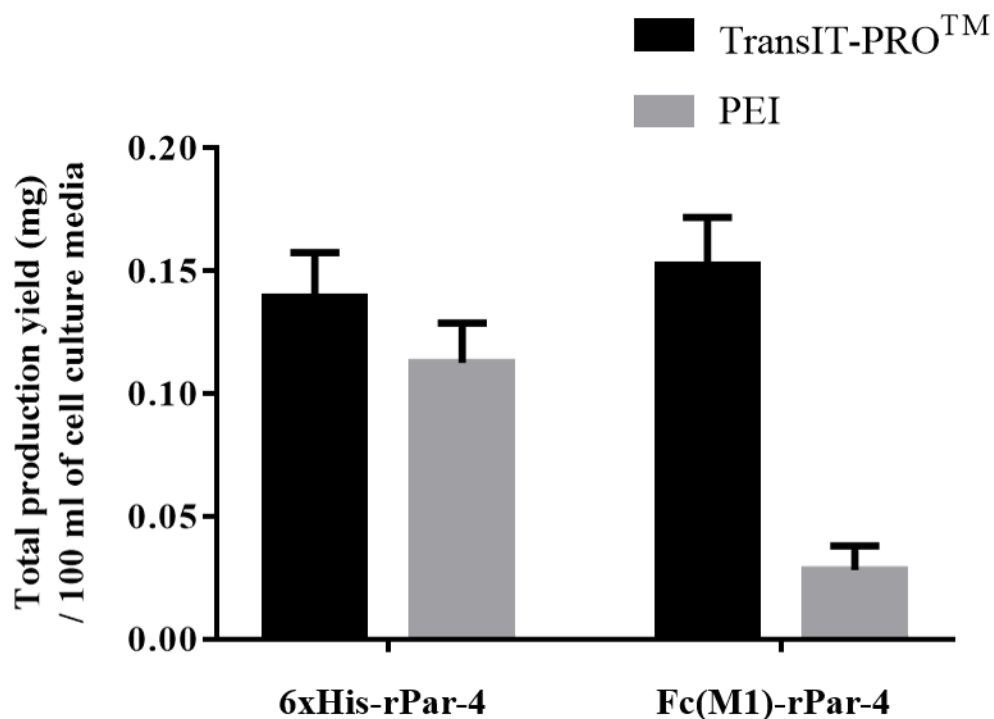


**Figure 5.5** Recombinant Par-4 protein is expressed at a scale of 100 ml using each of TransIT-PRO™ and PEI. Each bar represents the average of triplicates and the values are expressed as mean  $\pm$  S.D.

#### 5.3.2.4 Expression of recombinant Par-4 proteins using a bacterial expression system

Fc(M1)-Par-4 (~70 kD) was then prepared using the *E. coli* expressing system to obtain the amount of protein sufficient for the *in vivo* characterization study of the protein. Purification of the *E. coli*-derived soluble Fc(M1)-Par-4 protein was performed using protein A affinity chromatography, followed by an additional ion-exchange chromatographic step to obtain the purity required for a following *in vivo* characterization

study. (Fig. 5.6B & C)

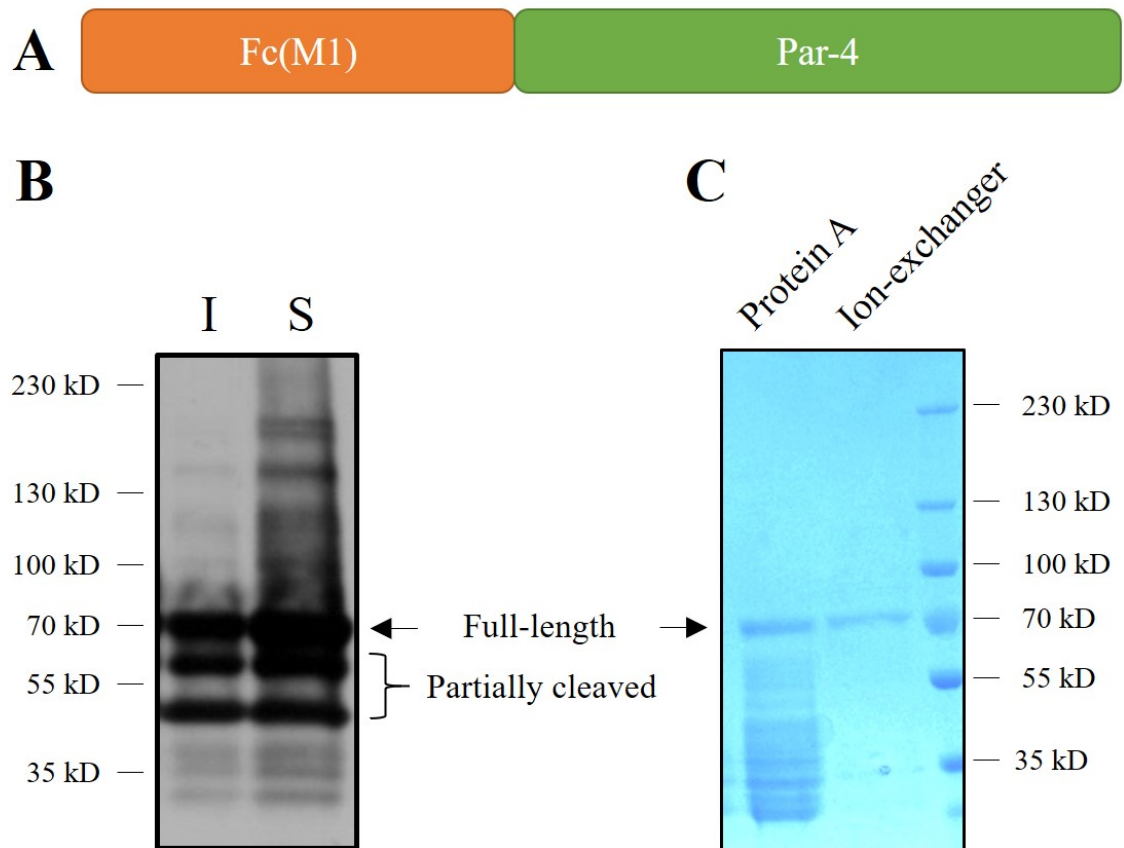


**Figure 5.6** Preparation of Fc(M1)-Par-4. (A) The schematic presentation of Fc(M1)-Par-4. (B) Western blot analysis of Par-4 protein in bacterial extract transformed with pET-22b(+)/6xhis-Par-4 and induced with IPTG. The soluble fraction (S) of the bacterial extract was separated from the insoluble fraction (I) by centrifugation before immunoblotting. (C) SDS-PAGE of the purified Fc(M1)-Par-4 protein. Soluble Fc(M1)-Par-4 protein was isolated by protein A chromatography (Protein A) followed by an additional ion-exchange chromatographic step (Ion exchanger) to achieve the purity required.

### ***5.3.2.5 Practical protocols for production of high yields of Fc-fused Par-4 protein using the *E. coli* expression system***

Although the established purification system yielded proteins of high purity, the yield after purification was still low (~1 mg/L bacterial culture for ~0.2 mg/L bacterial culture for Fc(M1)-Par-4). This low yield is mainly due to the formation of insoluble aggregates of Fc-fused Par-4 protein during high level expression in bacteria, and more complicated purification process. To obtain a higher quantity of Fc-fused Par-4 protein using the *E. coli* expression system, efforts have been focused on increasing production of the recombinant Par-4 protein.

#### ***1) Codon optimization***

The efficiency of heterologous protein expression in bacteria can be attenuated by biased codon usage. The approaches typically used to overcome this issue are site-directed mutagenesis to replace rare codons with other synonymous codon frequently used in bacteria, or the use of specialized cell lines supplying rare codon tRNAs such as Rosetta (DE3)<sup>TM</sup>.<sup>327</sup> Our *in silico* studies revealed that the open reading frame of Fc(M1)-Par-4 mRNA contains six rare codons in *E. coli* that may decrease protein expression (Fig. 5.7). However, we found that Fc(M1)-Par-4 protein production was not increased in Rosetta (DE3)<sup>TM</sup> cell (Fig. 5.8), which suggests that these six rare codons are not rate-limiting for protein synthesis.

In fact, the translation efficiency of mRNA is affected by a number of factors including codon adaptability (*e.g.* synonymous codon changes), the structure of mRNA, and different cis-acting elements involved in transcription and translation. With the help of a free online tool that takes these factors into consideration (built from Integrated DNA

Technologies), the full mRNA sequence of Fc(M1)-Par-4 was optimized for high yield production in *E. coli* and finally its expression was increased by a factor of about 3 after codon optimization (Fig. 5.9).

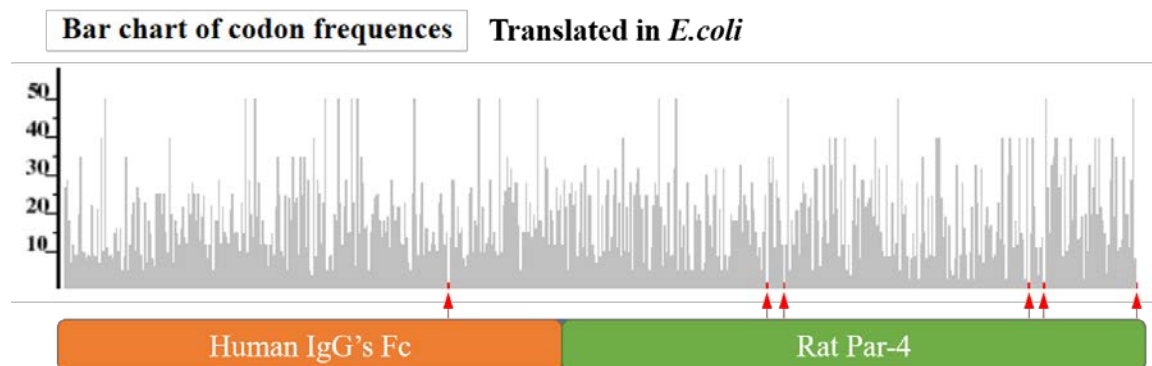


**Figure 5.7** Rare codons found in the coding region of Fc(M1)-Par4 gene. The rare codons are indicated by red arrow.

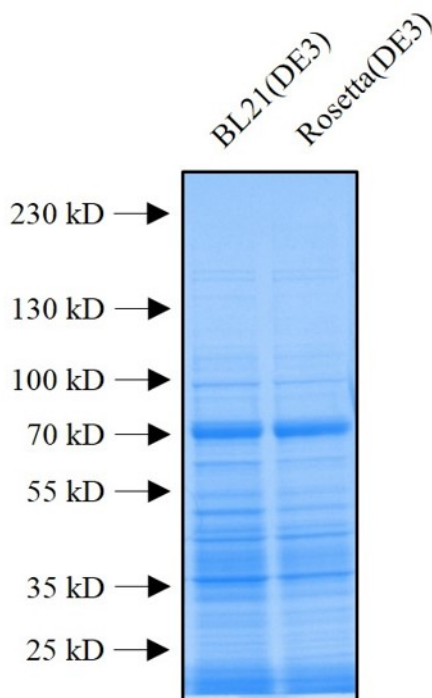


**Figure 5.8** SDS-PAGE analysis of Fc(M1)-Par-4 in the *E. coli* BL21 (DE3) and Rosetta

(DE3) transformed with pET-22b(+)/Fc(M1)-Par-4. Each 10 µg of soluble bacterial extract was loaded per lane.

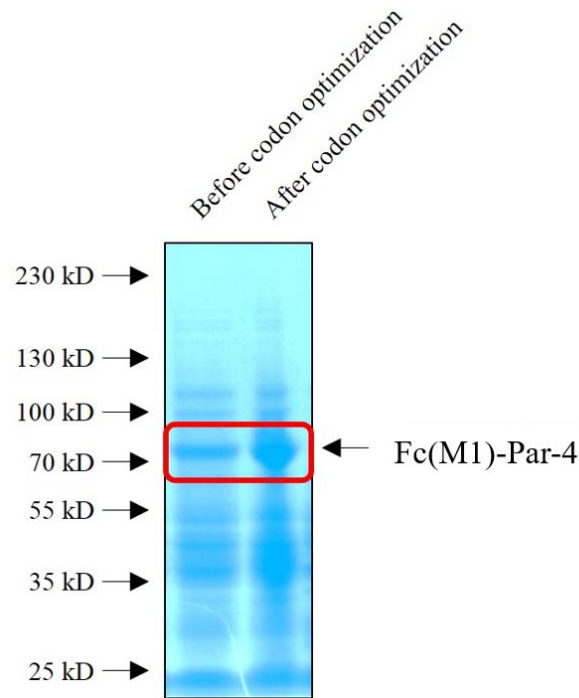


**Figure 5.9** Effects of computational codon optimization of Fc(M1)-Par-4 gene on its bacterial expression. Each 10 µg of soluble bacterial extract was loaded per lane.

## 2) *High cell-density culture of E. coli*

Terrific Broth (TB) is a nutritionally enriched medium developed by TARTOFF and HOBBS (1987) to increase yields in recombinant strains of *E. coli*. TB consists of tryptone, yeast extract, glycerol, and potassium phosphate. Excess potassium phosphate molecules keep the pH of the cell culture medium in a favorable range for the growth of *E. coli*, which allows cells to be protected against cell death due to decrease in pH. In addition, more nutrition (380% more yeast extract and 20% more tryptone than LB) in TB supports the



high cell-density growth of *E. coli* which is generally related to the elevated yield of recombinant protein production.

We have evaluated the process for Fc(M1)-Par-4 expression in the *E. coli* BL21 (DE3) transformed with pET-22b(+)/Fc(M1)-Par-4 in TB medium. First, to obtain overall growth rate curves of the transformed *E. coli* for two temperatures (18°C or 37°C) and to determine the time until exponential growth is observed (Absorbance at 600 nm (Abs<sub>600</sub>, also known as OD<sub>600</sub>) = 0.7) at these temperatures in a given condition, the transformed cells were cultivated at either 18°C or 37°C and monitored by measuring Abs<sub>600</sub> every 1 h. The results indicate that the transformed *E. coli* reached an OD<sub>600</sub> of 0.7 in about 7.5 hours at 18°C while it took 4 h to reach a similar absorbance at 37°C. The cell growth reaches saturation phase within 11 h at 37°C, but it took almost 18 h to reach the same absorbance at 18°C (Fig. 5.10).

Based on this information, we designed experiments to assess the effect of cell growth for induction (Abs<sub>ind</sub>) on cell growth and Fc(M1)-Par-4 protein expression in the *E. coli* BL21 (DE3) transformed with pET-22b(+)/Fc(M1)-Par-4. For this, the transformed *E. coli* was cultured at 18°C. Fc(M1)-Par-4 expression was induced at an Abs<sub>600</sub> of 0.7 or 2.0 by the addition of IPTG to a final concentration of 0.5 mM, followed by incubation for 10 h. The results reveal that the non-induction control group yields higher cell concentrations than the other two IPTG induction groups, which suggests that expression of Fc(M1)-Par-4 is toxic to the recombinant strain of *E. coli*. It was also observed that induction at Abs<sub>ind</sub> 2.0 leads to substantial increase in cell growth, compared to induction at Abs<sub>ind</sub> 0.7 (Fig. 5.11). However, no noticeable difference was observed in recombinant protein expression when Abs<sub>ind</sub> 2.0 was compared with 0.7 (Fig. 5.12). These data indicate that

total Fc(M1)-Par-4 protein production can increase if IPTG induction is done at a higher absorbance in the exponential phase.

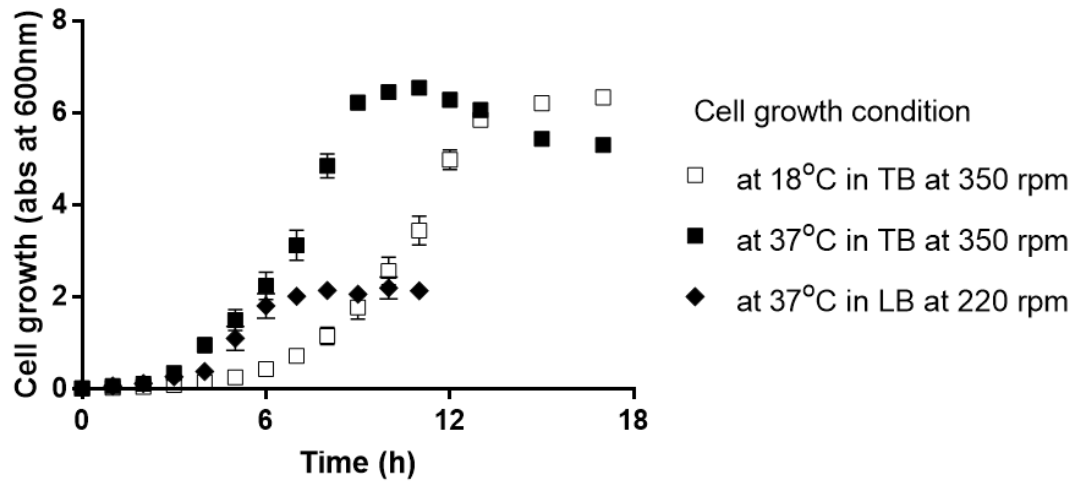


**Figure 5.10** Growth curves of the *E. coli* BL21 (DE3) transformed with pET-22b(+)/Fc(M1)-Par-4. Cell growth at 37°C in LB at 220 rpm, or at 37°C or 18°C in TB at 350 rpm. Each dot represents the average of duplicates and its values are expressed as the mean  $\pm$  standard deviation.

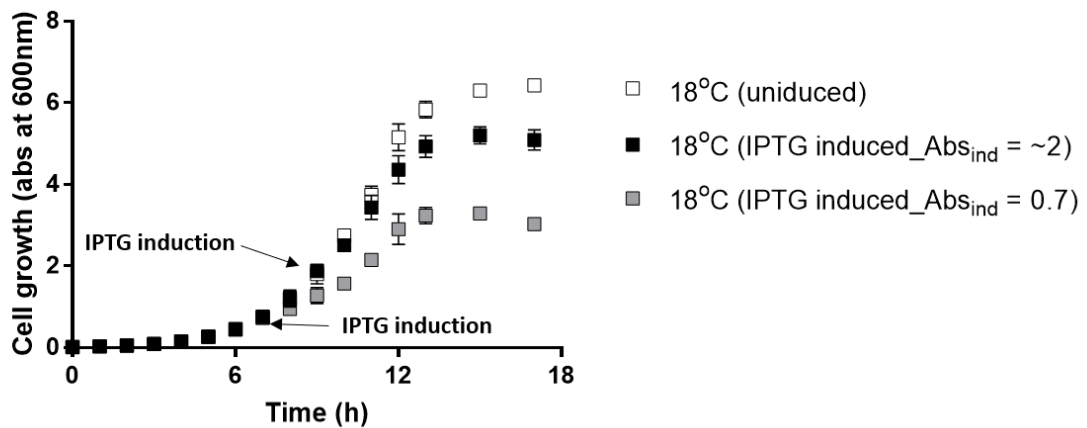


**Figure 5.11** Comparison between IPTG-induced and uninduced growth of the transformed

*E. coli* BL21 (DE3) at 18°C in TB at 350 rpm. Each dot is the representative of the average of duplicates and its values are expressed as the mean  $\pm$  standard deviation.

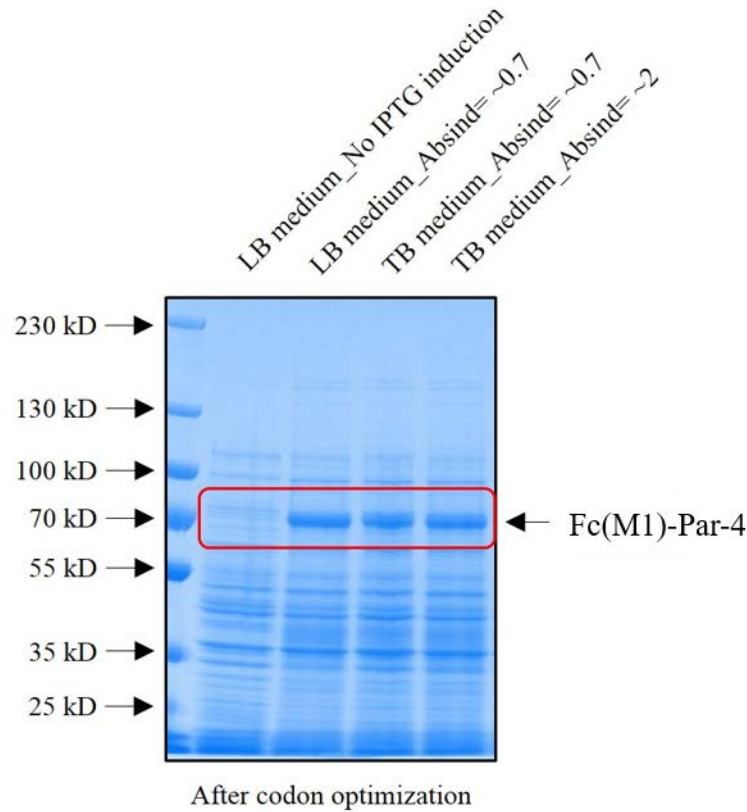


**Figure 5.12** Effects of the induction variables (OD600) on the expression of Fc(M1)-Par-4 in the *E. coli* BL21 (DE3) transformed with the gene.

### 5.3.3 *E. coli*-derived Par-4 proteins induce apoptosis in cancer cells

Before *in vivo* characterization of the purified recombinant Par-4 proteins, we first determined whether Fc fusion to the N-terminus of Par-4 diminishes its proapoptotic activity or not. To address this question, E0771 (murine breast cancer cell line) cells were treated with either 100 nM 6xHis-Par-4 or Fc(M1)-Par-4 protein, followed by incubation

for 24 h. Storage buffer (50 mM Hepes, 20% sorbitol, 1 M glycine, pH 7.4) was used as a vehicle control. It was observed that Fc(M1)-Par-4 and 6xHis-Par-4 proteins induced a similar level of apoptosis in E0771 cells in a given treatment condition (Fig. 5.13), which supports that anti-cancer activity of Par-4 is not significantly altered by Fc fusion to its N-terminus. This observation is very consistent with the findings of Zhao *et al.*<sup>321</sup> using TRX-Par-4.

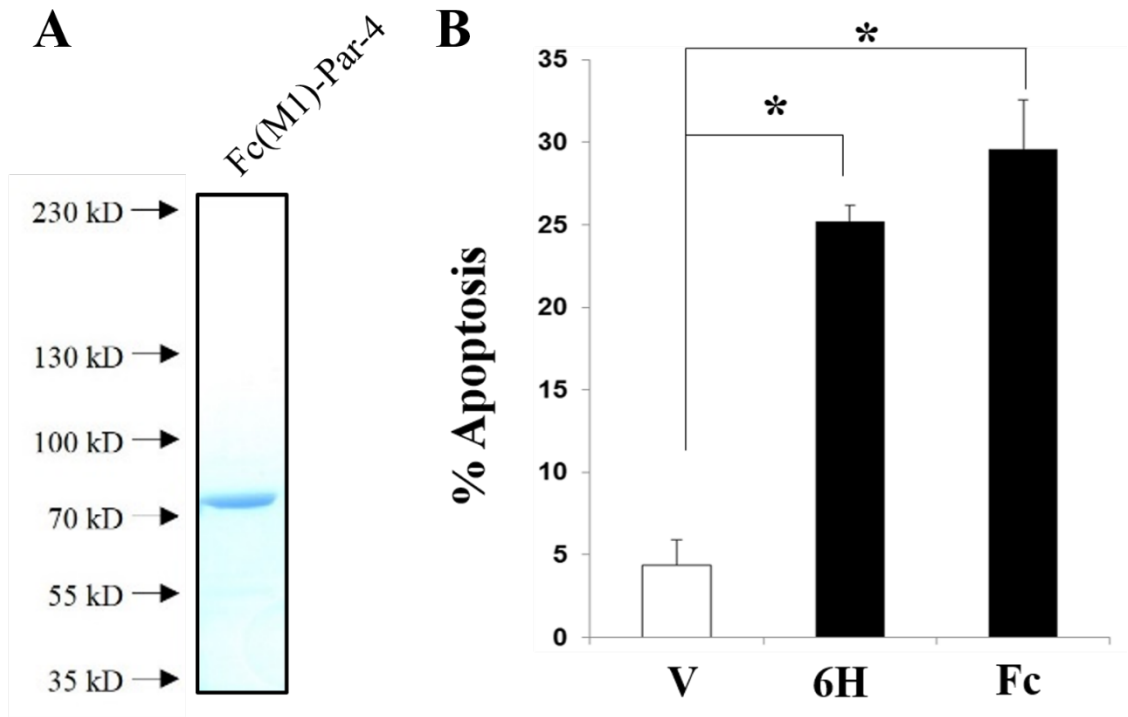


**Figure 5.13** Recombinant Par-4 elicits apoptosis in E0771 (murine breast cancer cell line) cells. (A) SDS-PAGE of the purified Fc(M1)-Par-4. (B) The cells were treated with vehicle (V), or purified 6xHis-Par-4 (6H) or Fc(M1)-Par-4 (Fc) (100 nM each). 24 h after treatment the cells were scored for apoptosis by immunocytochemistry (ICC) for caspase 3 activity. Results represent the average of triplicates and the values are expressed as mean  $\pm$  S.D.

Asterisk (\*) indicates the difference is statistically significant ( $p < 0.05$ ) by Student's t-test.

Dr. Nikhil Hebbar in the lab of Dr. Vivek M. Rangnekar provided this figure.

#### **5.3.4 Characterization of the *in vivo* profiles of recombinant Par-4**

To examine whether the protein fusion to an IgG Fc region really prolongs the biological half-life of Par-4 protein, a pharmacokinetic study was carried out in mice. The *in vivo* data were based on intravenous (*i.v.*) injection of each protein in the tested mice. The generated PK data are depicted in Fig. 5.14, and the biological half-lives obtained are summarized in Table 5.1. The results revealed that both Fc(M1)-Par-4 proteins prepared from CHO and *E. coli* cells have a substantially longer biological half-lives (up to ~23.8 h) than that (~3 h) of 6xHis-Par-4 protein. Aglycosylated Fc(M1)-Par-4 protein displays a biological half-life (~20.3 h) which is comparable to that of CHO-cell derived Fc(M1)-Par-4 protein (~23.8 h).

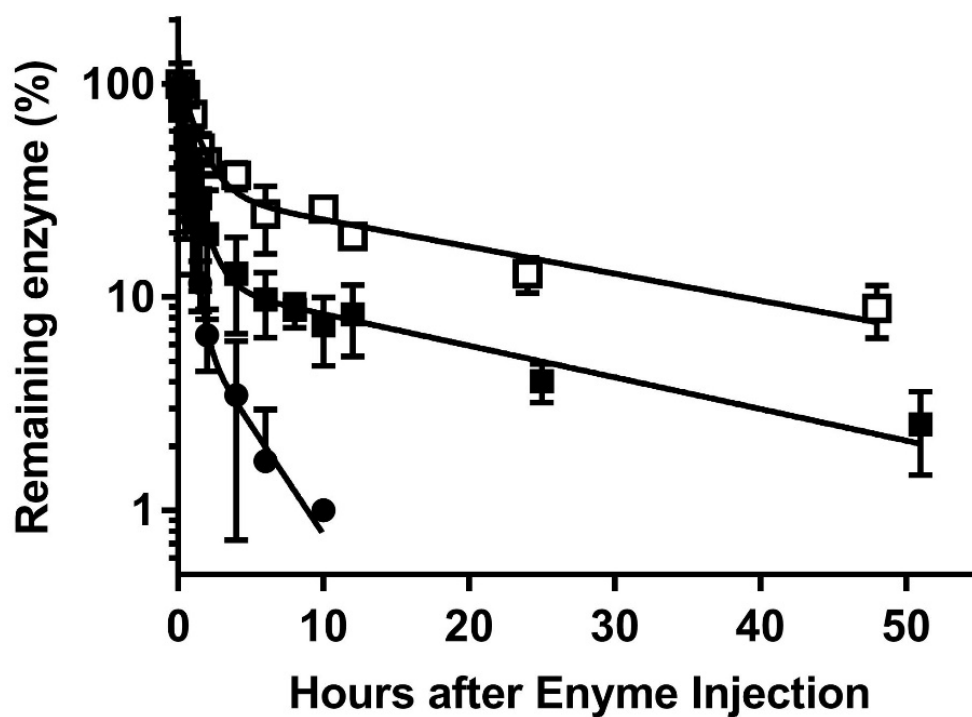


**Figure 5.14** Serum concentration (%) versus time profiles of recombinant Par-4 proteins in mice. CHO cell-derived Fc(M1)-Par-4 (□), *E. coli*-derived Fc(M1)-Par-4 (■) or *E. coli*-derived 6xHis-Par-4 (●) was administered *via i.v.* infusion at 5 mg/kg and the serum Par-4 protein concentrations were determined by ELISA. Results represent the average of triplicates per group and shown as mean  $\pm$  standard error.

**Table 5.1** The determined biological half-lives of recombinant Par-4 proteins in mice

Protein	Prepared from	$t_{1/2}$
6xHis-Par-4	<i>E. coli</i>	~3 hr
Fc(M1)-Par-4	<i>E. coli</i>	~20.3 hr
Fc(M1)-Par-4	CHO-S	~23.8 hr

### 5.3.5 *In vivo* characterization of recombinant Par-4 proteins for their potency in inhibiting metastatic tumor growth

To examine whether longer exposure due to half-life extension by Fc fusion improves *in vivo* antitumor activity of Par-4, we evaluated how efficiently Fc(M1)-Par-4 and 6xHis-Par-4 proteins inhibit lung metastasis of E0771 breast cancer cells in immunocompetent C57/BL6 mice. To address this question, the cells ( $1.5 \times 10^5$  cells) were injected through tail vein and then 250  $\mu$ g *E. coli*-derived 6xHis-Par-4 or Fc(M1)-Par-4 was administered intravenously every other day for 12 days (total of 1500  $\mu$ g of protein/mouse). It was observed that both Fc(M1)-Par-4 and 6xHis-Par-4 proteins significantly suppressed metastatic tumor growth *in vivo* compared to vehicle-treated control, but with no statistic difference between the two protein-treated groups in a given treatment condition (Fig. 5.15A). However, considering that the molecular weight of Fc(M1)-Par-4 protein (~70 kD) is approximately 1.7-fold higher than that of 6xHis-Par-4 protein (~35 kD), the mice have not been treated with equivalent molar concentrations of recombinant Par-4 proteins. This may suggest that Fc(M1)-Par-4 protein than 6xHis-Par-4 protein indeed would be more potent in inhibiting metastatic tumor growth *in vivo*, but the difference in their potency might become less evident at the high dose.

Therefore, to address this question, we further determined if the *in vivo* anti-tumor activity of Fc(M1)-Par-4 protein is diminished as the dose decreases. According to the data obtained (Fig. 5.15B), a 70%-reduced dose of Fc(M1)-Par-4 protein (75  $\mu$ g/injection) also induced substantial inhibition of lung metastasis in mice induced by E0771 breast cancer cells. Considering that lung metastasis by E0771 breast cancer cells was not significantly reduced at the low doses ( $\geq 250$   $\mu$ g/injection) of TRX-Par-4 in the previous studies,<sup>321</sup> these

results indicate that Fc-fusion has improved the potency of Par-4 protein in inhibiting in metastatic tumor growth *vivo*.

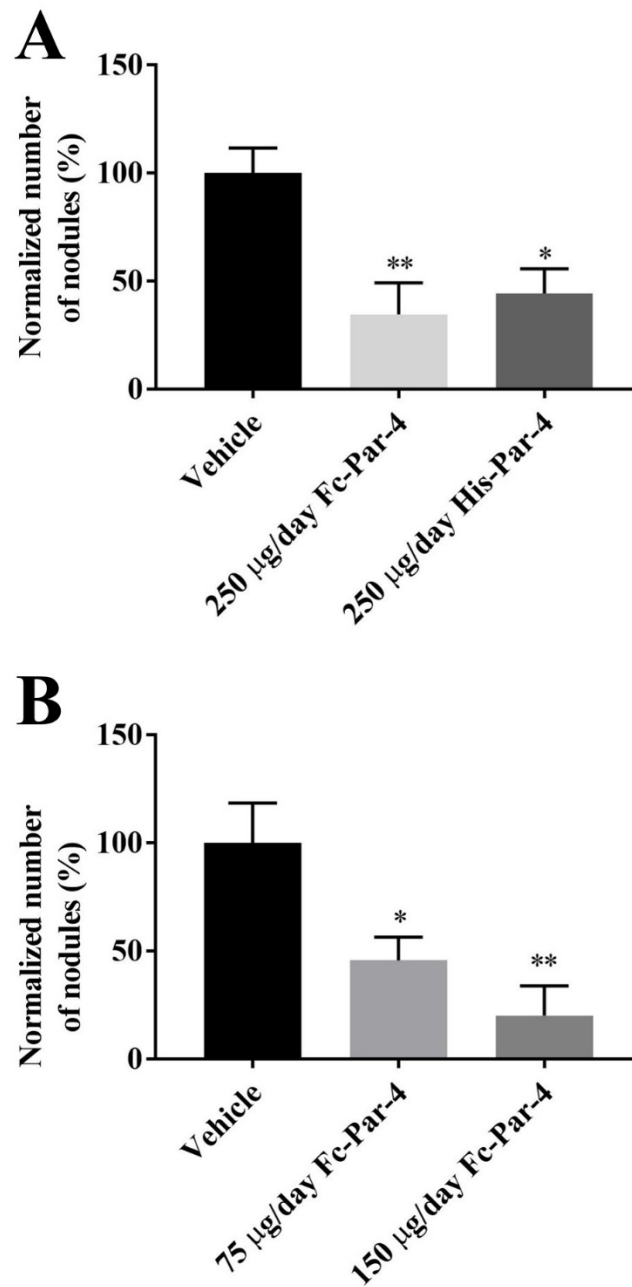


**Figure 5.15** Recombinant Par-4 protein suppresses the metastatic growth of tumor (E0771).



The cells ( $1.5 \times 10^5$  cells) were administered into tail vein in B6C3H mice (n=5). (A) 5 h after administration, vehicle, or 250  $\mu$ g purified 6xHis-Par-4 (**His-Par**) or Fc(M1)-Par-4 (**Fc-fuse-Par-4**) was injected through tail vein every alternate day for 12 days (total of 1500  $\mu$ g of protein/mouse). (B) 5 h after administration, vehicle, or 150 or 75  $\mu$ g purified Fc(M1)-Par-4 was injected through tail vein every alternate day for 12 days (total of 900 and 450  $\mu$ g of protein/mouse, respectively). Four weeks later, the mice were euthanized, and the number of the lung nodules were then counted. The data are expressed as the mean  $\pm$  SEM. The single and double asterisks indicate  $p < 0.05$  and  $p < 0.01$ , respectively.

## 5.4 Discussion

In 2011, Zhao *et al.*<sup>321</sup> showed that lung metastasis in immunocompetent mice induced by LLC1 lung cancer cells was substantially inhibited by the intravenous injection of 500  $\mu$ g recombinant TRX-Par-4 or TRX-SAC protein. However, the quantity of Par-4 protein used in the animal study seems substantially higher than usual because, assuming that the body weight of an adult mouse is 30 mg, the protein dose used can be calculated to be around 17 mg/kg (of body weight) which is comparable to a human dose of approximately 1000 mg per person for a typical body weight of 60 kg. Obviously, the protein dose of 1000 mg per person would be too high for practical clinical use. Both TRX-Par-4 and TRX-SAC proteins have proven their reasonable (and probably therapeutically valuable) *in vitro* and *in vivo* anti-cancer activity,<sup>311, 320-321</sup> but to my best knowledge their pharmacokinetic profiles have not yet been studied. This led us to examine whether TRX-Par-4 or unfused Par-4 protein has a sufficiently long serum persistence required for proper

*in vivo* activity. Our results showed that both TRX-Par-4 and 6xHis-Par-4 proteins stay in the circulatory system only for very short periods of time (< 120 min for TRX-Par-4 and < 60 min for 6xHis-Par-4) (Fig. 5.1), which suggests the possibility that the anti-tumor efficacy *in vivo* of Par-4 protein has been underestimated due to its short circulating half-life. In addition, considering that low-molecular-weight drugs whose mass are below the threshold for glomerular filtration ( $\leq \sim 40$  kD) usually undergo rapid clearance from the blood,<sup>328-332</sup> our data suggest that the relatively longer serum persistence of TRX-Par-4 protein ( $\sim 50$  kD) than that of 6xHis-Par-4 protein ( $\sim 35$  kD) would be largely attributed to its higher molecular weight than the threshold, and that natural Par-4 protein ( $\sim 35$  kD) released from cells to the blood stream might be short-lived due to its limited molecular size.

Par-4 was engineered to improve its pharmacokinetic performance so that it shows enhanced therapeutic response in mice. For this reason, Par-4 protein was genetically conjugated to the C-terminus of Fc(M1), a human IgG Fc variant. Fusion to IgG Fc is a preferably used method to extend the biological half-life of therapeutically valuable protein by exploiting the FcRn-mediated recycling mechanism.<sup>66-68</sup> The endothelial cellular neonatal Fc receptor (FcRn) has a critical role in maintaining the high circulating levels of IgG.<sup>59-60</sup> Indeed, IgG has a prolonged circulating half-life of 21 days in human mainly due to FcRn-mediated recycling that protects against intracellular endocytic-lysosomal degradation.<sup>61-62</sup> IgG Fc strongly interacts with FcRn in the acidic endosomal compartments after IgG is internalized into endocytic vesicles.<sup>63</sup> The receptor-bound proteins are then returned to the cell membrane for extracellular release, whereas other serum proteins in the vascular endothelium are eventually degraded by the endocytic-

lysosomal system.<sup>64-65</sup> Like IgG, Fc-fusion proteins can take the advantage of the FcRn-mediated recycling process for half-life extension.

In the present study, our effort was also made to produce a sufficiently large amount of recombinant Par-4 proteins for animal studies. The bacterial expression system was employed for large-scale production of Fc(M1)-Par-4. The *E. coli* expression system is considered one of preferable choices for large-scale production of therapeutic protein drugs mainly because of greater cost-effectiveness and easier cultivation of bacteria, compared to the CHO or HEK293 expression system. However, the deficiency of mechanisms for protein post-translational modification in bacterial cells has limited the use of bacteria for production of therapeutic protein agents that require proper modification for functional activity or stability. Therefore, one question to be asked about this approach is: how *E. coli*-derived Fc-fused Par-4 protein retains the functional activity and circulating half-life comparable to those of the fusion protein prepared from mammalian cells. However, there is a good possibility that aglycosylated Fc-fused Par-4 protein still can meet these requirements to be an effective therapeutic for cancer. First, previous studies have demonstrated that an aglycosylated IgG1 prepared from *E. coli* retains a sufficiently long *in vivo* half-life comparable to that of mammalian cell-derived immunoglobulins, and that aglycosylated and glycosylated antibodies show equivalent *in vitro* binding to FcRn.<sup>333-335</sup> These observations indicate that, in the case of immunoglobulin *in vivo* half-life, the motifs within the Fc portion responsible for the interaction with FcRn do not rely on post-translational modification including glycosylation. Second, it was already demonstrated that Par-4 protein prepared from bacteria retains reasonable *in vitro* and *in vivo* anti-tumor activity,<sup>321</sup> which implies that the post-translational modification of Par-4 is not critical for

its functional activity.

Although only less than 20% of Fc(M1)-Par-4 protein was expressed in *E. coli* as a soluble and intact form (Fig. 5.6B), we were able to obtain the amount of the recombinant Par-4 protein sufficient for the required *in vitro* and *in vivo* studies using the *E. coli* expression system. We also found that the *E. coli*-derived Fc(M1)-Par-4 protein not only retains considerable *in vitro* anti-cancer activity after purification (Fig. 5.13), but also has approximately 7 times longer biological half-life than 6xHis-Par-4 (Fig. 5.14 & Table 5.1). These results suggest that Fc fusion extends the biological half-life of Par-4 by both increasing its size high enough to escape glomerular filtration ( $\leq \sim 40$  kD) and implementing protection against cellular endolysosomal degradation. As the next step, it was further determined if Fc(M1)-Par-4 protein has improved antitumor activity in a mouse model for lung cancer metastasis induced by murine breast cancer cells. The results revealed that Fc(M1)-Par-4 protein is capable to substantially reduce lung metastatic growth *in vivo* at the low doses where TRX-Par-4 protein did not show significant *in vivo* anti-tumor activity in the same mouse model used in the previous studies<sup>321</sup> (Fig. 5.15). These results strongly support that increased exposure to Par-4 due to half-life extension improves the therapeutic efficacy of Par-4 for cancer. Overall, our study also shows a good possibility that the *E. coli* expression system can be utilized for the production of a therapeutically valuable form of Par-4 protein.

## 5.5 Experimental details

### 5.4.1 Cloning, expression and purification of 6xHis-Par-4 and Fc(M1)-Par-4

#### *The E. coli expression system*

Bacterial expression constructs for TRX-Par-4, 6xHis-Par-4, and Fc(M1)-Par-4 were produced by subcloning each gene into pET-22b(+) vector. The constructs TRX-Par-4 was prepared by subcloning the rat Par-4 sequence in frame with thioredoxin cDNA (TRX) in vector pThio-His (Invitrogen Corporation, Carlsbad, CA) as described in a previous reported by Burikhanov *et al.*<sup>311</sup> *E. coli* BL21 (DE3) Star<sup>TM</sup> cells (Thermo Fisher Scientific, Waltham, MA) were transformed with each construct and induced with 0.5 mM IPTG (Sigma-Aldrich, St. Louis, MO). The cells were harvested 10 h after IPTG induction. The cells were then washed with Tris-buffered saline (25 mM Tris base, pH 7.4, 138 mM NaCl, and 2.7 mM KCl) followed by a centrifugation at  $2,000 \times g$  for 5 min at 4°C. The cell homogenates were prepared through resuspending the cell pellets in 25 mM Tris-Cl, pH 7.4 and subjecting them to sonication. In order to remove cell debris or unbroken cells, the total cell homogenates were exposed to centrifugation at  $10,000 \times g$  for 20 min.

For purification of TRX-Par-4 or 6xHis-Par-4 protein, the resultant supernatant was loaded onto a HisPur<sup>TM</sup> Cobalt Resin (Thermo Fisher Scientific) which has been pre-equilibrated with a washing buffer (25 mM Tris, pH 7.4, 500 mM NaCl, 0.05% Triton X-100, and 50 mM imidazole). After extensive washing with the washing buffer, bound His-tagged proteins were eluted by a stepwise gradient elution with imidazole in the presence of 150 mM NaCl.

For purification of Fc(M1)-Par-4 protein, the resultant supernatant was loaded onto a rmp Protein A Sepharose Fast Flow (GE Healthcare Life Sciences) pre-equilibrated with

20 mM Tris·HCl (pH 7.4). Then, the mixture was packed in a column and washed with 5 column volume (CV) of 20 mM Tris·HCl (pH 7.4) containing 200 mM NaCl until an OD<sub>280</sub> < 0.02 was achieved; then the protein was eluted by 50 mM sodium acetate, pH 4.0, containing 200 mM NaCl. For buffer exchange, the eluate was dialyzed in 20 mM Tris·HCl (pH 7.4) by Millipore Centrifugal Filter Units. The protein solution was then loaded onto a Q-Sepharose Fast Flow (GE Healthcare Life Sciences, Pittsburgh, PA) pre-equilibrated with 20 mM Tris·HCl, pH 7.4, for the second-round chromatographic separation. Fc(M1)-Par-4 protein was eluted from the Q-Sepharose column with a stepwise gradient of NaCl (100–800 mM). For buffer exchange, the eluate was dialyzed in storage buffer (50 mM Hepes, 20% sorbitol, 1 M glycine, pH 7.4) by Millipore Centrifugal Filter Units. The entire purification process was performed in a cold room at 8°C and the purified proteins were stored at –80°C until the activity tests. Their purity was analyzed by SDS-PAGE on a 4–12% NuPAGE Novex Bis-Tris gel (Life Technologies).

### ***The CHO expression system***

Mammalian expression constructs for Fc(M1)-Par-4 were produced by subcloning each gene into pCMV-MCS vector. CHO-S cells were incubated in FreeStyle CHO Expression Medium (Life Technologies) with 8 mM l-glutamine (Life Technologies) at 37°C in a humidified atmosphere with 8% CO<sub>2</sub> and transfected with gene expression DNA constructs encoding the protein of interest using the TransIT-PRO Transfection Kit (Mirus Bio LLC, Madison, WI)) when the number of the cells reached  $1.0 \times 10^6$  cells/mL. The culture medium was harvested 6 days after transfection. Fc(M1)-Par-4 protein secreted into the culture medium was purified by protein A affinity chromatography. After removing cells by centrifugation, the cell-free culture medium was mixed with rmp Protein A

Sepharose Fast Flow (GE Healthcare Life Sciences) pre-equilibrated with 20 mM Tris·HCl, pH 7.4, and incubated for overnight at 6°C with occasional stirring. Then, the suspension was packed in a column and washed with 5 column volume (CV) of 20 mM Tris·HCl, pH 7.4, containing 200 mM NaCl until an  $OD_{280} < 0.02$  was achieved; then the protein was eluted by adjustment of the pH and salt concentration. The eluate was then dialyzed in storage buffer (50 mM Hepes, 20% sorbitol, 1 M glycine, pH 7.4) by Millipore Centrifugal Filter Units. The entire purification process was conducted on ice and the purified Par-4 proteins were stored at  $-20^{\circ}\text{C}$  until use. Their purity was analyzed by SDS-PAGE on a 4–12% NuPAGE Novex Bis-Tris gel (Life Technologies).

#### **5.4.2 Western blot**

Recombinant Par-4 proteins in bacterial extract transformed with pET-22b(+)/6xhis-Par-4 or pET-22b(+)/Fc(M1)-Par-4 were analyzed by western blot using goat anti-rat Par-4 IgG obtained from Santa Cruz Biotechnology (Dallas, Texas) (1:3000 dilution as described in the manufacturer's instructions). Pre-adsorbed, HRP-conjugated anti-goat IgG (Santa Cruz Biotechnology) was used at 1:4000 as a secondary antibody and Par-4 protein was finally detected by chemiluminescence using the SuperSignal West Dura Extended Duration Substrate from Pierce Biotechnology (Waltham, MA).

#### **5.4.3 Immunocytochemistry and apoptosis analysis**

Cells in chamber slides were exposed to 100 nM purified Fc(M1)-Par-4 or 6xHis-Par-4. 24 h after treatment the cells were subjected to immunocytochemistry (ICC) using the indicated anti-caspase 3 IgG and then stained with the appropriate secondary antibody

conjugated to Alexa Fluor-488 (green fluorescence) or Alexa Fluor-594 (red fluorescence) (Molecular Probes). Apoptotic nuclei were identified by TUNEL assay, caspase-3 immunostaining, or 4, 6-diamidino-2-phenylindole (DAPI) staining. A total of three independent experiments were performed; and approximately 300 cells were scored in each experiment for apoptosis under a fluorescent microscope, as described previously.<sup>336</sup>

#### **5.4.4 Pharmacokinetics studies in mice**

##### ***ELISA for Par-4***

Mice (n=3) were injected with each recombinant Par-4 protein or saline through the tail vein at a dose of 5 mg/kg of body weight. Blood samples were then obtained by needle puncture of the saphenous vein. Approximately 15-30  $\mu$ L of blood was collected into a heparin-treated capillary tube at differing time points after protein injection. The plasma was separated from the collected blood samples by centrifugation (15 min, at  $5,000 \times g$ ). 200 ng of plasma protein in 100  $\mu$ l 0.05M PBS, pH 7.4, was immobilized in a 96 well flat-bottomed EIA plate (Corning) at 4 °C overnight (or 37 °C for 2 h). The liquid was dumped from the plates and the rest was drained on paper towel. Coated wells were blocked with blocking buffer (0.05M PBS, pH 7.4, containing 1 mg/ml casein) (250  $\mu$ L/well) at RT for 30 min. After washing twice with washing buffer (0.05M PBS, pH 7.4) (250  $\mu$ L/well), 100  $\mu$ l of goat anti-rat Par-4 IgG (Santa Cruz Biotechnology) in blocking buffer was added to each well at a range of concentrations. The plate was then covered with an adhesive plastic and incubated, with continual shaking, at RT for 1 h. After washing three times with washing buffer, pre-adsorbed, HRP-conjugated secondary antibody (anti-goat IgG-HRP) (70  $\mu$ l/well), diluted with blocking buffer at a ratio of 1:30,000, was added into each well



and incubated at RT for 1 h on a shaker. The wells were then washed three times with washing buffer (250 µl/well) before 250 µl TMB substrate was added to the wells. The ELISA plate was kept in the dark until the desired color develops. The reaction was stopped with 100 µL of 0.5 M HCl. The absorbance (= the developed blue color) was measured at 450 nm using a microplate reader. All measurements were performed in triplicate or quadruplicate. The obtained PK data (time dependent enzyme concentrations) ( $[E]_t$ ) were fitted to a double-exponential equation <sup>247</sup> by GraphPad Prism 5.01 software:  $[E]_t = Ae^{-k_1t} + Be^{-k_2t}$ , which explains both the distribution process (the fast phase, associated with  $k_1$ ) and the elimination process (the slow phase, associated with  $k_2$ ) of the Fc-fused Coch3 protein in animals. The  $t_{1/2}$  associated with the elimination rate constant  $k_2$  of the fusion protein is known as the biological  $t_{1/2}$  or elimination  $t_{1/2}$ .

#### ***Western blot for Par-4***

The plasma protein was analyzed by western blot for Par-4, as described above.

#### **5.4.5 Lung metastasis of E0771 cells**

The E0771 cells ( $1.5 \times 10^5$  cells) were administered into tail vein in immunodeficient B6C3H mice (n=5). 5 h after administration, 6xHis-Par-4 or Fc(M1)-Par-4 was injected through tail vein every alternate day for 12 days (total of 1500 µg of protein/mouse). Four weeks later, the mice were euthanized, and the lungs were photographed. The number of the lung nodules were then counted.

#### **5.4.6 Statistical analysis**

Statistical analyses were performed with the Statistical Analysis System Software Version 9.2 (SAS Institute, Cary, NC). Unless stated explicitly otherwise, one-way ANOVA with *post hoc* analysis was utilized for the statistical analysis.

## Chapter VI. Conclusions and Future Directions

### 6.1 Cocaine abuse treatment

The first of our designed CocHs, *i.e.* CocH1, has been proven safe and promising for use in animals and humans in preclinical and clinical studies.<sup>84, 199</sup> However, a Phase II clinical trial of Albu-CocH1 for cocaine addiction treatment revealed that its actual therapeutic value for cocaine addiction treatment is still limited mainly due to its insufficiently long biological half-life which is 43-77 h in humans<sup>84</sup> or ~8 h in rats.<sup>198</sup>

The first part of my dissertation was focused on the development of a new CocH entity which is able to deliver a greater catabolic activity within the human body so that our CocH-based therapy for human cocaine addiction fits within the desirable once-weekly or longer dosing schedule. We found that Fc fusion greatly extended the serum persistence *in vivo* of CocH3 whose catalytic efficiency against cocaine is about 2-fold higher than that of CocH1. Enhanced FcRn binding by Fc engineering further improved its biological half-life in rats. Our rodent studies also demonstrated that the new CocH entity efficiently protected animals from the physiological and psychostimulant effects of cocaine, and more importantly, the anti-cocaine effect delivered by the enzymes remained in the circulatory system for prolonged periods of time. As for the next step, the potential efficacy of long-term administration of the enzyme as a treatment for cocaine addiction must be evaluated further. Given that many preclinical studies already have shown that therapies using a cocaine-metabolizing enzyme can significantly reduce cocaine-primed reinstatement and cocaine-self-administration,<sup>192-195</sup> the use of our new CocH entity with a prolonged duration of action will allow us to determine if this catalytic treatment can decrease the reinforcing action of cocaine for a sufficient period required to achieve long-term

extinction of drug-craving behavior in animals and humans.

Since heroin is one of the most frequently abused drugs with cocaine, in the second part of this dissertation we kinetically compared human recombinant AChE, BChE, and CocH1 with the aim to examine their catalytic efficiencies against heroin and 6-MAM. This allowed us to assess the interaction between cocaine and heroin or cocaine and 6-MAM in their hydrolysis reactions catalyzed by CocH1 in comparison with human enzymes AChE and BChE. According to the results obtained, both AChE and BChE can catalyze 6-MAM hydrolysis to morphine, with relatively lower catalytic efficiency compared to the corresponding enzyme catalyzing heroin hydrolysis. The data also strongly suggests that plasma BChE, but not AChE, is the primary enzyme responsible for the rapid enzymatic hydrolysis of the 3'-phenolic ester of heroin within the blood, which has led us to exam whether an effective blocker for BChE can be used as a novel therapeutic strategy for prevention of heroin overdose. Considering that heroin is regarded a prodrug which acts through its host's initial metabolites (6-MAM and morphine)<sup>264</sup> and that humans lacking functional BChE appear healthy,<sup>337</sup> there is a possibility that human BChE might be a potential target for prevention of cocaine intoxication, and our animal studies have produced promising results. In addition, the complete catalytic parameters obtained for CocH1 against heroin and 6-MAM revealed that concurrent use of heroin and cocaine is not expected to significantly affect the efficacy of CocH1 in cocaine detoxification.

## **6.2 Oligomerization and catalytic parameters of human UGT1A10**

In the third part of this dissertation, the complete catalytic parameters obtained for

recombinant UGT1A10 against therapeutically valuable two drugs, morphine and entacapone, demonstrated that the catalytic activities of recombinant UGT1A10 proteins are remarkably different, depending on which type of cell line is used to express the protein. Added to this, it was observed that recombinant human UGT1A10 protein expressed in HEK293 cells forms oligomerized complexes that are covalently cross-linked by disulfide bonds, but that expressed in CHO cells barely forms cross-linked disulfide bonds. Indeed, these findings are very meaningful in that this is not only the first demonstration of the oligomerized UGT1A10 complexes, but also the first evidence to show the presence of complicated disulfide bridges to form higher-order UGT complexes bigger than a dimer. Given that the covalently cross-linked homo-oligomers are not frequently observed in hepatic UGT1A1, 1A4, and 1A6 enzymes expressed in HEK293 cells,<sup>304</sup> the observed multiple disulfide bonds formed in the oligomerized complexes of extrahepatic UGT1A10 seem to be unique, which may be the first evidence to show the original differences between hepatic and extrahepatic UGT enzymes.

HEK293 is one of the most widely used cell lines for characterization of the enzymatic activity and oligomeric states of multiple human UGT isoforms. The use of the cell line has enabled us to compare our data with those reported by others. However, considering that UGT1A10 is an extrahepatic UGT isoform which is highly expressed in the large and small intestines, we might want to consider including intestinal epithelial cell lines for the gene expression in order to establish physiological relevance of our *in vitro* findings.

### **6.3 Cancer treatment**

The last part of this dissertation is focused on development of a new Par-4 entity

with a prolonged duration of action for cancer treatment. The results showed that Fc-fusion substantially prolonged the biological half-life of Par-4 protein. Aglycosylated Fc-fused Par-4 protein retained not only considerable *in vitro* and *in vivo* anti-cancer activity, but also increased serum persistence in mice, comparable to that of Fc-fused Par-4 protein prepared from mammalian cells. These data strongly suggest that the *E. coli* expression system is capable of producing a potentially therapeutically valuable form of Par-4 protein.

## **Chapter VII. Other Unpublished Works**

### **7.1 Development of potential antibody therapeutics for opioid use disorders**

#### **7.1.1 The main purpose of this study**

The main research goal of this project is to first develop the therapeutic antibody with high binding affinities for heroin and the psychoactive metabolites of heroin for heroin and morphine abuse treatment. Then, the discovered antibodies are going to be further engineered to have more broad specificity toward other opioids of abuse. In this study, I cloned and purified the protein used, and established the required binding affinity assays using isotope-labelled morphine ( $[^3\text{H}]$ morphine). Dr. Chunhui Zhang has taken over this work and further developed the project.

#### **7.1.2 Introduction**

##### ***Substance use disorder***

Continual use of psychoactive drugs can develop addiction. Addiction is defined as a chronic and relapsing brain disorder which is characterized by uncontrollable drug use, despite negative consequences. It is regarded a brain disorder since a drug changes the brain and how it works. These drug-induced changes in the brain can last for a long period of time and result in dangerous and self-destructive behaviors.

##### ***The journey to recovery from substance use disorder***

In general, acute withdrawal symptoms occur commonly hours after the last dose of a drug and diminish within weeks.<sup>112-114</sup> Acute withdrawal symptoms are generally followed by a protracted abstinence syndrome, including insomnia, dysphoria, irritability,

and fatigue for months. Symptom severity is generally associated with the several factors, *e.g.* what kind of narcotic has been used, and how long and much the drug has been abused. However, patients can abandon their recovery programs and return to drug use at any time during abstinent periods due to multiple potential factors like the priming effect of a drug, stress, and drug-related stimuli. This phenomenon is called “relapse”.

### ***Specific goals for substance use disorder treatment***

Goals for the treatment of substance use disorder include addressing withdrawal symptoms and drug craving in a proper way, normalizing physiological function that is changed in response to continual drug use, and more important, preventing patients against any exposure to drug again. However, limited success in opioid addiction treatment has been achieved with current therapeutic options. Historical data show that approximately 85% of patients undergo relapse within 2-years of intensive psychological interventions.<sup>338-339</sup> Maintenance treatment using opioid agonists (*e.g.* methadone or buprenorphine) has produced more promising results, but mean 1-year retention rates are still below 60%.<sup>340-345</sup> In addition, it has been observed in multiple clinical studies that patients on methadone maintenance with a history of heroin addiction remain vulnerable to the drug-related stimuli, such as images of morphine injection, which indicates a continuous vulnerability of patients on methadone maintenance treatment to relapse by drug-related stimuli through a day.<sup>346-348</sup>

### ***Current therapeutic options for illegal/prescription opioid use disorder***

- Opioid antagonist treatment: Naltrexone

Naltrexone is an opioid antagonist approved by the FDA for opioid use disorder treatment. The hypothesis for the use of an opioid antagonist in the treatment is a means of



blocking a conditioned response to drug.<sup>349</sup> Specifically, if the addicts cannot be successful in relieving the withdraw symptom- or craving-related negative state through opiate use because of competitive antagonism at the  $\mu$ -opioid receptor, the behavior of turning to opioid in these situations would be considerably reduced. However, multiple clinical trials of Naltrexone for opioid addiction treatment using either daily or thrice weekly schedule revealed that less than approximately 80% of patients returned to drug use within 6 months.<sup>350-352</sup>

- Opioid agonist maintenance treatment: Methadone & Buprenorphine

The FDA has approved two opioid agonists for the long-term treatment of opioid use disorder: methadone (a full opioid agonist), and buprenorphine (a partial opioid agonist). Methadone maintenance therapy (also denoted as “agonist-assisted relapse prevention treatments”) has produced better outcomes compared to any other intervention. Buprenorphine is more recently approved for narcotic addiction treatment and has proven to be as effective as methadone.<sup>353-354</sup> It has been demonstrated that both methadone and buprenorphine considerably reduce both the negative and positive reinforcing effects of short-acting opioids or natural opiates, and subside craving subsided, enable the addicted patients to focus on non-drug-related activities.<sup>353-354</sup> However, mean 1-year retention rate in the maintenance treatment is still below 60%.<sup>340-345</sup> In addition, many clinical studies have shown that, at any given time, approximately 15% of patients on methadone maintenance treatment will have the ongoing use of opiate.<sup>355-358</sup>

***The contributions we would like to make to opioid use disorder problem***

In the present study, we have developed antibody therapeutic candidates for opioid use disorder treatment. An antibody therapeutic is expected to have a mechanism and

therapeutic utility which distinctly different from the traditional small-molecule approaches to treatment. It has been demonstrated that antibodies with high binding affinity for a target opioid are capable to sequester the drug in the bloodstream and block the entry of the drug to the brain, markedly impairing any physiological effects of the drug.<sup>267, 359-361</sup> It is expected that the therapeutic antibody would have great potential to become available for complementing the existing pharmacologic treatment or for complementing the psychosocial tools needed for a transition to a medication-free and abstinent life.

### 7.1.3 Results and discussion

Based on the computational modeling and design, our most promising IgG1, denoted as MMBCmAb-H6M (Fig. 7.2) for convenience, with the overall highest binding affinities for the three heroin-related opioids, *i.e.* heroin ( $K_i = 11.8$  nM), 6-MAM ( $K_i = 11.9$  nM), and morphine ( $K_i = 127$  nM) as seen in Fig. 7.2 (panels B to D). Notably, compared to all of the mAbs reported so far (all with an affinity for 6-MAM at 150-300 nM),<sup>362-364</sup> MMBCmAb-H6M has the highest binding affinity for 6-MAM (the most toxic metabolite of heroin).

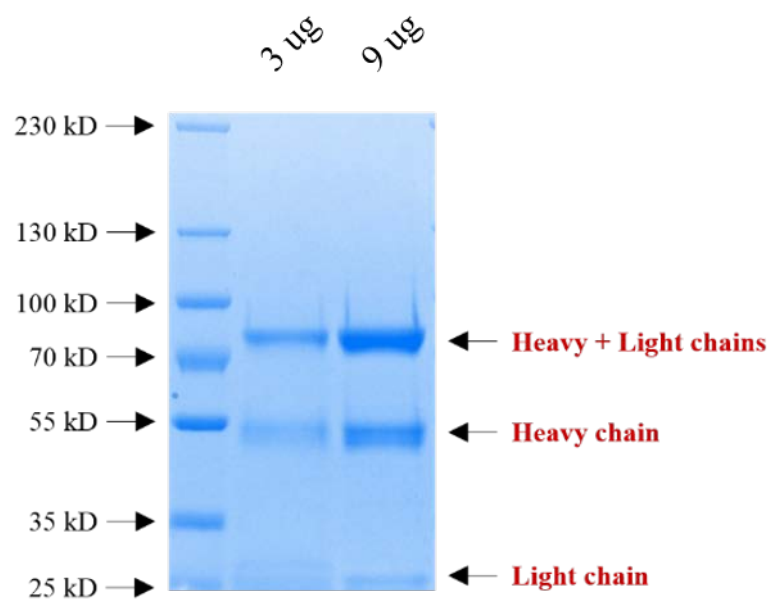


**Figure 7.1** SDS-PAGE of the purified mAb MMBCmAb-H6M. The different amounts of the purified antibody were loaded on the gel and visualized by Coomassie blue staining to determine its purity before a subsequent binding affinity test.

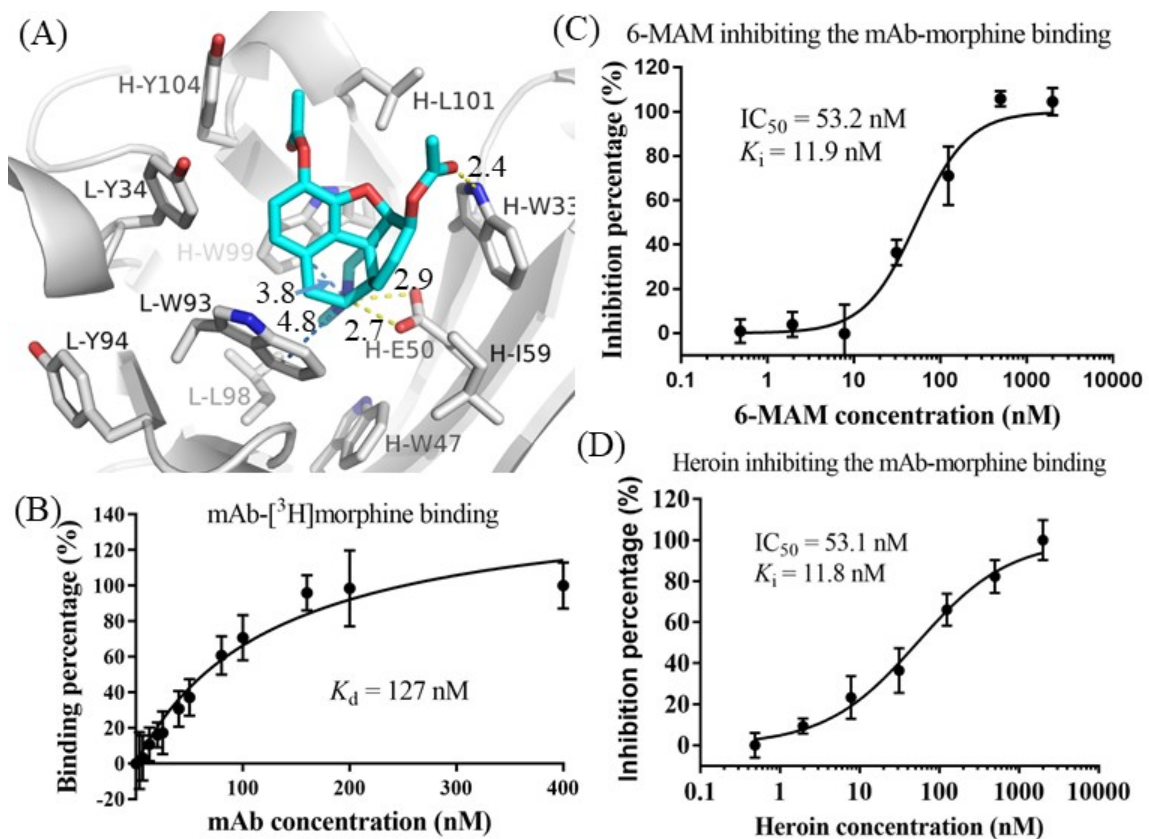


**Figure 7.2** The modeled structure and in vitro activities of mAb MMBCmAb-H6M: (A) mAb binding with heroin in which the distances are given in Å (the binding structures with 6-MAM and morphine are very similar to this one); (B) mAb-[<sup>3</sup>H]morphine binding saturation data (with [<sup>3</sup>H]morphine concentration being 2 nM); (C) 6-MAM inhibiting the mAb-[<sup>3</sup>H]morphine binding; (D) heroin inhibiting the mAb-[<sup>3</sup>H]morphine binding. For the competing binding assays, the [<sup>3</sup>H]morphine concentration was 2 nM, and the mAb concentration was 60 nM. All of the error bars of the *in vitro* data are represented in the standard deviation (SD).

#### **7.1.4 Materials and methods**

##### ***Protein preparation***

In our proof-of-principle studies, the mAb (MMBCmAb-H6M) genes were designed to carry both the heavy and light chains, with an Internal Ribosome Entry Site (IRES) inserted between them, so that both the heavy and light chains can be expressed at the same time. The genes were synthesized by GeneArt (Invitrogen), and were cloned into the pCMV-MCS vector (the same vector used to express many other proteins in our lab) between the BamHI and SalI sites.

The same experimental procedure<sup>365-366</sup> used in our accomplished studies to prepare various Fc-fusion protein variants was used to prepare MMBCmAb-H6M (and variants) in this investigation. Briefly, site-directed mutagenesis of the mAb cDNA (in the pCMV-MCS expression plasmid) was performed by using the QuikChange method.<sup>367</sup> Each variant was expressed in Chinese hamster ovary (CHO) cells in free-style CHO expression medium. Cells were grown first to a density of  $\sim 1.0 \times 10^6$  cells/ml in a 2 L shake flask and transfected using TransIT-PRO Transfectio Kit. Cells were incubated at 37°C in a CO<sub>2</sub> incubator for 5 days before the culture medium was harvested. The mAb (MMBCmAb-H6M or variant) protein expressed in the medium was purified by using MabSelect Protein A resin (GE Healthcare)<sup>38, 40</sup> and analyzed by SDS-PAGE.

##### ***In vitro binding assays***

The binding of the mAb with [<sup>3</sup>H]morphine was determined by using liquid scintillation counting. Briefly, 2 nM [<sup>3</sup>H]morphine was incubated with a varying concentration of mAb at room temperature for 60 min, with the total volume of the mixture being 100  $\mu$ L and the pH being 7.4. Then, it was filtered with EMD Millipore Amicon™

Ultra-0.5 Centrifugal Filter (30 kD) and EMD Millipore Amicon™ Ultra 0.5 mL Vials. 50  $\mu$ L of the filtrate was added to 3 mL of 3a70BTM complete counting cocktail (RPI Research Products) for liquid scintillation counting. The obtained mAb concentration-dependent data were analyzed by using the GraphPad Prism 7 software to determine the binding constant.

For the binding affinity of the mAb with other ligands, we first determined IC<sub>50</sub> for each ligand inhibiting the mAb-[<sup>3</sup>H]morphine binding through a competing binding assay. Briefly, 100  $\mu$ L of mixture (pH 7.4) containing 2 nM [<sup>3</sup>H]morphine, 60 nM mAb (or an mAb concentration close to the  $K_d$  of the mAb-[<sup>3</sup>H]morphine binding), and a varying concentration of the ligand under testing was incubated at room temperature for 60 min. Then the mixture was filtered with EMD Millipore Amicon™ Ultra-0.5 Centrifugal Filter (30 kD) and EMD Millipore Amicon™ Ultra 0.5 mL Vials, and 50  $\mu$ L of the filtrate was added to 3 mL of 3a70BTM complete counting cocktail (RPI Research Products) for liquid scintillation counting. The IC<sub>50</sub> (calculated by using the GraphPad Prism 7 software) was converted to  $K_i$  (or  $K_d$ ) by using the IC<sub>50</sub>-to- $K_i$  Converter.<sup>368</sup>

## **7.2 Development of mPGES-1 specific inhibitor as an anticancer agent for multiple therapeutic areas**

### **7.2.1 The main purpose of this study**

A growing body of evidence strongly suggest that prostaglandin E<sub>2</sub> (PGE<sub>2</sub>) plays a critical role in tumor development including proliferation in multiple types of cancer cells.<sup>369-372</sup> In PGE<sub>2</sub> biosynthesis, Cyclooxygenases (COX-1/COX-2) converts arachidonic acid arachidonic acid (AA) to prostaglandin H<sub>2</sub> (PGH<sub>2</sub>),<sup>373</sup> and microsomal PGE-synthase-1 (mPGES-1) converts PGH<sub>2</sub> to PGE<sub>2</sub>.<sup>374</sup> DU145 (human prostate cancer cell line), LLC-1 (murine lung cancer cell line), and A549 (human colon cancer cell line) express substantial amounts of MPGES-1 in a constitutive manner.<sup>369</sup> In the present study, we wanted to examine the possibility that an mPEGS-1 inhibitor has an anti-tumor activity and can be utilized for cancer treatment in combination with the first-line therapeutics for lung, colon, and prostate cancer including Cisplatin, Erlotinib, and Paclitaxel (PTX). I tested one of the mPGES-1 inhibitors (denoted as BAR002) discovered in our lab. It turned out that this mPGES-1 inhibitor had only mild anti-proliferation activity, but no strong cytotoxicity to both DU-145 or A549 cells. In addition, BAR002 did not show a promising synergistic anti-cancer activity when used in combination with the tested first-line drug.

### **7.2.2 Results and discussion**

Previously, our lab discovered a potent mPEGS-1 inhibitor, denoted as BAR002 here for convenience, whose IC<sub>50</sub> value is 33 nM against human mPEGS-1 and 157 nM against mouse mPGES-1.<sup>375-376</sup> First, the cytotoxicity of BAR002, Cisplatin, Erlotinib, and PTX were determined using MTT assay. Experiments were performed in triplicates and the

mean half maximal inhibitory concentration ( $IC_{50}$ ) was utilized to compare cytotoxicity. The determined  $IC_{50}$  values of these drugs for DU-145 cell growth (after 48 h of exposure) were summarized in Table 7.1 and depicted in Fig. 7.3. The results show that the  $IC_{50}$  value of BAR002 for the cell viability was  $\sim 23.6 \mu\text{M}$ , which implies that mPGES-1 inhibition by BAR002 is unlikely to be very toxic to DU-145 cells.

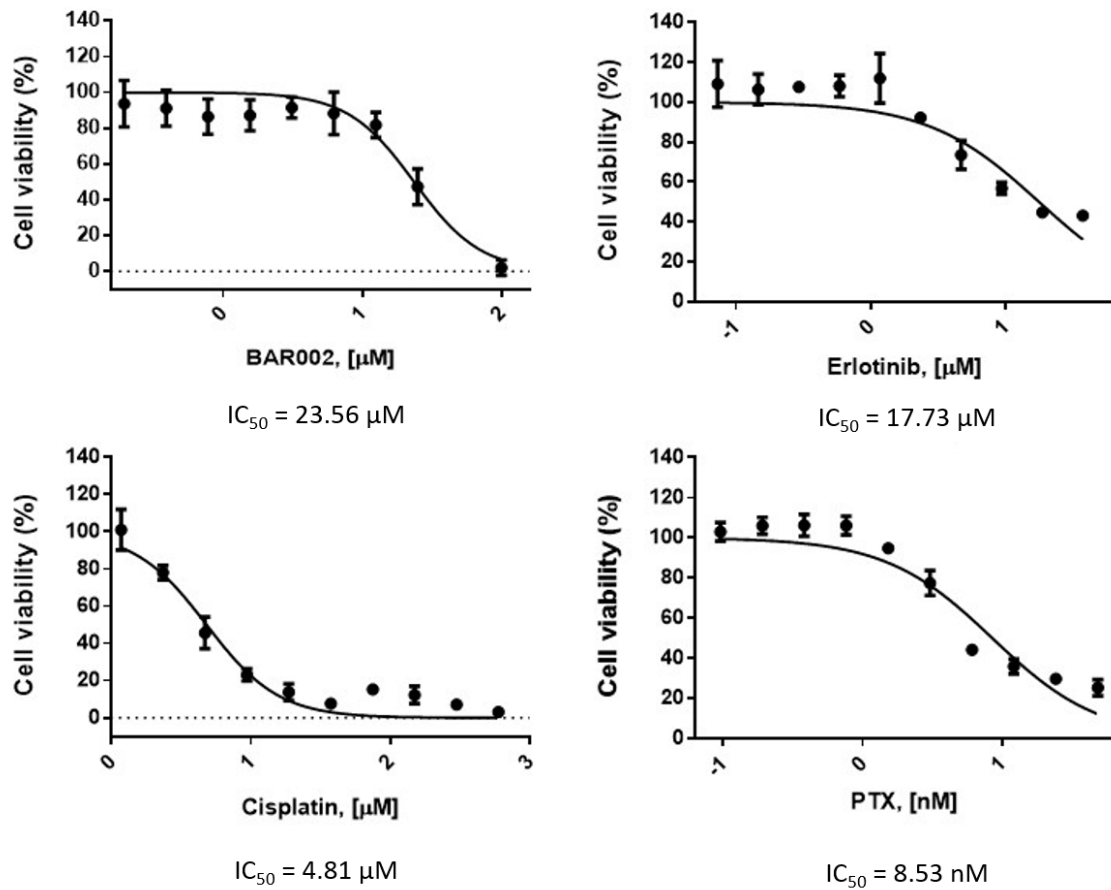


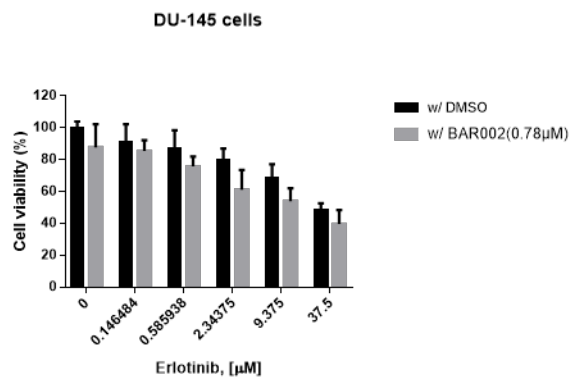
**Figure 7.3** Dose-response curves of Cisplatin, Erlotinib, or PTX in DU-145 cells (48 h of exposure, n = 3, mean  $\pm$  SD).



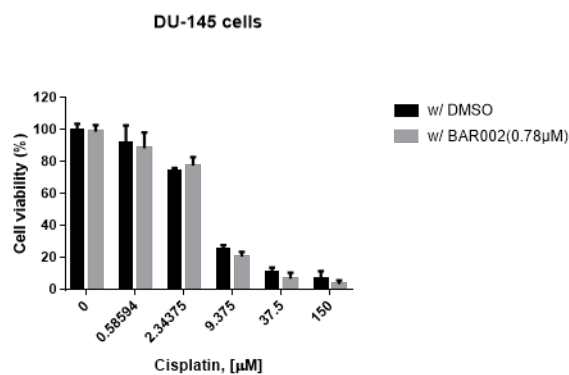
**Table 7.1** IC<sub>50</sub> values (μM) of BAR002, Cisplatin, Erlotinib, or PTX after 48 h of exposure (n = 3, mean ± SD)

	BAR002	Cisplatin	Erlotinib	PTX
DU-145	23.56 (±2.43)	4.81 (±0.12)	17.73 (±3.45)	<0.01

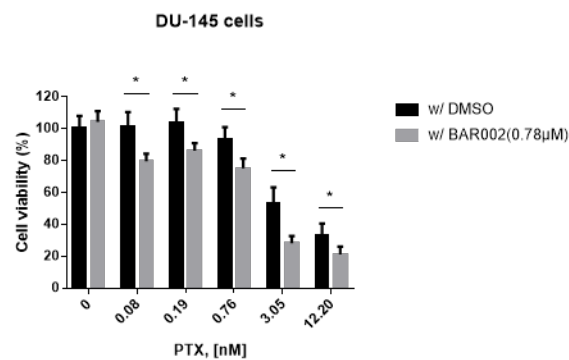
To evaluate the effect of combining BAR002 with the tested anti-cancer agents, DU-145 cells were exposed to a different concentration of Cisplatin, Erlotinib, or PTX in combination with 0.78 μM BAR002, followed by incubation for 48 h. Considering the low IC<sub>50</sub> value of BAR002 for human mPEGS-1 (33 nM)<sup>375</sup> and its IC<sub>50</sub> value determined for the growth of DU-145 cells (~23.6 μM), it is highly expected that BAR002 treatment at 1 μM concentration would strongly inhibit mPGES-1 activity of the cells, but not be significantly toxic to the cells. According to the results obtained (Fig. 7.4), BAR002 had subtle synergistic anti-cancer activity (about 10~20%) only with PTX, but not with Erlotinib or Cisplatin.



asterisks indicate p-value <0.05 with the Student t test



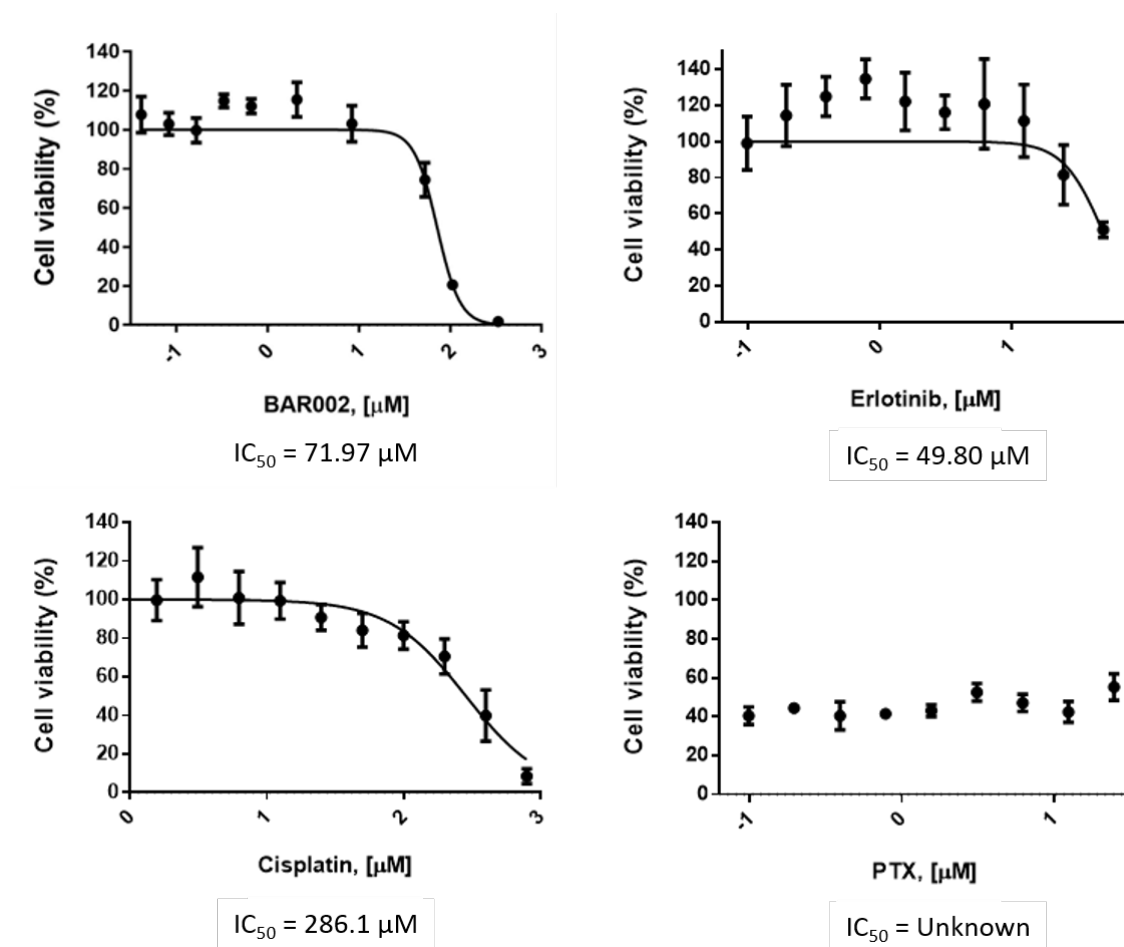
asterisks indicate p-value <0.05 with the Student t test



asterisks indicate p-value <0.05 with the Student t test

**Figure 7.4** Combination assays of BAR002 and anticancer agents Cisplatin, Erlotinib, and PTX. DU-145 cells were exposed to a different concentration of an anticancer agent with 0.78 μM BAR002.

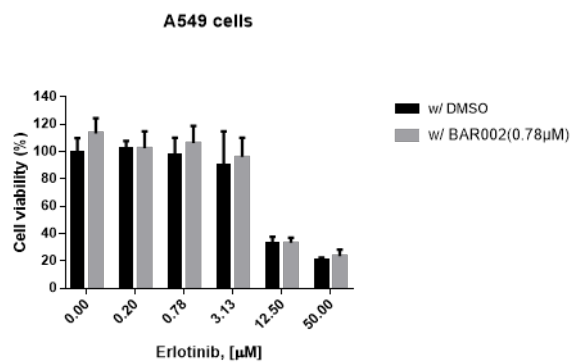
The cytotoxicity of BAR002, Cisplatin, Erlotinib, and PTX were also determined for A549 cells (colon cancer cell line). The determined IC<sub>50</sub> values of these drugs for the cell growth (after 48 h of exposure) were summarized in Table 7.2 (and also Fig. 7.5). According to the results obtained, A549 than DU-145 cells displayed relatively higher resistance to apoptotic cell death by the compounds tested. Interestingly, it was also observed that A549 cells were not completely died even at 25  $\mu$ M concentration of PTX. I do not know the reason why some of A549 clonal populations still had such strong resistance to the high dose of PTX, but this lead me to test whether BAR002 treatment makes A549 cells more vulnerable to apoptotic cells death by PTX or other anti-cancer reagents. For this, A549 cells were exposed to different concentrations of Cisplatin, Erlotinib, or PTX in combination with 0.78  $\mu$ M BAR002, followed by incubation for 48 h. The results showed that BAR002 neither increased the sensitivity of A549 cells to cell-death induced by PTX nor displayed significant synergistic anti-cancer activity with Erlotinib or Cisplatin (Fig. 7.6).



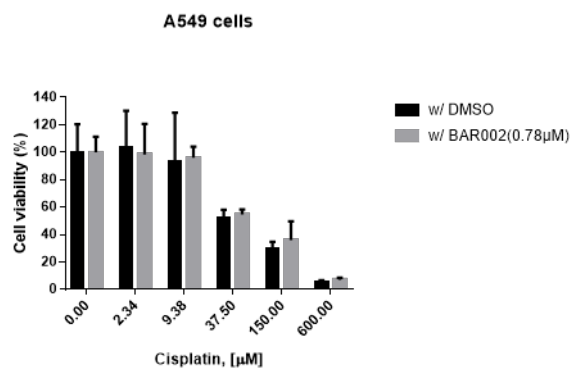
**Figure 7.5** Dose-response curves of Cisplatin, Erlotinib, or PTX in A549 cells (48 h of exposure,  $n = 3$ , mean  $\pm$  SD).

Table 7.2  $IC_{50}$  values (μM) of BAR002, Cisplatin, Erlotinib, or PTX after 48 h of exposure ( $n = 3$ , mean  $\pm$  SD)

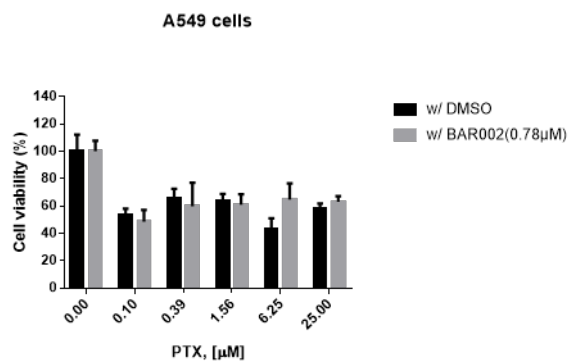
	BAR002	Cisplatin	Erlotinib	PTX
A549	71.97 ( $\pm 12.31$ )	286.1 ( $\pm 0.12$ )	49.80 ( $\pm 9.28$ )	Unknown



asterisks indicate p-value <0.05 with the Student t test



asterisks indicate p-value <0.05 with the Student t test



asterisks indicate p-value <0.05 with the Student t test

**Figure 7.6** Combination assays of BAR002 and anticancer agents Cisplatin, Erlotinib, and PTX. A549 cells were exposed to different concentrations of an anticancer agent with 0.78 μM BAR002.

We also determined whether BAR002 is capable of inhibiting the proliferation of DU-145 cells. DU-145 cells were treated with the BAR002 concentrations where the viability of DU-145 cells was not significantly affected. Viability was then measured over 5 days after the cells were exposed to BAR002. According to the results obtained (Fig. 7.7), proliferation in DU-145 cells was significantly compromised 4 days after exposure to BAR002. The antiproliferative effect of BAR002 was also observed even at the low BAR002 concentrations and became more obvious over time, which implies that the onset of the antiproliferative effect of BAR002 was slow. It is expected that the long-term BAR002 treatment would produce a more promising tumor growth suppression by the compound. In the future, we may have to further determine how efficiently BAR002 inhibits PEG<sub>2</sub> production in DU-145 cells overtime in the given treatment conditions. The combined results of the long-term effects of BAR002 on proliferation and PEG<sub>2</sub> production in DU-145 cells will let us know whether there is a positive correlation between those factors.

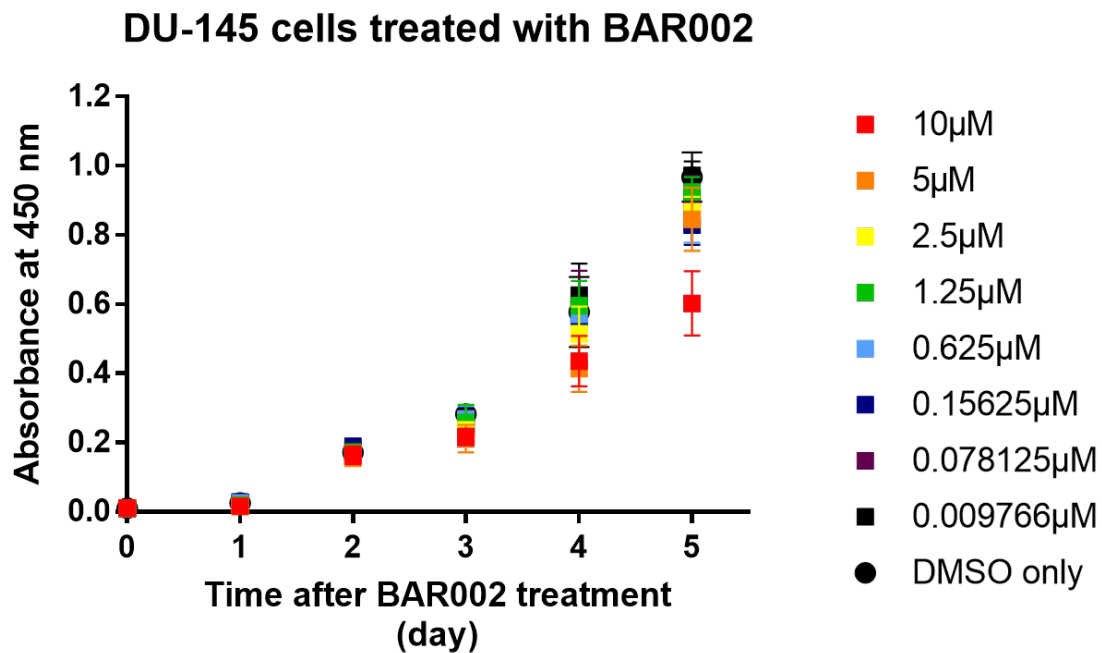


**Figure 7.7** Viability was measured over 5 days by MTT reduction after DU-145 cells were exposed to different concentrations of BAR002 (closed squares) and or controls (closed circles). Controls consisted of DMSO at the same concentration as in the BAR002-treatment experiments. Each experiment was performed in triplicates. Results are presented as the mean  $\pm$  S.D. of two separate experiments.

### **7.2.3 Materials and methods**

#### ***Cell viability assay***

Cells were seed onto a 96 well plate. (5000 cells/well). 24hr after cell seeding, the cells were incubated with differing concentrations of a designated compound for 48hr. Dye reduction was then initiated by the addition of 20  $\mu$ L of 5 mg/mL MTS to each well. After 2 h, the developed signals were measured at absorbance at 570 in a micro plate reader.

#### ***Cell proliferation assay***

Cells were seeded onto 96 well plate ( $5 \times 10^3$  cells/per) and incubated for 12 hr. The culture media was exchanged with fresh media right before incubation with different concentrations of an mPGES-1 inhibitor. The cell growth was measured over 3 days by MTS assay.



## References

1. Quianzon, C. C.; Cheikh, I., History of insulin. *J Community Hosp Intern Med Perspect* **2012**, 2 (2).
2. Cho, M. J.; Juliano, R., Macromolecular versus small-molecule therapeutics: drug discovery, development and clinical considerations. *Trends Biotechnol* **1996**, 14 (5), 153-8.
3. Lindsley, C. W., The top prescription drugs of 2012 globally: biologics dominate, but small molecule CNS drugs hold on to top spots. *ACS Chem Neurosci* **2013**, 4 (6), 905-7.
4. Graul, A. I.; Pina, P.; Cruces, E.; Stringer, M., The year's new drugs & biologics 2016: Part I. *Drugs Today (Barc)* **2017**, 53 (1), 27-74.
5. Lagasse, H. A.; Alexaki, A.; Simhadri, V. L.; Katagiri, N. H.; Jankowski, W.; Sauna, Z. E.; Kimchi-Sarfaty, C., Recent advances in (therapeutic protein) drug development. *FI000Res* **2017**, 6, 113.
6. Leader, B.; Baca, Q. J.; Golan, D. E., Protein therapeutics: a summary and pharmacological classification. *Nat Rev Drug Discov* **2008**, 7 (1), 21-39.
7. Berenson, D. F.; Weiss, A. R.; Wan, Z. L.; Weiss, M. A., Insulin analogs for the treatment of diabetes mellitus: therapeutic applications of protein engineering. *Ann N Y Acad Sci* **2011**, 1243, E40-E54.
8. Aviezer, D.; Golembo, M.; Yayon, A., Fibroblast growth factor receptor-3 as a therapeutic target for Achondroplasia--genetic short limbed dwarfism. *Curr Drug Targets* **2003**, 4 (5), 353-65.
9. Laron, Z.; Klinger, B.; Blum, W. F.; Silbergeld, A.; Ranke, M. B., IGF binding protein 3 in patients with Laron type dwarfism: effect of exogenous rIGF-I. *Clin Endocrinol (Oxf)* **1992**, 36 (3), 301-4.
10. Alvarez-Gallardo, H.; Kjelland, M. E.; Moreno, J. F.; Welsh, T. H., Jr.; Randel, R. D.; Lammoglia, M. A.; Perez-Martinez, M.; Lara-Sagahon, A. V.; Esperon-Sumano, A. E.; Romo, S., Gamete therapeutics: recombinant protein adsorption by sperm for increasing fertility via artificial insemination. *PLoS One* **2013**, 8 (6), e65083.
11. Pinevich, A. J.; Petersen, J., Erythropoietin therapy in patients with chronic renal failure. *West J Med* **1992**, 157 (2), 154-7.
12. Hoppe, H., Cerezyme--recombinant protein treatment for Gaucher's disease. *J Biotechnol* **2000**, 76 (2-3), 259-61.
13. Cox, T. M., Gaucher disease: clinical profile and therapeutic developments. *Biologics* **2010**, 4, 299-313.
14. Kintzing, J. R.; Filsinger Interrante, M. V.; Cochran, J. R., Emerging Strategies for Developing Next-Generation Protein Therapeutics for Cancer Treatment. *Trends Pharmacol Sci* **2016**, 37 (12), 993-1008.
15. Harada, H.; Kizaka-Kondoh, S.; Hiraoka, M., Antitumor protein therapy; application of the protein transduction domain to the development of a protein drug for cancer treatment. *Breast Cancer* **2006**, 13 (1), 16-26.
16. Chakrabarty, A. M.; Bernardes, N.; Fialho, A. M., Bacterial proteins and peptides in cancer therapy: today and tomorrow. *Bioengineered* **2014**, 5 (4), 234-42.
17. Adler, M. J.; Dimitrov, D. S., Therapeutic antibodies against cancer. *Hematol Oncol*

*Clin North Am* **2012**, 26 (3), 447-81, vii.

18. Johnson-Leger, C.; Power, C. A.; Shomade, G.; Shaw, J. P.; Proudfoot, A. E., Protein therapeutics--lessons learned and a view of the future. *Expert Opin Biol Ther* **2006**, 6 (1), 1-7.
19. Nichols, T. C.; Dillow, A. M.; Franck, H. W.; Merricks, E. P.; Raymer, R. A.; Bellinger, D. A.; Arruda, V. R.; High, K. A., Protein replacement therapy and gene transfer in canine models of hemophilia A, hemophilia B, von willebrand disease, and factor VII deficiency. *ILAR J* **2009**, 50 (2), 144-67.
20. Youjin, S.; Jun, Y., The treatment of hemophilia A: from protein replacement to AAV-mediated gene therapy. *Biotechnol Lett* **2009**, 31 (3), 321-8.
21. Mahler, H. C., Developing protein therapeutics. *J Pharm Pharmacol* **2018**, 70 (5), 583.
22. Carter, P. J., Introduction to current and future protein therapeutics: a protein engineering perspective. *Exp Cell Res* **2011**, 317 (9), 1261-9.
23. Vasserot, A. P.; Dickinson, C. D.; Tang, Y.; Huse, W. D.; Manchester, K. S.; Watkins, J. D., Optimization of protein therapeutics by directed evolution. *Drug Discov Today* **2003**, 8 (3), 118-26.
24. Caravella, J.; Lugovskoy, A., Design of next-generation protein therapeutics. *Curr Opin Chem Biol* **2010**, 14 (4), 520-8.
25. Steinmetz, N. A.; Koch, C.; Harris, K. D.; Carandini, M., Challenges and opportunities for large-scale electrophysiology with Neuropixels probes. *Curr Opin Neurobiol* **2018**, 50, 92-100.
26. Mello, C. V.; Clayton, D. F., The opportunities and challenges of large-scale molecular approaches to songbird neurobiology. *Neurosci Biobehav Rev* **2015**, 50, 70-6.
27. Lautala, P. T.; Hilliard, M. R.; Webb, E.; Busch, I.; Richard Hess, J.; Roni, M. S.; Hilbert, J.; Handler, R. M.; Bittencourt, R.; Valente, A.; Laitinen, T., Opportunities and Challenges in the Design and Analysis of Biomass Supply Chains. *Environ Manage* **2015**, 56 (6), 1397-415.
28. Putney, S. D.; Burke, P. A., Improving protein therapeutics with sustained-release formulations. *Nat Biotechnol* **1998**, 16 (2), 153-7.
29. Marshall, S. A.; Lazar, G. A.; Chirino, A. J.; Desjarlais, J. R., Rational design and engineering of therapeutic proteins. *Drug Discov Today* **2003**, 8 (5), 212-21.
30. Chennamsetty, N.; Voynov, V.; Kayser, V.; Helk, B.; Trout, B. L., Design of therapeutic proteins with enhanced stability. *Proc Natl Acad Sci U S A* **2009**, 106 (29), 11937-42.
31. Liu, W. P.; Chen, Y. H.; Ming, X.; Kong, Y., Design and Synthesis of a Novel Cationic Peptide with Potent and Broad-Spectrum Antimicrobial Activity. *Biomed Res Int* **2015**, 2015, 578764.
32. Hwang, I.; Park, S., Computational design of protein therapeutics. *Drug Discov Today Technol* **2008**, 5 (2-3), e43-8.
33. Jeal, W.; Goa, K. L., Aldesleukin (recombinant interleukin-2): a review of its pharmacological properties, clinical efficacy and tolerability in patients with renal cell carcinoma. *BioDrugs* **1997**, 7 (4), 285-317.
34. Amaria, R. N.; Reuben, A.; Cooper, Z. A.; Wargo, J. A., Update on use of aldesleukin for treatment of high-risk metastatic melanoma. *Immunotargets Ther* **2015**, 4, 79-89.

35. Interleukin-2 (IL-2, Proleukin). *Proj Inf Perspect* **1999**, (27), 21-2.
36. Alex, S.; Gupta, S. L.; Minor, J. R.; Turcovski-Corrales, S.; Gallelli, J. F.; Taub, D.; Piscitelli, S. C., Compatibility and activity of aldesleukin (recombinant interleukin-2) in presence of selected drugs during simulated Y-site administration: evaluation of three methods. *Am J Health Syst Pharm* **1995**, 52 (21), 2423-6.
37. Dillman, R. O., What to do with IL-2? *Cancer Biother Radiopharm* **1999**, 14 (6), 423-34.
38. Atkins, M. B., Interleukin-2: clinical applications. *Semin Oncol* **2002**, 29 (3 Suppl 7), 12-7.
39. Yang, J. C.; Sherry, R. M.; Steinberg, S. M.; Topalian, S. L.; Schwartzentruber, D. J.; Hwu, P.; Seipp, C. A.; Rogers-Freezer, L.; Morton, K. E.; White, D. E.; Liewehr, D. J.; Merino, M. J.; Rosenberg, S. A., Randomized study of high-dose and low-dose interleukin-2 in patients with metastatic renal cancer. *J Clin Oncol* **2003**, 21 (16), 3127-32.
40. Rao, B. M.; Driver, I.; Lauffenburger, D. A.; Wittrup, K. D., High-affinity CD25-binding IL-2 mutants potently stimulate persistent T cell growth. *Biochemistry* **2005**, 44 (31), 10696-701.
41. Rao, B. M.; Driver, I.; Lauffenburger, D. A.; Wittrup, K. D., Interleukin 2 (IL-2) variants engineered for increased IL-2 receptor alpha-subunit affinity exhibit increased potency arising from a cell surface ligand reservoir effect. *Mol Pharmacol* **2004**, 66 (4), 864-9.
42. Osusky, M.; Teschke, L.; Wang, X.; Wong, K.; Buckley, J. T., A chimera of interleukin 2 and a binding variant of aerolysin is selectively toxic to cells displaying the interleukin 2 receptor. *J Biol Chem* **2008**, 283 (3), 1572-9.
43. Peraino, J. S.; Zhang, H.; Rajasekera, P. V.; Wei, M.; Madsen, J. C.; Sachs, D. H.; Huang, C. A.; Wang, Z., Diphtheria toxin-based bivalent human IL-2 fusion toxin with improved efficacy for targeting human CD25(+) cells. *J Immunol Methods* **2014**, 405, 57-66.
44. Kelley, V. E.; Bacha, P.; Pankewycz, O.; Nichols, J. C.; Murphy, J. R.; Strom, T. B., Interleukin 2-diphtheria toxin fusion protein can abolish cell-mediated immunity in vivo. *Proc Natl Acad Sci U S A* **1988**, 85 (11), 3980-4.
45. Duvic, M.; Talpur, R., Optimizing denileukin diftitox (Ontak) therapy. *Future Oncol* **2008**, 4 (4), 457-69.
46. Fuentes, A. C.; Szwed, E.; Spears, C. D.; Thaper, S.; Dang, L. H.; Dang, N. H., Denileukin Diftitox (Ontak) as Maintenance Therapy for Peripheral T-Cell Lymphomas: Three Cases with Sustained Remission. *Case Rep Oncol Med* **2015**, 2015, 123756.
47. Wong, K. K.; deLeeuw, R. J.; Dosanjh, N. S.; Kimm, L. R.; Cheng, Z.; Horsman, D. E.; MacAulay, C.; Ng, R. T.; Brown, C. J.; Eichler, E. E.; Lam, W. L., A comprehensive analysis of common copy-number variations in the human genome. *Am J Hum Genet* **2007**, 80 (1), 91-104.
48. Woetmann, A.; Lovato, P.; Eriksen, K. W.; Krejsgaard, T.; Labuda, T.; Zhang, Q.; Mathiesen, A. M.; Geisler, C.; Svejgaard, A.; Wasik, M. A.; Odum, N., Nonmalignant T cells stimulate growth of T-cell lymphoma cells in the presence of bacterial toxins. *Blood* **2007**, 109 (8), 3325-32.
49. Bandaranayake, A. D.; Almo, S. C., Recent advances in mammalian protein production. *FEBS letters* **2014**, 588 (2), 253-60.
50. Butler, M.; Meneses-Acosta, A., Recent advances in technology supporting

biopharmaceutical production from mammalian cells. *Appl Microbiol Biotechnol* **2012**, 96 (4), 885-94.

51. Zhu, J., Mammalian cell protein expression for biopharmaceutical production. *Biotechnol Adv* **2012**, 30 (5), 1158-70.

52. Tobin, P. H.; Richards, D. H.; Callender, R. A.; Wilson, C. J., Protein engineering: a new frontier for biological therapeutics. *Curr Drug Metab* **2014**, 15 (7), 743-56.

53. Wurm, F. M., Production of recombinant protein therapeutics in cultivated mammalian cells. *Nat Biotechnol* **2004**, 22 (11), 1393-8.

54. Lutz, S., Beyond directed evolution--semi-rational protein engineering and design. *Curr Opin Biotechnol* **2010**, 21 (6), 734-43.

55. Turecek, P. L.; Bossard, M. J.; Schoetens, F.; Ivens, I. A., PEGylation of Biopharmaceuticals: A Review of Chemistry and Nonclinical Safety Information of Approved Drugs. *J Pharm Sci* **2016**, 105 (2), 460-475.

56. Levin, D.; Golding, B.; Strome, S. E.; Sauna, Z. E., Fc fusion as a platform technology: potential for modulating immunogenicity. *Trends Biotechnol* **2015**, 33 (1), 27-34.

57. Rath, T.; Baker, K.; Dumont, J. A.; Peters, R. T.; Jiang, H.; Qiao, S. W.; Lencer, W. I.; Pierce, G. F.; Blumberg, R. S., Fc-fusion proteins and FcRn: structural insights for longer-lasting and more effective therapeutics. *Crit Rev Biotechnol* **2015**, 35 (2), 235-54.

58. Andersen, J. T.; Pehrson, R.; Tolmachev, V.; Daba, M. B.; Abrahmsen, L.; Ekblad, C., Extending half-life by indirect targeting of the neonatal Fc receptor (FcRn) using a minimal albumin binding domain. *J Biol Chem* **2011**, 286 (7), 5234-41.

59. Sockolosky, J. T.; Szoka, F. C., The neonatal Fc receptor, FcRn, as a target for drug delivery and therapy. *Adv Drug Deliv Rev* **2015**, 91, 109-24.

60. Kuo, T. T.; Aveson, V. G., Neonatal Fc receptor and IgG-based therapeutics. *MAbs* **2011**, 3 (5), 422-30.

61. Mankarious, S.; Lee, M.; Fischer, S.; Pyun, K. H.; Ochs, H. D.; Oxelius, V. A.; Wedgwood, R. J., The half-lives of IgG subclasses and specific antibodies in patients with primary immunodeficiency who are receiving intravenously administered immunoglobulin. *J Lab Clin Med* **1988**, 112 (5), 634-40.

62. Correia, I. R., Stability of IgG isotypes in serum. *MAbs* **2010**, 2 (3), 221-32.

63. Oganessian, V.; Damschroder, M. M.; Cook, K. E.; Li, Q.; Gao, C.; Wu, H.; Dall'Acqua, W. F., Structural insights into neonatal Fc receptor-based recycling mechanisms. *J Biol Chem* **2014**, 289 (11), 7812-24.

64. Schmidt, M. M.; Townson, S. A.; Andreucci, A. J.; King, B. M.; Schirmer, E. B.; Murillo, A. J.; Dombrowski, C.; Tisdale, A. W.; Lowden, P. A.; Masci, A. L.; Kovalchin, J. T.; Erbe, D. V.; Wittrup, K. D.; Furfine, E. S.; Barnes, T. M., Crystal structure of an HSA/FcRn complex reveals recycling by competitive mimicry of HSA ligands at a pH-dependent hydrophobic interface. *Structure* **2013**, 21 (11), 1966-78.

65. Christianson, G. J.; Sun, V. Z.; Akilesh, S.; Pesavento, E.; Proetzel, G.; Roopenian, D. C., Monoclonal antibodies directed against human FcRn and their applications. *MAbs* **2012**, 4 (2), 208-16.

66. Czajkowsky, D. M.; Hu, J.; Shao, Z.; Pleass, R. J., Fc-fusion proteins: new developments and future perspectives. *EMBO Mol Med* **2012**, 4 (10), 1015-28.

67. Kenanova, V. E.; Olafsen, T.; Salazar, F. B.; Williams, L. E.; Knowles, S.; Wu, A. M., Tuning the serum persistence of human serum albumin domain III: diabody fusion

proteins. *Protein Eng Des Sel* **2010**, 23 (10), 789-98.

68. Carter, J.; Zhang, J.; Dang, T. L.; Hasegawa, H.; Cheng, J. D.; Gianan, I.; O'Neill, J. W.; Wolfson, M.; Siu, S.; Qu, S.; Meininger, D.; Kim, H.; Delaney, J.; Mehlin, C., Fusion partners can increase the expression of recombinant interleukins via transient transfection in 2936E cells. *Protein Sci* **2010**, 19 (2), 357-62.

69. Xu, J.; Zhang, C., Human IgG Fc promotes expression, secretion and immunogenicity of enterovirus 71 VP1 protein. *J Biomed Res* **2016**, 30 (3), 209-16.

70. Carlson, K. R.; Pomerantz, S. C.; Li, J.; Vafa, O.; Naso, M.; Strohl, W.; Mains, R. E.; Eipper, B. A., Secretion of Fc-amidated peptide fusion proteins by Chinese hamster ovary cells. *BMC Biotechnol* **2015**, 15, 61.

71. Park, K., Albumin: a versatile carrier for drug delivery. *J Control Release* **2012**, 157 (1), 3.

72. Evans, D. R.; Macniven, R. P.; Labanca, M.; Walker, J.; Notarnicola, S. M., Purification of an Fc-fusion biologic: clearance of multiple product related impurities by hydrophobic interaction chromatography. *J Chromatogr A* **2008**, 1177 (2), 265-71.

73. Kimchi-Sarfaty, C.; Schiller, T.; Hamasaki-Katagiri, N.; Khan, M. A.; Yanover, C.; Sauna, Z. E., Building better drugs: developing and regulating engineered therapeutic proteins. *Trends in pharmacological sciences* **2013**, 34 (10), 534-48.

74. Borrok, M. J.; Wu, Y.; Beyaz, N.; Yu, X. Q.; Oganessian, V.; Dall'Acqua, W. F.; Tsui, P., pH-dependent binding engineering reveals an FcRn affinity threshold that governs IgG recycling. *J Biol Chem* **2015**, 290 (7), 4282-90.

75. Dall'Acqua, W. F.; Woods, R. M.; Ward, E. S.; Palaszynski, S. R.; Patel, N. K.; Brewah, Y. A.; Wu, H.; Kiener, P. A.; Langermann, S., Increasing the affinity of a human IgG1 for the neonatal Fc receptor: biological consequences. *J Immunol* **2002**, 169 (9), 5171-80.

76. Dall'Acqua, W. F.; Kiener, P. A.; Wu, H., Properties of human IgG1s engineered for enhanced binding to the neonatal Fc receptor (FcRn). *The Journal of biological chemistry* **2006**, 281 (33), 23514-24.

77. Yeung, Y. A.; Leabman, M. K.; Marvin, J. S.; Qiu, J.; Adams, C. W.; Lien, S.; Starovasnik, M. A.; Lowman, H. B., Engineering human IgG1 affinity to human neonatal Fc receptor: impact of affinity improvement on pharmacokinetics in primates. *J Immunol* **2009**, 182 (12), 7663-71.

78. Keating, G. M., Bevacizumab: a review of its use in advanced cancer. *Drugs* **2014**, 74 (16), 1891-1925.

79. Yeung, M. L.; Bennasser, Y.; Watashi, K.; Le, S. Y.; Houzet, L.; Jeang, K. T., Pyrosequencing of small non-coding RNAs in HIV-1 infected cells: evidence for the processing of a viral-cellular double-stranded RNA hybrid. *Nucleic acids research* **2009**, 37 (19), 6575-86.

80. Monnet, C.; Jorieux, S.; Urbain, R.; Fournier, N.; Bouayadi, K.; De Romeuf, C.; Behrens, C. K.; Fontayne, A.; Mondon, P., Selection of IgG Variants with Increased FcRn Binding Using Random and Directed Mutagenesis: Impact on Effector Functions. *Front Immunol* **2015**, 6, 39.

81. Yeung, Y. A.; Wu, X.; Reyes, A. E., 2nd; Vernes, J. M.; Lien, S.; Lowe, J.; Maia, M.; Forrest, W. F.; Meng, Y. G.; Damico, L. A.; Ferrara, N.; Lowman, H. B., A therapeutic anti-VEGF antibody with increased potency independent of pharmacokinetic half-life. *Cancer Res* **2010**, 70 (8), 3269-77.

82. Zheng, F.; Zhan, C. G., Are pharmacokinetic approaches feasible for treatment of cocaine addiction and overdose? *Future medicinal chemistry* **2012**, *4* (2), 125-8.
83. Nutt, D.; King, L. A.; Saulsbury, W.; Blakemore, C., Development of a rational scale to assess the harm of drugs of potential misuse. *Lancet* **2007**, *369* (9566), 1047-53.
84. Cohen-Barak, O.; Wildeman, J.; van de Wetering, J.; Hettinga, J.; Schuilenga-Hut, P.; Gross, A.; Clark, S.; Bassan, M.; Gilgun-Sherki, Y.; Mendzelevski, B.; Spiegelstein, O., Safety, Pharmacokinetics, and Pharmacodynamics of TV-1380, a Novel Mutated Butyrylcholinesterase Treatment for Cocaine Addiction, After Single and Multiple Intramuscular Injections in Healthy Subjects. *J Clin Pharmacol* **2015**, *55*, 573-583.
85. Gilgun-Sherki, Y.; Eliaz, R. E.; McCann, D. J.; Loupe, P. S.; Eyal, E.; Blatt, K.; Cohen-Barak, O.; Hallak, H.; Chiang, N.; Gyaw, S., Placebo-controlled evaluation of a bioengineered, cocaine-metabolizing fusion protein, TV-1380 (AlbuBChE), in the treatment of cocaine dependence. *Drug Alcohol Depend.* **2016**, *166*, 13-20.
86. Kyungbo Kim, T. Z., Xirong Zheng, Fang Zheng, Chang-Guo Zhan, An efficient long-lasting cocaine hydrolase prevents both cocaine-induced hyper-locomotion activity and dopamine transporter trafficking to cell surface in the brains of rats. **2018**.
87. Chen, X.; Xue, L.; Hou, S.; Jin, Z.; Zhang, T.; Zheng, F.; Zhan, C. G., Long-acting cocaine hydrolase for addiction therapy. *Proc Natl Acad Sci U S A* **2016**, *113* (2), 422-7.
88. Heard, K.; Palmer, R.; Zahniser, N. R., Mechanisms of acute cocaine toxicity. *The open pharmacology journal* **2008**, *2* (9), 70-78.
89. Foltin, R. W.; Fischman, M. W.; Levin, F. R., Cardiovascular effects of cocaine in humans: laboratory studies. *Drug and alcohol dependence* **1995**, *37* (3), 193-210.
90. Schindler, C. W.; Tella, S. R.; Erzouki, H. K.; Goldberg, S. R., Pharmacological mechanisms in cocaine's cardiovascular effects. *Drug and alcohol dependence* **1995**, *37* (3), 183-91.
91. Goldfrank, L. R.; Hoffman, R. S., The cardiovascular effects of cocaine. *Annals of emergency medicine* **1991**, *20* (2), 165-75.
92. Das, G., Cardiovascular effects of cocaine abuse. *International journal of clinical pharmacology, therapy, and toxicology* **1993**, *31* (11), 521-8.
93. Havakuk, O.; Rezkalla, S. H.; Kloner, R. A., The Cardiovascular Effects of Cocaine. *Journal of the American College of Cardiology* **2017**, *70* (1), 101-113.
94. Zhou, J., Norepinephrine transporter inhibitors and their therapeutic potential. *Drugs of the future* **2004**, *29* (12), 1235-1244.
95. Muscholl, E., Effect of cocaine and related drugs on the uptake of noradrenaline by heart and spleen. *British journal of pharmacology and chemotherapy* **1961**, *16*, 352-9.
96. Hurd, W. W.; Smith, A. J.; Gauvin, J. M.; Hayashi, R. H., Cocaine blocks extraneuronal uptake of norepinephrine by the pregnant human uterus. *Obstetrics and gynecology* **1991**, *78* (2), 249-53.
97. Rosenberg, M. B.; Carroll, F. I.; Negus, S. S., Effects of monoamine reuptake inhibitors in assays of acute pain-stimulated and pain-depressed behavior in rats. *The journal of pain : official journal of the American Pain Society* **2013**, *14* (3), 246-59.
98. Phillips, K.; Luk, A.; Soor, G. S.; Abraham, J. R.; Leong, S.; Butany, J., Cocaine cardiotoxicity: a review of the pathophysiology, pathology, and treatment options. *American journal of cardiovascular drugs : drugs, devices, and other interventions* **2009**, *9* (3), 177-96.
99. Rezkalla, S. H.; Kloner, R. A., Cocaine-induced acute myocardial infarction.

*Clinical medicine & research* **2007**, 5 (3), 172-6.

100. Nestler, E. J., The neurobiology of cocaine addiction. *Sci Pract Perspect* **2005**, 3 (1), 4-10.

101. Karila, L.; Petit, A.; Lowenstein, W.; Reynaud, M., Diagnosis and consequences of cocaine addiction. *Current medicinal chemistry* **2012**, 19 (33), 5612-8.

102. Kosten, T. R.; George, T. P., The neurobiology of opioid dependence: implications for treatment. *Science & practice perspectives* **2002**, 1 (1), 13-20.

103. Morton, W. A., Cocaine and Psychiatric Symptoms. *Primary care companion to the Journal of clinical psychiatry* **1999**, 1 (4), 109-113.

104. Ahmadi, J.; Kampman, K.; Dackis, C.; Sparkman, T.; Pettinati, H., Cocaine withdrawal symptoms identify "Type B" cocaine-dependent patients. *The American journal on addictions* **2008**, 17 (1), 60-4.

105. Banks, M. L.; Negus, S. S., Effects of extended cocaine access and cocaine withdrawal on choice between cocaine and food in rhesus monkeys. *Neuropsychopharmacology : official publication of the American College of Neuropsychopharmacology* **2010**, 35 (2), 493-504.

106. Sofuoglu, M.; Dudish-Poulsen, S.; Poling, J.; Mooney, M.; Hatsukami, D. K., The effect of individual cocaine withdrawal symptoms on outcomes in cocaine users. *Addictive behaviors* **2005**, 30 (6), 1125-34.

107. Kampman, K. M.; Pettinati, H.; Volpicelli, J.; Kaempf, G.; Turk, E.; Insua, A.; Lipkin, C.; Sparkman, T.; O'Brien, C. P., Concurrent cocaine withdrawal alters alcohol withdrawal symptoms. *Journal of addictive diseases* **2002**, 21 (4), 13-26.

108. Helmus, T. C.; Downey, K. K.; Wang, L. M.; Rhodes, G. L.; Schuster, C. R., The relationship between self-reported cocaine withdrawal symptoms and history of depression. *Addictive behaviors* **2001**, 26 (3), 461-7.

109. Cornelius, J. R.; Thase, M. E.; Salloum, I. M.; Cornelius, M. D.; Black, A.; Mann, J. J., Cocaine use associated with increased suicidal behavior in depressed alcoholics. *Addictive behaviors* **1998**, 23 (1), 119-21.

110. Sperry, K.; Sweeney, E. S., Suicide by intravenous injection of cocaine. A report of three cases. *Journal of forensic sciences* **1989**, 34 (1), 244-8.

111. Darke, S.; Kaye, S., Attempted suicide among injecting and noninjecting cocaine users in Sydney, Australia. *Journal of urban health : bulletin of the New York Academy of Medicine* **2004**, 81 (3), 505-15.

112. Aviram, M.; Dornfeld, L., Pomegranate juice consumption inhibits serum angiotensin converting enzyme activity and reduces systolic blood pressure. *Atherosclerosis* **2001**, 158 (1), 195-8.

113. Dursteler, K. M.; Berger, E. M.; Strasser, J.; Caflisch, C.; Mutschler, J.; Herdener, M.; Vogel, M., Clinical potential of methylphenidate in the treatment of cocaine addiction: a review of the current evidence. *Substance abuse and rehabilitation* **2015**, 6, 61-74.

114. Palmer, R. S.; McMahon, T. J.; Moreggi, D. I.; Rounsaville, B. J.; Ball, S. A., College Student Drug Use: Patterns, Concerns, Consequences, and Interest in Intervention. *Journal of college student development* **2012**, 53 (1).

115. Murphy, J. L., Jr., Hypertension and pulmonary oedema associated with ketamine administration in a patient with a history of substance abuse. *Canadian journal of anaesthesia = Journal canadien d'anesthesie* **1993**, 40 (2), 160-4.

116. Holman, B. L.; Carvalho, P. A.; Mendelson, J.; Teoh, S. K.; Nardin, R.; Hallgring,

- E.; Hebben, N.; Johnson, K. A., Brain perfusion is abnormal in cocaine-dependent polydrug users: a study using technetium-99m-HMPAO and ASPECT. *Journal of nuclear medicine : official publication, Society of Nuclear Medicine* **1991**, 32 (6), 1206-10.
117. Amara, S. G.; Kuhar, M. J., Neurotransmitter transporters: recent progress. *Annual review of neuroscience* **1993**, 16, 73-93.
118. Horne, M. K.; Lee, J.; Chen, F.; Lanning, K.; Tomas, D.; Lawrence, A. J., Long-term administration of cocaine or serotonin reuptake inhibitors results in anatomical and neurochemical changes in noradrenergic, dopaminergic, and serotonin pathways. *Journal of neurochemistry* **2008**, 106 (4), 1731-44.
119. Gorelick, D. A.; Kim, Y. K.; Bencherif, B.; Boyd, S. J.; Nelson, R.; Copersino, M. L.; Dannals, R. F.; Frost, J. J., Brain mu-opioid receptor binding: relationship to relapse to cocaine use after monitored abstinence. *Psychopharmacology* **2008**, 200 (4), 475-86.
120. McClure, E. A.; Gipson, C. D.; Malcolm, R. J.; Kalivas, P. W.; Gray, K. M., Potential role of N-acetylcysteine in the management of substance use disorders. *CNS drugs* **2014**, 28 (2), 95-106.
121. Schmitz, J. M.; Green, C. E.; Stotts, A. L.; Lindsay, J. A.; Rathnayaka, N. S.; Grabowski, J.; Moeller, F. G., A two-phased screening paradigm for evaluating candidate medications for cocaine cessation or relapse prevention: modafinil, levodopa-carbidopa, naltrexone. *Drug and alcohol dependence* **2014**, 136, 100-7.
122. Dackis, C.; O'Brien, C., Neurobiology of addiction: treatment and public policy ramifications. *Nature neuroscience* **2005**, 8 (11), 1431-6.
123. Volkow, N. D.; Fowler, J. S.; Wolf, A. P.; Schlyer, D.; Shiue, C. Y.; Alpert, R.; Dewey, S. L.; Logan, J.; Bendriem, B.; Christman, D.; et al., Effects of chronic cocaine abuse on postsynaptic dopamine receptors. *The American journal of psychiatry* **1990**, 147 (6), 719-24.
124. Volkow, N. D.; Fowler, J. S.; Wang, G. J.; Hitzemann, R.; Logan, J.; Schlyer, D. J.; Dewey, S. L.; Wolf, A. P., Decreased dopamine D2 receptor availability is associated with reduced frontal metabolism in cocaine abusers. *Synapse* **1993**, 14 (2), 169-77.
125. Volkow, N. D.; Wang, G. J.; Fowler, J. S.; Logan, J.; Gatley, S. J.; Hitzemann, R.; Chen, A. D.; Dewey, S. L.; Pappas, N., Decreased striatal dopaminergic responsiveness in detoxified cocaine-dependent subjects. *Nature* **1997**, 386 (6627), 830-3.
126. Martinez, D.; Broft, A.; Foltin, R. W.; Slifstein, M.; Hwang, D. R.; Huang, Y.; Perez, A.; Frankle, W. G.; Cooper, T.; Kleber, H. D.; Fischman, M. W.; Laruelle, M., Cocaine dependence and d2 receptor availability in the functional subdivisions of the striatum: relationship with cocaine-seeking behavior. *Neuropsychopharmacology : official publication of the American College of Neuropsychopharmacology* **2004**, 29 (6), 1190-202.
127. Malison, R. T.; Best, S. E.; van Dyck, C. H.; McCance, E. F.; Wallace, E. A.; Laruelle, M.; Baldwin, R. M.; Seibyl, J. P.; Price, L. H.; Kosten, T. R.; Innis, R. B., Elevated striatal dopamine transporters during acute cocaine abstinence as measured by [123I] beta-CIT SPECT. *The American journal of psychiatry* **1998**, 155 (6), 832-4.
128. Crits-Christoph, P.; Newberg, A.; Wintering, N.; Ploessl, K.; Gibbons, M. B.; Ring-Kurtz, S.; Gallop, R.; Present, J., Dopamine transporter levels in cocaine dependent subjects. *Drug Alcohol Depend* **2008**, 98 (1-2), 70-6.
129. Wang, G. J.; Volkow, N. D.; Fowler, J. S.; Fischman, M.; Foltin, R.; Abumrad, N. N.; Logan, J.; Pappas, N. R., Cocaine abusers do not show loss of dopamine transporters with age. *Life sciences* **1997**, 61 (11), 1059-65.



130. Narendran, R.; Lopresti, B. J.; Martinez, D.; Mason, N. S.; Himes, M.; May, M. A.; Daley, D. C.; Price, J. C.; Mathis, C. A.; Frankle, W. G., In vivo evidence for low striatal vesicular monoamine transporter 2 (VMAT2) availability in cocaine abusers. *The American journal of psychiatry* **2012**, *169* (1), 55-63.
131. Little, K. Y.; Krolewski, D. M.; Zhang, L.; Cassin, B. J., Loss of striatal vesicular monoamine transporter protein (VMAT2) in human cocaine users. *The American journal of psychiatry* **2003**, *160* (1), 47-55.
132. Wilson, J. M.; Levey, A. I.; Bergeron, C.; Kalasinsky, K.; Ang, L.; Peretti, F.; Adams, V. I.; Smialek, J.; Anderson, W. R.; Shannak, K.; Deck, J.; Niznik, H. B.; Kish, S. J., Striatal dopamine, dopamine transporter, and vesicular monoamine transporter in chronic cocaine users. *Annals of neurology* **1996**, *40* (3), 428-39.
133. Jacobsen, L. K.; Staley, J. K.; Malison, R. T.; Zoghbi, S. S.; Seibyl, J. P.; Kosten, T. R.; Innis, R. B., Elevated central serotonin transporter binding availability in acutely abstinent cocaine-dependent patients. *The American journal of psychiatry* **2000**, *157* (7), 1134-40.
134. Little, K. Y.; Patel, U. N.; Clark, T. B.; Butts, J. D., Alteration of brain dopamine and serotonin levels in cocaine users: a preliminary report. *The American journal of psychiatry* **1996**, *153* (9), 1216-8.
135. Matuskey, D.; Bhagwagar, Z.; Planeta, B.; Pittman, B.; Gallezot, J. D.; Chen, J.; Wanyiri, J.; Najafzadeh, S.; Ropchan, J.; Geha, P.; Huang, Y.; Potenza, M. N.; Neumeister, A.; Carson, R. E.; Malison, R. T., Reductions in brain 5-HT1B receptor availability in primarily cocaine-dependent humans. *Biological psychiatry* **2014**, *76* (10), 816-22.
136. Yang, S.; Salmeron, B. J.; Ross, T. J.; Xi, Z. X.; Stein, E. A.; Yang, Y., Lower glutamate levels in rostral anterior cingulate of chronic cocaine users - A (1)H-MRS study using TE-averaged PRESS at 3 T with an optimized quantification strategy. *Psychiatry research* **2009**, *174* (3), 171-6.
137. Little, J. M.; Kurkela, M.; Sonka, J.; Jantti, S.; Ketola, R.; Bratton, S.; Finel, M.; Radomska-Pandya, A., Glucuronidation of oxidized fatty acids and prostaglandins B1 and E2 by human hepatic and recombinant UDP-glucuronosyltransferases. *J Lipid Res* **2004**, *45* (9), 1694-703.
138. Volkow, N. D.; Fowler, J. S.; Wang, G. J.; Swanson, J. M.; Telang, F., Dopamine in drug abuse and addiction: results of imaging studies and treatment implications. *Archives of neurology* **2007**, *64* (11), 1575-9.
139. Thomas, M. J.; Kalivas, P. W.; Shaham, Y., Neuroplasticity in the mesolimbic dopamine system and cocaine addiction. *British journal of pharmacology* **2008**, *154* (2), 327-42.
140. Kauer, J. A.; Malenka, R. C., Synaptic plasticity and addiction. *Nature reviews. Neuroscience* **2007**, *8* (11), 844-58.
141. Koob, G. F.; Caine, B.; Markou, A.; Pulvirenti, L.; Weiss, F., Role for the mesocortical dopamine system in the motivating effects of cocaine. *NIDA Res Monogr* **1994**, *145*, 1-18.
142. Kalivas, P. W., Neurobiology of cocaine addiction: implications for new pharmacotherapy. *The American journal on addictions* **2007**, *16* (2), 71-8.
143. Schmitt, K. C.; Reith, M. E., Regulation of the dopamine transporter: aspects relevant to psychostimulant drugs of abuse. *Annals of the New York Academy of Sciences* **2010**, *1187*, 316-40.

144. Ali, S. F.; Onaivi, E. S.; Dodd, P. R.; Cadet, J. L.; Schenk, S.; Kuhar, M. J.; Koob, G. F., Understanding the Global Problem of Drug Addiction is a Challenge for IDARS Scientists. *Current neuropharmacology* **2011**, 9 (1), 2-7.
145. Koob, G. F.; Volkow, N. D., Neurocircuitry of addiction. *Neuropsychopharmacology : official publication of the American College of Neuropsychopharmacology* **2010**, 35 (1), 217-38.
146. Melemis, S. M., Relapse Prevention and the Five Rules of Recovery. *The Yale journal of biology and medicine* **2015**, 88 (3), 325-32.
147. Kleber, H. D., Pharmacologic treatments for opioid dependence: detoxification and maintenance options. *Dialogues in clinical neuroscience* **2007**, 9 (4), 455-70.
148. Kreek, M. J.; LaForge, K. S.; Butelman, E., Pharmacotherapy of addictions. *Nature reviews. Drug discovery* **2002**, 1 (9), 710-26.
149. Gorelick, D. A., Pharmacokinetic strategies for treatment of drug overdose and addiction. *Future medicinal chemistry* **2012**, 4 (2), 227-43.
150. Kampman, K. M., New medications for the treatment of cocaine dependence. *Psychiatry* **2005**, 2 (12), 44-8.
151. Kim, J. H.; Lawrence, A. J., Drugs currently in Phase II clinical trials for cocaine addiction. *Expert opinion on investigational drugs* **2014**, 23 (8), 1105-22.
152. Grabowski, J.; Rhoades, H.; Stotts, A.; Cowan, K.; Kopecky, C.; Dougherty, A.; Moeller, F. G.; Hassan, S.; Schmitz, J., Agonist-like or antagonist-like treatment for cocaine dependence with methadone for heroin dependence: two double-blind randomized clinical trials. *Neuropsychopharmacology : official publication of the American College of Neuropsychopharmacology* **2004**, 29 (5), 969-81.
153. Grabowski, J.; Rhoades, H.; Schmitz, J.; Stotts, A.; Daruzska, L. A.; Creson, D.; Moeller, F. G., Dextroamphetamine for cocaine-dependence treatment: a double-blind randomized clinical trial. *Journal of clinical psychopharmacology* **2001**, 21 (5), 522-6.
154. Shearer, J.; Wodak, A.; van Beek, I.; Mattick, R. P.; Lewis, J., Pilot randomized double blind placebo-controlled study of dexamphetamine for cocaine dependence. *Addiction* **2003**, 98 (8), 1137-41.
155. Schmitz, J. M.; Lindsay, J. A.; Stotts, A. L.; Green, C. E.; Moeller, F. G., Contingency management and levodopa-carbidopa for cocaine treatment: a comparison of three behavioral targets. *Experimental and clinical psychopharmacology* **2010**, 18 (3), 238-44.
156. Dackis, C. A.; Kampman, K. M.; Lynch, K. G.; Pettinati, H. M.; O'Brien, C. P., A double-blind, placebo-controlled trial of modafinil for cocaine dependence. *Neuropsychopharmacology : official publication of the American College of Neuropsychopharmacology* **2005**, 30 (1), 205-11.
157. Anderson, A. L.; Reid, M. S.; Li, S. H.; Holmes, T.; Shemanski, L.; Slee, A.; Smith, E. V.; Kahn, R.; Chiang, N.; Vocci, F.; Ciraulo, D.; Dackis, C.; Roache, J. D.; Salloum, I. M.; Somoza, E.; Urschel, H. C., 3rd; Elkashef, A. M., Modafinil for the treatment of cocaine dependence. *Drug and alcohol dependence* **2009**, 104 (1-2), 133-9.
158. Baranski, J. V.; Pigeau, R.; Dinich, P.; Jacobs, I., Effects of modafinil on cognitive and meta-cognitive performance. *Human psychopharmacology* **2004**, 19 (5), 323-32.
159. Turner, D. C.; Robbins, T. W.; Clark, L.; Aron, A. R.; Dowson, J.; Sahakian, B. J., Cognitive enhancing effects of modafinil in healthy volunteers. *Psychopharmacology* **2003**, 165 (3), 260-9.

160. Kalechstein, A. D.; Mahoney, J. J., 3rd; Yoon, J. H.; Bennett, R.; De la Garza, R., 2nd, Modafinil, but not escitalopram, improves working memory and sustained attention in long-term, high-dose cocaine users. *Neuropharmacology* **2013**, *64*, 472-8.
161. Meini, M.; Capovani, B.; Sbrana, A.; Massei, G. J.; Ravani, L.; Massimetti, G.; Daini, L.; Scaramelli, D.; Moncini, M., A pilot open-label trial of ropinirole for cocaine dependence. *The American journal on addictions* **2008**, *17* (2), 165-6.
162. Meini, M.; Moncini, M.; Cecconi, D.; Cellesi, V.; Biasci, L.; Simoni, G.; Ameglio, M.; Pellegrini, M.; Forgione, R. N.; Rucci, P., Aripiprazole and ropinirole treatment for cocaine dependence: evidence from a pilot study. *Current pharmaceutical design* **2011**, *17* (14), 1376-83.
163. Schmitz, J. M.; Mooney, M. E.; Moeller, F. G.; Stotts, A. L.; Green, C.; Grabowski, J., Levodopa pharmacotherapy for cocaine dependence: choosing the optimal behavioral therapy platform. *Drug and alcohol dependence* **2008**, *94* (1-3), 142-50.
164. Vorspan, F.; Bellais, L.; Keijzer, L.; Lepine, J. P., An open-label study of aripiprazole in nonschizophrenic crack-dependent patients. *Journal of clinical psychopharmacology* **2008**, *28* (5), 570-2.
165. Haney, M.; Rubin, E.; Foltin, R. W., Aripiprazole maintenance increases smoked cocaine self-administration in humans. *Psychopharmacology* **2011**, *216* (3), 379-87.
166. Lofwall, M. R.; Nuzzo, P. A.; Campbell, C.; Walsh, S. L., Aripiprazole effects on self-administration and pharmacodynamics of intravenous cocaine and cigarette smoking in humans. *Experimental and clinical psychopharmacology* **2014**, *22* (3), 238-47.
167. Lile, J. A.; Stoops, W. W.; Glaser, P. E.; Hays, L. R.; Rush, C. R., Discriminative stimulus, subject-rated and cardiovascular effects of cocaine alone and in combination with aripiprazole in humans. *Journal of psychopharmacology* **2011**, *25* (11), 1469-79.
168. Johnson, B. A.; Roache, J. D.; Ait-Daoud, N.; Gunderson, E. W.; Haughey, H. M.; Wang, X. Q.; Liu, L., Topiramate's effects on cocaine-induced subjective mood, craving and preference for money over drug taking. *Addiction biology* **2013**, *18* (3), 405-16.
169. Kampman, K. M.; Pettinati, H.; Lynch, K. G.; Dackis, C.; Sparkman, T.; Weigley, C.; O'Brien, C. P., A pilot trial of topiramate for the treatment of cocaine dependence. *Drug and alcohol dependence* **2004**, *75* (3), 233-40.
170. Johnson, B. A.; Ait-Daoud, N.; Wang, X. Q.; Penberthy, J. K.; Javors, M. A.; Seneviratne, C.; Liu, L., Topiramate for the treatment of cocaine addiction: a randomized clinical trial. *JAMA psychiatry* **2013**, *70* (12), 1338-46.
171. Reis, A. D.; Castro, L. A.; Faria, R.; Laranjeira, R., Craving decrease with topiramate in outpatient treatment for cocaine dependence: an open label trial. *Revista brasileira de psiquiatria* **2008**, *30* (2), 132-5.
172. Harris, J. A.; Westbrook, R. F., Evidence that GABA transmission mediates context-specific extinction of learned fear. *Psychopharmacology* **1998**, *140* (1), 105-15.
173. Chhatwal, J. P.; Myers, K. M.; Ressler, K. J.; Davis, M., Regulation of gephyrin and GABAA receptor binding within the amygdala after fear acquisition and extinction. *The Journal of neuroscience : the official journal of the Society for Neuroscience* **2005**, *25* (2), 502-6.
174. Mariani, J. J.; Pavlicova, M.; Bisaga, A.; Nunes, E. V.; Brooks, D. J.; Levin, F. R., Extended-release mixed amphetamine salts and topiramate for cocaine dependence: a randomized controlled trial. *Biological psychiatry* **2012**, *72* (11), 950-6.
175. Shoptaw, S.; Yang, X.; Rotheram-Fuller, E. J.; Hsieh, Y. C.; Kintaudi, P. C.;

- Charuvastra, V. C.; Ling, W., Randomized placebo-controlled trial of baclofen for cocaine dependence: preliminary effects for individuals with chronic patterns of cocaine use. *The Journal of clinical psychiatry* **2003**, *64* (12), 1440-8.
176. Kahn, R.; Biswas, K.; Childress, A. R.; Shoptaw, S.; Fudala, P. J.; Gorgon, L.; Montoya, I.; Collins, J.; McSherry, F.; Li, S. H.; Chiang, N.; Alathari, H.; Watson, D.; Liberto, J.; Beresford, T.; Stock, C.; Wallace, C.; Gruber, V.; Elkashef, A., Multi-center trial of baclofen for abstinence initiation in severe cocaine-dependent individuals. *Drug and alcohol dependence* **2009**, *103* (1-2), 59-64.
177. Elliott, H. L.; Meredith, P. A.; Sumner, D. J.; McLean, K.; Reid, J. L., A pharmacodynamic and pharmacokinetic assessment of a new alpha-adrenoceptor antagonist, doxazosin (UK33274) in normotensive subjects. *British journal of clinical pharmacology* **1982**, *13* (5), 699-703.
178. Newton, T. F.; De La Garza, R., 2nd; Brown, G.; Kosten, T. R.; Mahoney, J. J., 3rd; Haile, C. N., Noradrenergic alpha(1) receptor antagonist treatment attenuates positive subjective effects of cocaine in humans: a randomized trial. *PloS one* **2012**, *7* (2), e30854.
179. Shorter, D.; Lindsay, J. A.; Kosten, T. R., The alpha-1 adrenergic antagonist doxazosin for treatment of cocaine dependence: A pilot study. *Drug and alcohol dependence* **2013**, *131* (1-2), 66-70.
180. Self, T.; Rogers, M. L.; Mancell, J.; Soberman, J. E., Carvedilol therapy after cocaine-induced myocardial infarction in patients with asthma. *The American journal of the medical sciences* **2011**, *342* (1), 56-61.
181. Kampman, K. M.; Volpicelli, J. R.; Mulvaney, F.; Alterman, A. I.; Cornish, J.; Gariti, P.; Cnaan, A.; Poole, S.; Muller, E.; Acosta, T.; Luce, D.; O'Brien, C., Effectiveness of propranolol for cocaine dependence treatment may depend on cocaine withdrawal symptom severity. *Drug and alcohol dependence* **2001**, *63* (1), 69-78.
182. Brunet, A.; Poundja, J.; Tremblay, J.; Bui, E.; Thomas, E.; Orr, S. P.; Azzoug, A.; Birmes, P.; Pitman, R. K., Trauma reactivation under the influence of propranolol decreases posttraumatic stress symptoms and disorder: 3 open-label trials. *Journal of clinical psychopharmacology* **2011**, *31* (4), 547-50.
183. Saladin, M. E.; Gray, K. M.; McRae-Clark, A. L.; Larowe, S. D.; Yeatts, S. D.; Baker, N. L.; Hartwell, K. J.; Brady, K. T., A double blind, placebo-controlled study of the effects of post-retrieval propranolol on reconsolidation of memory for craving and cue reactivity in cocaine dependent humans. *Psychopharmacology* **2013**, *226* (4), 721-37.
184. Zheng, F.; Zhan, C. G., Enzyme-therapy approaches for the treatment of drug overdose and addiction. *Future medicinal chemistry* **2011**, *3* (1), 9-13.
185. Kinsey, B. M.; Kosten, T. R.; Orson, F. M., Anti-cocaine vaccine development. *Expert review of vaccines* **2010**, *9* (9), 1109-14.
186. Leader, A. E.; Lerman, C.; Cappella, J. N., Nicotine vaccines: will smokers take a shot at quitting? *Nicotine & tobacco research : official journal of the Society for Research on Nicotine and Tobacco* **2010**, *12* (4), 390-7.
187. Moreno, A. Y.; Azar, M. R.; Warren, N. A.; Dickerson, T. J.; Koob, G. F.; Janda, K. D., A critical evaluation of a nicotine vaccine within a self-administration behavioral model. *Molecular pharmaceutics* **2010**, *7* (2), 431-41.
188. Norman, A. B.; Tabet, M. R.; Norman, M. K.; Tsibulsky, V. L., Using the self-administration of apomorphine and cocaine to measure the pharmacodynamic potencies and pharmacokinetics of competitive dopamine receptor antagonists. *Journal of*

*neuroscience methods* **2011**, *194* (2), 252-8.

189. Hubbard, J. J.; Laurenzana, E. M.; Williams, D. K.; Gentry, W. B.; Owens, S. M., The fate and function of therapeutic antiaddiction monoclonal antibodies across the reproductive cycle of rats. *The Journal of pharmacology and experimental therapeutics* **2011**, *336* (2), 414-22.

190. Pan, Y.; Gao, D.; Yang, W.; Cho, H.; Yang, G.; Tai, H. H.; Zhan, C. G., Computational redesign of human butyrylcholinesterase for anticocaine medication. *Proc Natl Acad Sci U S A* **2005**, *102* (46), 16656-61.

191. Yang, W.; Xue, L.; Fang, L.; Chen, X.; Zhan, C. G., Characterization of a high-activity mutant of human butyrylcholinesterase against (-)-cocaine. *Chem Biol Interact* **2010**, *187* (1-3), 148-52.

192. Gao, Y.; LaFleur, D.; Shah, R.; Zhao, Q.; Singh, M.; Brimijoin, S., An albumin-butyrylcholinesterase for cocaine toxicity and addiction: catalytic and pharmacokinetic properties. *Chem Biol Interact* **2008**, *175* (1-3), 83-7.

193. Anker, J. J.; Brimijoin, S.; Gao, Y.; Geng, L.; Zlebnik, N. E.; Parks, R. J.; Carroll, M. E., Cocaine hydrolase encoded in viral vector blocks the reinstatement of cocaine seeking in rats for 6 months. *Biol Psychiatry* **2012**, *71* (8), 700-5.

194. Gao, Y.; Geng, L.; Orson, F.; Kinsey, B.; Kosten, T. R.; Shen, X.; Brimijoin, S., Effects of anti-cocaine vaccine and viral gene transfer of cocaine hydrolase in mice on cocaine toxicity including motor strength and liver damage. *Chem Biol Interact* **2013**, *203* (1), 208-11.

195. Geng, L.; Gao, Y.; Chen, X.; Hou, S.; Zhan, C. G.; Radic, Z.; Parks, R. J.; Russell, S. J.; Pham, L.; Brimijoin, S., Gene transfer of mutant mouse cholinesterase provides high lifetime expression and reduced cocaine responses with no evident toxicity. *PLoS One* **2013**, *8* (6), e67446.

196. Sun, H.; Shen, M. L.; Pang, Y. P.; Lockridge, O.; Brimijoin, S., Cocaine metabolism accelerated by a re-engineered human butyrylcholinesterase. *J Pharmacol Exp Ther* **2002**, *302* (2), 710-6.

197. Xie, W.; Altamirano, C. V.; Bartels, C. F.; Speirs, R. J.; Cashman, J. R.; Lockridge, O., An improved cocaine hydrolase: the A328Y mutant of human butyrylcholinesterase is 4-fold more efficient. *Mol Pharmacol* **1999**, *55* (1), 83-91.

198. Brimijoin, S.; Gao, Y.; Anker, J. J.; Gliddon, L. A.; LaFleur, D.; Shah, R.; Zhao, Q.; Singh, M.; Carroll, M. E., A Cocaine Hydrolase Engineered from Human Butyrylcholinesterase Selectively Blocks Cocaine Toxicity and Reinstatement of Drug Seeking in Rats. *Neuropsychopharmacology* **2008**, *33* (11), 2715-2725.

199. Shram, M. J.; Cohen-Barak, O.; Chakraborty, B.; Bassan, M.; Schoedel, K. A.; Hallak, H.; Eyal, E.; Weiss, S.; Gilgun, Y.; Sellers, E. M.; Faulknor, J.; Spiegelstein, O., Assessment of Pharmacokinetic and Pharmacodynamic Interactions Between Albumin-Fused Mutated Butyrylcholinesterase and Intravenously Administered Cocaine in Recreational Cocaine Users. *J Clin Psychopharmacol* **2015**, *35*, 396-405.

200. Zhang, T.; Zheng, X.; Zhou, Z.; Chen, X.; Jin, Z.; Deng, J.; Zhan, C.-G.; Zheng, F., Clinical potential of an enzyme-based novel therapy for cocaine overdose. *Sci. Rep.* **2017**, *7*, 15303.

201. Zheng, X.; Zhou, Z.; Zhang, T.; Jin, Z.; Chen, X.; Deng, J.; Zhan, C.-G.; Zheng, F., Effectiveness of a cocaine hydrolase for cocaine toxicity treatment in male and female rats. *AAPS J.* **2018**, *20*, 3. <https://doi.org/10.1208/s12248-017-0167-4>.

202. Xue, L.; Ko, M. C.; Tong, M.; Yang, W.; Hou, S.; Fang, L.; Liu, J.; Zheng, F.; Woods, J. H.; Tai, H. H.; Zhan, C. G., Design, preparation, and characterization of high-activity mutants of human butyrylcholinesterase specific for detoxification of cocaine. *Molecular pharmacology* **2011**, *79* (2), 290-7.
203. Zheng, F.; Yang, W.; Xue, L.; Hou, S.; Liu, J.; Zhan, C. G., Design of high-activity mutants of human butyrylcholinesterase against (-)-cocaine: structural and energetic factors affecting the catalytic efficiency. *Biochemistry* **2010**, *49* (42), 9113-9.
204. Zheng, F.; Xue, L.; Hou, S.; Liu, J.; Zhan, M.; Yang, W.; Zhan, C. G., A highly efficient cocaine-detoxifying enzyme obtained by computational design. *Nat Commun* **2014**, *5*, 3457.
205. Huang, X.; Zheng, F.; Zhan, C. G., Binding structures and energies of the human neonatal Fc receptor with human Fc and its mutants by molecular modeling and dynamics simulations. *Mol Biosyst* **2013**, *9* (12), 3047-58.
206. Feng, Y.; Gong, R.; Dimitrov, D. S., Design, expression and characterization of a soluble single-chain functional human neonatal Fc receptor. *Protein Expr Purif* **2011**, *79* (1), 66-71.
207. Raghavan, M.; Bonagura, V. R.; Morrison, S. L.; Bjorkman, P. J., Analysis of the pH dependence of the neonatal Fc receptor/immunoglobulin G interaction using antibody and receptor variants. *Biochemistry* **1995**, *34* (45), 14649-57.
208. Raghavan, M.; Gastinel, L. N.; Bjorkman, P. J., The class I major histocompatibility complex related Fc receptor shows pH-dependent stability differences correlating with immunoglobulin binding and release. *Biochemistry* **1993**, *32* (33), 8654-60.
209. Ghetie, V.; Ward, E. S., Multiple roles for the major histocompatibility complex class I-related receptor FcRn. *Annu Rev Immunol* **2000**, *18*, 739-66.
210. He, W.; Ladinsky, M. S.; Huey-Tubman, K. E.; Jensen, G. J.; McIntosh, J. R.; Bjorkman, P. J., FcRn-mediated antibody transport across epithelial cells revealed by electron tomography. *Nature* **2008**, *455* (7212), 542-6.
211. Ghetie, V.; Hubbard, J. G.; Kim, J. K.; Tsen, M. F.; Lee, Y.; Ward, E. S., Abnormally short serum half-lives of IgG in beta 2-microglobulin-deficient mice. *Eur J Immunol* **1996**, *26* (3), 690-6.
212. Pyzik, M.; Rath, T.; Lencer, W. I.; Baker, K.; Blumberg, R. S., FcRn: The Architect Behind the Immune and Nonimmune Functions of IgG and Albumin. *J Immunol* **2015**, *194* (10), 4595-603.
213. Chaudhury, C.; Mehnaz, S.; Robinson, J. M.; Hayton, W. L.; Pearl, D. K.; Roopenian, D. C.; Anderson, C. L., The major histocompatibility complex-related Fc receptor for IgG (FcRn) binds albumin and prolongs its lifespan. *J Exp Med* **2003**, *197* (3), 315-22.
214. Gastinel, L. N.; Simister, N. E.; Bjorkman, P. J., Expression and crystallization of a soluble and functional form of an Fc receptor related to class I histocompatibility molecules. *Proc Natl Acad Sci U S A* **1992**, *89* (2), 638-42.
215. Maeda, A.; Iwayanagi, Y.; Haraya, K.; Tachibana, T.; Nakamura, G.; Nambu, T.; Esaki, K.; Hattori, K.; Igawa, T., Identification of human IgG1 variant with enhanced FcRn binding and without increased binding to rheumatoid factor autoantibody. *MAbs* **2017**, *9* (5), 844-853.
216. Abdiche, Y. N.; Yeung, Y. A.; Chaparro-Riggers, J.; Barman, I.; Strop, P.; Chin, S. M.; Pham, A.; Bolton, G.; McDonough, D.; Lindquist, K.; Pons, J.; Rajpal, A., The neonatal

Fc receptor (FcRn) binds independently to both sites of the IgG homodimer with identical affinity. *MAbs* **2015**, 7 (2), 331-43.

217. Robbie, G. J.; Criste, R.; Dall'acqua, W. F.; Jensen, K.; Patel, N. K.; Losonsky, G. A.; Griffin, M. P., A novel investigational Fc-modified humanized monoclonal antibody, motavizumab-YTE, has an extended half-life in healthy adults. *Antimicrob Agents Chemother* **2013**, 57 (12), 6147-53.

218. Simister, N. E.; Rees, A. R., Isolation and characterization of an Fc receptor from neonatal rat small intestine. *Eur J Immunol* **1985**, 15 (7), 733-8.

219. Kim, J. K.; Tsen, M. F.; Ghetie, V.; Ward, E. S., Localization of the site of the murine IgG1 molecule that is involved in binding to the murine intestinal Fc receptor. *Eur J Immunol* **1994**, 24 (10), 2429-34.

220. Popov, S.; Hubbard, J. G.; Kim, J.; Ober, B.; Ghetie, V.; Ward, E. S., The stoichiometry and affinity of the interaction of murine Fc fragments with the MHC class I-related receptor, FcRn. *Mol Immunol* **1996**, 33 (6), 521-30.

221. Tesar, D. B.; Cheung, E. J.; Bjorkman, P. J., The chicken yolk sac IgY receptor, a mammalian mannose receptor family member, transcytoses IgY across polarized epithelial cells. *Mol Biol Cell* **2008**, 19 (4), 1587-93.

222. Lee, C. H.; Choi, D. K.; Choi, H. J.; Song, M. Y.; Kim, Y. S., Expression of soluble and functional human neonatal Fc receptor in *Pichia pastoris*. *Protein Expr Purif* **2010**, 71 (1), 42-8.

223. Andersen, J. T.; Justesen, S.; Berntzen, G.; Michaelsen, T. E.; Lauvrak, V.; Fleckenstein, B.; Buus, S.; Sandlie, I., A strategy for bacterial production of a soluble functional human neonatal Fc receptor. *J Immunol Methods* **2008**, 331 (1-2), 39-49.

224. Sanchez, L. M.; Penny, D. M.; Bjorkman, P. J., Stoichiometry of the interaction between the major histocompatibility complex-related Fc receptor and its Fc ligand. *Biochemistry* **1999**, 38 (29), 9471-6.

225. Firan, M.; Bawdon, R.; Radu, C.; Ober, R. J.; Eaken, D.; Antohe, F.; Ghetie, V.; Ward, E. S., The MHC class I-related receptor, FcRn, plays an essential role in the maternofetal transfer of gamma-globulin in humans. *Int Immunol* **2001**, 13 (8), 993-1002.

226. Neuber, T.; Frese, K.; Jaehrling, J.; Jager, S.; Daubert, D.; Felderer, K.; Linnemann, M.; Hohne, A.; Kaden, S.; Kolln, J.; Tiller, T.; Brocks, B.; Ostendorp, R.; Pabst, S., Characterization and screening of IgG binding to the neonatal Fc receptor. *MAbs* **2014**, 6 (4), 928-42.

227. Lockridge, O.; Schopfer, L. M.; Winger, G.; Woods, J. H., Large Scale Purification of Butyrylcholinesterase from Human Plasma Suitable for Injection into Monkeys; a Potential New Therapeutic for Protection against Cocaine and Nerve Agent Toxicity. *J. Med. Chem. Biol. Radiol. Def.* **2005**, 3, nihms5095.

228. Schultz, W., Predictive reward signal of dopamine neurons. *J Neurophysiol* **1998**, 80 (1), 1-27.

229. Torres, G. E.; Gainetdinov, R. R.; Caron, M. G., Plasma membrane monoamine transporters: structure, regulation and function. *Nat Rev Neurosci* **2003**, 4 (1), 13-25.

230. Vaughan, R. A.; Foster, J. D., Mechanisms of dopamine transporter regulation in normal and disease states. *Trends Pharmacol Sci* **2013**, 34 (9), 489-96.

231. Amara, S. G.; Sonders, M. S., Neurotransmitter transporters as molecular targets for addictive drugs. *Drug Alcohol Depend* **1998**, 51 (1-2), 87-96.

232. Gainetdinov, R. R.; Wetsel, W. C.; Jones, S. R.; Levin, E. D.; Jaber, M.; Caron, M.

- G., Role of serotonin in the paradoxical calming effect of psychostimulants on hyperactivity. *Science* **1999**, 283 (5400), 397-401.
233. Greenwood, T. A.; Alexander, M.; Keck, P. E.; McElroy, S.; Sadovnick, A. D.; Remick, R. A.; Kelsoe, J. R., Evidence for linkage disequilibrium between the dopamine transporter and bipolar disorder. *Am J Med Genet* **2001**, 105 (2), 145-51.
234. Laasonen-Balk, T.; Kuikka, J.; Viinamaki, H.; Husso-Saastamoinen, M.; Lehtonen, J.; Tiihonen, J., Striatal dopamine transporter density in major depression. *Psychopharmacology (Berl)* **1999**, 144 (3), 282-5.
235. Segal, D. S.; Kuczenski, R., Repeated cocaine administration induces behavioral sensitization and corresponding decreased extracellular dopamine responses in caudate and accumbens. *Brain Res* **1992**, 577 (2), 351-5.
236. Cass, W. A.; Gerhardt, G. A.; Gillespie, K.; Curella, P.; Mayfield, R. D.; Zahniser, N. R., Reduced clearance of exogenous dopamine in rat nucleus accumbens, but not in dorsal striatum, following cocaine challenge in rats withdrawn from repeated cocaine administration. *J Neurochem* **1993**, 61 (1), 273-83.
237. Zahniser, N. R.; Larson, G. A.; Gerhardt, G. A., In vivo dopamine clearance rate in rat striatum: regulation by extracellular dopamine concentration and dopamine transporter inhibitors. *J Pharmacol Exp Ther* **1999**, 289 (1), 266-77.
238. David, D. J.; Zahniser, N. R.; Hoffer, B. J.; Gerhardt, G. A., In vivo electrochemical studies of dopamine clearance in subregions of rat nucleus accumbens: differential properties of the core and shell. *Exp Neurol* **1998**, 153 (2), 277-86.
239. Fleckenstein, A. E.; Haughey, H. M.; Metzger, R. R.; Kokoshka, J. M.; Riddle, E. L.; Hanson, J. E.; Gibb, J. W.; Hanson, G. R., Differential effects of psychostimulants and related agents on dopaminergic and serotonergic transporter function. *Eur J Pharmacol* **1999**, 382 (1), 45-9.
240. Daws, L. C.; Callaghan, P. D.; Moron, J. A.; Kahlig, K. M.; Shippenberg, T. S.; Javitch, J. A.; Galli, A., Cocaine increases dopamine uptake and cell surface expression of dopamine transporters. *Biochem Biophys Res Commun* **2002**, 290 (5), 1545-50.
241. Mash, D. C.; Pablo, J.; Ouyang, Q.; Hearn, W. L.; Izenwasser, S., Dopamine transport function is elevated in cocaine users. *J Neurochem* **2002**, 81 (2), 292-300.
242. Little, K. Y.; Elmer, L. W.; Zhong, H.; Scheys, J. O.; Zhang, L., Cocaine induction of dopamine transporter trafficking to the plasma membrane. *Mol Pharmacol* **2002**, 61 (2), 436-45.
243. Chi, L.; Reith, M. E., Substrate-induced trafficking of the dopamine transporter in heterologously expressing cells and in rat striatal synaptosomal preparations. *J Pharmacol Exp Ther* **2003**, 307 (2), 729-36.
244. Staley, J. K.; Hearn, W. L.; Ruttenber, A. J.; Wetli, C. V.; Mash, D. C., High affinity cocaine recognition sites on the dopamine transporter are elevated in fatal cocaine overdose victims. *J Pharmacol Exp Ther* **1994**, 271 (3), 1678-85.
245. Zheng, F.; Zhan, C. G., Modeling of pharmacokinetics of cocaine in human reveals the feasibility for development of enzyme therapies for drugs of abuse. *PLoS Comput Biol* **2012**, 8 (7), e1002610.
246. Fang, L.; Chow, K. M.; Hou, S.; Xue, L.; Chen, X.; Rodgers, D. W.; Zheng, F.; Zhan, C. G., Rational design, preparation, and characterization of a therapeutic enzyme mutant with improved stability and function for cocaine detoxification. *ACS Chem Biol* **2014**, 9 (8), 1764-72.



247. Lockridge, O.; Schopfer, L. M.; Winger, G.; Woods, J. H., Large Scale Purification of Butyrylcholinesterase from Human Plasma Suitable for Injection into Monkeys; a Potential New Therapeutic for Protection against Cocaine and Nerve Agent Toxicity. *J Med Chem Biol Radiol Def* **2005**, *3*, nihms5095.
248. Kyungbo Kim, J. Y., Zhenyu Jin, Fang Zheng, Chang-Guo Zhan, Kinetic characterization of cholinesterases and a therapeutically valuable cocaine hydrolase for their catalytic activities against heroin and its metabolite 6-monoacetylmorphine. *Chem Biol Interact* **2018**.
249. Kim, K.; Yao, J.; Jin, Z.; Zheng, F.; Zhan, C. G., Kinetic characterization of cholinesterases and a therapeutically valuable cocaine hydrolase for their catalytic activities against heroin and its metabolite 6-monoacetylmorphine. *Chem Biol Interact* **2018**, *293*, 107-114.
250. Kamendulis, L. M.; Brzezinski, M. R.; Pindel, E. V.; Bosron, W. F.; Dean, R. A., Metabolism of cocaine and heroin is catalyzed by the same human liver carboxylesterases. *J Pharmacol Exp Ther* **1996**, *279* (2), 713-7.
251. Siegal, H. A.; Carlson, R. G.; Wang, J.; Falck, R. S.; Stephens, R. C.; Nelson, E. D., Injection drug users in the Midwest: an epidemiologic comparison of drug use patterns in four Ohio cities. *J Psychoactive Drugs* **1994**, *26* (3), 265-75.
252. Hasin, D. S.; Grant, B. F.; Endicott, J.; Harford, T. C., Cocaine and heroin dependence compared in poly-drug abusers. *Am J Public Health* **1988**, *78* (5), 567-9.
253. Grella, C. E.; Anglin, M. D.; Wugalter, S. E., Patterns and predictors of cocaine and crack use by clients in standard and enhanced methadone maintenance treatment. *Am J Drug Alcohol Abuse* **1997**, *23* (1), 15-42.
254. Magura, S.; Kang, S. Y.; Nwakeze, P. C.; Demsky, S., Temporal patterns of heroin and cocaine use among methadone patients. *Subst Use Misuse* **1998**, *33* (12), 2441-67.
255. Lauzon, P.; Vincelette, J.; Bruneau, J.; Lamothe, F.; Lachance, N.; Brabant, M.; Soto, J., Illicit use of methadone among i.v. drug users in Montreal. *J Subst Abuse Treat* **1994**, *11* (5), 457-61.
256. Dolan, M. P.; Black, J. L.; Deford, H. A.; Skinner, J. R.; Robinowitz, R., Characteristics of drug abusers that discriminate needle-sharers. *Public Health Rep* **1987**, *102* (4), 395-8.
257. Rowlett, J. K.; Woolverton, W. L., Self-administration of cocaine and heroin combinations by rhesus monkeys responding under a progressive-ratio schedule. *Psychopharmacology (Berl)* **1997**, *133* (4), 363-71.
258. Perez de los Cobos, J.; Trujols, J.; Ribalta, E.; Casas, M., Cocaine use immediately prior to entry in an inpatient heroin detoxification unit as a predictor of discharges against medical advice. *Am J Drug Alcohol Abuse* **1997**, *23* (2), 267-79.
259. Downey, K. K.; Helmus, T. C.; Schuster, C. R., Contingency management for accurate predictions of urinalysis test results and lack of correspondence with self-reported drug use among polydrug abusers. *Psychol Addict Behav* **2000**, *14* (1), 69-72.
260. Leri, F.; Bruneau, J.; Stewart, J., Understanding polydrug use: review of heroin and cocaine co-use. *Addiction* **2003**, *98* (1), 7-22.
261. Boerner, U., The metabolism of morphine and heroin in man. *Drug Metab Rev* **1975**, *4* (1), 39-73.
262. Qiao, Y.; Han, K.; Zhan, C.-G., Reaction pathways and free energy profiles for cholinesterase-catalyzed hydrolysis of 6-monoacetylmorphine. *Org. Biomol. Chem.* **2014**,

12, 2214-2227 (Cover Article).

263. Qiao, Y.; Han, K. L.; Zhan, C.-G., Fundamental reaction pathway and free energy profile for butyrylcholinesterase-catalyzed hydrolysis of heroin. *Biochemistry* **2013**, *52*, 6467-6479.

264. Gottas, A.; Oiestad, E. L.; Boix, F.; Vindenes, V.; Ripel, A.; Thaulow, C. H.; Morland, J., Levels of heroin and its metabolites in blood and brain extracellular fluid after i.v. heroin administration to freely moving rats. *Br J Pharmacol* **2013**, *170* (3), 546-56.

265. Andersen, J. M.; Ripel, A.; Boix, F.; Normann, P. T.; Morland, J., Increased locomotor activity induced by heroin in mice: pharmacokinetic demonstration of heroin acting as a prodrug for the mediator 6-monoacetylmorphine in vivo. *J Pharmacol Exp Ther* **2009**, *331* (1), 153-61.

266. Boix, F.; Andersen, J. M.; Morland, J., Pharmacokinetic modeling of subcutaneous heroin and its metabolites in blood and brain of mice. *Addict Biol* **2013**, *18* (1), 1-7.

267. Bogen, I. L.; Boix, F.; Nerem, E.; Morland, J.; Andersen, J. M., A monoclonal antibody specific for 6-monoacetylmorphine reduces acute heroin effects in mice. *J Pharmacol Exp Ther* **2014**, *349* (3), 568-76.

268. Garrett, E. R.; Gurkan, T., Pharmacokinetics of morphine and its surrogates II: methods of separation of stabilized heroin and its metabolites from hydrolyzing biological fluids and applications to protein binding and red blood cell partition studies. *J Pharm Sci* **1979**, *68* (1), 26-32.

269. Garrett, E. R.; Gurkan, T., Pharmacokinetics of morphine and its surrogates IV: Pharmacokinetics of heroin and its derived metabolites in dogs. *J Pharm Sci* **1980**, *69* (10), 1116-34.

270. Owen, J. A.; Nakatsu, K., Diacetylmorphine (heroin) hydrolases in human blood. *Can J Physiol Pharmacol* **1983**, *61* (8), 870-5.

271. Nakamura, G. R.; Thornton, J. I.; Noguchi, T. T., Kinetics of heroin deacetylation in aqueous alkaline solution and in human serum and whole blood. *J Chromatogr* **1975**, *110* (1), 81-9.

272. Smith, D. A.; Cole, W. J., Rapid and sensitive gas chromatographic determination of diacetylmorphine and its metabolite monoacetylmorphine in blood using a nitrogen detector. *J Chromatogr* **1975**, *105* (2), 377-81.

273. Salmon, A. Y.; Goren, Z.; Avissar, Y.; Soreq, H., Human erythrocyte but not brain acetylcholinesterase hydrolyses heroin to morphine. *Clin Exp Pharmacol Physiol* **1999**, *26* (8), 596-600.

274. Lockridge, O.; Mottershaw-Jackson, N.; Eckerson, H. W.; La Du, B. N., Hydrolysis of diacetylmorphine (heroin) by human serum cholinesterase. *J Pharmacol Exp Ther* **1980**, *215* (1), 1-8.

275. Alberty, R. A., Effects of pH in rapid-equilibrium enzyme kinetics. *J. Phys. Chem. B* **2007**, *111*, 14064-14068.

276. Lockridge, O.; Mottershaw-Jackson, N.; Eckerson, H. W.; LaDu, B. N., Hydrolysis of diacetylmorphine (heroin) by human serum cholinesterase. *J. Pharmacol. Exp. Ther.* **1980**, *215*, 1-8.

277. Rook, E. J.; van Ree, J. M.; van den Brink, W.; Hillebrand, M. J.; Huitema, A. D.; Hendriks, V. M.; Beijnen, J. H., Pharmacokinetics and pharmacodynamics of high doses of pharmaceutically prepared heroin, by intravenous or by inhalation route in opioid-dependent patients. *Basic Clin Pharmacol Toxicol* **2006**, *98* (1), 86-96.

278. Gyr, E.; Brenneisen, R.; Bourquin, D.; Lehmann, T.; Vonlanthen, D.; Hug, I., Pharmacodynamics and pharmacokinetics of intravenously, orally and rectally administered diacetylmorphine in opioid dependents, a two-patient pilot study within a heroin-assisted treatment program. *Int J Clin Pharmacol Ther* **2000**, 38 (10), 486-91.
279. Girardin, F.; Rentsch, K. M.; Schwab, M. A.; Maggiorini, M.; Pauli-Magnus, C.; Kullak-Ublick, G. A.; Meier, P. J.; Fattinger, K., Pharmacokinetics of high doses of intramuscular and oral heroin in narcotic addicts. *Clin Pharmacol Ther* **2003**, 74 (4), 341-52.
280. Qiao, Y.; Han, K.; Zhan, C.-G., Reaction pathways and free energy profiles for cholinesterase-catalyzed hydrolysis of 6-monoacetylmorphine. *Organic & Biomolecular Chemistry* **2014**, 12 (14), 2214-2227.
281. Qiao, Y.; Han, K.; Zhan, C.-G., Fundamental Reaction Pathway and Free Energy Profile for Butyrylcholinesterase-Catalyzed Hydrolysis of Heroin. *Biochemistry* **2013**, 52 (37), 6467-6479.
282. Brimijoin, S.; Gao, Y.; Anker, J. J.; Gliddon, L. A.; Lafleur, D.; Shah, R.; Zhao, Q.; Singh, M.; Carroll, M. E., A cocaine hydrolase engineered from human butyrylcholinesterase selectively blocks cocaine toxicity and reinstatement of drug seeking in rats. *Neuropsychopharmacology* **2008**, 33 (11), 2715-25.
283. Zheng, F.; Yang, W.; Ko, M. C.; Liu, J.; Cho, H.; Gao, D.; Tong, M.; Tai, H. H.; Woods, J. H.; Zhan, C. G., Most efficient cocaine hydrolase designed by virtual screening of transition states. *J Am Chem Soc* **2008**, 130 (36), 12148-55.
284. Pan, Y.; Gao, D.; Yang, W.; Cho, H.; Zhan, C.-G., Free Energy Perturbation (FEP) Simulation on the Transition States of Cocaine Hydrolysis Catalyzed by Human Butyrylcholinesterase and Its Mutants. *Journal of the American Chemical Society* **2007**, 129 (44), 13537-13543.
285. Pan, Y.; Gao, D.; Yang, W.; Cho, H.; Yang, G.; Tai, H.-H.; Zhan, C.-G., Computational redesign of human butyrylcholinesterase for anticocaine medication. *Proceedings of the National Academy of Sciences of the United States of America* **2005**, 102 (46), 16656-16661.
286. Kyungbo Kim, F. Z., Chang-Guo Zhan, Oligomerization and Catalytic Parameters of Human UDP-glucuronosyltransferase 1A10. *Drug Metab Dispos* **2018**.
287. Kim, K.; Zheng, F.; Zhan, C. G., Oligomerization and catalytic parameters of human UDP-glucuronosyltransferase 1A10: Expression and characterization of the recombinant protein. *Drug Metab Dispos* **2018**.
288. Meech, R.; Mackenzie, P. I., Structure and function of uridine diphosphate glucuronosyltransferases. *Clin Exp Pharmacol Physiol* **1997**, 24 (12), 907-15.
289. Wiffen, P. J.; Wee, B.; Moore, R. A., Oral morphine for cancer pain. *Cochrane Database Syst Rev* **2013**, (7), CD003868.
290. Milne, R. W.; Nation, R. L.; Somogyi, A. A., The disposition of morphine and its 3- and 6-glucuronide metabolites in humans and animals, and the importance of the metabolites to the pharmacological effects of morphine. *Drug Metab Rev* **1996**, 28 (3), 345-472.
291. Christrup, L. L., Morphine metabolites. *Acta Anaesthesiol Scand* **1997**, 41 (1 Pt 2), 116-22.
292. Dechelotte, P.; Sabouraud, A.; Sandouk, P.; Hackbarth, I.; Schwenk, M., Uptake, 3-, and 6-glucuronidation of morphine in isolated cells from stomach, intestine, colon, and

liver of the guinea pig. *Drug Metab Dispos* **1993**, 21 (1), 13-7.

293. Stone, A. N.; Mackenzie, P. I.; Galetin, A.; Houston, J. B.; Miners, J. O., Isoform selectivity and kinetics of morphine 3- and 6-glucuronidation by human udp-glucuronosyltransferases: evidence for atypical glucuronidation kinetics by UGT2B7. *Drug Metab Dispos* **2003**, 31 (9), 1086-9.

294. Matern, H.; Matern, S.; Gerok, W., Isolation and characterization of rat liver microsomal UDP-glucuronosyltransferase activity toward chenodeoxycholic acid and testosterone as a single form of enzyme. *J Biol Chem* **1982**, 257 (13), 7422-9.

295. Ghosh, S. S.; Sappal, B. S.; Kalpana, G. V.; Lee, S. W.; Chowdhury, J. R.; Chowdhury, N. R., Homodimerization of human bilirubin-uridine-diphosphoglucuronate glucuronosyltransferase-1 (UGT1A1) and its functional implications. *J Biol Chem* **2001**, 276 (45), 42108-15.

296. Operana, T. N.; Tukey, R. H., Oligomerization of the UDP-glucuronosyltransferase 1A proteins: homo- and heterodimerization analysis by fluorescence resonance energy transfer and co-immunoprecipitation. *J Biol Chem* **2007**, 282 (7), 4821-9.

297. Finel, M.; Kurkela, M., The UDP-glucuronosyltransferases as oligomeric enzymes. *Curr Drug Metab* **2008**, 9 (1), 70-6.

298. Kurkela, M.; Garcia-Horsman, J. A.; Luukkanen, L.; Morsky, S.; Taskinen, J.; Baumann, M.; Kostianen, R.; Hirvonen, J.; Finel, M., Expression and characterization of recombinant human UDP-glucuronosyltransferases (UGTs). UGT1A9 is more resistant to detergent inhibition than other UGTs and was purified as an active dimeric enzyme. *J Biol Chem* **2003**, 278 (6), 3536-44.

299. Kato, Y.; Izukawa, T.; Oda, S.; Fukami, T.; Finel, M.; Yokoi, T.; Nakajima, M., Human UDP-glucuronosyltransferase (UGT) 2B10 in drug N-glucuronidation: substrate screening and comparison with UGT1A3 and UGT1A4. *Drug Metab Dispos* **2013**, 41 (7), 1389-97.

300. Radominska-Pandya, A.; Bratton, S.; Little, J. M., A historical overview of the heterologous expression of mammalian UDP-glucuronosyltransferase isoforms over the past twenty years. *Curr Drug Metab* **2005**, 6 (2), 141-60.

301. He, G.; Troberg, J.; Lv, X.; Xia, Y. L.; Zhu, L. L.; Ning, J.; Ge, G. B.; Finel, M.; Yang, L., Identification and characterization of human UDP-glucuronosyltransferases responsible for xanthotoxol glucuronidation. *Xenobiotica* **2018**, 48 (2), 109-116.

302. Zhang, H.; Patana, A. S.; Mackenzie, P. I.; Ikushiro, S.; Goldman, A.; Finel, M., Human UDP-glucuronosyltransferase expression in insect cells: ratio of active to inactive recombinant proteins and the effects of a C-terminal his-tag on glucuronidation kinetics. *Drug Metab Dispos* **2012**, 40 (10), 1935-44.

303. Tukey, R. H.; Tephly, T. R., Purification of properties of rabbit liver estrone and p-nitrophenol UDP-glucuronosyltransferases. *Arch Biochem Biophys* **1981**, 209 (2), 565-78.

304. Fujiwara, R.; Nakajima, M.; Yamanaka, H.; Katoh, M.; Yokoi, T., Interactions between human UGT1A1, UGT1A4, and UGT1A6 affect their enzymatic activities. *Drug Metab Dispos* **2007**, 35 (10), 1781-7.

305. Ohno, S.; Nakajin, S., Determination of mRNA expression of human UDP-glucuronosyltransferases and application for localization in various human tissues by real-time reverse transcriptase-polymerase chain reaction. *Drug Metab Dispos* **2009**, 37 (1), 32-40.

306. Oda, S.; Kato, Y.; Hatakeyama, M.; Iwamura, A.; Fukami, T.; Kume, T.; Yokoi, T.;

- Nakajima, M., Evaluation of expression and glycosylation status of UGT1A10 in Supersomes and intestinal epithelial cells with a novel specific UGT1A10 monoclonal antibody. *Drug Metab Dispos* **2017**, *45* (9), 1027-1034.
307. Nakamura, A.; Nakajima, M.; Yamanaka, H.; Fujiwara, R.; Yokoi, T., Expression of UGT1A and UGT2B mRNA in human normal tissues and various cell lines. *Drug Metab Dispos* **2008**, *36* (8), 1461-4.
308. Sato, Y.; Nagata, M.; Tetsuka, K.; Tamura, K.; Miyashita, A.; Kawamura, A.; Usui, T., Optimized methods for targeted peptide-based quantification of human uridine 5'-diphosphate-glucuronosyltransferases in biological specimens using liquid chromatography-tandem mass spectrometry. *Drug Metab Dispos* **2014**, *42* (5), 885-9.
309. Xue, L.; Hou, S.; Tong, M.; Fang, L.; Chen, X.; Jin, Z.; Tai, H. H.; Zheng, F.; Zhan, C. G., Preparation and in vivo characterization of a cocaine hydrolase engineered from human butyrylcholinesterase for metabolizing cocaine. *Biochem J* **2013**, *453* (3), 447-54.
310. Sells, S. F.; Wood, D. P., Jr.; Joshi-Barve, S. S.; Muthukumar, S.; Jacob, R. J.; Crist, S. A.; Humphreys, S.; Rangnekar, V. M., Commonality of the gene programs induced by effectors of apoptosis in androgen-dependent and -independent prostate cells. *Cell Growth Differ* **1994**, *5* (4), 457-66.
311. Burikhanov, R.; Zhao, Y.; Goswami, A.; Qiu, S.; Schwarze, S. R.; Rangnekar, V. M., The tumor suppressor Par-4 activates an extrinsic pathway for apoptosis. *Cell* **2009**, *138* (2), 377-88.
312. Gurumurthy, S.; Rangnekar, V. M., Par-4 inducible apoptosis in prostate cancer cells. *J Cell Biochem* **2004**, *91* (3), 504-12.
313. Kogel, D.; Reimertz, C.; Mech, P.; Poppe, M.; Fruhwald, M. C.; Engemann, H.; Scheidtmann, K. H.; Prehn, J. H., Dlk/ZIP kinase-induced apoptosis in human medulloblastoma cells: requirement of the mitochondrial apoptosis pathway. *Br J Cancer* **2001**, *85* (11), 1801-8.
314. Boehrer, S.; Chow, K. U.; Puccetti, E.; Ruthardt, M.; Godzisard, S.; Krapohl, A.; Schneider, B.; Hoelzer, D.; Mitrou, P. S.; Rangnekar, V. M.; Weidmann, E., Deregulated expression of prostate apoptosis response gene-4 in less differentiated lymphocytes and inverse expressional patterns of par-4 and bcl-2 in acute lymphocytic leukemia. *Hematol J* **2001**, *2* (2), 103-7.
315. El-Guendy, N.; Rangnekar, V. M., Apoptosis by Par-4 in cancer and neurodegenerative diseases. *Exp Cell Res* **2003**, *283* (1), 51-66.
316. Hebbar, N.; Wang, C.; Rangnekar, V. M., Mechanisms of apoptosis by the tumor suppressor Par-4. *J Cell Physiol* **2012**, *227* (12), 3715-21.
317. Chakraborty, M.; Qiu, S. G.; Vasudevan, K. M.; Rangnekar, V. M., Par-4 drives trafficking and activation of Fas and FasL to induce prostate cancer cell apoptosis and tumor regression. *Cancer Res* **2001**, *61* (19), 7255-63.
318. El-Guendy, N.; Zhao, Y.; Gurumurthy, S.; Burikhanov, R.; Rangnekar, V. M., Identification of a unique core domain of par-4 sufficient for selective apoptosis induction in cancer cells. *Mol Cell Biol* **2003**, *23* (16), 5516-25.
319. Burikhanov, R.; Sviripa, V. M.; Hebbar, N.; Zhang, W.; Layton, W. J.; Hamza, A.; Zhan, C. G.; Watt, D. S.; Liu, C.; Rangnekar, V. M., Arylquins target vimentin to trigger Par-4 secretion for tumor cell apoptosis. *Nat Chem Biol* **2014**, *10* (11), 924-926.
320. Burikhanov, R.; Hebbar, N.; Noothi, S. K.; Shukla, N.; Sledziona, J.; Araujo, N.; Kudrimoti, M.; Wang, Q. J.; Watt, D. S.; Welch, D. R.; Maranchie, J.; Harada, A.;

- Rangnekar, V. M., Chloroquine-Inducible Par-4 Secretion Is Essential for Tumor Cell Apoptosis and Inhibition of Metastasis. *Cell Rep* **2017**, *18* (2), 508-519.
321. Zhao, Y.; Burikhanov, R.; Brandon, J.; Qiu, S.; Shelton, B. J.; Spear, B.; Bondada, S.; Bryson, S.; Rangnekar, V. M., Systemic Par-4 inhibits non-autochthonous tumor growth. *Cancer Biol Ther* **2011**, *12* (2), 152-7.
322. Berndt, C.; Lillig, C. H.; Holmgren, A., Thioredoxins and glutaredoxins as facilitators of protein folding. *Biochim Biophys Acta* **2008**, *1783* (4), 641-50.
323. Maxwell, L. J.; Singh, J. A., Abatacept for rheumatoid arthritis: a Cochrane systematic review. *J Rheumatol* **2010**, *37* (2), 234-45.
324. Boussif, O.; Lezoualc'h, F.; Zanta, M. A.; Mergny, M. D.; Scherman, D.; Demeneix, B.; Behr, J. P., A versatile vector for gene and oligonucleotide transfer into cells in culture and in vivo: polyethylenimine. *Proc Natl Acad Sci U S A* **1995**, *92* (16), 7297-301.
325. Sonawane, N. D.; Szoka, F. C., Jr.; Verkman, A. S., Chloride accumulation and swelling in endosomes enhances DNA transfer by polyamine-DNA polyplexes. *J Biol Chem* **2003**, *278* (45), 44826-31.
326. Longo, P. A.; Kavran, J. M.; Kim, M. S.; Leahy, D. J., Transient mammalian cell transfection with polyethylenimine (PEI). *Methods Enzymol* **2013**, *529*, 227-40.
327. Mauro, V. P.; Chappell, S. A., A critical analysis of codon optimization in human therapeutics. *Trends Mol Med* **2014**, *20* (11), 604-13.
328. Knop, K.; Hoogenboom, R.; Fischer, D.; Schubert, U. S., Poly(ethylene glycol) in drug delivery: pros and cons as well as potential alternatives. *Angew Chem Int Ed Engl* **2010**, *49* (36), 6288-308.
329. Miner, J. H., The glomerular basement membrane. *Exp Cell Res* **2012**, *318* (9), 973-8.
330. Sztal, T.; Berger, S.; Currie, P. D.; Hall, T. E., Characterization of the laminin gene family and evolution in zebrafish. *Dev Dyn* **2011**, *240* (2), 422-31.
331. Suh, J. H.; Jarad, G.; VanDeVoorde, R. G.; Miner, J. H., Forced expression of laminin beta1 in podocytes prevents nephrotic syndrome in mice lacking laminin beta2, a model for Pierson syndrome. *Proc Natl Acad Sci U S A* **2011**, *108* (37), 15348-53.
332. Hausmann, R.; Kuppe, C.; Egger, H.; Schweda, F.; Knecht, V.; Elger, M.; Menzel, S.; Somers, D.; Braun, G.; Fuss, A.; Uhlig, S.; Kriz, W.; Tanner, G.; Floege, J.; Moeller, M. J., Electrical forces determine glomerular permeability. *J Am Soc Nephrol* **2010**, *21* (12), 2053-8.
333. Simmons, L. C.; Reilly, D.; Klimowski, L.; Raju, T. S.; Meng, G.; Sims, P.; Hong, K.; Shields, R. L.; Damico, L. A.; Rancatore, P.; Yansura, D. G., Expression of full-length immunoglobulins in *Escherichia coli*: rapid and efficient production of aglycosylated antibodies. *J Immunol Methods* **2002**, *263* (1-2), 133-47.
334. Hobbs, S. M.; Jackson, L. E.; Hoadley, J., Interaction of aglycosyl immunoglobulins with the IgG Fc transport receptor from neonatal rat gut: comparison of deglycosylation by tunicamycin treatment and genetic engineering. *Mol Immunol* **1992**, *29* (7-8), 949-56.
335. Tao, M. H.; Morrison, S. L., Studies of aglycosylated chimeric mouse-human IgG. Role of carbohydrate in the structure and effector functions mediated by the human IgG constant region. *J Immunol* **1989**, *143* (8), 2595-601.
336. Goswami, A.; Burikhanov, R.; de Thonel, A.; Fujita, N.; Goswami, M.; Zhao, Y.; Eriksson, J. E.; Tsuruo, T.; Rangnekar, V. M., Binding and phosphorylation of par-4 by akt

- is essential for cancer cell survival. *Mol Cell* **2005**, 20 (1), 33-44.
337. Primo-Parmo, S. L.; Sorenson, R. C.; Teiber, J.; La Du, B. N., The human serum paraoxonase/arylesterase gene (PON1) is one member of a multigene family. *Genomics* **1996**, 33 (3), 498-507.
338. Vaillant, G. E., A 20-year follow-up of New York narcotic addicts. *Archives of general psychiatry* **1973**, 29 (2), 237-41.
339. MJ, P., Follow-up study of treated narcotics addicts. *public health reports* **1943**, (170), 1-18.
340. Johnson, R. E.; Chutuape, M. A.; Strain, E. C.; Walsh, S. L.; Stitzer, M. L.; Bigelow, G. E., A comparison of levomethadyl acetate, buprenorphine, and methadone for opioid dependence. *The New England journal of medicine* **2000**, 343 (18), 1290-7.
341. Strain, E. C.; Bigelow, G. E.; Liebson, I. A.; Stitzer, M. L., Moderate- vs high-dose methadone in the treatment of opioid dependence: a randomized trial. *JAMA : the journal of the American Medical Association* **1999**, 281 (11), 1000-5.
342. Ling, W.; Wesson, D. R.; Charuvastra, C.; Klett, C. J., A controlled trial comparing buprenorphine and methadone maintenance in opioid dependence. *Archives of general psychiatry* **1996**, 53 (5), 401-7.
343. Bart, G., Maintenance medication for opiate addiction: the foundation of recovery. *Journal of addictive diseases* **2012**, 31 (3), 207-25.
344. Kakko, J.; Svanborg, K. D.; Kreek, M. J.; Heilig, M., 1-year retention and social function after buprenorphine-assisted relapse prevention treatment for heroin dependence in Sweden: a randomised, placebo-controlled trial. *Lancet* **2003**, 361 (9358), 662-8.
345. Mattick, R. P.; Ali, R.; White, J. M.; O'Brien, S.; Wolk, S.; Danz, C., Buprenorphine versus methadone maintenance therapy: a randomized double-blind trial with 405 opioid-dependent patients. *Addiction* **2003**, 98 (4), 441-52.
346. Langleben, D. D.; Ruparel, K.; Elman, I.; Busch-Winokur, S.; Pratiwadi, R.; Loughhead, J.; O'Brien, C. P.; Childress, A. R., Acute effect of methadone maintenance dose on brain fMRI response to heroin-related cues. *The American journal of psychiatry* **2008**, 165 (3), 390-4.
347. Childress, A. R.; McLellan, A. T.; O'Brien, C. P., Conditioned responses in a methadone population. A comparison of laboratory, clinic, and natural settings. *Journal of substance abuse treatment* **1986**, 3 (3), 173-9.
348. Walter, M.; Wiesbeck, G. A.; Bloch, N.; Aeschbach, S.; Olbrich, H. M.; Seifritz, E.; Dursteler-MacFarland, K. M., Psychobiological responses to drug cues before and after methadone intake in heroin-dependent patients: a pilot study. *European neuropsychopharmacology : the journal of the European College of Neuropsychopharmacology* **2008**, 18 (5), 390-3.
349. Martin, W. R., Realistic goals for antagonist therapy. *The American journal of drug and alcohol abuse* **1975**, 2 (3-4), 353-6.
350. O'Brien, C. P.; Greenstein, R. A.; Mintz, J.; Woody, G. E., Clinical experience with naltrexone. *The American journal of drug and alcohol abuse* **1975**, 2 (3-4), 365-77.
351. Hollister, L. E.; Schwin, R. L.; Kasper, P., Naltrexone treatment of opiate-dependent persons. *Drug and alcohol dependence* **1977**, 2 (3), 203-9.
352. Judson, B. A.; Carney, T. M.; Goldstein, A., Naltrexone treatment of heroin addiction: efficacy and safety in a double-blind dosage comparison. *Drug and alcohol dependence* **1981**, 7 (4), 325-46.

353. Dole, V. P.; Nyswander, M. E.; Kreek, M. J., Narcotic blockade. *Archives of internal medicine* **1966**, *118* (4), 304-9.
354. Dole, V. P.; Nyswander, M., A Medical Treatment for Diacetylmorphine (Heroin) Addiction. A Clinical Trial with Methadone Hydrochloride. *JAMA : the journal of the American Medical Association* **1965**, *193*, 646-50.
355. Marsch, L. A.; Stephens, M. A.; Mudric, T.; Strain, E. C.; Bigelow, G. E.; Johnson, R. E., Predictors of outcome in LAAM, buprenorphine, and methadone treatment for opioid dependence. *Experimental and clinical psychopharmacology* **2005**, *13* (4), 293-302.
356. Kelly, S. M.; O'Grady, K. E.; Mitchell, S. G.; Brown, B. S.; Schwartz, R. P., Predictors of methadone treatment retention from a multi-site study: a survival analysis. *Drug and alcohol dependence* **2011**, *117* (2-3), 170-5.
357. Belding, M. A.; McLellan, A. T.; Zanis, D. A.; Incmikoski, R., Characterizing "nonresponsive" methadone patients. *Journal of substance abuse treatment* **1998**, *15* (6), 485-92.
358. Villafranca, S. W.; McKellar, J. D.; Trafton, J. A.; Humphreys, K., Predictors of retention in methadone programs: a signal detection analysis. *Drug and alcohol dependence* **2006**, *83* (3), 218-24.
359. Sulima, A.; Jalah, R.; Antoline, J. F. G.; Torres, O. B.; Imler, G. H.; Deschamps, J. R.; Beck, Z.; Alving, C. R.; Jacobson, A. E.; Rice, K. C.; Matyas, G. R., A Stable Heroin Analogue That Can Serve as a Vaccine Hapten to Induce Antibodies That Block the Effects of Heroin and Its Metabolites in Rodents and That Cross-React Immunologically with Related Drugs of Abuse. *J Med Chem* **2018**, *61* (1), 329-343.
360. Schlosburg, J. E.; Vendruscolo, L. F.; Bremer, P. T.; Lockner, J. W.; Wade, C. L.; Nunes, A. A.; Stowe, G. N.; Edwards, S.; Janda, K. D.; Koob, G. F., Dynamic vaccine blocks relapse to compulsive intake of heroin. *Proc Natl Acad Sci U S A* **2013**, *110* (22), 9036-41.
361. Anton, B.; Leff, P., A novel bivalent morphine/heroin vaccine that prevents relapse to heroin addiction in rodents. *Vaccine* **2006**, *24* (16), 3232-40.
362. Bogen, I. L.; Boix, F.; Nerem, E.; Mørland, J.; Andersen, J. M., A Monoclonal Antibody Specific for 6-Monoacetylmorphine Reduces Acute Heroin Effects in Mice. *J. Pharmacol. Exp. Ther.* **2014**, *349*, 568-576.
363. Kvello, A. M. S.; Andersen, J. M.; Elisabeth Leere Øiestad; Mørland, J.; Bogen, I. L., Pharmacological Effects of a Monoclonal Antibody against 6-Monoacetylmorphine upon Heroin-Induced Locomotor Activity and Pharmacokinetics in Mice. *J. Pharmacol. Exp. Ther.* **2016**, *358*, 181-189.
364. Moghaddama, A.; Borgenb, T.; Stacyb, J.; Kausmallyb, L.; Bjørg Simonsenb; Marvikb, O. J.; Brekkeb, O. H.; Braunagel, M., Identification of scFv antibody fragments that specifically recognise the heroin metabolite 6-monoacetylmorphine but not morphine. *J. Immunol. Methods* **2003**, *280*, 139-155.
365. Chen, X.; Xue, L.; Hou, S.; Jin, Z.; Zhang, T.; Zheng, F.; Zhan, C.-G., Long-acting cocaine hydrolase for addiction therapy. *Proc. Natl. Acad. Sci. USA* **2016**, *113*, 422-427.
366. Chen, X.; Zheng, X.; Zhou, Z.; Zhan, C.-G.; Zheng, F., Effects of a cocaine hydrolase engineered from human butyrylcholinesterase on metabolic profile of cocaine in rats. *Chem. Biol. Interact.* **2016**, *259*, 104-109.
367. Braman, J.; Papworth, C.; Greener, A., Site-directed mutagenesis using double-stranded plasmid DNA templates. *Methods Mol. Biol.* **1996**, *57*, 31-44.



368. BotDB-Sponsored by U. S. Army Medical Research Institute of Infectious Diseases (USAMRIID), IC50-to-Ki Converter (<https://botdb-abcc.ncifcrf.gov/toxin/kiConverter.jsp>).
369. Hanaka, H.; Pawelzik, S. C.; Johnsen, J. I.; Rakonjac, M.; Terawaki, K.; Rasmuson, A.; Sveinbjornsson, B.; Schumacher, M. C.; Hamberg, M.; Samuelsson, B.; Jakobsson, P. J.; Kogner, P.; Radmark, O., Microsomal prostaglandin E synthase 1 determines tumor growth in vivo of prostate and lung cancer cells. *Proc Natl Acad Sci U S A* **2009**, *106* (44), 18757-62.
370. Chang, H. H.; Meuillet, E. J., Identification and development of mPGES-1 inhibitors: where we are at? *Future Med Chem* **2011**, *3* (15), 1909-34.
371. Gudis, K.; Tatsuguchi, A.; Wada, K.; Futagami, S.; Nagata, K.; Hiratsuka, T.; Shinji, Y.; Miyake, K.; Tsukui, T.; Fukuda, Y.; Sakamoto, C., Microsomal prostaglandin E synthase (mPGES)-1, mPGES-2 and cytosolic PGES expression in human gastritis and gastric ulcer tissue. *Lab Invest* **2005**, *85* (2), 225-36.
372. Payner, T.; Leaver, H. A.; Knapp, B.; Whittle, I. R.; Trifan, O. C.; Miller, S.; Rizzo, M. T., Microsomal prostaglandin E synthase-1 regulates human glioma cell growth via prostaglandin E(2)-dependent activation of type II protein kinase A. *Mol Cancer Ther* **2006**, *5* (7), 1817-26.
373. Kudo, I.; Murakami, M., Prostaglandin E synthase, a terminal enzyme for prostaglandin E2 biosynthesis. *J Biochem Mol Biol* **2005**, *38* (6), 633-8.
374. Fahmi, H., mPGES-1 as a novel target for arthritis. *Curr Opin Rheumatol* **2004**, *16* (5), 623-7.
375. Ding, K.; Zhou, Z.; Zhou, S.; Yuan, Y.; Kim, K.; Zhang, T.; Zheng, X.; Zheng, F.; Zhan, C. G., Design, synthesis, and discovery of 5-((1,3-diphenyl-1H-pyrazol-4-yl)methylene)pyrimidine-2,4,6(1H,3H,5H)-triones and related derivatives as novel inhibitors of mPGES-1. *Bioorg Med Chem Lett* **2018**, *28* (5), 858-862.
376. Ding, K.; Zhou, Z.; Hou, S.; Yuan, Y.; Zhou, S.; Zheng, X.; Chen, J.; Loftin, C.; Zheng, F.; Zhan, C. G., Structure-based discovery of mPGES-1 inhibitors suitable for preclinical testing in wild-type mice as a new generation of anti-inflammatory drugs. *Sci Rep* **2018**, *8* (1), 5205.

## Vitae

### Kyungbo Kim

#### EDUCATION:

- 2018 PhD candidate, Pharmaceutical Sciences, University of Kentucky at Lexington, USA
- 2011 M.S. in Bioscience and biotechnology, Konkuk University in Korea
- 2008 Bioscience and Bioformatics, Myungji University in Korea

#### EXPERIENCE:

- 2013-2018 Graduate Research Fellow, University of Kentucky, College of Pharmacy
- 2012-2013 Research Assistant, University of Kentucky, College of Pharmacy  
01/2012 – 03/2013 (15 months)
- 2009-2011 Graduate Research Fellow, Konkuk University

#### TEACHING:

- 2009 Fall Teaching Assistant, Biological Sciences and Biotechnology, Konkuk University

#### MANUSCRIPTS PUBLISHED OR SUBMITTED (\*: Co-first author)

- 1) **Kyungbo Kim\***, Bokhui Lee\*, Sangtaek Oh, Joon Sig Choi, Jong-Sang Park, Dal-Hee Min, and Dong-Eun Kim (\*: Co-first author) "Suppression of Hepatitis C Virus Genome Replication in Cells with RNA-Cleaving DNA Enzymes and Short-Hairpin RNA", *OLIGONUCLEOTIDES*, 20, 285-296 (2010)
- 2) Mi Kyoung Kim, Mi-Sun Yu, Hye Ri Park, **Kyungbo Kim**, Chaewoon Lee, Suh Young Cho, Jihoon Kang, Hyunjun Yoon, Dong-Eun Kim, Hyunah Choo, Yong-Joo Jeong, and Youhoon Chong "2,6-Bis-arylmethoxy-5-hydroxychromones with antiviral activity against both hepatitis C virus (HCV) and SARS-associated coronavirus (SCV)", *EUROPEAN JOURNAL OF MEDICINAL CHEMISTRY*, 46, 5698-5704 (2011)

- 3) Sun Young Park, Seho Kim, Hana Yoon, **Kyungbo Kim**, Sheetal S. Kalme, Sangtaek Oh, Chang Seon Song, and Dong-Eun Kim "Selection of an Antiviral RNA Aptamer Against Hemagglutinin of the Subtype H5 Avian Influenza Virus", *NUCLEIC ACID THERAPEUTICS*, 21, 395-402 (2011)
- 4) Joon Soo Park, **Kyungbo Kim**, Dong-Eun Kim "DNA helicase reduces production of aberrant run-off transcripts during in vitro RNA synthesis with T7 RNA polymerase", *Bull. Korean Chem. Soc.* 2011, 32, No. 10 3779-3782 (2011)
- 5) Soo-Ryoon Ryoo, Hongje Jang, Ki-Sun Kim, Bokhui Lee, **Kyungbo Kim**, Young-Kwan Kim, Woon-Seok Yeo, Younghoon Lee, Dong-Eun Kim, and Dal-Hee Min "Functional delivery of DNzyme with iron oxide nanoparticles for hepatitis C virus gene knockdown", *BIOMATERIALS*, 33, 2754-2761 (2012)
- 6) Ji Eun Park, Lin Ao, Zachary Miller, **Kyungbo Kim**, Ying Wu, Eun Ryoung Jang, Eun Young Lee, Kyung Bo Kim, and Woon Lee. "PSMB9 codon 60 polymorphisms have no impact on the activity of the immunoproteasome catalytic subunit  $\beta$ 1i expressed in multiple types of solid cancer." *PLoS One*. 2013, 8(9):e73732.
- 7) Nilay Thakkar, **Kyungbo Kim**, Eun Ryoung Jang, Songhee Han, Kyunghwa Kim, Donghern Kim, Nipun Merchant, A. Craig Lockhart, and Woon Lee. "A cancer-specific variant of the SLCO1B3 gene encodes a novel human organic anion transporting polypeptide 1B3 (OATP1B3) localized mainly in the cytoplasm of colon and pancreatic cancer cells." *Mol Pharm.* 10(1):406-16 (2013)
- 8) **Kyungbo Kim\***, Songhee Han\*, Nilay Thakkar\*, Donghak Kim, and Woon Lee. (\*: Co-first author) "Role of hypoxia inducible factor-1 $\alpha$  in the regulation of the cancer-specific variant of organic anion transporting polypeptide 1B3 (OATP1B3), in colon and pancreatic cancer." *Biochem Pharmacol.* 86(6):816-23 (2013)
- 9) Si Eun Baek, Hyoseon Kim, **Kyungbo Kim**, Soojin Yoon, Jungwoo Choe, Wonhee Suh, Yong-Joo Jeong, Yo Han Cho, Dong-Eun Kim, "Dual effects of duplex RNA harboring 5'-terminal triphosphate on gene silencing and RIG-I mediated innate immune response", *Biochem Biophys Res Commun.* 456(2):591-7 (2015)
- 10) **Kyungbo Kim**, Jianzhuang Yao, Zhenyu Jin, Fang Zheng, and Chang-Guo Zhan "Kinetic characterization of cholinesterases and a therapeutically valuable cocaine hydrolase for their catalytic activities against heroin and its metabolite 6-monoacetylmorphine", *Chem. Biol. Interact.* 293:107-114 (2018).

- 11) **Kyungbo Kim**, Fang Zheng, and Chang-Guo Zhan “Oligomerization and Catalytic Parameters of Human UDP-glucuronosyltransferase 1A10”, *Drug Metab Dispos.* 2018 Aug 15. pii: dmd.118.082495 (Epub ahead of print).